UNIVERSITY OF SOUTHAMPTON

DEPARTMENT OF MECHANICAL ENGINEERING

A NUMERICAL STUDY OF SOLIDIFICATION AND NATURAL CONVECTION DURING CRYOGENIC PIPE FREEZING

Alison Clare Keary

Submitted for Degree of Doctor of Philosophy 1995

UNIVERSITY OF SOUTHAMPTON

ABSTRACT

FACULTY OF ENGINEERING AND APPLIED SCIENCE
DEPARTMENT OF MECHANICAL ENGINEERING

Doctor of Philosophy

A NUMERICAL STUDY OF SOLIDIFICATION AND NATURAL CONVECTION DURING CRYOGENIC PIPE FREEZING

by
Alison Clare Keary

Cryogenic pipe freezing is a pipeline maintenance technique which can be used to isolate sections of pipeline; the pipe is cooled externally over a short length, freezing the liquid inside the pipe and forming a solid plug. The effect of natural convection on freezing in a vertical pipe containing water was investigated by modelling the process. As a first stage, the literature was reviewed and the results from previous experimental research for freezing in vertical pipes were summarised.

An analytical model was developed, assuming one-dimensional solidification and using an integral solution for the heat transfer coefficient for laminar natural convection adjacent to a heated vertical flat plate. The results obtained, assuming no decay in the water temperature during freezing, displayed good qualitative agreement with the experimental data. A method for defining the effect of convection on freezing in terms of the pipe radius and bulk temperature was proposed. A simple criterion based on the Grashof number for the temperature at which turbulent mixing becomes sufficient to halt freezing was extracted from experimental results. The formulation of a simple model of the processes which control the bulk temperature decay was undertaken and this was incorporated into the freezing model. The poor agreement with measurements of bulk temperature demonstrated the need for an improved understanding of the mixing processes.

A numerical model of pipe freezing was developed using the finite volume methodology, with the SIMPLER algorithm to predict convection, and the enthalpy method used to include solidification. A fixed (non-transforming) grid was used and the buoyancy-driven flows were assumed to be laminar. The numerical model was validated against experimental data and the dependence on numerical factors such as grid density was investigated. The development of the buoyancy-driven flows in the absence of freezing was studied and it was found that a complex mixing region forms which controls the bulk temperature inside the freezing zone. This flow development is dependent on the initial temperature and the pipe diameter, and has a negligible effect on the bulk temperature in pipes over a critical size. Plug formation was included in the model and the effects of varying the initial water temperature, the length of the pipe and the 'freezing' boundary condition were investigated. Interaction between the downwards boundary layer and the upwards core flow was noted at the plug neck, with the boundary layer becoming entrained in the core flow at the neck. The water above the neck becomes increasingly isolated from that below the neck, causing a decrease in bulk temperature and, if convection is sufficient to affect plug formation, neck migration up the plug. This agreed with experimental observations. The accuracy of the bulk temperature prediction was found to depend on the length of pipe that was modelled; this was demanding on computer resources and an 'open' bottom boundary condition was developed as a compromise. This allowed flow into and out of the domain and also made it possible to specify the bulk temperature. The results obtained using the different modelling approaches were analysed and the limitations of the methods discussed. Recommendations for further development were made. A series of criteria were defined (accounting for the effect of convection, turbulence and bulk temperature decay) to indicate which modelling approach to apply depending on pipe diameter and initial water temperature.

ACKNOWLEDGEMENTS

Firstly, I would like to acknowledge the continued advice, support and encouragement of my supervisor, Mr. R. J. Bowen, throughout this research. I am indebted to Dr. A. C. R. Tavner for many helpful discussions and also for proof-reading this thesis. I would like to thank Dr. M. Burton for his considerable help in developing the numerical model and in encoding the SIMPLE algorithm. The financial support of PowerGen (formerly C.E.G.B.) for the first three years of this project is also gratefully acknowledged; also the interest of Dr. D. Hobson at PowerGen.

On the more personal side, there are a number of people who I would like to thank. Firstly, my friends and colleagues at the University, especially Angus (again), Giles, William, Ian, Alastair, Russ, Martin, Paul, Jonathon, Kevin (for his help in creating colour bitmaps) and Steve (for all his help). I would also like to thank my parents for their encouragement and my late grandfather for financial support. Outside the University, I would like to thank all my friends, especially Chris, Dave, Lucy and Hazel. Holly deserves recognition for being a wonderful cat, despite doing her best to sit on the keyboard when I was programming at home. Finally, I wish to thank Peter for his support, advice, encouragement (in many forms !) and patience, especially while I was writing up.

NOMENCLATURE

GEOMETRY

x	horizontal co-ordinate; horizontal direction	(m)
r	radial co-ordinate; radial direction	(m)
z	vertical co-ordinate; vertical direction	(m)
dr	radial grid spacing	(m)
dz	vertical grid spacing	(m)
R_i	interface radius	(m)
R_w	inner pipe radius	(m)
H	jacket length	(m)
θ	angle between flow and grid orientation	(radians)

VARIABLES

T	temperature	(°C)
H	enthalpy	(J/kg)
u	radial velocity	(m/s)
w	vertical velocity	(m/s)
U	speed	(m/s)
p	pressure	(Pa)
t	time	(s)
Q	heat flow	(W)
q	heat flux	(W/m^2)
S	streamfunction	(m^3/s)

PROPERTIES

α	thermal diffusivity	(m^2/s)
β	expansivity	(K^{-1})
Γ	(general) diffusivity	
μ	dynamic viscosity	(Pa s)
ν	kinematic viscosity	(m^2/s)
ρ	density	(kg/m^3)
k	conductivity	(W/m K)
c	specific heat capacity	(J/kg K)
h	heat transfer coefficient (no subscript: heat transfer from water to ice interface)	
h_{c2b}	coef. for heat transfer between boundary layer and core flow	(W/m^2K)

L	latent heat capacity	(J/kg)
ε	porosity	
g	standard gravitational acceleration	(m/s^2)

MISCELLANEOUS

A	area	(m^2)
V	volume	(m^3)
Δ	change in ..	
T_∞	ambient temperature	(°C)
δ_v	velocity boundary layer thickness	(m)
δ_T	thermal boundary layer thickness	(m)
A_h	vertical distance between plug neck and bottom of jacket as fraction of jacket length	
f_s	solid fraction	
f_v	immobilisation factor (Chapter 5)	
f_x	factor for x ($x=v,\delta_T,\delta_v$) (Appendix I)	
q	ratio δ_v/δ_T (Appendix I)	
F	mass flow	(kg/s)
B_x	extra source term in momentum equations (x=u,w)	

SUBSCRIPTS

l	liquid
s	solid
w	wall
c	coolant
b	bulk
i	interface
core	core
f	freezing zone
m	mixing zone
bl	boundary layer
j	jacket
v	velocity boundary layer
T	thermal boundary layer
e,w,n,s	east, west, north, south (Appendix II only)

DIMENSIONLESS NUMBERS

Prandtl number

$$Pr = \frac{\mu c_p}{k}$$

Grashof number

$$Gr_H = \frac{\beta g \Delta T \rho^2 H^3}{\mu^2}$$

Rayleigh number

$$Ra_H = \frac{\beta g \Delta T \rho^2 H^3 c_p}{\mu k} = Gr_H . Pr$$

Nusselt number

$$Nu = \frac{hx}{k}$$

Biot Number

$$Bi = \frac{h}{k/L}$$

Stefan Number

$$Ste = \frac{c_s (T_f - T_{in})}{L}$$

Fourier Number

$$Fo = \frac{k_s}{c_s \rho_s L^2} t$$

CONTENTS

1. INTRODUCTION

1.1 INTRODUCTION TO PIPE FREEZING

Pipe freezing is a pipeline maintenance technique which can be used to isolate sections of a liquid filled pipeline. A jacket is placed round the pipe and filled with a cryogen such as liquid nitrogen, which cools the fluid in the pipe causing it to freeze and form a plug. This process is shown in figure 1.1. If this is repeated at another point, the section in between is isolated and may be opened in order to effect a repair or add, for instance, a valve or junction. Once the work has been completed the jacket can be removed and the plug allowed to thaw.

Using pipe freezing can eliminate the need to shut down and drain the system and therefore removes the need to decommission a large section of the plant. It is also less expensive than other plugging techniques which require more complex equipment as well as good access to the pipe. A thorough review of these alternative techniques is provided by Burton[1].

Although pipe freezing appears to be a simple technique, the actual processes taking place inside the pipe as the plug grows may be complicated. For example, freezing is very sensitive to flow in the pipe and the temperature of the liquid. It is also difficult to gauge what is happening inside a pipeline during a freeze and one of the important problems in performing a freeze lies in determining when the plug has sealed the pipe. If the pipe is opened before the plug is totally formed, the resulting flow will bring warmer liquid into the cooled region, destroying the existing ice layer.

Pipe freezing is regularly used in a range of situations. For instance, pipe freezing kits (usually using carbon dioxide gas as the cryogen) can be obtained from tool hire outlets to perform freezing in domestic plumbing situations. For larger scale applications, pipe freezing is a specialist activity and contractors rely on experience both in gauging the likely success of a potential freeze and in deciding when the pipe is blocked.

In order to provide a better scientific background to the subject, a research programme, funded by several interested companies and the S.E.R.C., was started at Southampton in 1981. The first two phases of this programme were mainly experimental studies of pipe freezing under a range of conditions. These investigations have looked at the effect of parameters such as flow, pipe diameter, orientation, initial fluid temperature and also investigated freezing different fluids. During phases three and four (currently in progress) the stresses induced in the pipe itself by freezing are considered.

One of the main aims of the research at Southampton was to determine the range of conditions under which pipe freezing can be successfully applied. The effect of natural convection on the plug formation is one important parameter: the temperature of the fluid in the pipe is often significantly higher than its freezing temperature. The effect of natural convection on freezing in vertical water-filled pipes have been studied in numerous experiments. The results from these studies showed that a complex flow field develops which interacts with the forming plug. When the water temperature was sufficiently high, the plug formation stopped before the plug sealed the pipe.

Further investigations were required to cover the range of conditions encountered in practice; these included, for instance, the fluid properties, pipe geometry and orientation, flow, freezing methods and environmental conditions. It was decided to develop a numerical model of the freezing and convection processes in order to investigate the interaction between convection and solidification in more detail. The main advantage of developing a numerical model is that pipe freezing can be studied under a range of conditions without the expense and effort required to construct, instrument and operate new experimental rigs. A numerical investigation also offers complete data in the whole area modelled whereas experimental studies can only provide data at positions where instrumentation is installed (which also risk affecting the local flow). This is especially important in the case of pipe freezing, given the inherent problems involved in observing fluid movement and plug formation inside the pipe.

1.2 INTRODUCTION TO NUMERICAL MODELLING

In order to investigate the freezing process theoretically, the fundamental energy conservation and Navier-Stokes equations for the flow and temperature distributions must be solved. Over the past 20 years or so, techniques for solving these equations have developed into a discipline called computational fluid dynamics (abbreviated to CFD). The governing second order partial differential equations are turned into a set of highly interlinked simultaneous equations for the value of each dependant variable at a series of points inside the region of interest. A computer program can be written to solve these equations using matrix inversion or iterative techniques. For a transient process, the time scale is also divided into a series of time steps at which the equations are solved. The resulting computer model can be used to predict the plug shape, the temperature distributions inside the frozen and liquid regions and the velocity distributions in the liquid

regions throughout the freezing process. This can be used to study the interaction between the convection and solidification processes and the effect of varying the governing parameters can be investigated.

1.3 AIMS OF THE NUMERICAL INVESTIGATION

The objectives of this investigation were as follows :

1. To develop a numerical model which predicts the plug formation and the buoyancy driven flow in a vertical pipe containing water.
2. Validate the model by comparing the predictions obtained using it with the results obtained from the experiments.
3. To use the model to understand the way in which the plug formation and the flow interact; in particular :
   - how the freezing time is affected by convection
   - the effect of increasing the initial temperature
   - how the processes vary with the pipe diameter

A vertical pipe was chosen for two reasons; firstly, detailed experimental results were available for this geometry and secondly because it can be treated as two-dimensional (axisymmetric) and is therefore more straightforward to model than a full three-dimensional situation.

1.4 ORGANISATION OF THE THESIS

This thesis is organised on a broadly chronological basis. In chapter 2, the background to this investigation is established by reviewing the experimental work which has been carried out in pipe freezing and related problems. The numerical and analytical research into pipe freezing and also into more general phase change and convection problems is reviewed.

As a preliminary stage to numerical modelling, the importance of convection on the freezing process was briefly studied by using an integral solution for the boundary layer velocities and thickness to a greatly simplified situation. In addition, a simple model of the flow development in the pipe was formulated. The method, results and limitations

with this approach are described in chapter 3.

The detailed description of the development of the numerical model has not been included in this thesis. The methods used in the numerical model are well established and the development of the model included extensive comparison with published data which does not form a major part of the investigation into pipe freezing. In order to make the presentation of this thesis clearer, the description of the numerical model has been summarised in chapter 4 with the detailed description moved to a separate report[2].

The validation of the numerical model for pipe freezing is described in chapter 5, comparing the predicted behaviour with the available experimental data.

The main body of results is presented in chapter 6. The development of the flow field inside the pipe without freezing is described and the interaction between the flow and the forming plug is investigated. The effect of varying the initial temperature, the pipe diameter, the length of the pipe and the applied cooling rate is studied. The results obtained using an open bottom model are described.

The conclusions, in chapter 7, draw together the results from this numerical investigation. Finally, the proposals for further work are detailed in chapter 8.

2. LITERATURE REVIEW

The purpose of a literature review into pipe freezing is to gather together the existing knowledge on pipe freezing and related fields which provides the background to the current research. There are several approaches which have been used to investigate problems that are relevant to pipe freezing. They can be split into the following areas.

- Experimental investigations: the problem of interest is reproduced as closely as possible in the laboratory and experiments are carried out. By installing instrumentation, such as thermocouples, in the rig, detailed information can be obtained during the experiment.
- Analytical investigations: the equations governing freezing and convection are complicated, however by making assumptions about the general behaviour it is possible to simplify the problem to a point at which the equations can be solved. Solution of the final equations often requires numerical techniques, especially for evaluating complicated integrals.
- Numerical investigations: the governing equations are solved without making assumptions about the general behaviour. The basis of the method is to divide the area of interest into a grid of points and to relate the value of the dependent variable at one point to the values at the neighbouring points using the governing equations. In a transient problem, the time scale must also be divided up and the equations solved at a series of points in time. The resulting sets of equations are interlinked and are solved either iteratively or by employing more complicated techniques, normally using a computer program. The analytical solutions are obtained by making fairly detailed assumptions but provide equations which are fairly quick to solve, whereas the numerical methods require very few specific assumptions but generally demand significant computer resources.

The literature review is split into these categories and has concentrated on natural convection and freezing problems. Some studies combine approaches, for example experimental research from which empirical constants are extracted and used in analytical models; these investigations are categorised on the basis of the major part of the work. A complete review of research into pipe freezing would cover a wide range of problems, such as freezing flowing liquids which, although interesting, are not of direct relevance to the current work and are therefore not included. In addition, problems involving materials which do not solidify at a discrete temperature are not reported in great detail because there are significant differences between these processes and those involved in freezing water.

2.1 REVIEW OF EXPERIMENTAL WORK

The relevant experimental research consists of studies into pipe freezing and also general investigations into freezing with convection. Firstly, the results from the entire research programme at Southampton are summarised in section 2.1.1.1. The investigations into the effect of convection on freezing water in vertical pipes is described in more detail in section 2.1.1.2. Research into pipe freezing performed outside Southampton is described in section 2.1.1.3. In section 2.1.2, relevant studies in the wider field of freezing and natural convection are summarised.

2.1.1 Research into Pipe Freezing

2.1.1.1 General Pipe Freezing Research at Southampton

Research has been carried out since 1981, investigating pipe freezing in depth. The work is described in detail by Wigley[3] and Bowen[4]. Detailed overall reviews are provided by Burton[1] and Tavner[5]; these results were used by Wigley[6] to propose a set of guidelines for pipe freezing practice.

The first phase of the research ran from 1981 to 1985 with the general objective of establishing the processes which control the plug formation. During the second phase (1986-1990) the research into freezing water and crude oil was continued and the development of non-invasive methods of gauging when the plug was closed was investigated. Phase three was started in late 1993 with the aim of investigating the stresses induced in the pipe wall during freezing; the results from the third phase are described by Keary[7]. This work is continued in phase four which started at the end of 1994.

Freezing was carried out in vertical pipes for a range of pipe sizes and water temperatures and showed that the freezing time was proportional to the square of the pipe diameter at low values of initial water temperature. As the temperature was increased, the freezing time increased and eventually reached a limiting temperature at which a solid plug could not be formed. The limiting temperature was lower for larger pipes. The results showing the time to freeze in different size pipes is shown in figure 2.1 and are discussed in more detail in section 2.1.1.2. Freezing static water in a horizontal pipe showed that natural convection caused the ice to form faster at the bottom of the pipe, with the plug finally closing at a point above the centre of the pipe.

Freezing flowing water was also explored for pipes of various size and material and generally required longer freezing times than static water because of the increased heat transfer into the freezing zone. The effect of initial temperature and flowrate was investigated for vertical and horizontal pipes. These conditions, combined with the pump head, were found to influence the success of the freeze. Investigations also showed that the ice formation could display cyclic melting and freezing behaviour and also that the position of the plug neck could change during freezing. Formation of multiple necks was observed in situations with high flowrates and relatively long freezing jackets. This is an area of interest because of the danger to the pipeline when the plug necks close and trap water in between; the confined expansion on freezing will cause high stresses which can cause the pipe to fail.

The effect of freezing on the pipe itself was investigated and it was concluded that the thermal stresses generated by the shock cooling lie within the elastic limit for steel but not for materials such as glass reinforced plastic which are more sensitive to thermal shock. However, it was noted that reducing the temperature to that of the cryogen will cause mild steels to undergo transition from a ductile to brittle state and therefore shock loading such pipes should be avoided. A numerical and analytical study of the stresses in the pipe wall is currently in progress.

Freezing hydrocarbons such as fuel oils, motor oil, paraffin and various crude oils was studied and it was found that, due to the increased convection, those with low viscosity are more difficult to freeze. Since hydrocarbons do not solidify at a discrete temperature but become more viscous as the temperature drops, solidification was judged by the ability of the plug to withstand pressure. In the experiments carried out on crude oil, this was found to be at core temperatures between -100°C and -120°C. During a freeze on live Kuwait crude oil in a large (250mm (10") diameter, 9m (30ft) length) horizontal steel pipe, the pipe had to be insulated to prevent heat transfer from the environment and forming a solid plug was only possible for initial temperatures below 13°C. Freezing times were over 36 hours, compared to around 2 hours for water in the same pipe.

The practice of freezing oil filled pipelines by introducing water into the pipe and freezing an ice plug is common. Investigations showed that the pressures that could be resisted by the plug were considerably lower than those held in a clean pipe because the layer of oil on the pipe wall reduced the adhesion between the ice and the wall. In horizontal pipes the oil collects at the top of the pipe and any drop in liquid nitrogen level could endanger the freeze because the oil must be below -120°C to hold pressure.

Both water and oil plugs in various pipes were tested to determine how much pressure could be safely held. Ice plugs in a 50mm (2") diameter pipe were found to withstand

pressures of up to 207 bar (3 ksi). The ability to hold pressure is thought to be due to the 'necking' of the pipe and the strength of the interfacial bond between the wall and the solid. These mechanisms are being studied in the current phase.

Considerable work has been carried out looking into non-invasive methods of monitoring the progress of a plug in order to improve the methods of gauging when it is safe to open the pipe. Monitoring wall temperatures was found to give no indication of plug close-off. Ultrasonic methods were tried and both heat flux and acoustic emission were monitored. Both pulse-echo and through-transmission ultrasound methods were used. Monitoring the initial plug growth was possible but as the internal plug diameter became smaller, the signals became more difficult to understand due to scattering caused by cracks in the ice. Both transmitters and receivers were intolerant to low temperatures and therefore could not be located inside the jacket. Another method which was found to give encouraging results was the acoustic emission technique; cracking sounds are heard as a freeze progresses with a burst of activity just before the plug closes off. This method is easier and cheaper to apply than ultrasound, especially as the sensor can be mounted away from the freezing section, but it provides less information about the progress of the freeze and merely monitoring for a peak in emission could lead to a false indication of freeze off. Heat flux measurement provides more information on the progress of the freeze. The steady state value of heat flux for a plug with a small but finite neck diameter is calculated and when the measured heat flux drops below that value, the plug can be said to be frozen. Because the calculation neglects axial heat transfer and transient effects, the critical value is under-predicted, effectively incorporating a safety factor into the method.

2.1.1.2 Freezing in Vertical Water Filled Pipes

Burton[1] studied the formation of ice plugs in vertical pipes, both experimentally and numerically. A 100mm diameter (4") stainless steel pipe with a 200mm long jacket was used to investigate the effect of initial temperature on plug formation. Experiments were carried out in two ways; with the pipe blanked off at the bottom and with the bottom of the pipe left open and placed on top of a tank. In the first arrangement the entire bulk of the water inside the pipe was cooled during freezing whereas in the second arrangement the bulk temperature inside the freezing zone was maintained at the initial value. Burton concluded that these two configurations represented extreme cases of mixing between the freezing zone and the water in the surrounding pipework.

Burton observed that at temperatures below 20°C, the heat transfer was limited to the freezing section and the presence of the tank made little difference. At higher temperatures, using the tank lengthened the freezing time greatly and also resulted in more asymmetric plug profiles with the neck offset towards the top of the plug.

Burton proposed that there are three stages in plug formation; during the first stage, the cooled water flows down over the growing ice and is replaced by an upwards core flow. When the plug reaches a critical size, the two flows interfere, causing the core flow to be turned at the neck and join the downwards moving boundary layer. The top section is now isolated and cools rapidly, freezing off first. During the third stage the plug grows axially. This is sketched in figure 2.2. This theory was supported by the heat flux data which was obtained from temperature measurements from different parts of the freezing section. Later work by Bowen and Burton[8] modified this theory slightly by suggesting that a mixing region formed when the core flow and boundary layer flows started to interfere. Burton also developed a numerical model of one-dimensional solidification; this is described in section 2.2.2.1.

Further investigations were carried out by Bowen and Burton during the second phase of the pipe freezing research, studying freezing water in vertical pipes ranging from 100mm to 250mm in diameter. The results showed that when the initial water temperature was low the freeze times were roughly proportional to the diameter of the pipe. Using this data, Bowen et al[9] performed a one-dimensional analysis to investigate the effect of pipe diameter on the maximum temperature which can be frozen by considering the case at which the heat fluxes balance and therefore solidification stops. Consideration of the heat balance equation shows that there is a critical value of the plug radius; if the plug grows to this size then it will completely solidify. This critical plug radius is proportional to the pipe radius. Using the relationship for the critical neck radius and assuming a constant heat transfer coefficient for the heat transfer from the water to the freezing front, the limiting temperature is found to be inversely proportional to the pipe radius. The proportionality constant can be defined using the experimental results for one pipe diameter, providing an estimate of the limiting temperature for any pipe size.

Bowen also considered the difference between the freezing time at low initial water temperatures and that at higher temperatures and, by assuming the difference to be due to convection, obtained an estimate of the heat transfer coefficient.

The design of the freezing jacket was also investigated and found to affect the freezing time. This was investigated using the 100mm diameter pipe and a narrow annulus jacket made from aluminium alloy and a larger annulus stainless steel jacket.

The aim of the work carried out by Tavner[5] was to observe the effects of convection on plug formation in vertical pipes by using flow visualisation techniques. A vertical 100mm diameter (4") stainless steel pipe with a 200mm long jacket was used. Tavner developed the experimental rig in several stages; the bulk of the useful results were obtained using the final rig. In order to allow the forming plug to be seen, the pipe was cut in half axially and a perspex window was bolted onto the front of the half-pipe. The thermal conductivity of perspex is three orders of magnitude lower than that of steel and so the window was considered to be adiabatic. The other difference between using a whole and half pipe is the shear at the window; in a whole pipe, the velocity gradient would be zero, whereas in the half pipe, the velocity is zero. However, this will only effect the behaviour near the wall and the overall formation of the plug should be unchanged and was still considered two dimensional. The pipe was placed on top of a 1m long, 300mm (12") diameter tank of water which could be maintained at a desired temperature by immersion heaters. The role of the tank was to simulate the thermal mass of water in a long length of pipe. Both flowing and static water was frozen.

This rig allowed the plug formation to be observed and photographed. Various flow visualisation techniques were attempted and the thymol blue method was found to be the most appropriate. This method is described in depth by Tavner[5]. Briefly, the thymol-blue solution is an indicator dye and is yellow in colour when added to the water. When a voltage is placed across it, the solution near the cathode becomes depleted in H_3O^+ ions and turns blue. The dye remains blue for several minutes. A cathode wire was positioned across the pipe (the pipe itself was the anode) and a voltage applied to generate the blue dye. This made the flow patterns visible (these were photographed). The resulting velocity profiles were W-shaped, showing the boundary layers flowing downwards over the ice and the core flow up the centre of the pipe. In some cases, an upwards flowing sub-layer was observed next to the ice where the temperature was below the density inversion temperature of 4°C. The speed of the flow was obtained by measuring the distance covered by the blue dye over a set time period.

A series of experiments were also carried out with an array of 20 thermocouples positioned inside the freezing zone, providing data for the temperature variation inside the ice and water as the freeze progressed.

Another series of experiments used a thermocouple, mounted on a traversing mechanism, to obtain temperature readings at a single point throughout the freeze. The thermocouple was positioned before the freeze began and the temperature logged as the freeze progressed until the thermocouple became embedded in the ice. This was repeated with the same initial conditions to obtain the temperature - time history at different positions in the

pipe.

The three stages of plug development, deduced by Burton[1] from temperature measurements, were observed by Tavner although they were not as distinct as Burton suggested. A 'mixing region' was identified below the plug, where the boundary layer and core flow interfere. The extent of this region was found to depend on the bulk temperature. Tavner noted that the bulk temperature of the water inside the freezing region away from the ice started to decay soon after the freeze started.

2.1.1.3 External Research on Pipe Freezing

Very little research has been carried out on pipe freezing apart from that described above. Both Burton[1] and Tavner[5] review the relevant literature in detail. In addition to the research at Southampton, pipe freezing has been studied by Lannoy[10], Lannoy and Flaix[11] and by Law[12].

Lannoy and Flaix attempted to reproduce specific situations where freezes had to be carried out. Tests were performed on horizontal and inclined steel pipes of diameters ranging from 360mm (14") to 230mm (8.5") containing static and flowing liquid. One motivation for the work was to observe the effect of the shock cooling on the pipe itself and also the effect on any weld sites. The stress and strain on the pipe were measured and temperature readings in and on the pipe wall were taken. Pressure testing of the plugs was also carried out.

The results showed that the thermal stresses induced in the pipe were lower than the elastic limit for both austenitic and ferritic steel and that it was possible to freeze a pipe more than once at the same location without harming the pipe. They recommended that attention should be paid to reducing the risk of thermal shock by precooling the pipe before freezing takes place.

Law[12] carried out experiments in pipe freezing and also modelled the process using analytical and numerical techniques. The modelling is described separately in sections 2.2.1 and 2.2.2 and Tavner[5] reviews the experimental results in depth. Law attempted to freeze water, diesel fuel and kerosene in horizontal 100mm (4") and 150mm (6") pipes, under static and flow conditions. Different jacket lengths and different methods of cooling the wall were used and the feasibility of freezing carbon dioxide gas was also investigated. There was a disagreement between Law's results and those obtained by Bowen[4] concerning the limiting temperature at which a plug would form in a 150mm (6") diameter pipe which can be attributed to the fact that Law made no effort to maintain the bulk temperature inside the pipe

during the freeze.

2.1.2 Other Relevant Studies

The work related to the unintentional freezing of pipes in cold climates concerns situations which are significantly different to the type of pipe freezing considered here. Freezing in cold climates generally involves liquid flowing through long lengths of pipeline at a low ambient temperature. The geometry of the problem is different and, because the actual temperature differences are small, there is little heat transfer by conduction or natural convection.

General studies into natural convection with freezing have been carried out for a variety of situations. Generally, these studies involved more simple geometries and conditions than those found in pipe freezing. Some examples are described below.

Sparrow et al[13] et al observed the effect of natural convection on the solidification of n-eicosane paraffin. The freezing was initiated by placing a cooled rod into a vertical cylinder containing paraffin. Their results showed that in the presence of natural convection the shape of the solidification front was altered, the time to freeze was increased and with sufficient initial superheat, solidification would stop at a critical thickness.

Sparrow and Souza Mendes[14] determined the local heat transfer coefficients at the ice/water interface. The heat transfer by conduction through the solid was equated with the convective heat transfer when the ice growth stopped, thus obtaining a steady state heat transfer coefficient. Bathelt and Viskanta[15] experimented with paraffin and obtained the heat transfer coefficient for paraffin.

Sparrow and Broadbent[16] considered the solidification of paraffin resulting from external cooling. A vertical tube containing paraffin was immersed in a chilled water bath and the initial superheat of the liquid and the subcooling of the bath were varied. Four component energies were evaluated from the results and the latent heat of fusion was found to be dominant although the sensible energies released from the subcooled frozen solid and superheated liquid were significant at larger amounts of superheat. The effect of natural convection was found to be small because the initial superheat decayed rapidly.

Boger and Westwater[17] observed the effect of buoyancy on the melting and freezing of water in a cavity. The sides of the cavity were insulated and the top and bottom could be heated or cooled. They concluded that natural convection is negligible at Rayleigh numbers lower than a critical value of 1700.

2.2 REVIEW OF ANALYTICAL AND NUMERICAL WORK

The purpose of the review of analytical and numerical work was to identify research into similar problems and to see which solution methods were used. The review was limited to problems which combined phase change with natural convection. General literature reviews are published regularly, for instance Patankar[18] provides an excellent overview of CFD problems, Ostrach[19] has reviewed natural convection problems and Viskanta[20] has reviewed heat transfer in solidifying metal.

The literature can be broadly divided into two groups; analytical solutions and numerical solutions. In order to use analytical methods, assumptions must be applied to the problem to simplify the governing equations, however they do provide a method of analysing the problem without requiring lengthy computer programs. Indeed before the development of computers, only analytical solutions could be used.

2.2.1 Analytical Studies

This section is further subdivided into three, considering phase change in the absence of convection and with forced and natural convection. Analytical studies of freezing in pipes published up to 1985 were reviewed by Law[12], who also applied and extended some of the models to pipe freezing situations. In addition, studies of natural convection driven by a heated or cooled vertical flat plate are described.

2.2.1.1 Phase Change without Convection

The work by London and Seban[21] concentrated on one dimensional (radial) plug growth with zero superheat in the liquid and neglected thermal heat capacity in the solid. A similar theory was used by Luikov[22] and Shamsundar[23] (although the formulation by Shamsundar incorporated a 'shape factor' to account for the two-dimensional plug form) resulting in the same expression for freezing time. These studies differed from the method of London and Seban mainly in the choice of boundary condition on the outside of the solid region. The London and Seban theory used a convective boundary condition whereas Luikov used an isothermal boundary. The resulting relationship for freezing time was proportional to the square of the pipe radius and inversely proportional to the difference between the freezing

temperature and the coolant temperature.

Lannoy[10] used a similar method to describe freezing and extended it to take account of forced convection (as described in the following section). One dimensional solidification was assumed and the rate of interface movement was formulated by a heat balance at the interface. The steady heat flux between the solid/liquid interface and the coolant (incorporating a heat transfer coefficient for the heat transfer between the pipe wall and coolant) was equated with flux required to extract the latent and sensible heat energies from the liquid in order to advance the interface position. The resulting expression for freeze time was the same as that obtained in the previously mentioned studies except that the sensible energy of the liquid was included.

The methods of London and Seban, Luikov, and Shamsundar were used by Law and were found to underestimate the freezing times compared to Law's experimental results. Law extended the model of London and Seban[21] to try to take the initial water superheat and also thermal heat capacity of the ice into account. The expression for the water superheat was the same as that used by Lannoy and the resulting freeze time was extended by the incorporation of the sensible heat in the ice region. Law noted that this improved the results but added that it was based on arbitrary assumptions of the temperature distribution in the ice and water. Law applied the predictions obtained with the Luikov model to cases with initial superheat by introducing a scale factor equal to the superheat energy and latent heat divided by the latent heat.

2.2.1.2 Phase Change with Forced Convection

Lannoy[10] extended the one-dimensional model to investigate the effect of forced convection. An extra flux term was included in the heat balance and formulated for the case of both laminar and turbulent forced convection. The circumstances under which freezing is possible were investigated for varying pressure heads.

Other studies attempted to predict the steady state plug form for the two-dimensional situation. Assumptions were made, notably concerning the velocity profile inside the pipe, the boundary condition on the outside of the solid and neglecting axial conduction and free convection. Mathematical analysis was carried out to obtain the solutions for the liquid zone. The steady state temperature distribution inside the solid region is specified in terms of the solid front radius and, by enforcing heat balance across the solid/liquid boundary, the position of the boundary can be calculated. This is described by Zerkle and Sunderland[24], who used

a constant external temperature whereas Sadeghipour et al[25] applied a convective boundary condition. The convective boundary condition complicated matters by resulting in a section of the pipe at the inlet where there was flow and cooling but no freezing. In order to solve the problem, some simplifying assumptions had to be made. These two methods predicted the steady state plug profile and were used to see whether, under certain conditions, the plug would reach the centre of the pipe. These two methods were employed by Law to investigate the effect of jacket length, initial temperature and flowrate on the success of the freeze. Law noted that the first method (Zerkle et al) was overly pessimistic about the limiting flowrate and temperatures (compared to experimental results) whereas the second method (Sadeghipour et al) gave more realistic results.

2.2.1.3 Phase Change with Natural Convection

Bowen et al[9] performed a simple one dimensional analysis and, by assuming that the heat transfer coefficient is constant, predicted that the highest temperature that can be frozen in a given pipe is inversely proportional to the pipe diameter. By choosing the proportionality constant to give the limiting temperature for one pipe size from experimental results, the limiting temperature for any pipe size was obtained.

Since 1985 several papers have been published describing analytical solutions for natural convection and phase change. Huang[26] studied the effect of natural convection on melting assuming that the temperature distribution could be obtained from the solution to the Neumann equation (ie. conduction controlled and one-dimensional (cartesian)). By applying simplifying assumptions to the velocity equation, the velocity distribution could be predicted and the interface movement calculated.

Bejan[27] looked at the problem of melting with natural convection in the melt. A solid initially at its fusion temperature was placed in contact with a vertical wall which was maintained above the fusion temperature. The solution was divided into two parts. Firstly, the quasi-steady melting case when the liquid region was sufficiently wide that it could be divided into a cooled boundary layer flowing downward over the solid, a warmed upwards flowing boundary layer by the wall and a core region in between. By using boundary layer theory, the velocity and temperature distributions in the boundary layers were specified and the velocity and temperature distributions in the core region defined. From these equations the thickness of the two boundary layers and the core temperature were calculated and the interface velocity predicted. The second part was obtained by considering the early stages when the width of

the liquid region was small and the temperature distribution inside the liquid was dominated by one-dimensional conduction. The temperature distribution and interface position could then be determined using the Neumann solution. By applying simplifications to the equation for vertical velocity, the velocity profile and thence the convective flux were calculated and the resulting interface movement predicted.

In the same year, Zhang and Bejan[28] published a paper describing melting with natural convection in a semi-infinite region but with conduction in the solid. The boundary layer velocity and temperature profiles were predicted using boundary layer theory and movement of the interface was calculated.

2.2.1.4 Convection over a Vertical Flat Plate

Scale analysis, carried out by Bejan[29], used the governing equations, simplified for the boundary layer and considered the magnitude of the inertia, friction and buoyancy components. Bejan then obtained relationships for the order of magnitude of the peak boundary layer velocity and the thicknesses of the thermal and velocity boundary layers for the two cases of Prandtl Number greater and less than one. This was based on the assumption of a homogenous constant property fluid. Bejan then went on to derive more exact expressions for these quantities using integral analysis, assuming velocity and temperature distributions inside the boundary layer. The integral analysis for a high Prandtl number fluid such as water is detailed in Appendix I.

2.2.2 Numerical Studies

Since the 1970s, as computer power and availability has increased, the interest in solving problems numerically has grown. A numerical solution allows complex problems to be solved and is especially attractive in problems where the geometry is complex, for instance in modelling heat flow in castings or where the boundary conditions are complicated.

This section is subdivided into four problem types. Firstly, the numerical work that has been carried out specifically into cryogenic pipe freezing is described. This is kept separate from the research labelled 'pipe blockage' because there are fundamental differences between the two problems. 'Pipe blockage' refers to the (normally undesired) freezing of long lengths of pipes, typically in cold regions. The next section gives an overview of the particular problems associated with alloy solidification and finally the fundamental research using simplified geometries is described. In each section the similarities and differences between the problems modelled and the current work are outlined.

The numerical methods used in each example are not described here in detail.

2.2.2.1 Pipe Freezing

Numerical modelling of pipe freezing has been carried out by Burton[1] and by Law[12]. Burton modelled one-dimensional, radial, solidification with conduction in the water and ice regions. Firstly, the equivalent heat capacity method was used but instability was experienced in trying to model the discrete phase change temperature. The boundary immobilisation method was used instead, thus solving the conduction equation in the water and ice regions separately and using the heat balance at the interface to calculate the movement of the interface. The pipe wall was incorporated into the model and the cryogen boiling on the wall was simulated using a heat flux-wall temperature correlation for the outer boundary condition. The model overestimated freezing times by a consistent amount which was attributed to the difficulties in formulating the boiling curve for liquid nitrogen. Apart from this, the results agreed well with experimental data at values of initial temperatures when the assumption of zero convection is valid.

Law[12] used a finite element package (PAFEC) to model the plug formation in two dimensions, neglecting convection. The solidification was solved using a fixed grid and varying the specific heat capacity to account for the phase change. The pipe wall was not included in the solution but a convective boundary condition was applied which was

formulated assuming that the temperature on the outside of the pipe wall was constant at -186°C. Law observed that the predicted freezing times were less than the experimental values and attributes this to neglecting convection. However, closer observation of the predicted and measured temperatures on the inside of pipe wall would suggest that the cooling rate was over-estimated by assuming that the temperature on the outside of the pipe immediately dropped to -186°C and that this is responsible for the difference in freeze times.

2.2.2.2 Pipe Blockage

Liquid-filled pipelines in environments where the ambient temperature falls below the freezing temperature of the liquid run the risk of becoming blocked by the pipe freezing shut. This can be prevented by maintaining a small flow in the pipe and therefore research is needed to establish the required flowrate.

Pipe blockage problems differ from cryogenic pipe freezing for several reasons. The ambient temperature inside the pipe will be near the freezing temperature so there will be negligible levels of natural convection although forced convection is often included in the investigations. In addition, the amount of subcooling will be low and the length of pipe cooled is much longer than that used for pipe freezing.

One problem that has attracted interest is the formation of a wavy ice profile inside the pipe due to the flow changing between laminar and turbulent. This has been investigated experimentally (for instance, by Hirata and Matsuzawa[30]), analytically (eg. Wiegand and Beer[31]) and numerically (eg. Albert[32]).

2.2.2.3 Alloy Solidification

Casting has been modelled by numerous researchers both with and without natural convection in the melt. Whilst pure substances and eutectic mixtures solidify at a discrete temperature, binary and multicomponent alloys solidify over a range of temperatures, thus there is a temperature (and spatial) range over which liquid and solid phases coexist in equilibrium. This is known as a mushy region. On a microscopic scale, this region contains complicated, usually dendritic, structures. Although complex on the microscopic scale, on the macroscopic scale methods have been developed to model the region. This can actually make the prediction easier because the change in properties and enthalpy occur across a temperature

and spacial range instead of occurring suddenly at the interface. The particular problems associated with mushy regions in alloy solidification are not relevant to pipe freezing.

2.2.2.4 General Applications

Interest in phase change as a method of storing energy has also fuelled research in this area, for instance Bellecci and Conti[33] who modelled the transient freezing in a solar storage module. Other areas of research encountered include crystal growth, freezing biological cells (either cryopreservation or for food storage) and freezing porous media such as soils.

There are also a large number of papers describing more fundamental research. These include papers describing modelling phase change with natural convection in simplified geometries. One typical geometry is a vertical enclosure with an adiabatic top and bottom and isothermal sides, for instance Ramachandran et al[34], Gadgil and Gobin[35], Ho and Viskanta[36], Benard et al[37], Beckermann and Viskanta[38], de Vahl Davis et al[39]. All the above examples used a transforming grid so that the position of the solid/liquid interface was fixed in relation to the grid. Yoo and Ro[40] modelled the melting of a solid initially at its fusion temperature in a rectangular cavity with adiabatic top and bottom and warmed sides. This differed from other research in that it included the effect of a solid-liquid density change on the velocity at the interface. In this situation with a PCM (n-octadecane) with a 5% decrease in density on melting, Yoo et al noted that the density change was important early in the melting process. However, Gadgil and Gobin[35] state results for paraffin which undergoes a 10% density decrease on melting and quote that the effect of this is negligible in comparison with the boundary layer velocities. The other geometry frequently modelled is a two-dimensional slice through a horizontal cylinder and either involves phase change around the outside of the cylinder, for instance Yao and Cherney[41] and Ho and Chen[42] or phase change inside the cylinder, for instance Rieger et al[43]. Sparrow et al[44] modelled melting from a warm cylinder embedded in a cylinder containing a PCM (phase change material) at its fusion temperature. Later, Sparrow and Ohkubo[45] considered the problem of ice formation inside a vertical pipe using the finite volume approach, a transforming grid and the SIMPLER algorithm. This problem differed significantly from the pipe freezing configuration in that the entire vertical wall was maintained at one temperature and the top and bottom of the domain were adiabatic.

These situations differed from that of pipe freezing because of the constant boundary condition and its effect on the resulting flow. Pipe freezing involves cooling only a section of the wall. Thus a layer of ice grows from the wall to meet in the centre of the pipe and the

flow pattern becomes disrupted as the boundary layer flows down the wall, curves over the ice and back to the wall.

Several attempts to solve the problem of flow entering a pipe which has a step change in the boundary conditions near the entrance, changing from adiabatic to cooled and therefore results in a high gradient of the solid/liquid profile. Hibbert et al[46] used the commercial CFD package, PHOENICS, with the enthalpy method to predict the transient plug formation with flow but no buoyancy effects. The cooled wall condition extends from close to the entrance to the pipe to the end of the domain. Bennon and Incropera[47] also used the enthalpy method to predict the steady state plug formation between parallel vertical plates and included the effect of natural convection. Their predictions showed that the local cooling at the solid/liquid interface accelerated the flow next to the interface such that flow reversal in the fluid core could take place near the exit. Albert[32] modelled the flow and phase change in a similar configuration using finite volume method and a transforming grid. Natural convection was neglected but the turbulent flow was included in the model in order to investigate the wavy ice formation.

2.2.3 **Discussion**

The problem of interest in this work is the deliberate freezing of the contents in a section of pipeline in order to form a temporary seal. The cooling is therefore applied to a section of the pipe wall and there are changes in boundary condition at the top and bottom of the jacket. The problem also includes the interaction between the natural convection and the growing plug.

The literature above is split into analytical and numerical work. In order to solve the problem analytically, simplifications must be applied to the definition of the problem. Analytical solutions are a good method of gaining a preliminary step in studying the mechanisms involved in plug growth and were used by Law[12] to do this. The work of Bejan[27] and Zhang and Bejan[28], if it were extended to cylindrical co-ordinates, could be useful in investigating the effect of natural convection on plug formation, however, this would still require assumptions to be made concerning, for instance, the core temperature and the formation of separate regions above and below the plug neck could not be included. The scope of the problem investigated in this work was considered to be too complex for analytical solutions to be practical.

Very little analytical or numerical work has been carried out specifically into pipe

freezing. A large number of methods have been developed and a wide range of problems have been solved numerically but only a small number of these applications are of direct relevance to this work. The only relevant work was by Burton[1] and by Law[12], both of whom neglected natural convection.

Most of the papers found in the literature review describe simplified geometries, typically rectangular enclosures with adiabatic top and bottom, or horizontal cylinders with phase change occurring inside or around the outside of the cylinder. The presence of two changes in the boundary conditions (ie. the top and bottom of the jacket) was found to be unusual. These conditions are important as they result in a steep solid-liquid interface in the regions at the top and bottom of the freezing region and also cause a large degree of distortion to the liquid region. The development of a numerical model of pipe freezing and natural convection has not been attempted. Similar problems have been modelled but there are significant disparities between them and pipe freezing which make it impossible to apply the results to pipe freezing.

2.3 SUMMARY OF PREVIOUS WORK

The important results from the previous sections are summarised into the following sections for reference. The definition of the characteristic dimensionless numbers are included in Appendix IV together with example values.

2.3.1 Effect of Pipe Size and Initial Temperature on Freezing

The freezing times for static water in vertical pipes for varying initial temperatures and four pipe sizes (100mm, 150mm, 200mm and 250mm diameter) are shown in figure 2.1. At low temperatures, the freezing times are roughly proportional to the square of the diameter, ie. proportional to the cross-sectional area. As the initial temperature is increased, the freezing time increases almost linearly and then starts to increase more rapidly until a limiting temperature is reached at which the plug will not form. The limiting temperature is lower for larger diameter pipes.

This behaviour is explained in the following discussion. If convection is negligible, the freezing time is determined by the rate at which the latent heat and sensible heat can be removed from the pipe. Freezing consists of removing the latent heat and the sensible heat from the ice and also removing the sensible heat of the water. The sensible heat of the water is proportional to the initial water temperature and both components are proportional to the ratio of the volume to length of freezing zone (ie. the cross-sectional area). The relationship between pipe size and freezing time when the water is initially at the freezing temperature is predicted by the analytical models of London and Seban, Luikov, Shamsumdar and Lannoy. The model of Lannoy and the extensions of the London and Seban and the Luikov models by Law predict the linear increase with initial temperature.

When convection is important, there will be an extra component to the freezing time because convection increases the rate at which heat is supplied to the ice interface and therefore slows the ice growth. When the temperature is sufficiently high, the heat flux to the interface can balance the rate at which heat is removed by conduction through the ice to the cryogen and at this point the ice growth stops. The rate at which heat can be conducted away from the interface decreases as the ice layer grows and therefore the value of initial temperature which is sufficient to stop ice growth is lower for larger diameter pipes. The analysis by Bowen et al implies that, if the coefficient for the heat transfer between the water and ice can be assumed to be constant, the limiting temperature is inversely proportional to

the pipe diameter.

2.3.2 Development of the Buoyancy Driven Flows

Burton[1], and Burton and Bowen[8] deduced that there are three stages in plug formation, illustrated in figure 2.2. In the first stage, the cooled water flows down over the growing ice and an equal flowrate moves up the centre of the pipe. The second stage begins when the plug has reached a critical size (Burton states that this happens when the neck diameter is about 30mm in a 100mm (4") diameter pipe) and the two flows begin to interfere, causing a mixing region at the plug neck where the boundary layer and the core flow interfere. If the bulk temperature below the neck is maintained, the freezing in this region is retarded. The water above the neck is isolated and the ice growth is more rapid, causing the neck to migrate up the plug. In the third stage, the plug grows axially.

The three stage theory was broadly supported by Tavner, with the qualification that the stages were not as distinct as Burton proposed and that the critical neck diameter increased with initial water temperature. Tavner noted that a mixing region forms below the plug, where the boundary layer and core flow interfere. The distance that this region extended upwards into the freezing zone and downwards into the pipe was found to depend on the initial temperature. The effect on the bulk temperature inside the freezing zone is discussed in section 2.3.3.

2.3.3 Variation of Bulk Temperature inside the Freezing Zone

Tavner noted that the bulk temperature of the water inside the freezing region away from the ice started to decay soon after the freeze started. This was attributed to the mixing region causing stratification inside the freezing zone. At initial temperatures above about 30°C the bulk temperature did not decay and it was therefore concluded that the mixing region had extended down the pipe into the tank.

The role of the tank in maintaining the bulk temperature was also implied by comparing Tavner's temperature measurements with those obtained by Burton. In Burton's experiments the tank was located nearer the freezing section than in Tavner's rig (200mm (two pipe diameters) compared to 400mm (four pipe diameters), respectively) and there was very little decay in bulk temperature even at 20°C.

2.3.4 Effect of Convection on Plug Profiles

If the cooling rate is uniform in the jacket and there is negligible convection, the ice front will be vertical except near the top and bottom of the jacket. In practice, the process of filling the jacket means that the plug first starts to grow at the bottom of the jacket. This is augmented by the effect of convection which also causes the ice to form more rapidly near the bottom of the jacket.

When the plug reaches a critical size, the interaction between the flow field and the forming plug results in the water above the plug neck becoming isolated from the surrounding water. The bulk temperature above the neck drops rapidly and the freezing rate increases. The position of the plug neck migrates upwards, leading to the plug closing off above the mid-point of the jacket.

Burton compared the plug profiles obtained with and without a tank. When the tank was not used, the position of the plug neck was near the bottom of the jacket at the beginning of the freeze and moved up the plug during the freeze so that the plug froze off at around half-way up the jacket. The plug extended above and below the freezing zone. The bulk temperature decayed throughout the freeze and therefore the initial water temperature had very little effect on the shape of the ice plug.

When the tank was included in the rig, the bulk temperature inside the freezing zone did not decay. The volume of ice formed was lower, with the plug being restricted to the freezing zone. The neck position moved further up the plug so that the plug froze off above the centre of the jacket; it was noted that this asymmetry increased with increasing initial temperatures.

This effect was also noted in Tavner's results. It was modified by the extra cooling at the bottom of the jacket ('cooled fin'); this resulted in asymmetric plug profiles at low initial temperatures with the neck position below the centre of the plug.

3. DEVELOPMENT OF ANALYTICAL MODEL OF PIPE FREEZING

Several attempts have been made to investigate freezing using analytical models of varying complexity. These were reviewed in chapter 2. The early models[21,22,23] addressed the Stefan problem in which the liquid is initially at its fusion temperature. More recently, attempts have been made to predict freezing when the initial temperature is greater than the fusion temperature by making assumptions concerning the change in sensible heat which occurs during the interface movement. Other models have included the heat flow from the liquid to the freezing front; Bowen et al[9] used a heat transfer coefficient derived from experimental data for natural convection, and Lannoy[10] included a forced convection coefficient to predict freezing with forced flow.

The work by Bejan[29] offers an attractive way of extending the analysis further. Bejan predicted the flow and heat transfer due to laminar natural convection driven by a cooled or heated vertical plate by making assumptions about the velocity and temperature profiles in the boundary layer and thereby solving the governing equations (this analysis is reproduced in Appendix I). This resulted in equations for the heat transfer coefficient, boundary layer velocity and velocity and thermal boundary layer thicknesses in terms of the fluid properties, bulk temperature and cooled wall length. The predicted heat transfer coefficients were around 50% larger than those obtained experimentally by Tavner for the same water temperature. This was attributed to the fact that the analytical solution was derived for a fluid with constant properties; cooling water below 4°C results in an up-flowing boundary layer next to the cooled wall and a down-flowing layer away from the wall. In addition, the plug growth will distort the flow field which will affect the heat transfer at the plug neck and the assumption of laminar flow becomes less accurate at higher temperatures and in larger pipes.

The development of an analytical model of pipe freezing is described in the following sections. In section 3.1, freezing with no decay in the water temperature in the freezing zone is considered. In section 3.2, the variation of the water temperature is predicted by making assumptions about the development of the flow field. Finally, in section 3.3, the two models are linked and the effect of bulk temperature decay on the freezing time is investigated.

3.1 DEVELOPMENT OF THE FREEZING MODEL WITH NO BULK TEMPERATURE DECAY

A one dimensional (radial) model is described, based on a heat balance at the solid/liquid interface at the plug neck. Estimates of freezing times for different sizes of pipe and initial temperature are presented and approximate relationships between the governing parameters are defined for the limiting case (when the plug will only just freeze across the pipe).

3.1.1 Derivation

The heat conducted away from the freezing front through the solid, assuming steady conduction and ignoring the thermal resistance of the pipe wall, is given by equation 3.1.

$$Q_{cond} = \frac{2\pi R_w (T_i - T_c)}{\frac{1}{h_c} + \frac{R_w}{k_s} \ln \frac{R_w}{R_i}} \qquad T_i = 0 \tag{3.1}$$

where the conductivity in the ice, k_s, depends on the coolant temperature.

The heat flux from the liquid to the interface is given in equation 3.2.

$$Q_{conv} = 2\pi R_i h (T_b - T_i) \qquad T_i = 0 \tag{3.2}$$

The difference between the heat conducted away from the interface and that arriving at the interface is equal to the change in enthalpy caused by the interface movement. In order to account for the change in sensible heat, the assumption made by both Law and by Lannoy was employed, ie. that the layer of liquid which solidifies was at the bulk temperature. Thus the rate of interface movement is given by equation 3.3.

$$\frac{dR_i}{dt} = \frac{hT_b - \frac{R_w(-T_c)}{R_i(\frac{1}{h_c} + \frac{R_w}{k_s} \ln \frac{R_w}{R_i})}}{\rho L + \rho c T_b} \tag{3.3}$$

The heat balance was applied at the plug neck because this is the point of interest when assessing plug closure and also because axial conduction is minimised at this position. Bejan's prediction of heat transfer coefficient for flow over a flat vertical plate, (equation I.16

in Appendix I), is formulated in terms of a distance, z, which, for this case, is the length of cooled wall above the plug neck (the extra length due to the curvature of the ice plug was neglected). The heat transfer coefficient decreases with increasing cooled wall length and therefore it is expected that the plug neck will be near the bottom of the jacket. It is assumed that the vertical position of the plug neck is proportional to the jacket length for all pipe sizes and initial temperatures and that it remains at the same vertical position throughout the freeze. The rate of interface advance becomes equation 3.4.

$$\frac{dR_i}{dt} = \frac{1}{\rho L + \rho c T_b}\left[\frac{A_h^{0.25} k_l \, Ra_H^{0.25} T_b h}{H} - \frac{R_w \, T_c}{R_i\left(\frac{1}{h_c} + \frac{R_w}{k_s}\ln\frac{R_w}{R_i}\right)}\right] \tag{3.4}$$

where A_h is the ratio of the length of the cooled wall above the plug neck to the total length of cooled wall and H is the total length of the cooled wall (ie. the jacket length).

This equation can be further manipulated to investigate the effects of the governing parameters on freezing and this is described in the following sections.

3.1.2 Results

Two investigations were carried out. Firstly, freezing times were calculated for four pipe diameters and various initial water temperatures and, secondly, the effect of the pipe size, jacket length and coolant temperature on the highest value of temperature which can be frozen successfully was investigated.

3.1.2.1 Predicted Freezing Times

If the heat transfer between the liquid and solid/liquid interface can be neglected, equation 3.4 can be solved to give the following equation for the time to freeze the pipe. (This equation is presented by Law and by Lannoy.)

$$TTF = \frac{\rho L + \rho c T_b}{2\,|T_c|} R_w \left(\frac{1}{h_c} + \frac{R_w}{2k_s}\right) \tag{3.5}$$

Further manipulation of the values of heat transfer coefficient (see Appendix I) gives

the following relationship for heat transfer coefficient (equation 3.6).

$$h(z) \approx 25.880\ T_b^{0.680}\ z^{-0.25}$$
$$\therefore\ h(A_hH) \approx 25.880\ T_b^{0.680}\ (A_hH)^{-0.25} \qquad (3.6)$$

The existence of a non-zero heat transfer coefficient complicates the solution, however, results can be obtained by employing a simple numerical approximation. The interface position at time t+δt, making use of equation 3.6, is given by the following equation.

$$R_i^{t+\delta t} \approx R_i^t + \frac{\delta t}{\rho L + \rho c T_b}\left[\frac{25.880\ T_b^{1.680}}{(A_hH)^{0.25}} - \frac{R_w\ T_c}{R_i\left(\frac{1}{h_c} + \frac{R_w}{k_s}\ln\frac{R_w}{R_i}\right)}\right] \qquad (3.7)$$

The freezing time can be obtained by repeatedly updating the interface position (set equal to the pipe radius at time zero) until the interface reaches the centre of the pipe. (If the heat transfer between the solid and the coolant is assumed to be perfect, then an initial ice layer will be necessary to obtain a finite value for the gradient dR/dt.) By repeating the process with decreasing values of the time step δt, the estimated freezing time will converge to the accurate solution.

A program was written to solve equation 3.7 for varying values of initial temperature and pipe size. Freezing times for water at initial temperatures between 0°C and 30°C in pipes of diameter 100mm (4"), 150mm (6"), 200mm (8") and 250mm (10") were obtained using the following parameters :

T_c	-196°C	(liquid nitrogen)
h_c	2000 W/m²K	(nucleate boiling)
k_s	3.67 W/mK	(average in range 0°C to -196°C)
A_h	1	(neck at bottom of jacket)
	½	(neck at centre of jacket)

The value for the coefficient of heat transfer to the liquid nitrogen assumes nucleate boiling conditions; it will therefore overestimate the heat transfer at the beginning of the freeze when the liquid nitrogen is separated from the wall by a layer of nitrogen vapour.

The resulting freeze times are shown in figure 3.1. There are four sets of curves for the four pipe sizes and each set comprises of two curves obtained with the ratio A_h set to 1 and ½. Each curve shows the roughly linear increase in freezing time as the initial temperature increases from zero. Over this range the ratio A_h has very little effect because the heat transfer coefficient is low and the effect of the initial temperature is due to the sensible heat term

rather than the convected heat flux term. At higher temperatures, the freezing times start to increase more rapidly and the results obtained using the different definitions of A_h diverge. The curves rise rapidly until a limiting temperature is reached above which a complete plug cannot be frozen. As expected, the limiting temperature is lower when the neck is assumed to be at the centre of the jacket (A_h=½) than when it is at the bottom of the jacket (A_h=1). The freezing times for water initially at 0°C increase roughly proportionally to the square of the pipe size; the limiting temperatures decrease with pipe diameter.

The corresponding experimental results for the same temperature and pipe diameter ranges are shown in figure 2.1. Comparison between the two sets of data shows that the general behaviour is predicted well but the actual values are less accurate. The differences can be split into two areas, as follows.

Firstly, the predicted freezing times for water initially at 0°C are much lower than the experimental results, typically by a factor of about 60%. There are several reasons for this difference, described in the following four points.

- The definition of the heat removed from the interface through the ice used the steady state temperature profile. The temperature gradient on the ice side of the interface is therefore inversely proportional to the natural logarithm of the ratio of pipe radius to interface radius. Experimental results obtained by Tavner showed a more linear temperature profile (ie. that the movement of the interface acts to 'straighten out' the steady state temperature profile). This gives a lower heat flux than the steady case and therefore using the steady state temperature profile results in shorter overall freeze times.
- The conductivity of the ice varies with temperature. The average conductivity was therefore defined as the average between 0°C and T_c; it should have been the average in the range 0°C to the temperature at the pipe wall. The temperature at the pipe wall, and therefore the average conductivity, will vary throughout the freeze and incorporating this variation would complicate the solution. Because the conductivity used in the predictions was the maximum possible value, defining the conductivity more accurately will increase the predicted freeze times; for example, if the value for a wall temperature of -100°C were used (2.6 W/mK instead of 3.7 W/mK), the freeze times would increase by around 38%.
- One parameter in equation 3.7 which is not known accurately is the coefficient which is used to quantify the heat transfer between the ice and the coolant; in the case of heat transfer to liquid nitrogen, as the wall temperature drops, the boiling changes from film boiling (with lower heat transfer) to nucleate boiling. The previous analysis used a value from the nucleate boiling region which will give faster freezing times.
- The jacket was filled during the initial few minutes of the experiment which would cause

the position of the plug neck to move up the plug; the assumption of zero axial conduction in the ice is therefore not correct over this period. The heat conducted away from interface through the ice (and therefore the freezing rate) was over-predicted during this period.

The second observation which can be made from figure 3.1 concerns the prediction of the highest value of initial temperature which can be frozen to block the pipe for each pipe size; the predicted values are higher than the experimental results. The limiting temperature is not affected by the assumptions about the steady state temperature profiles and the bulk temperature in the pipe was deliberately maintained at the initial temperature during the experiments and therefore the condition in the prediction was realistic for comparison with these experimental results. The factors which affect the limiting temperature are described in the following three points.

- Comparison between the experimentally derived heat transfer coefficients (from Tavner[5]) and the predicted values indicate that the predicted heat transfer coefficient is higher than expected at temperatures below 25°C; at higher temperatures the heat transfer coefficient will increase as turbulence becomes increasingly significant and therefore the predicted values may be too low, unrealistically increasing the range of temperatures where freezing is possible.
- The value of heat transfer coefficient used to define heat flux between the ice and the nitrogen will affect the limiting temperature. The value used here which was a maximum using the published data from Flynn et al[48]; decreasing this will decrease the limiting temperature.
- The remaining assumption which could be responsible for the predicted limiting temperatures being lower than the experimental data is the assumption that axial conduction can be neglected. Axial conduction will become more important at higher temperatures; the experimental data obtained by Burton[1], Burton and Bowen[8] and by Tavner[5] showed that interaction between the flow and the plug resulted in significant differences in the conditions above and below the plug neck causing the plug neck to move up the plug. This indicates that at these temperatures axial conduction is significant.

3.1.2.2 Parametric Study of Limiting Temperature

From the preceding analysis, an indication of the highest value of initial water temperature that can be frozen was obtained for each pipe size considered. This method of predicting the maximum temperature uses the heat transfer coefficient derived for laminar natural convection driven by a cooled/heated flat plate. Near the limiting temperature the flow

may become turbulent and there will be an increased risk of neck migration (and therefore a breakdown in the flow development and increased axial conduction in the ice). This must be taken into consideration during the following investigation into the effect of varying the pipe size, jacket length and coolant temperature on the limiting temperature.

The plug will form a solid cylinder (ie. the pipe will be sealed) if the rate of interface movement (dR/dt) is less than zero for all values of interface radius between the pipe inner radius (R_w) and zero. Therefore, considering equation 3.4, the first term on the right hand side of the equation must always be less than the second term. This first term is independent of the plug radius and for a given water temperature and pipe size remains constant throughout the freeze. The second term varies with the interface radius; as the radius decreases, the denominator of this term increases then decreases to equal zero when the radius is zero. There is a maximum thermal resistance between the interface and coolant at an intermediate point in the freeze and therefore a related minimum heat flux. The interface radius for this critical point is given by equation 3.8.

$$R_i^{crit} = R_w \, e^{-1+\frac{k_s}{h_c R_w}} \tag{3.8}$$

Therefore the condition for the plug to freeze-seal the pipe can be simplified to equation 3.9.

$$hT_b < \frac{k_s \, |T_c|}{R_w e^{-1} e^{\frac{k_s}{h_c R_w}}} \tag{3.9}$$

The limiting temperature is the value for which the two terms are equal. If the heat transfer coefficient were constant, the maximum temperature which could be frozen would be inversely proportional to the pipe radius. The limiting temperature is therefore given in equation 3.10 (substituting equation 3.6 for the heat transfer coefficient).

$$T_b^{\lim} = \left[\frac{k_s \, |T_c| \, (A_h H)^{0.25}}{25.880 R_w e^{-1} e^{\frac{k_s}{h_c R_w}}} \right]^{\frac{1}{1.680}} \tag{3.10}$$

The effect of varying the pipe diameter, jacket length and cryogen temperature on the limiting temperature was studied. The results are described in the following sections.

Effect of Varying Pipe Size

With a constant coolant temperature (-196°C) and ratio of jacket length to pipe diameter (2), the highest values of water temperature which can be frozen are plotted in figure 3.2 for the two neck positions (A_h=1,½) and two values of the heat transfer coefficient for the heat transfer to the liquid nitrogen h_c (600, 2000 W/m²K). The experimental data are also included in figure 3.2 and it is noted that the experimental results drop off more rapidly with increasing pipe size than the predicted values.

The lines corresponding to the Grashof number at the bottom of the jacket (2D) and at the centre of the jacket equal to $1.3x10^9$ are also included; this is the criterion for transition to turbulent flow listed by Bejan[29] for flow over an isothermal vertical flat plate[3.1] (data from Mahajan and Gebhart[49]).

The experimental values lie on a line which is defined *both* by equation 3.9 with a constant heat transfer coefficient (h=630 W/m²K) *and* by the line for constant Grashof number ($Gr_{2D}=2.1x10^9$: above transition to turbulent flow). This line crosses the line defined by limiting temperature under laminar conditions at approx. 60°C in 100mm (4") diameter pipe using h_c=2000 W/m²K and (A_h=1) and at approx. 48°C in 130mm (5.2") diameter pipe for h_c=2000 W/m²K and (A_h=½). The link between the experimental results and Grashof number indicates that the critical temperature is possibly controlled by turbulent heat transfer in pipes greater than a critical value. This critical point depends on the heat transfer to the liquid nitrogen; if the film boiling layer collapses, increasing the heat transfer, the critical diameter is in the range 100mm-130mm (4-5.2") (the lower heat transfer under film boiling conditions decreases the limiting temperature and therefore means that the limiting temperature is controlled by laminar heat transfer up to a critical diameter of approximately 150mm (6")). Turbulent mixing increases the heat transfer to the freezing front and decreases the maximum water temperature which can be frozen successfully. If the transition criterion ($Gr=1.3x10^9$) is applicable, this implies that freezing will stop when the boundary layer flow has become turbulent over ($(1.3/2.1)^{1/3}\Rightarrow$) 85% of the jacket length. There is therefore an intermediate region between $Gr_{2D}=1.3x10^9$ and $Gr_{2D}=2.1x10^9$ in which the flow is turbulent at the very bottom of the jacket which will increase the freezing time. This implies that in pipes less than the critical diameter, the maximum temperature is controlled by laminar natural convection and above the critical diameter, it is controlled by turbulent convection heat transfer. Extrapolating from the experimental results to predict the maximum water temperature by assuming a constant heat transfer coefficient (as suggested by Bowen et al[9]) will therefore

---

[3.1]Note that the criterion for transition between laminar and turbulent flow may vary by up to an order of magnitude from one study to another.

over-predict the maximum temperature in pipes less than 100mm (4") in diameter. Some corroboration of this theory is provided by the experimental results for freezing time (figure 2.1); this shows that there is a much steeper increase in freezing time with increasing temperature in the 150mm (6"), 200mm (8") and 250mm (10") diameter pipes than in the 100mm (4") diameter pipe.

It has been noted that the analytical solution predicted larger values of heat transfer coefficient than those recorded from experimental data by Tavner. In addition, it was noted at the beginning of this section that the use of the flat plate heat transfer coefficient becomes increasingly inaccurate at high temperatures due to the breakdown in flow field; the assumption of no axial conduction also becomes increasingly inaccurate at these temperatures. These points must be taken into account in trying to establish the break-point between the two controlling mechanisms (laminar and turbulent). Without improved data for the heat transfer coefficient, an accurate prediction of maximum temperature under laminar conditions (in the range 0-150mm (6") diameter) is not possible.

Effect of Varying Jacket Length

With constant coolant temperature (-196°C), ratio of jacket length to pipe diameter (2), neck position (A_h=1) and heat transfer coefficient between the ice and liquid nitrogen (h_c=2000 W/m²K), the relationship between the ratio of jacket length to pipe diameter and limiting temperature of four pipe sizes (assuming laminar conditions) is plotted in figure 3.3. This shows an approximately linear increase in the limiting temperature with increasing jacket length. The effect is slightly greater in a 100mm (4") diameter pipe (≈15°C increase obtained by increasing the jacket length from one pipe diameter to five) than in a 250mm (10") diameter pipe (≈10°C over the same range). Using longer jackets decreases the temperature at which the flow becomes turbulent, especially in the larger pipes and this will affect the limiting temperature. The lines defined by ($Gr=2.1x10^9$) at the bottom of the jacket are included (dashed) in figure 3.3. These show that increasing the jacket length may decrease the limiting temperature by making the flow turbulent inside the freezing zone. The existence of a laminar region and a turbulent region may cause the formation of multiple necks in the ice plug, with associated risks on freeze-off.

Effect of Varying the Coolant Temperature

The relationship between the limiting temperature and the coolant temperature is plotted in figure 3.4, for four pipe sizes, with the other parameters held constant (jacket length equal to two pipe diameters, h_c=2000 W/m²K and A_h=1). This shows a roughly linear decrease

in limiting temperature with increasing (decreasing magnitude) coolant temperature. The effect is greater in the 100mm (4") diameter pipe than in the larger pipes. These results have practical implications for the use of carbon dioxide as a cryogen and also higher temperature ('controlled temperature') freezing methods.

3.1.3 Scaling Criterion for the Effect of Natural Convection on Freezing

One aim of this investigation is to develop the understanding of the processes involved in pipe freezing so that it is possible to deduce the behaviour under conditions which have not been studied in detail. For instance, a large number of experiments have been conducted looking at the effect of convection on freezing using a 100mm (4") diameter pipe (Burton[1] and Tavner[5]); a way of scaling these results to understand what is happening during freezes in larger pipes has not yet been developed.

The effect of convection on freezing can be defined using the ratio of the convected flux (at the interface) to the conducted flux (removed through the ice layer). If the thermal resistance between the ice and coolant is neglected (h_c=BIG) and the critical interface radius is used (equation 3.8), this ratio is given by equation 3.11.

$$\frac{Q_{conv}}{Q_{cond}} = \frac{R_w e^{-1} h T_b}{k_s |T_c|} \tag{3.11}$$

For a fixed coolant temperature, the product '$h\ T_b\ R_w$' provides a measure of the effect of convection on freezing (heat flow per unit length). This is defined as the 'effective heat flux' (e.h.f). Using the approximation for the heat transfer coefficient (equation 3.6), the relationship between temperature and pipe radius (assuming that the jacket length is a constant multiple of pipe diameters) is given in equation 3.12.

$$T_b R_w^{0.446} = constant \quad \Rightarrow constant\ effective\ heat\ flux \tag{3.12}$$

Applying this relationship it can be deduced that the effect of convection on freezing in a 100mm (4") diameter pipe with a water temperature of 20°C is equal to that at approximately 15°C in a 200mm (8") diameter pipe.

This approach was used to produce figure 3.5, showing the effect of convection on pipe freezing. Seven lines of equal effective heat flux (e.h.f.) are plotted (these are the thin lines, including dashed line); these lines are defined by the seven values of e.h.f.

corresponding to temperatures of 10°C, 20°C, 30°C, 40°C, 50°C, 60°C and 70°C in a 100mm (4") diameter pipe. The thick lines denote Grashof number equal to $1.3x10^9$ at the bottom and at the mid-point of the jacket, together with the line ($Gr_{2D}=2.1x10^9$) which fits the experimental data for the maximum water temperature which can be frozen. The lines of equal e.h.f. can be used to deduce the processes involved during freezing; for instance, both Burton[1] and Tavner[5] noted that convection has very little effect on freezing below 20°C in a 100mm diameter pipe; this can be scaled to other pipe sizes using the relationship ($20x(0.05/R_w)^{0.446}$) (eg. 15°C in a 200mm (8") diameter) pipe). This scaling criterion assumes laminar natural convection and therefore becomes inaccurate if the combination of temperature and pipe size lie above the line ($Gr_{2D}=1.3x10^9$).

Burton noted that the plug neck moved up the plug during freezing when the initial temperature was 30°C and the bulk temperature was maintained; no neck migration was noted at 20°C. The plug neck will migrate up the pipe above the centre of the plug when the heat flow to the interface is sufficiently large to slow freezing and when the difference in the heat flow to the ice above and below the neck becomes significant. *This can be characterised by a constant value of e.h.f.*. When this occurs the one-dimensional, flat plate based model starts to break down. This 'breakdown' line is highlighted in figure 3.5 by the dashed line as a suggestion of the limit of application of this scaling method. The effect on the freezing time is partially controlled by the point during the freeze at which neck migration commences; this depends on the shear between the boundary layer and core flow which, in turn, increases with increasing temperature.

3.1.4 Conclusions

To the author's knowledge, this has been the first attempt to solve the problem of pipe freezing with natural convection using relationships derived from purely analytical studies. As such the results have been very interesting, however, comparison with experimental results has highlighted problems with the assumptions made during the analysis.

The predictions show the same general behaviour as that recorded in the experiments although the definition of the heat transfer between the ice and the cryogen resulted in the freeze times for water initially at 0°C being under-predicted.

The study of the maximum temperature which can be frozen in varying pipe sizes yielded two useful results. Firstly, it appears that in pipes less than 100-150mm (4-6") in diameter, the maximum temperature which can be frozen is controlled by laminar natural

convection; in larger pipes, the flow conditions become turbulent and the maximum temperature which can be frozen decreases. Thus the freeze-no freeze boundary on a 'map' of temperature against pipe size consists of two sections, the first defined by constant $h.T_b.R_w$ and the second defined by constant Grashof number ($Gr_{2D}=2.1x10^9$). The second result which emerged from this study was the definition of a criterion to scale the effect of convection on freezing between pipe sizes under laminar conditions. This analysis showed that constant $T_b.R_w^{0.446}$ implies constant effect of convection on freezing; this relationship becomes increasingly inaccurate as the effect of convection increases and destroys the grounds for assuming flat plate conditions (20-30°C in a 100mm (4") diameter pipe) and also as the conditions near transition to turbulence.

In order to develop a more accurate model for predicting the freezing times for relatively high temperature freezes it is necessary to include axial conduction. In order to do this, a numerical, rather than analytical, approach is recommended. This would allow transient conduction in the ice region to be included. The heat transfer to the coolant (and the time delay caused by filling the jacket) must be defined more rigorously and the variation of the conductivity of ice included. It will also be necessary to obtain a relationship for the heat transfer coefficient in the water which includes the effect of the density inversion on the boundary layer. In order to predict the freezing times in larger pipes and at higher temperatures, the effect of turbulence on the heat transfer coefficient must be quantified.

3.2 DEVELOPMENT OF THE FLOW MODEL

In the previous section, an analytical model of the freezing process was presented, using a prediction of the heat transfer coefficient for the heat transfer between the ice and water. The model showed good agreement with the experimental data; however, in the experiments a tank was placed below the freezing zone which prevented bulk temperature decay. The model was limited by the assumption that the temperature of the water inside the freezing zone was maintained at the initial water temperature. Tavner[5] observed that the average temperature of the water inside the freezing zone away from the ice front decayed during freezing. This was attributed to convection causing and maintaining inverted stratification in the water. The mechanism controlling this is proposed as follows; the water next to the cold wall cools, becomes denser and starts to fall, thereby establishing a convection cell. The cooled layer moves down the wall and entrains water from the core which increases the layer thickness as it moves down the pipe. Below the jacket, where the flow is no longer cooled by the cold wall, heat transfer with the warmer entrained water causes the water in the layer to warm up and slow down. The cooled boundary layer moving downwards is balanced by an equal flowrate of water moving up the centre of the pipe; this core flow is cooled by the downward flowing cold layer at the pipe wall, resulting in a decay of the bulk temperature in the freezing zone. This in turn decreases the heat flux to the forming ice plug.

In order to obtain an idea of the effect of initial temperature, pipe length and pipe diameter on the water temperature, a simple analytical model was proposed to describe the effect of cooling a section of the pipe wall to 0°C. The derivation and results are described in the following sections.

3.2.1 Derivation

Conservation of energy in the cooled region and the mixing region (defined by the extent of the convection-driven flow) assuming zero net heat flow out of the top of the cooled zone and zero conduction through the pipe wall above and below the cooled zone, gives the following equations (equations 3.13-3.15). The general arrangement of cooled region and the mixing region is sketched in figure 3.6.

FREEZING ZONE:

$$\rho c V_f \frac{dT_f^{av}}{dt} = \rho c F (T_{core} - T_{bl}) - hA_j T_f^{av} \qquad (3.13)$$

$$F = \int_{bl} w dA = A_{bl} w_{bl}^{av}$$

MIXING REGION:

$$\rho c V_m \frac{dT_m}{dt} = \rho c (T_{in} - T_m) \frac{dV_m}{dt} - \rho c F (T_{core} - T_{bl}) \qquad (3.14)$$

COMBINED REGIONS:

$$\rho c V_{total} \frac{dT_{total}^{av}}{dt} = \rho c (T_{in} - T_{total}^{av}) \frac{dV_{total}}{dt} - hA_j T_f^{av} \qquad (3.15)$$

The regions of interest are the freezing zone (volume V_f) and the mixing region (volume V_m, total volume $V_{total}=V_f+V_m$). The temperature distribution is represented by four values: T_{bl} (boundary layer), T_{core} (core flow), T_f^{av} (average temperature in freezing zone) and T_{total}^{av} (average overall temperature). The subscripts m, bl, j, f refer to mixing region, boundary layer, jacket and freezing zone, respectively.

The following simplifying assumptions are made in order to reduce equations 3.13-3.15 to a form in which they can be solved.

Assumption 1 : $T_f^{av}=T_{core}=T_b$

This will slightly overestimate T_f^{av} because it neglects the cooled boundary layer. It will therefore be more accurate in larger diameter pipes, when the thickness of the boundary layer is small in proportion to the pipe diameter.

Assumption 2 : $T_{total}^{av}=\frac{1}{2}(T_{in}+T_f^{av})=\frac{1}{2}(T_{in}+T_b)=T_{av}$

This will slightly overestimate T_{av} because the temperature in the boundary layer is ignored. Again, it will be more accurate in larger diameter pipes.

Using these assumptions, equations 3.13-3.15 can be rewritten as equations 3.16 and 3.17.

$$V_f \frac{dT_b}{dt} = F(T_b - T_{bl}) - \frac{hA_j}{\rho c} T_b$$
$$\therefore T_{bl} = \left(1 - \frac{hA_j}{\rho c F}\right) T_b - \frac{V_f}{F}\frac{dT_b}{dt} \qquad (3.16)$$
$$F = A_{bl} w_{bl}^{av} \approx A_{bl} \frac{w_{bl}}{2}$$

$$V_{total} \frac{dT_b}{dt} = (T_{in} - T_b)\frac{dV_{total}}{dt} - \frac{2hA_j}{\rho c} T_b \qquad (3.17)$$

The convection parameters, h, A_{bl} and w_{bl} are functions of T_b and the cooled wall length and can be estimated using the flat plate solutions proposed by Bejan[29] (see Appendix I). Note that the heat transfer coefficient, h, is the average coefficient over the length of the jacket (cooled wall) and is 33⅓% greater than the value at the bottom of the jacket. The time for the flow to develop from its initial static state is ignored.

The second equation (equation 3.17) relates the bulk temperature and the volume occupied by the convection cell. This equation cannot be solved unless the relationship between the length of the mixing zone and the temperature distribution is known. It is interesting to note that if the length of the mixing region is fixed, ie. if the pipe is blocked at some distance below the freezing zone, the bulk temperature will decay exponentially to zero, as given in equation 3.18. (The heat transfer coefficient, h, will vary as the bulk temperature decays; h_{ef} is the effective heat transfer coefficient over the temperature range.)

$$T_b = T_{in}\, e^{-\frac{2h_{ef} A_j t}{\rho c V_{total}}} \qquad (3.18)$$

Assuming that the jacket length is a constant multiple of pipe diameter and ignoring the variation of the properties of water with temperature, the initial temperature decay rate will be proportional to the bulk temperature (to the power 1.25), inversely proportional to the length of pipe and inversely proportional to the pipe radius (to the power 0.25).

In order to develop this model further, the relationship between the volume of the mixing region and the bulk temperature must be estimated. Two further assumptions were therefore proposed.

Assumption 3 :

The flow turns inwards and off the pipe wall when the boundary layer temperature

reaches the initial temperature. Having left the wall, the flow proceeds up the centre of the pipe.

Assumption 4 :

The average heat flux to the down-flowing water is proportional to the difference between the average temperature in the mixing region and the average temperature of the down-flowing water. The average temperature of the downwards flow is halfway between the average temperature of the flow leaving the freezing zone and the initial water temperature. Similarly, the average temperature of the core flow is halfway between the bulk temperature, T_b, and the initial temperature, T_{in}. The coefficient, h_{c2b} (core to boundary layer) quantifies the heat transfer between the boundary layer and the core flow.

Employing these assumptions gives the following relationship (equation 3.19) for the length of the mixing region.

$$\rho cF\frac{dT_{down}}{dz}\Big|_{av} = h_{c2b}(T_{up}^{av} - T_{down}^{av})2\pi(R_w - \delta_v)$$

$$\therefore \frac{T_{in}-T_{bl}}{L_m} = \frac{h_{c2b}2\pi(R_w-\delta_v)}{\rho cF}\frac{1}{2}(T_{in}+T_b-(T_b+T_{bl})) \qquad (3.19)$$

$$\therefore L_m = \frac{2\rho cF}{h_{c2b}2\pi(R_w-\delta_v)}\left(\frac{T_{in}-T_{bl}}{T_b-T_{bl}}\right)$$

The governing equations can be summarised (equation 3.20) using the approximation that the flowrate, F, is equal to $(2\pi R_w \delta_v w_{bl}/2)$.

$$T_{bl} = \left(1 - \frac{hA_j}{\rho c\pi R_w \delta_v w_{bl}}\right)T_b - \frac{V_f}{\pi R_w \delta_v w_{bl}}\frac{dT_b}{dt}$$

$$V_{total} = V_f + \pi R_w^2\left(\frac{\rho cR_w\delta_v w_{bl}}{h_{c2b}(R_w-\delta_v)}\right)\left(\frac{T_{in}-T_{bl}}{T_b-T_{bl}}\right) \qquad (3.20)$$

$$V_{total}\frac{dT_b}{dt} = (T_{in}-T_b)\frac{dV_{total}}{dt} - \frac{2hA_j}{\rho c}T_b$$

There are three equations and three unknowns, T_{bl}, V_{total} (or V_m) and T_b. Given the level of interlinking between the three equations, it was decided to use a numerical solution procedure. The set of equations was rewritten in approximate form (equation 3.21):

$$T_{bl} \approx \left(1 - \frac{hA_j}{\rho c \pi R_w \delta_v w_{bl}} - \frac{V_f}{\pi R_w \delta_v w_{bl} \delta t}\right) T_b + \frac{V_f}{\pi R_w \delta_v w_{bl} \delta t} T_b'$$

$$V_{total} = V_f + \pi R_w^2 \left(\frac{\rho c R_w \delta_v w_{bl}}{h_{c2b}(R_w - \delta_v)}\right)\left(\frac{T_{in} - T_{bl}}{T_b - T_{bl}}\right) \qquad (3.21)$$

$$T_b \approx \frac{T_b' V_{total} + T_{in}(V_{total} - V_{total}')}{2V_{total} - V_{total}' + \frac{2hA_j \delta t}{\rho c}}$$

where ' denotes values at previous time step.

The solution procedure for each time step (δt) was as follows :

1. calculate w_{bl}, h (Appendix I)
2. calculate T_{bl}, V_{total}, T_b
3. if converged - next time step else repeat from step 1.

(Convergence was assessed by monitoring the change in T_b between successive iterations.)

Refinement to this solution procedure was necessary because problems were experienced in obtaining convergence: divergence was noted in some circumstances, with negative or high ($>T_{in}$) values of bulk temperature. This was tracked to the 'dT_b/dt' term in the definition of boundary layer temperature. If, at some intermediate iteration during solution, the bulk temperature decay rate increased to more than a critical value, the boundary layer temperature could increase, which would cause a decrease in length of the mixing region and therefore cause the bulk temperature to decrease further, thereby causing divergence. In order to keep this term under control, under-relaxation was used. A new term, S, was substituted for the term '$(T_b - T_b')/\delta t$' and this was updated during successive iterations by $\alpha((T_b - T_b')/\delta t - S)$. In addition to this, the bulk temperature was under-relaxed; in each iteration, the bulk temperature was updated by $ß(T_b(\text{new value}) - T_b)$. Therefore, during successive iterations, the predictions of both T_b and S (and T_{bl}) were both converging towards their final values. Values of 0.05 and 0.5 were required for the under-relaxation factors α and ß; δt was 5 seconds.

The definition of the coefficient of heat transfer between the upwards flow and the downwards flow (h_{c2b}) was required in order to obtain a solution. The value of h_{c2b} was defined such that the bulk temperature dropped from 20°C to 12°C over 20 minutes. This data was taken from bulk temperature measurements reported by Tavner[5], who also stated that the mixing region did not reach the tank under these conditions (implied from the fact that the bulk temperature inside the freezing zone continued to decay throughout the freeze). This gave a value of 600 W/m²K; for comparison a value of 60 W/m²K was also used.

3.2.2 Results

The variation of bulk temperature with time was predicted for the situation of water initially at 20°C in a 100mm (4") diameter pipe. The resulting decay in bulk temperature is plotted against time in figure 3.7 showing that the temperature decay rate decreases over time but does not reach zero; therefore the bulk temperature will not stabilise until it is equal to 0°C. The decay rate was lower for the lower value of heat transfer coefficient, h_{c2b}=60 W/m²K. The predicted bulk temperatures differed from the experimental data; the predicted decay rate decreased over time whereas the measured data showed an approximately constant decay rate.

The length of the mixing region is also plotted in figure 3.7. There is a disparity between the predictions and the experimental results; the predicted extent of the mixing region was nearly 2½m (h_{c2b}=600 W/m²K) and 13m (h_{c2b}=60 W/m²K) over the 20 minute period compared to less than 0.4m in the experiments. A further simulation was run with the mixing region length set at 0.4m and the resulting bulk temperature plotted in figure 3.7. The temperature decayed exponentially, as indicated by equation 3.18, to nearly 3°C at 20 minutes. This highlights the fact that there are significant problems in the results and therefore in the assumptions used in the derivation of the model.

3.2.3 Discussion

Five assumptions were used in the fixed length model which are discussed below.

- It was assumed that the average temperature in the combined regions was equal to the average of the bulk temperature inside the freezing zone and the initial temperature. If the average temperature in the combined regions was equal to the average temperature in the freezing zone then the temperature would drop from 20°C to 7.5°C in 20 minutes.
- The accuracy of using the prediction of heat transfer coefficient obtained from flat plate analysis has been discussed in the previous sections; the experimental results obtained by Tavner[5] indicated that the heat transfer coefficient was less than that predicted by Bejan[29]. This will result in a slower decay in bulk temperature.
- The time required for the convection driven flow to become established and the time to fill the jacket with liquid nitrogen were neglected. Including these effects will decrease the initial temperature decay. The time to fill the jacket was of the order of 2 minutes and scale analysis by Bejan estimated that the time for the fluid to move from rest to the steady state solution was of the order of 4 minutes. Over a time scale of 20 minutes, these two effects will be

important. If the product ($h_c A_j$) increased from zero to its final value over, say, a 10 minute period, the temperature would decay more linearly.

- The walls above and below the jacket were assumed to be perfectly lagged; any heat flux through the wall from the surroundings will decrease the rate at which the bulk temperature decays.
- The assumption made by Tavner that the bulk temperature will stabilise as soon as the mixing region reaches the tank may be incorrect; there may be an intermediate state where the flow partially enters the tank causing a slower bulk temperature decay.

The predictions of bulk temperature and mixing length obtained using the 'infinite pipe' assumptions (3 and 4) disagree significantly with the experimental results. Using these assumptions, it is not possible to express the heat transfer from the core flow to the downwards flow using a heat transfer coefficient and predict both the bulk temperature decay and the length of the mixing region correctly. This may be attributed to the points discussed in the previous paragraph or may be an indication that the assumptions (3-4) require further development.

3.2.4 Conclusions

The predictions of bulk temperature and mixing length can only be considered as qualitative. Without more experimental data, in particular measurements of the length of the mixing region, it is difficult to establish which of the assumptions are responsible for the difference between the prediction and the measured bulk temperature. The following comments can be made.

- Both the fixed and the infinite length pipe models predict that the bulk temperature will decay to (nearly) zero. The decay rate decreases with decreasing temperature and is lower in the infinite pipe model than in a fixed length of pipe.
- Poor heat transfer from the core up flow to the down flow results in a longer mixing region and a lower rate of temperature decay.
- The temperature decay rate depends on both the volume of the mixing region and the rate at which it expands. The decay rate is therefore partially controlled by the initial temperature; the length of the mixing region will be greater in the case of water initially at 40°C and decayed to 20°C than the case of water initially at 30°C and decayed to 20°C; the rate at which the temperature continues to decay below 20°C will be lower with an initial temperature of 40°C than with an initial temperature of 30°C.

- Additional investigations not detailed above showed that if the *rate* at which the length of the mixing region increased was proportional to the difference between the bulk temperature and the ambient (initial) temperature, then the bulk temperature would stabilise at a value greater than 0°C.
- The derivation of the heat transfer coefficient and the assumption of the flow development assumed laminar flow conditions and therefore they should not be applied under turbulent flow conditions (discussed in the previous section).
- The derivation above has assumed that the pipe wall is perfectly lagged. Heat flux to the down flow through the wall may alter the flow field. If the downwards flow is warmed entirely by the heat flux through the wall, the temperature of the core flow and therefore of the water in the cooled/freezing zone will not decay.

3.3 DEVELOPMENT OF THE FREEZING MODEL WITH BULK TEMPERATURE DECAY

The two models derived in the previous sections were combined to investigate the effect of bulk temperature decay on the freeze times. The decrease in bulk temperature affected the freezing rate by decreasing the heat flux from the water to the ice front during the freeze. The assumptions used in developing the flow model were not changed and the model was run assuming an infinite pipe length, using values of the heat transfer coefficient for the heat flow from the core flow to the downwards flow equal to 60 and 600 W/m²K, as before. The plug neck was assumed to be at the centre of the jacket (A_h=½) and the jacket length was assumed to be twice the pipe diameter. The heat transfer coefficient for the heat flux to the liquid nitrogen (h_c) was equal to 2000 W/m²K.

3.3.1 Results

The resulting freeze times are plotted in figure 3.8, for 100mm (4"), 150mm (6"), 200mm (8") and 250mm (10") diameter pipes, clearly demonstrating the effect of including a bulk temperature decay on the freezing time. With h_{c2b} equal to 600 W/m²K the freeze times increase gradually with increasing temperature; with h_{c2b} equal to 600 W/m²K, the freeze times increase more rapidly and approach a limiting-type of curve. The fact that the bulk temperature will continue to decay means that it will always be possible to freeze the pipe given a finite (but large) length of time and liquid nitrogen supply.

3.3.2 Discussion

The bulk temperature does not level out until it reaches 0°C. This implies that it should be possible to form a complete plug in a *finite* length of time, irrespective of the initial water temperature and the pipe length. The freezing time therefore consists of the time for the temperature to decay to below the highest value which can be frozen with maintained bulk temperature plus the time for the pipe to freeze at that temperature. The temperature decay rate decreases with time as the length of the mixing region increases and therefore the freezing times will increase non-linearly with temperature. If the heat transfer to the cooled boundary layer is poor, the bulk temperature in the freezing zone will decay very slowly and, for

practical purposes, the freeze times will appear to display limiting behaviour.

If the flow field were controlled by an alternative mechanism, namely that the length of the mixing region increased at a rate proportional to the difference between the initial and bulk temperatures, the bulk temperature will stabilise above 0°C. Under these conditions, limiting behaviour (ie. a maximum initial temperature above which it will not be possible complete a freeze) will be encountered. This emphasises the need for an improved understanding of the mechanisms which control the development of the flow field.

This analysis assumed laminar flow conditions and therefore cannot be used to imply the behaviour under conditions where the combination of water temperature and pipe diameter results in turbulent flow.

Extra heat flow into the pipe through the pipe walls will decrease the rate at which the bulk temperature decays. This may result in the bulk temperature stabilising above 0°C and therefore result in the freeze times displaying limiting behaviour.

3.4 CONCLUSIONS

In this chapter, the freezing process and the development of the natural convection-driven flow have been considered using simplified 'analytical' models. Firstly, freezing with convection in the water was considered assuming that the water temperature remained constant throughout the freeze. Convection was simulated by including the analytical solution for the heat transfer to a vertical plate from Bejan[29]. The second situation which was considered was the development of the flow field when a section of the pipe wall is cooled (without freezing) and the effect on the bulk water temperature was predicted. The final case coupled the previous two models together to predict the effect of a bulk temperature decay in the freezing zone on the freeze times.

The first model demonstrated that with a maintained bulk temperature and convection the freezing times display a limiting behaviour and there is a maximum initial temperature above which it is impossible to form a complete plug. The maximum temperature decreased in larger diameter pipes. This agreed with the experimental results obtained by Bowen et al[9]. Differences between the predictions and the experimental data was split into two areas. The predicted freeze times in water initially at 0°C were lower than the experimental values, this was attributed to neglecting axial conduction and inaccuracies in the definition of the heat flux to the liquid nitrogen. The predicted maximum values of water temperature which could be frozen were generally higher than the experimental values and this was attributed to the assumption of laminar conditions. The experimental results for the maximum temperature were found to fall on a line of equal Grashof number which crossed the line defining the maximum temperature under laminar conditions at between 100mm and 150mm (4-6") pipe diameter (the range was due to variations in neck position and thermal resistance between the ice and the liquid nitrogen). It was therefore concluded that two equations are required to define the limiting temperature; below 100mm (4") the relationship[3.2] is controlled by a critical value of the product ($h.T_b.R_w \approx T_b.R_w^{0.446}$) and above 150mm (6") the limiting temperature is the temperature at which the Grashof number (defined using the jacket length) is 2.1×10^9. Further investigations are required to define the break-point in pipe diameter more rigorously, either through experiment or improving the prediction of heat transfer coefficient.

The effect of varying the jacket length and coolant temperature on the limiting temperatures was also investigated. The effect of jacket length on the limiting temperature was found to be weak; an approximately 25% increase in the maximum temperature could be

[3.2]Assuming that the ratio of jacket length above plug neck to pipe diameter remains constant.

obtained by increasing the jacket length from 1 to 5 pipe diameters. The effect of decreasing the coolant temperature was more significant, with large reductions in maximum temperature resulting from decreasing the coolant temperature (for example, increasing the coolant temperature from -200°C to -100°C decreases the maximum temperature from 60°C to 33°C in a 100mm (4") diameter pipe).

The study of the variation of limiting temperature provided a method of scaling the effect of convection on freezing between pipe sizes. A parameter termed the 'effective heat flux' (e.h.f.) was defined as the product ($h.T_b.R_w$); equal values of e.h.f. indicate an equivalent effect of convection on freezing. The values of heat transfer coefficient predicted using the integral analysis by Bejan were manipulated with the result that, for equal e.h.f., the product $T_b.R_w^{0.446}$ is constant. (For instance, the effect of convection on freezing at 20°C in a 100mm (4") diameter pipe is equal to that at 15°C in a 200mm (8") diameter pipe and at 27°C in a 50mm (2") pipe.) This scaling can only be applied under laminar conditions and in situations where there is no significant neck migration because this causes a breakdown in the flat plate conditions used in the derivation of the heat transfer coefficient. This limits this scaling rule to below approximately 30°C in a 100mm (4") diameter pipe, 41°C in a 50mm (2") diameter pipe and 22°C in a 200mm (8") diameter pipe.

The experimental data from Bowen was obtained with the test pipe placed over a tank, thereby deliberately maintaining the bulk temperature of the water in the freezing zone: the same conditions as those assumed in the analytical model. Tavner[5] observed that the temperature inside the freezing zone decayed if the convection-driven flow did not reach the tank. In order to investigate this temperature decay in more detail, a simple model was proposed. The bulk temperature decay in both short (finite) and infinite pipes was considered. Freezing was not included at this stage.

The resulting predictions were compared with experimental data using Tavner's measurements of bulk temperature during a 20°C freeze during which the flow probably did not reach the tank. The predictions of bulk temperature obtained when the length of pipe was fixed equal to the length of pipe above the tank decayed considerably more rapidly than the measured temperatures. This was partially attributed to the fact that the time to cool the outside of the pipe and the time for the water to move from rest were neglected. Other possible causes were neglecting heat transfer through the pipe wall from the surroundings, the assumptions made in defining the bulk temperature in the freezing zone and the definition of heat transfer coefficient.

Predictions of the bulk temperature and length of mixing region in an infinite length of pipe employed the assumption that the downwards flow was warmed up by heat transfer

from the core flow. These results were controlled by the value of the coefficient used to characterise this heat flux. Decreasing this value resulted in a longer mixing zone and lower bulk temperature decay. A heat transfer coefficient was obtained to give the same drop in bulk temperature as measured in the experiments; this predicted that the mixing region extended six times further than the distance between the tank and the freezing zone.

The most important result from the consideration of the bulk temperature decay was the conclusion that, under the assumptions employed, the bulk temperature would continue to decay to 0°C and therefore it would be possible to freeze water at any initial temperature. This then implies that the conclusion from the experimental data that there is a maximum temperature at which it is possible to perform a freeze was a result of using a tank in the experiments. On closer examination, this result is dependent on a number of assumptions; in particular, the assumption of laminar flow conditions, the relationships governing the bulk temperature decay and the assumption of zero heat flux through the pipe wall. When the predicted bulk temperature decay was included in the freezing model, giving the third 'analytical' model, an approximation to the limiting type behaviour was obtained using a low heat transfer coefficient for the heat flux between the core flow and the downwards flow. The resulting freeze times at high initial temperatures were large but finite.

At present, therefore, it is not possible to conclude whether or not the bulk temperature inside the freezing zone will continue to decay to 0°C and therefore whether it will be possible to form a plug at any initial temperature given sufficient time and liquid nitrogen. This investigation has emphasised the need to study the heat flux to the ice front due to both laminar and turbulent convection in the water and therefore the effect of convection on the bulk temperature inside the freezing zone. An improved understanding of the mechanisms which control the bulk temperature decay would allow the further development of the analytical model.

4. DEVELOPMENT OF THE NUMERICAL MODEL AND POST-PROCESSING FACILITIES

There are two possible approaches that can be used in developing a numerical model: a computer program can be written to solve the governing equations for the problem or a general purpose CFD modelling package can be used. At the beginning of this research, the only CFD package that was available for this work at the University was PHOENICS 87, mounted on the University's IBM 3090 mainframe. From a brief attempt using this software it did not appear user-friendly and there was very little expertise and support available to help those using it. In addition, the IBM 3090 was heavily used by both undergraduates and postgraduates and was slow on actual run-times. It was concluded that PHOENICS offered little advantage over producing a numerical model 'in house' specifically to predict pipe freezing.

The numerical model was developed using established numerical methods to solve the flow and energy equations and predict the convection and freezing processes. The development process included several validation stages during which the model was modified to predict results for comparison with published analytical and numerical results. The model development is described in detail in a separate report[2] and is briefly summarised in the following sections. This allows the important details to be described without devoting a large amount of space to the technicalities of numerical modelling and validation tests, since these are not of overall importance to pipe freezing itself.

In addition to the model, techniques for analysing the results also had to be developed. Numerical analyses (especially transient analyses) produce an immense amount of data which has to be examined to explain the processes taking place. The best way of doing this is to present the results graphically. Computer software was developed which allows interactive analysis of the results data set. A detailed description of the facilities offered by this software is included with the details of the model development[2] and is summarised in section 4.2.

4.1 DEVELOPMENT OF THE NUMERICAL MODEL

The basis of a numerical method is to divide the physical area of interest into smaller subregions. Assumptions about the way in which the dependent variables are related to the values in the neighbouring regions are made based on the governing equations and a set of interlinked equations is obtained. The methods used to do this are broadly divided into finite difference, finite volume, finite element and boundary element methods. The finite volume methodology was chosen, partly on the grounds of computer power requirements and partly because some (unpublished) preliminary development of a model of convection in a pipe had been carried out by Burton using this method.

The flow problem was formulated in terms of the primitive variables (the pressure and the radial and vertical components of velocity) rather than streamfunction and vorticity variables. Using streamfunction and vorticity as the dependent variables reduces the number of variables by one (the pressure drops out of the equations) in two dimensional problems but actually increases the number of variables in three dimensional problems. The primitive variable approach was chosen for this work partly because it yields results which are straightforward to understand and partly because the numerical work was ultimately aimed at modelling horizontal or inclined pipes which are three dimensional problems.

The physical processes involved in pipe freezing are complicated, even in a vertical pipe. A thin annulus of ice grows to block the pipe; this is controlled by cooling a section of the outside of the pipe, normally by the complex process of a cryogen boiling against the outside of the pipe. For an accurate prediction, the pipe wall must be included in the problem so that conduction axially along the wall and through the wall is included. The freezing process is also affected by natural convection in the water and the geometry of this water region gradually changes as the plug forms. The problem is further complicated because the properties of ice and those of water vary with temperature (for instance, the density maximum at about 4°C). The flow was assumed to be laminar which was a reasonable assumption for most of the conditions under which experimental investigations had been carried out. Applying flat plate correlations indicated that it is possible that the flow may become turbulent under more extreme pipe freezing conditions depending on the water temperature and the pipe diameter; this is discussed in the previous chapter (section 3.1.2.2).

The model was developed in stages; firstly looking at modelling the buoyancy driven flow and the solidification processes separately and then coupling the two models together to produce the final model of plug formation in a pipe. The same structure is retained in the following sections.

4.1.1 Development of the Convection Model

The numerical method used to solve the momentum, energy and continuity equations was the SIMPLER algorithm. This is a development of the earlier SIMPLE algorithm, both of which were developed by S.V. Patankar[50]. The name SIMPLE stands for Semi-Implicit Pressure Linked Equations (and SIMPLER is SIMPLE-Revised). This was fully and clearly described by Patankar and has since been used widely (for example, the modelling package PHOENICS uses the SIMPLEST algorithm, which is also based on SIMPLE).

The physical domain is divided into a grid of control volumes (hereafter called CVs) and the governing equations are integrated over a CV. (These 'new' equations are actually the original equations from which the governing equations were derived, in the limit of the size of the CV decreasing to zero.) A set of equations is formulated for pressure, velocity (both components), pressure correction, velocity correction and temperature. Each equation typically involves the other dependent variables (for instance, the vertical velocity equation involves temperature, pressure and the values of velocity at the four neighbouring CVs. This interlinking is handled iteratively so that, for instance, the equation for vertical velocity at one CV uses the latest calculated values for the horizontal (radial) velocity, pressure and temperature. The resulting equations relate the value of the dependent variable at one CV to the values at the 4 neighbouring CVs and therefore, if the equations for all the grid points are written in matrix form, the matrix of the coefficients is populated on the main diagonal and on the two diagonals on either side (giving a penta-diagonal matrix). (If the problem is one-dimensional, the matrix is tri-diagonal.) Directly inverting the matrix is extremely time-consuming in all but the simplest problems and therefore most solution methods apply iterative techniques combined with the standard Tri-Diagonal Matrix Algorithm (TDMA) which (as the name suggests) gives the exact solution for a tri-diagonal matrix. The method used in this work was to apply the line-by-line method to solve each equation; the equations were solved for a row or column of CVs at a time with the 'off-line' variables kept constant. Multiple iterations were performed, changing the direction of the calculation (row/column) to obtain a converged solution.

If the pressure equation is formulated using the same set of grid points as the velocity equation, two sets of equations are obtained for pressure: one for even and one for the odd numbered nodes. The resulting pressure distribution can resemble a checkerboard, with the distribution on the even-numbered nodes being offset from that on the odd nodes. In order to avoid this, the staggered grid approach was taken which meant that the pressures were solved on a different grid to that used for the velocity solution.

An important stage in deriving the discretised (solvable) equations from the integrated governing equations is the choice to how to interpolate between nodes in order to obtain the value of a variable on the face of a CV. Linear interpolation can be used when there is very little flow and/or when a fine grid is used, but in stronger flows the upstream value will become increasingly dominant. In this analysis the power-law method was used. This fits between the central difference (linear) and the upwind (where the intermediate value is set to the upstream value) methods and is an approximation of the so-called 'exact' solution. The 'exact' solution is the analytical solution for the variation between two points in one dimensional steady flow with constant properties and without sources in a rectangular geometry. It contains exponentials and is therefore computationally expensive to evaluate.

The model was formulated to predict convection in rectangular and radial geometries. The set of equations for a radial geometry differed from those in a rectangular geometry in that the areas of the CV faces varied with the radial position and that there was an extra term in the horizontal (radial) velocity equation. The derivation of the equations for the radial co-ordinate system was based on that used by Sparrow and Ohkubo[51].

Natural convection is driven by variations in the density resulting from a non-constant temperature distribution. One peculiarity of water is the density inversion at around 4°C; cooling water down to 4°C increases the density but if water is cooled further the density will decrease. This causes an up-flowing sub-layer in the boundary layer (observed in experiments by Tavner[5]). The variation of density with temperature was used in the formulation of the velocity source term by means of interpolation from a look-up table. The variation of density was ignored when considering continuity; proper consideration would require incorporating an inflow to maintain overall continuity because the bulk density will increase on cooling (an outflow will be required when the density change on solidification is considered). This was not considered to be an important factor in the overall process and therefore was neglected.

The convection modelled was validated using two benchmark problems. Convection in a square cavity with heated and cooled vertical walls and lagged top and bottom walls was modelled and the resulting steady state solution compared with the published results by de Vahl Davis and Jones[52] and by Markatos and Pericleous[53]. The fluid in the cavity was assumed to have constant properties and a constant expansion coefficient and therefore the conditions were easily condensed into dimensionless form. Four cases were modelled, varying the Rayleigh number between 10^3 and 10^6 and resulting velocity and temperature distributions were found to agree well with the published data (comparing the values of velocity at designated points and also by means of velocity, streamline and temperature plots).

Convection in a cylinder with heated vertical and top walls and cold bottom wall was

modelled for comparison with the results of Huang and Hsieh[54]. Steady state velocity and temperature distributions were presented for different combinations of Prandtl and Grashof numbers, and Nusselt numbers describing the heat transfer at the walls were listed. The agreement with the published data was good, with the exception of the average Nusselt numbers over the top, side and bottom walls, possibly due to differences in the method used to calculate the temperature gradient (not described by Huang and Hsieh). There were problems in calculating the temperature gradient at the bottom outside corner due to the discontinuity in the temperature distribution.

4.1.2 **Development of the Solidification Model**

The methods which have been used to model freezing and melting problems can be divided into fixed grid (or weak) methods and transforming grid (strong) methods. For the former, the equations are formulated in such a way that they are valid in both solid and liquid regions and therefore the position of the solid/liquid interface does not need to be tracked. If a transforming grid is used, the domain is divided into solid and liquid regions and therefore the interface remains at a fixed position in the grid. The boundary conditions on the interface are zero velocity in both directions and fixed temperature and therefore the problem can be solved in both regions separately. The interface position, and therefore the deformation of the grid, is obtained by applying a heat balance between the solid and liquid sides of the interface.

One of the problems in modelling water is the thickness of the boundary layers (Tavner's experimental results showed temperature boundary layer thicknesses of the order of 5mm); using a transforming grid would allow grid refinement in this area. However, the degree of grid distortion which would arise in modelling the growth of the ice plug is high and this caused concern as to the applicability of the transforming grid method to this problem. If a fixed grid approach were taken, it would be necessary to refine the whole grid in order to resolve the boundary layer, resulting in unwanted refinement outside the area of interest. A study was made of the available literature (1990); this showed that the transforming grid method had invariably been applied to problems which had involved very little grid distortion. The literature describing problems which involved high interface gradient (Bennon and Incropera[47] and Hibbert et al[46]) consistently used the fixed grid method. It was therefore decided to use a fixed grid method for this work together with a fine grid.

The equation for temperature used in the single phase models is derived from the enthalpy equation (enthalpy is replaced by the product of specific heat and temperature). Phase

change problems are more complicated because the latent heat contribution to the enthalpy varies between solid and liquid regions. There are two dependent variables in the enthalpy equation, the temperature and enthalpy distributions. Several methods have been developed which attempt to simplify the equation to a single dependent variable so that they can be solved more quickly. Examples include the equivalent heat capacity method (which incorporates the latent heat into an equivalent heat capacity) and the enthalpy method of Voller et al[55] (latent heat change incorporated into source term). Neither method appeared to be suitable for this problem; the equivalent heat capacity method can only be used to model solidification over a temperature range and substituting sensible or total enthalpy for temperature in the governing equation gives problems in incorporating the steel pipe wall into the domain. It was therefore decided to retain the enthalpy and temperature as dependent variables, employing the enthalpy method of Shamsundar et al[56].

Two validation tests were applied; firstly one dimensional solidification from a cold wall in a semi-infinite (ie. cartesian) medium was modelled. The resulting interface positions and temperature distributions were compared with the analytical Neumann solution. This showed that the interface position moves forwards unsteadily, 'stepping' around the analytical solution (figure 4.1). This is a characteristic of the enthalpy method and is due to the assumption that the temperature in the CV remains at the freezing point while the interface passes through the CV. Reducing the grid spacing makes the interface move more smoothly. Methods of smoothing the interface movement after the enthalpy distribution has been obtained have been suggested by Hill and Dewynne[57] and Shamsundar and Rooz[58]. It is noted (eg. by Lee and Tzong[59]) that this 'stepping' interface movement represents a drawback to the method because it results in slow convergence. Other researchers (eg. Cao and Faghri[60], Shamsundar and Rooz[58]) state that it also causes corresponding oscillations in the nodal enthalpies.

Solidification of a material in a square cavity initially at its freezing temperature and cooled on its external boundaries was also modelled for comparison with the results presented by Shamsundar and Sparrow[56] and Shamsundar and Rooz[58]. Interface positions, solid fractions and surface integrated heat flux throughout the freeze were compared for two combinations of Biot and Stefan number. The results were found to be nearly exactly the same as the published data, which was reassuring because the same method, time step, grid layout and grid density were employed in both cases. The excellent agreement demonstrated that the method was properly employed.

4.1.3 **Model of Convection and Solidification**

The algorithm used to predict convection iteratively called routines for calculating the pressure, velocity, pressure correction, velocity correction and temperature until a converged solution is obtained. The enthalpy method fits neatly into this framework, replacing the temperature calculation stage, and the convective terms can be included in the enthalpy equation in the same way as in the temperature equation. In order to decrease the velocities to zero in solidifying CVs, a source term was included into the velocity equations which forced the velocity towards zero as the liquid fraction in the CV decreased. An exponential variation of this source term with the liquid fraction was used which caused an initially small then increasing decay in the velocity as the liquid fraction dropped. This is described by Voller et al[55] and it was found to give much better stability than changing the viscosity with the liquid fraction in the CV.

4.2 DEVELOPMENT OF POST-PROCESSING METHODS

One feature of a numerical model is the quantity of data that is produced. With a 56x130 grid (used in the following chapters to model a 1022mm length of 100mm diameter pipe), the radial and vertical velocities and enthalpy distributions add up to some (3x56x130=) 21,840 values. Over a typical prediction of, say, 25 minutes, storing the distributions every 30 seconds gives some 1,092,000 floating point numbers which must be analysed to explain the processes occurring during the freeze.

The traditional method of displaying the results has been to plot them graphically - giving snapshots of the velocity distributions or the temperature distributions. More recently, the improvement in computer graphics has lead to more sophisticated techniques; for instance, the results can be used to produce a simulation of the process, showing the movement of the solid/liquid interface and movement of the liquid, using colour to show the temperature distribution. These methods can lead to a vast improvement in the understanding of the processes involved but are actually more demanding in terms of computer requirements than the numerical model itself. In order to communicate the results in journals or report form, the results must be produced on paper and preferably in black and white. (It should be noted that the difficulties in displaying the results from a two-dimensional model are completely dwarfed by the complexity of showing the results from a three-dimensional simulation.)

There is an extra problem associated with displaying the results from modelling pipe freezing which is due to the high aspect ratio (long and thin) of the domain. If the results (velocity vectors, isotherm plot, etc.) are plotted to scale, the detail in the radial direction is very difficult to see. However, if the radial scale is expanded, the results are easily misinterpreted. This has important consequences if the quality of the output device (printer, photograph, etc.) is poor. In addition, since the process is transient, the development of the plug and the flow field is of interest. It is therefore desirable to be able to display plots at time intervals throughout the freeze on the same page which also imposes limits on the size of each individual plots. It is necessary to choose the data (eg. number and size of velocity vectors, number of isotherms and streamlines) carefully so that the results are communicated clearly.

Software for analysing the results was developed during this project. The software was PC based and written in the programming language C, making the software more flexible and interactive than FORTRAN would allow. The software made full use of the Super-VGA screen quality and provided high quality output in black and white via a laser printer and in colour using the standard 'bitmap' format. The traditional ways of presenting velocity (ie. as

vector and streamline[4.1] plots) and temperature distributions (isotherm plots or colour-coding the velocity vector and streamline plots) were used.

This program (FgMaker) was designed to be as flexible as possible so that no changes were required to the code to plot results obtained in different grids while displaying sufficient data (such as initial conditions and jacket position) to produce figures for reports and presentations. The main features of this program are described in the following sections.

4.2.1 Normal Mode

In this mode, the results obtained for one point in time can be studied in depth. The data can be examined using vector plots colour-coded for temperature, streamline plots (also colour-coded) and isotherm plots. The velocity vectors are shown by lines drawn from the grid point, the position of which is emphasised by a dot, in the direction of the flow and with length proportional to the magnitude of the velocity. In 'quick vel' mode, a reduced set of velocity vectors are drawn with arrow heads to indicate the direction more clearly. In 'show' mode, the user can move a pointer around the grid and the velocity and temperature is displayed on screen. The streamline for a selected point can be plotted. The isotherms can be annotated.

A further option allows the user to 'zoom' in on an area and carry out all the above operations. This was found to be invaluable to analyse the flows and plug formation in a long domain. Another option allows '3zoom', where a region in the domain is selected and three sub-plots of isotherms, colour-coded velocity vectors and streamlines are displayed.

4.2.2 Time Development Mode

In this mode, a series of snapshots in standard formats at user-specified times are displayed, showing, for instance, the flow, temperature or plug development during the freeze. The user can choose between colour-coded velocity vectors, colour-coded streamlines, isotherms, vectors and isotherms, and streamlines and isotherms. The area which is displayed can also be selected, this allows a 'zoom' in on areas of interest, such as the plug development

[4.1] The streamline plot is a contour plot of the streamfunction distribution which is calculated from the velocity distribution within the software. The definitions of streamfunction, solution method and boundary conditions are detailed in Appendix II.

in the freezing zone (eg. figures 6.13a-d). The isotherm levels can be annotated.

4.2.3 **Hardcopy Methods**

Black and White Output (Laser Printer): The screen is written to a binary file. Either two or four screens can be printed on the same page and a separate program (DumpFig) is used to combine the screen-dump files together to give a binary file which can be sent to a laser printer. The Hewlett-Packard Laserjet format was used because it is a standard format which is emulated by most other laser printers.

Colour Output : The screen can also be 'dumped' to a file using the 'bitmap' format. This is a standard format and allows the user to import the file into other applications and to print on a wide range of printers.

5. MODEL VALIDATION

A model of freezing with convection in the liquid region was developed, as described in the previous chapter, providing a numerical model which could be used to predict natural convection and phase change inside a vertical pipe. The component parts (ie. the separate convection and solidification solution routines) had been validated using test cases which were significantly different to pipe freezing. It was therefore decided that more rigorous validation was necessary before the model could be used to explore the processes involved in pipe freezing. Computer models are subject to errors arising from both programming (a significant problem considering the size and complexity of the code) and from a lack of resolution in the grid spacing and time step size. In addition, the assumptions used to define the boundary conditions must be checked.

One complexity in modelling pipe freezing which was still unresolved was how to incorporate the boiling nitrogen into the model. The mechanisms controlling the rate at which the boiling nitrogen removes heat from the water are highly complex and also affected by a range of conditions. It was therefore concluded that it would not be possible (or even desirable) to quantify the process exactly; using a temperature dependent heat flux as the boundary condition was chosen instead. By imposing a heat flux boundary condition as the boundary condition to the model, the relationship between the wall temperature and heat flux can be varied until good agreement between the predicted temperatures and the experimental results is obtained. Before this can be carried out, the numerical model must be validated.

There are three methods of validating numerical models; comparison with an exact or analytical solution, comparison with an existing benchmark numerical solution and comparison with experimental data. While analytical and numerical solutions offer repeatable and reproducible solutions without requiring an expensive experimental program, they only offer solutions under a set of simplifying assumptions. In order for a computer model to be accepted, it should be tested against experimental results. The experimental work by Tavner[5] produced results for the temperature distribution and plug profiles during pipe freezing and also gained some information on the convective flows during the freeze by using flow visualisation techniques.

The freezing prediction was validated incorporating Tavner's measurements of wall temperature for the jacket boundary condition for initial water temperatures at which natural convection is insignificant. The boundary condition was then modified to a varying heat flux condition and the relationship between wall temperature and heat flux optimised to duplicate the wall temperature measurements during the freeze. The convection and solidification models were combined and the effect of certain parameters used in the numerical method was studied and the solution convergence behaviour was explored. The predictions of flow field

and plug development were then compared with the experimental data obtained by Tavner and by Burton[1].

5.1 MODEL OF PIPE FREEZING IN THE ABSENCE OF CONVECTION

The model was used to predict the plug formation in situations where natural convection can be ignored. The experimental results showed that this was for values of initial temperature below around 20°C in a 100mm (4") diameter pipe. The following section describes model validation using temperature measurements obtained by Tavner as the boundary condition for the jacket. These results were presented at the Seventh International Conference on Numerical Methods in Thermal Problems; this paper is included in Appendix V. In the second section below, the formulation of a temperature dependent heat flux to simulate the boiling nitrogen is described.

5.1.1 Preliminary Model: Prescribed Wall Temperatures

The computational domain was 400mm long and 50mm wide (100mm (4") diameter pipe). The 'jacket' was 200mm (8") long and positioned centrally. The boundary condition in this region was set using experimental data and the pipe wall was not included in the domain. Tavner had measured the temperatures at four positions on the outside of the pipe wall every 30 seconds and linear interpolation was used both in space and time to calculate the temperatures for all the nodes lying on the boundary during the freeze. The radial heat flux out of the pipe above and below the freezing zone was assumed to be zero and the top and bottom of the domain were isothermal and maintained at the initial water temperature.

Both the conductivity and specific heat capacity of ice vary with temperature; the conductivity increases from 2.2 W/mK at 0°C to 6.5 W/mK at -200°C and the specific heat capacity decreases approximately linearly from 2.1 kJ/kgK at 0°C to 0.56 kJ/kgK, giving a quadratic relationship between enthalpy and temperature. The density of ice is 920 kg/m^3. The density, conductivity and specific heat capacity of water were 1000 kg/m^3, 0.6 W/mK and 4.2 kJ/kgK, respectively. The latent heat of fusion of water was taken as 333.5 kJ/kg.

Investigations were carried out with 40x51, 40x102 and 80x102 grids and times steps of 1 second and 0.5 seconds. There was very little difference between the results and therefore the 40x51 grid and the 1 second time step were used, giving a grid spacing of 10mm in the

vertical direction and of 1mm in the radial direction.

The model was run for initial temperatures of 8°C, 23°C and 26°C (temperatures determined by the experimental results of Tavner).

5.1.1.1 Results

The predictions were compared with the experimental data by considering the freezing time, the temperature profiles across the pipe during freezing and the plug development during the freeze. Only the temperature profiles from the 8°C and 26°C freezes and the plug profiles from the 23°C freeze are compared here.

Figure 5.1 plots freezing time against the initial temperature. The predicted freezing times increase linearly with increasing initial temperature; the general trend is plotted with the dashed line to estimate the freezing time at higher temperatures. This general trend agrees with the experimental results for initial water temperatures below 25°C and the predicted freeze times lie within a minute of the measured times. This difference can be attributed partly to possible human error in assessing close-off visually and partly to neglecting the heat transfer through the perspex window. At higher temperatures, the measured freezing time increases rapidly because convection becomes more important.

Figures 5.2a,b show the temperature distribution inside the pipe during freezing for the 8°C and 26°C freezes. Each sub-plot shows a cross-section through the pipe, with the centre of the pipe on the left (dashed line) and the jacket on the right (denoted by a rectangle). The temperature profiles are plotted for the four vertical positions at which experimental data was available and these profiles are positioned on the plot at the corresponding vertical positions (0%, 50%, 75% and 100% of the jacket length from the bottom of the jacket). In each of these four graphs, the predicted temperature distribution is indicated by the line and the experimental data is shown as dots.

The results for the 8°C freeze show excellent agreement with the experimental data until the ice front reaches the centre of the pipe. This behaviour is also noted in the results for the 26°C freeze. In the 26°C freeze, it can be seen that the solidification takes place more slowly than predicted particularly at the bottom of the jacket. This is consistent with the effect of convection causing an asymmetric plug profile.

At first sight, the difference between the predicted and measured temperatures in the ice after close-off appears to be a major failing in the model. However, temperature measurements made by Burton differed from those recorded by Tavner and showed flat

temperature distributions similar to the predicted variation. The difference can be attributed to the heat flux through the perspex window in Tavner's rig. When the temperature of the perspex drops below 0°C, water vapour in the air on the outside of the pipe condenses and freezes on the outside of the window, causing a significant heat flow. In addition, because the conductivity of ice is higher than that of water, any heat flux through the window will have a greater effect on the temperature distribution once the ice has reached the window.

The plug profiles for the 23°C freeze at 5 minute intervals during the freeze are plotted in figure 5.3, showing excellent agreement with the experimental data (again denoted by dots). The wall temperature data (which were used as the temperature boundary condition for the numerical model) and the plug profiles were measured during different freezes and therefore variations in the liquid nitrogen level account for the differences between the predicted and measured ice profiles, especially at the top of the jacket.

5.1.1.2 Discussion

The agreement between the predictions and the experimental results is excellent when the initial water temperature is less than 26°C. Freezing times are predicted to within a minute and the temperature distributions agree well with the measurements. The accuracy of the temperature predictions at the bottom of the jacket is better for the 8°C freeze than the 26°C freeze, showing that convection is becoming important by 26°C.

5.1.2 Development of Heat Flux Jacket Boundary Condition

A major part of modelling a practical problem lies in defining the conditions on the boundary of the model. The wall is cooled by the liquid nitrogen boiling inside the jacket. The liquid nitrogen enters the jacket at less than -196°C (it is stored under a slight pressure (0.5-1 barg)) and hits the jacket and pipe walls which are at room temperature. This temperature difference is so large that any nitrogen in contact with the wall boils rapidly and a layer of nitrogen vapour forms between the liquid nitrogen and the wall, which insulates the wall and liquid. As the wall cools, the temperature difference between the wall and the liquid nitrogen drops until the vapour film layer collapses and nucleate boiling takes over. This causes a sharp rise in the heat flux and a corresponding drop in wall temperature. This relationship between heat flux and temperature depends on a range of conditions, such as the surface roughness and

geometry.

The experimental results obtained by Tavner and by Burton have shown that different boiling characteristics can be obtained using the same pipe size and orientation due to differences in the width of the jacket annulus. Burton's jacket was wider than Tavner's and comparison of wall temperatures shows a faster decay inside Burton's rig and shows that the transition from film to nucleate boiling (which causes the sharp drop in wall temperature) occurs much earlier with the larger jacket. In fact, Tavner's temperature measurements indicate that the film boiling regime persisted for a large proportion of the length of the freeze. The difference between the boiling characteristics of the different jackets is attributed to the ease of dispersal of the nitrogen vapour; the larger jacket allows the nitrogen vapour to escape easily and promotes the transition to nucleate boiling. This has important implications in improving the jacket design and this is an area in which further research would be useful.

The boiling process is clearly complex and it would be beyond the scope of the present work to attempt to describe it thoroughly. It was decided to define a relationship between the heat flux and the wall temperature to simulate the nitrogen boiling in the jacket. In order to be able to use Tavner's results to validate the model, it was necessary to establish a relationship which simulated the characteristics of Tavner's jacket.

Two methods of doing this were considered. The heat flux could be calculated using Tavner's measurements of temperature, however, the spacing of the thermocouples was too large to be able to neglect axial conduction and therefore this method was rejected. Instead, the heat flux-temperature relationship was included into the model as the outer boundary condition and modified iteratively until good agreement with Tavner's wall temperature data was obtained.

The numerical model described above was modified to incorporate the steel pipe wall into the domain. This had the added advantage that the axial conduction in the pipe wall could be included. The process of filling the jacket was also incorporated, using a fill time of 2 minutes (established from Tavner's temperature measurements). The nitrogen level was assumed to increase linearly over the first two minutes, with the heat flux boundary conditions only imposed on control volumes below the nitrogen level. The boundary condition above the nitrogen level was assumed to be adiabatic; this simplification slightly underestimates the cooling rate above the nitrogen level but is only important during the filling stage. The heat flux imposed on the control volume which lay at the nitrogen surface was multiplied by the proportion of the height of the control volume which was below the nitrogen level. It was assumed that the nitrogen level in the jacket was maintained at the top of the jacket once it was filled.

The comparison between experiment and prediction should ideally be made using a situation in which convection is negligible. Tavner carried out one freeze at 2.1°C and five on water at between 17°C-20°C. (The 8°C freeze was affected by the 2.1°C freeze which had been carried out earlier that day.) At first sight, the 2.1°C freeze would appear to be the best choice, however, since only one freeze had been carried out at this temperature there was a risk that this could be an atypical freeze. The results for the freezes of water around 20°C agreed with each other well and the previous results implied that at around 20°C convection does not play an important part in the plug formation. The 20°C results were therefore selected.

The boiling curve was tuned to predict the temperature on the inside of the pipe wall half-way up the jacket. The temperature measurements from the top and bottom of the jacket were not used because, by welding the jacket to the pipe, the top and bottom walls of the jacket acted as cooled fins and the cooling was increased in these regions. The temperature measurements from the top of the jacket were also affected by any variations in the liquid nitrogen level. These effects were not included in the model and so the agreement between model and measurements was expected to be poorer in those regions.

5.1.2.1 **Results**

The relationship between heat flux and wall temperature which predicted the wall temperatures best in the 20°C freeze is plotted in figure 5.4, together with published data from Flynn et al[48] and Hanson and Richards[61].

The predictions of the inner wall temperatures at the centre of the jacket which were obtained using this relationship are plotted in figures 5.5a,b for initial water temperatures of 17°C and 2°C, respectively, together with the experimental results. The agreement between predicted and measured wall temperature at 17°C is excellent, both in terms of wall temperature decay and the transition from film to nucleate boiling. During the 2°C freeze (figure 5.5b), the predicted wall temperature drops less rapidly than the measured data and the transition from film boiling to nucleate boiling takes place over 1 minute later than recorded in the experimental data.

The heat flux correlation was used to predict freezing water initially at 23°C and the resulting plug profiles compared with those obtained using the measured wall temperatures in figure 5.6. The main difference is clear at the bottom and tops of the plug, where the plug grows axially due to axial heat conduction along the pipe wall. In addition, because the

'cooled fin' effect at the top and bottom of the jacket was not included, the plug growth in these regions was slightly slower than that obtained using measured wall temperatures.

5.1.3 **Discussion**

The solidification routines have been validated and the boiling nitrogen boundary condition has been established in a form which is easy to apply to the model. The boundary condition is specific to the boiling characteristics of Tavner's jacket but could easily be modified to use other data (eg. Flynn et al[48]) for the variation of heat flux during boiling. The agreement between the predicted wall temperatures and the measured values was good in the region away from the ends of the jacket. The differences at the top and bottom of the jacket were greater than at the centre of the jacket because the extra cooling at the top and bottom of the jacket due to the increased cooled surface area afforded by the welded jacket was not included in the model. In addition, variations from freeze to freeze in the rate at which the jacket was filled and in the success of maintaining a full jacket will cause small differences between the measured and predicted wall temperatures.

5.2 MODEL OF PIPE FREEZING INCLUDING CONVECTION

The conduction model was extended to include natural convection in the water, as described in chapter 4 and in detail by Keary[2]. The Navier-Stokes and continuity equations were solved together with the energy (enthalpy) equation to give the transient flow and pressure field development in parallel with the plug development. This added the calculations of radial and vertical components of velocity, pressure and pressure difference into the solution procedure. In addition, by including the effects of convection into the model, the length of pipe below the freezing zone which is modelled becomes more important. The act of cooling the wall causes a downwards flow next to the pipe wall and a corresponding upwards flow at the centre of the pipe with a complicated mixing region below the freezing zone. The definition of the bottom and top boundaries of the computational domain, both in terms of position and the prescribed conditions at the boundary, is therefore more important than in the case when convection is neglected. The aim of the research was to be able to predict plug formation in an infinite length of pipe in order to obtain general results. The experimental work by Burton[1] (see section 2.1.1.2) demonstrated the effect of using a short length of pipe on the bulk temperature during freezing and the corresponding effect on the plug development. However, it was not possible to solve the problem numerically using an infinitely long computational domain and therefore assumptions of the pipe length and the velocity and temperature variation on the boundaries were necessary.

In order to be able to compare the results with experimental results of Tavner[5] and Burton, a 100mm (4") diameter pipe was modelled. This determined the location of the vertical boundaries. Experience suggested that the boundary condition at the bottom of the domain was more important than that at the top of the domain. The condition of zero inflow and a maintained temperature were applied and the top boundary was positioned approximately 1½ diameters above the top of the freezing zone.

It was clear that, as there were no obvious ways of defining the velocity profile immediately below the freezing zone, the length of pipe to be modelled had to be as long as possible. The number of grid points which could be used was constrained by the available computer power and memory and increasing the grid spacing would cause a decrease in accuracy. It was decided to apply a zero inflow condition on the bottom boundary and observe the effects of the closed ends by varying the length of pipe that was modelled. As an attempt to simulate the thermal mass of water in an infinite pipe, the temperatures of the bottom and top boundaries were maintained at the initial water temperature.

This section is divided into two; firstly (section 5.2.1), the sensitivity of the solution

to certain numerical factors is investigated and the general behaviour of the iterative solution described, and in section 5.2.2, the numerical model is used to predict freezing under a series of conditions for comparison with the experimental results obtained by Tavner[5] and by Burton[1].

Two pipe geometries were modelled in the following sections. A short (630mm (25.2")) pipe with a mild steel wall was used to model the prototype rig used by Tavner. This was a 100mm (4") diameter and 600mm (24") long mild steel pipe with the jacket located centrally. It was placed inside a tank of water and lifted approximately 25mm (1") off the bottom of the tank in an attempt to allow mixing with the water in the tank and to maintain the bulk temperature inside the pipe. A longer stainless steel pipe was modelled to simulate Tavner's final rig. The final rig included a tank section located 400mm (16") below the freezing zone and therefore a long domain length was required to model the rig accurately. The choice of pipe length was limited by the required grid spacing and the computer power available. The resulting domain was 654mm long with the 'jacket' positioned 343mm above the bottom of the domain, slightly shorter than the actual rig. In both geometries the internal diameter of the pipe was 100mm (4") and the pipe wall was 5mm (0.2") thick.

Over a 200mm (8") length on the outside of the pipe, the temperature dependent heat flux was applied to simulate boiling nitrogen inside the jacket. This boundary condition was applied gradually from the bottom of the 'jacket' over the first 2 minutes to simulate the process of filling the jacket. The wall above and below the 'jacket' was adiabatic.

The thermal properties of ice and water were described earlier (section 5.1). A look-up table for the variation of density with temperature was incorporated into the numerical model, including the density inversion at 4°C. The Boussinesq-type assumption was applied, ie. it was assumed that the variation of density is only significant in the velocity source and the variation was not included in the formulation of the continuity equation. The density, conductivity and specific heat capacity of mild steel were 7950 kg/m^3, 52 W/mK and 460 J/kgK, respectively, and of stainless steel were 7810 kg/m^3, 16 W/mK and 460 J/kgK, respectively.

5.2.1 Sensitivity to Numerical Factors

Before a numerical model can be used, the sensitivity to numerical factors must be examined. In this section, the effect of varying the grid spacing in both horizontal and vertical directions is investigated together with the factor which is used to set the velocities in solid

regions to zero. Because the computer resources available were limited, the short pipe length, corresponding to Tavner's prototype rig (described above), was used for the tests. The effect of varying the time step was not investigated; a constant value of one second was used throughout this work (experience showed that freezing takes place over a time scale of greater than the order of seconds). The behaviour of the iterative numerical scheme is described in section 5.2.1.3 and the effect of the numerical phenomenon generally referred to as false, or numerical, diffusion is described in section 5.2.1.4.

The grid spacing was determined by the thickness of the thermal boundary layer in the water next to the ice; the analytical solution by Bejan[29] (Appendix I) predicts a maximum thickness at the bottom of the plug of 1-2mm for water temperatures below 60°C and Tavner's temperature measurements indicated a thickness of around 5mm. The grid spacing was also restricted by the characteristic 'stepping' movement of the ice front, which is a product of using the enthalpy method (figure 4.1).

The method used to stop the flow in solid regions has a significant effect on the accuracy of the numerical scheme because it controls the heat convected to the forming solid. The method used in this model was proposed by Voller et al[55] and was based on the Darcy equation for flow in a porous media. This was a purely numerical 'fix' and there was no implication that a mushy region was present at the interface. The momentum equation was modified to resemble the Darcy equation ($\partial p/\partial x \propto -u/\varepsilon$, where ε is the porosity), providing an extra source term in the vertical and radial velocity equations which was proportional to the appropriate component of velocity, inversely proportional to the liquid fraction and proportional to the volume of the control volume. As the control volume solidifies, this source term becomes increasingly dominant and forces the velocity to decrease in magnitude. The formulation of the source term which was employed in this research (similar to that proposed by Voller et al) is given in equation 5.1.

$$B_u = -f_v\,(e^{f_s}-1)\,\Delta V\,u, \quad B_w = -f_v\,(e^{f_s}-1)\,\Delta V\,w \tag{5.1}$$

Using an exponential gives a non-linear variation with solid fraction which causes a slow decrease in velocity as the solid fraction increases from zero with a more rapid decrease as the solid fraction approaches unity. The degree of non-linearity can be varied by including a multiplying factor in the exponential term (a larger factor will decrease the initial increase in B_u, B_w); in this analysis, this factor was set at unity. The velocity in the solidified regions is controlled by the factor, f_v; this was set such that the velocity in solidified regions was less than 0.05% of the velocity in liquid regions. This definition required knowledge of the magnitude of the coefficient for the velocity at the grid point in the discretised velocity

equations. The most significant term in this coefficient (under the conditions modelled here) was '$\rho\Delta V/\delta t$' (i.e. ~$10^3\Delta V$), giving a value of 10^6 for the factor f_v.

The effect of varying grid density is investigated and described in section 5.2.1.1; three values of grid spacing in each direction were used and the immobilisation factor was set at 10^6. In section 5.2.1.2, the effect of varying the immobilisation factor was investigated, using three values. The results are compared on the basis of the flow development, the boundary layer velocity, the bulk temperature inside the freezing zone and the interface position during the freeze.

5.2.1.1 Grid Sensitivity

Three values of horizontal grid spacing (0.5mm, 1.0mm and 2.0mm grid spacing) and three values of vertical spacing (5.0mm, 8.0mm and 16.0mm) were used. This gives 9 possible combinations of radial and vertical grid spacing. In order to simplify the exercise, the sensitivity of the radial grid spacing was investigated with the vertical spacing set at 8.0mm and the sensitivity to the vertical grid spacing was studied with the horizontal grid spacing set to 1.0mm. The results are described in the following paragraphs.

Flow Field

The development of the plug and flow field is shown in figures 5.7a-e. The notes in Appendix VI explain the general layout used in the production of these figures. In the series of plots, the development of the velocity and temperature distributions and the growth of the ice plug can be seen. These plots show a large amount of information which is discussed in more detail in the following sections and chapters. At this stage, the most important point to note is the effect of the failure to resolve the boundary layer sufficiently which is responsible for significant differences in flow field which is exaggerated by including the density inversion in the model. Flow reversal is noted in situations where the local temperature is below 4°C; smearing the boundary layer cools a larger mass of water next to the ice to below 4°C causing it to move upwards. This is visible in the flow field at 15 minutes in the 'coarse radial' (dr=2mm;dz=8mm) solution (figure 5.7d), where the boundary layer moves upwards and the core flow is downwards. Sub-cells (with the water moving upwards next to the ice and downwards away from the ice) are visible from 8 minutes onwards in both the 'coarse radial' grid (dr=2mm;dz=8mm) and the 'coarse vertical' grid (dr=1mm;dz=16mm). This change in flow field can be traced back to a thickening in boundary layer immediately below the plug

neck which can be seen at 6 minutes in the 'coarse radial' grid (dr=2mm;dz=8mm), and at 4 minutes in the 'coarse vertical' grid (dr=1mm;dz=16mm). It is just visible at 15 minutes in the 'standard' grid (dr=1mm;dz=8mm). Complete reversal of the convection cell in the freezing zone takes place at different points in time with the different grids; in the 'coarse radial' grid (dr=2mm;dz=8mm) the water flows downwards through the plug core at 15 minutes, whereas with the 'standard' (dr=1mm;dz=8mm) and 'coarse vertical' (dr=1mm;dz=16mm) grids the flow is static from 15 minutes onwards. With the finer grids ((dr=1mm;dz=5mm) and (dr=0.5mm;dz=8mm)) there is still an upwards flow through the flow core at 15 minutes.

Another difference between the five sets of results is that by 2 minutes the main convection cell predicted using the coarser vertical grid occupies a greater proportion of the pipe length than predicted using the other grids. This is because the cooled flow is smeared across a greater volume and therefore falls further. The effect is most noticeable with the coarsest vertical grid.

Boundary Layer Velocity

The measured values of peak velocity in the boundary layer were obtained by Tavner using thymol blue traces during freezing with initial water temperature of 18°C. The measurements started 8 minutes after the freeze began and continued at intervals until the plug had frozen across the pipe. Over this period the velocity decreased from around 5mm/s to zero. The decrease in velocity is partly due to the drop in bulk temperature, therefore decreasing the temperature difference between the water and the ice, and partly to the narrowing of the plug neck, which alters the flow field and decreases the flow through the plug neck.

The predicted values were obtained by interpolating the radial and vertical velocity distributions to obtain values for both components on the main grid points and then calculating the magnitude of the speed (ie. $\sqrt{(u^2+w^2)}$) at these points. The maximum speed of downwards flow near to the ice was taken as the peak velocity in the boundary layer.

The variation of boundary layer velocity during the freeze is plotted in figures 5.8a,b, together with the measured velocity data from Tavner[5], showing the effect of varying the grid density in the radial and vertical directions, respectively. The velocities are not plotted after the flow reverses (at 11 minutes with the 'coarse radial' grid (dr=2mm;dz=8mm) and at 19 minutes with the 'coarse vertical' grid (dr=1mm;dz=16mm). The two graphs clearly show that the radial grid spacing is more significant than the vertical grid spacing.

Bulk Temperature

Similar results were obtained when the bulk temperature inside the freezing zone was considered (figures 5.9a,b), with almost no difference obtained by varying the vertical grid spacing (slightly slower initial decay with finer grid); varying the radial grid spacing was more significant (with significantly faster decay predicted with the coarsest grid spacing). The values predicted using a 1mm radial grid spacing were closer to those predicted using a 0.5mm spacing than those obtained using a 2mm spacing.

Interface Position

Comparison of ice front position during the freeze and overall freezing times (figures 5.10a,b) showed almost no difference between the five sets of data (the initial freezing rate is slightly slower with the 'coarse radial' grid, possibly linked to slightly higher boundary layer velocity at around 3 minutes), showing that convection does not significantly affect freezing in this case.

Discussion

From these results, it can be concluded that the solution is more sensitive to variations in the radial grid spacing than to variations in the vertical spacing. It appears that a grid spacing of 1mm in the radial direction and of 8mm in the vertical direction gives a reasonable prediction of the flow inside the freezing zone; certainly no significant gains can be obtained with higher resolution in the vertical direction. Increasing the grid density in the radial direction has a noticeable effect on the results, with a greater effect obtained by halving the spacing from 2mm to 1mm than by decreasing the grid spacing below 1mm. The difference obtained by decreasing the grid spacing below 1mm was not considered sufficiently important to warrant the increased memory requirements and run-times of a finer grid.

5.2.1.2 Velocity Immobilisation Factor

The effect of varying the immobilisation factor (f_v) was investigated using the same test case as that used in the grid sensitivity tests[5.1]. Three tests were run, each using a 56x81

[5.1]Varying the immobilisation factor will change the level of heat apparently convected to a solidifying control volume and therefore change the solidification rate. The results obtained from the grid dependency tests showed that the bulk temperature dropped rapidly and that convection had very little effect on the solidification rate. However, because the pipe length is fixed and relatively short, (continued...)

grid (dr=1mm;dz=8mm) and velocity immobilisation factors of 10^5, 10^6 and 10^7.

Flow Field

The developing flow field through the freeze predicted using the three values of immobilisation factor are incorporated as figures 5.11a-c. The effect of changing the velocity immobilisation factor was highlighted by flow reversal. This was exhibited clearly in the predictions obtained with the 'low' factor ($f_v=10^5$) which included 9 separate subcells next to the ice plug at 8 minutes, a single complete inverted subcell at 10 minutes and full reversal by 15 minutes. The predicted flow field obtained with the 'standard' factor ($f_v=10^6$) does not include subcells; by 15 minutes the water in the freezing zone is stagnant and by 20 minutes the flow has reversed. The predictions obtained using the 'high' factor ($f_v=10^7$) were similar to those obtained with the 'standard' factor ($f_v=10^6$), with the exception that the velocities were slightly higher from 6 minutes onwards and there was still a small upwards flow through the plug core at 15 minutes.

Boundary Layer Velocity

The peak velocities in the downwards flowing boundary layer throughout the freeze are plotted in figure 5.12, together with the measurements taken by Tavner[5]. Over the first 10 minutes, the velocities predicted using the lowest immobilisation factor ($f_v=10^5$) were higher than those obtained with the higher values ($f_v=10^6$, 10^7) with very little difference between the velocities predicted using the two higher values. The boundary layer turns to flow upwards by 13 minutes with the lowest value ($f_v=10^5$) and therefore the velocities were not plotted. From 10 minutes onwards the velocities predicted using the highest value of immobilisation factor ($f_v=10^7$) were slightly greater than those predicted using the 'standard' value ($f_v=10^6$). In all cases, however, the predictions were within 1mm/sec of the measured velocities.

Bulk Temperature

The variation of average temperature inside the freezing zone (away from the ice and boundary layer) throughout the freeze is plotted in figure 5.13. From 2 minutes onwards, the bulk temperature predicted using the lowest value of immobilisation factor ($f_v=10^5$) decayed more rapidly than predicted using the higher factors ($f_v=10^6$ and 10^7). Over the initial 6

[5.1](...continued)
the 'prototype rig' model is reasonably quick to run and is therefore the most suitable model for carrying out multiple computer runs.

minutes, there is very little difference between the temperatures predicted using the two higher values, after which the bulk temperature predicted using the 'standard' factor ($f_v=10^6$) started to decay more rapidly than that predicted using the highest value ($f_v=10^7$). The bulk temperature levelled out at approximately 7°C in all three cases.

Interface Position

The interface position (minimum plug radius) throughout the freeze is plotted in figure 5.14. Differences between the three curves are minimal, due to the relative insignificance of convection on solidification in this example. The plug radius is slightly greater with the 'low' factor ($f_v=10^5$) in the period between 5 and 10 minutes than predicted using the higher values ($f_v=10^6$, 10^7), with no noticeable difference between the predicted position obtained with the two higher values of immobilisation factor. After 15 minutes, this trend reverses, with similar values of neck radii predicted using the two lower factors ($f_v=10^5$ and 10^6) which are slightly smaller than that predicted with the 'high' value ($f_v=10^7$).

Discussion

Whilst a low value of immobilisation factor results in higher velocities early in the freeze by allowing higher velocities near the ice front, the combination of the density inversion and a low immobilisation factor causes up-flowing sub-layers next to the ice front which isolate the down-flow from the ice and therefore cause a decrease in the velocity of the down-flowing boundary layer later on in the freeze. Using a low value of immobilisation factor results in the cold water next to the ice front being free to move and therefore the bulk temperature drops more quickly.

Over the first 5 minutes of the freeze, the results obtained using the two higher values of immobilisation factor appear very similar. The results obtained with the lowest value ($f_v=10^5$) exhibit higher boundary layer velocities, slightly retarded solidification and a greater decay in bulk temperature, culminating in a reversal of flow direction during the second half of the freeze. From 7 minutes onwards, differences appear between the results obtained with the two higher factors ($f_v=10^6$ and 10^7), with lower values of both velocity and bulk temperature predicted with the 'standard' factor ($f_v=10^6$). This is the opposite of the behaviour noted with the lowest value ($f_v=10^5$) where a higher bulk temperature decay was linked to higher boundary layer velocities. It appears that small variations in the velocity and temperature distributions during the first 5 minutes led to a slightly lower bulk temperature

in the lower recirculation region with the 'standard' factor ($f_v=10^6$) than with the highest factor[5.2] ($f_v=10^7$), causing lower bulk temperatures in the freezing zone later in the freeze. This in turn causes lower velocities and slightly faster freezing.

The results obtained with the lowest factor ($f_v=10^5$) clearly disagree with the experimental results. This test has not been able to show that a higher value causes significantly greater freezing rates because the effect of convection on solidification has been minimal. Caution must be used when choosing a high value because of possible adverse affects under conditions when convection is important; Hibbert et al[46] state that a discontinuous switch-off (equivalent to a very high value of immobilisation factor) causes unrealistically high freezing rates. The value of 10^6 was therefore chosen, on the grounds that it was the lowest value which produced reasonable agreement with the experimental results.

5.2.1.3 Solution Convergence

The velocity, pressure and pressure difference distributions were predicted using a line-by-line procedure which makes use of the tri-diagonal matrix algorithm (TDMA) to calculate the values of the dependent variable for all the nodes on each row (or column) simultaneously with the nodal values 'off-row' (or column) kept at the value from the previous iteration. The solution procedure then alternated between row and column solution. The velocity calculation was under-relaxed (only updated by a proportion (80%) of the predicted change in nodal values between iterations) to improve convergence. The energy equation could not be solved using the line-by-line method because there were two dependent variables: enthalpy and temperature. Instead the more primitive point-by-point procedure was used; each node was visited in turn and updated using the latest values at the neighbouring nodes. This method is more time consuming than the line-by-line method and also more prone to instability.

Modelling phase change also causes problems in solution convergence of the energy equation due to the abrupt change in properties and velocity between water and ice. This causes oscillations in the enthalpy-temperature distribution both in solidifying control volumes and also at surrounding positions. This is noted to a small extent (causing temperature variations of the order of 0.1°C) in one dimensional solidification; it is more serious in two dimensional problems (both with and without convection) with multiple control volumes undergoing solidification and oscillations in the rows above and below the solidifying control

---

[5.2]Investigations detailed in the next chapter (section 6.1.1.1) show that the main (upper) recirculation region mixes periodically with this lower region.

volume. There is also a further effect involved in convection-solidification problems when the velocity is forced to zero as the control volume solidifies. This effect is lessened by using an exponential term in the immobilisation routine.

The major effect causing oscillation was found to be the change in conductivity (0.6 W/m^2K in water to 2.2 W/m^2K in ice) at the ice-water interface and the problem was more significant in two dimensional problems. Changes in enthalpy in solidifying control volumes of the order of ±1000 J/kg (equivalent to an interface movement of approximately 3μm) were noted together with changes in temperature at surrounding nodes of several degrees (greater at the nodes above and below the solidifying control volume). Occasionally, the position of the interface oscillated between two control volumes.

The formulation of the enthalpy method used in this model assumed that the temperature at the node in a solidifying control volume remained at zero while the enthalpy decreased from the latent heat to zero; this causes a zig-zag (stepped) interface movement (see figure 4.1). This can be explained by dividing the solidification of a single CV into two stages as follows:

Stage 1: CV starts solidifying

T set to 0°C (average temperature (expected) greater than 0°C)

Ice side : temperature difference therefore heat flux is less than it should be

Water side : temperature difference therefore heat flux is greater

⇒ enthalpy decays less quickly therefore interface moves more slowly

Stage 2. CV almost entirely solidified

T set to 0°C (average temperature (expected) less than 0°C)

reverse of above

⇒ enthalpy decays more quickly therefore interface moves quickly

Hence the interface position 'steps' around the exact solution for one-dimensional solidification. This behaviour causes problems in defining the interface profile in two dimensional problems[5.3]. The conductivity around the solidifying control volume was assigned on the basis of the temperature on the sides of the control volume, giving either the conductivity of water or of ice (except between two solidifying control volumes, when the temperature gradient would be zero). If the conductivity were assigned on the basis of a smoothed interface, then the change in conductivity would be more gradual. A recent paper by Lee and Tzong[59] proposed a modified enthalpy method which supplied an even latent heat

[5.3]The smooth ice profiles shown in the figures were obtained by assuming that the average interface position (calculated by summing the liquid fractions) was located at the vertical centre of the control volume and linking these positions.

evolution during freezing (and therefore a smoother interface movement) and also included the application of a weighting scheme to deal with the jump in properties at the interface. This was published since this model was finalised; however, the model could benefit further development in this area.

This problem of oscillations in the enthalpy-temperature calculation can be minimised by only updating the conductivity distribution at the beginning of the time step. This introduces a small inaccuracy in the position of the interface, however if the time steps are sufficiently small this should not cause a significant overall error in freeze time.

A more crude method of dealing with the problem is to effectively ignore it in terms of judging convergence if a large number (around 40) iterations have been performed. There is normally a variable number of convergent iterations before the oscillations set in and therefore, by using a constant cut-off number of iterations, sometimes the interface will move forwards and sometimes it will be retarded and therefore the error in interface position should cancel out over a period of time. This method is slower than the method described in the previous paragraph because, in a two dimensional problem with a curved ice-water interface, oscillatory behaviour is encountered regularly. (Although this does ensure a high level of convergence in the other distributions.)

Predictions obtained using both methods showed no noticeable differences and the first method was used because it was faster.

5.2.1.4 **False (or Numerical) Diffusion**

False diffusion is a problem found in most numerical discretisation schemes. It is encountered in situations when the flow is not aligned with the grid direction and there is a significant gradient of the dependant variable in the direction perpendicular to the flow, resulting in a local artificially increased diffusion coefficient for the dependant variable. This problem originates from the assumption that the flow across the control volume faces is locally one-dimensional. Patankar[50] quotes an approximate relationship for the value of this extra coefficient (Γ_f) from de Vahl Davis, given in equation 5.2 which expresses Γ_f in terms of the flow velocity (U), density, grid size (Δx,Δy) and the angle (θ) between the flow and the horizontal direction.

The diffusion coefficient for water in the momentum equation, ie. viscosity, is approximately 10^{-3} kg/ms, whereas the diffusivity in the energy equation (k/c) is an order of magnitude lower (0.14×10^{-3} kg/ms). Under 'standard' conditions for the convection problem

$$\Gamma_f = \frac{\rho U \, \Delta x \, \Delta y \sin 2\theta}{4(\Delta y \sin^3\theta + \Delta x \cos^3\theta)}$$

$$\Gamma_f^{max}(\theta=45°) = \frac{\rho U}{\sqrt{2}} \left(\frac{\Delta x}{1+\frac{\Delta x}{\Delta y}} \right) \tag{5.2}$$

(Δx=1mm, Δy=8mm, U=10mm/s, $\rho=10^3$) the maximum value of the false diffusion coefficient is approximately 50×10^{-3} kg/ms, an order of magnitude greater than viscosity and two orders of magnitude greater than the thermal diffusivity. In order to reduce the false diffusivity to less than the thermal diffusivity, a grid spacing in the horizontal direction of approximately 0.04mm ($\Delta x=\Delta y$) would be required (ie. a 50mmx1000mm domain would require a 1250x25000 grid).

In the case of pipe freezing, significant angles between the grid and the flow direction and a high gradient of both temperature and velocity perpendicular to the flow direction will arise at the ends of the plug. The angle between the interface and the grid at the bottom of the plug will be greater than that at the top, partly as a result of applying the 'jacket' boundary condition gradually to simulate the process of filling the jacket and partly due to the effects of convection; in addition, the velocity is higher at the bottom of the plug. Any effects of false diffusion on the solution will therefore be most noticeable below the plug neck.

Both velocity and temperature calculations will be affected by this to some degree because both experience an increase in diffusivity; the effect on the temperature distribution will be greater than that on the velocity calculation. This will affect the temperature distribution by gradually smearing the high temperature gradient at the interface as the flow moves downstream giving an artificially thickened thermal boundary layer. The false diffusion coefficient is also proportional to the speed of the flow and therefore the effect will be more significant for higher values of initial temperature.

In addition to the top and bottom of the plug, false diffusion may also affect the solution at the point where the boundary layer flow turns off the wall to flow inwards and across the pipe before returning to the freezing zone up the centre of the pipe. At the point that the water leaves the pipe wall, there will be both temperature and velocity gradients in the direction perpendicular to the flow.

One way of avoiding false diffusion around the plug would be to use a transforming grid to model the solidification process, producing a grid which is aligned with the flow direction. This method of modelling solidification was considered (described briefly in chapter 4 and in more detail by Keary[2]) and was rejected because there were doubts as to its suitability for a problem which would include a high degree of distortion. The effect of false

diffusion can be minimised by using a discretisation scheme which takes into account the two-dimensional flow, for instance, the Skewed Upwind Differencing Scheme (SUDS) proposed by Raithby[62]. This includes more neighbouring control volumes in the discretisation scheme and therefore increases the complexity of the solution.

At this stage it was envisaged that false diffusion would produce localised effects at the bottom of the plug and cause little effect on the overall freezing time, which is controlled by the conditions at the plug neck. In the results obtained for the grid sensitivity tests (figures 5.7a-e), the angle between the grid and the ice interface increased as the ice plug grew, giving a maximum angle of approximately 25° (between the interface and the vertical direction) at 20 minutes and 35° at 25 minutes, after the plug has closed off. The angle between the flow and the grid will be greater in stainless steel pipes, because the conductivity of stainless steel is 31% of that of mild steel and therefore the plug will be confined to the freezing zone to a greater extent. There appears to be no indication of false diffusion below the plug because by the time that there is a significant angle between the grid and the flow, the bulk temperature and velocity, had decreased. The flow reversal when the temperature dropped below 4°C complicated the flow and obscured any effects of false diffusion. At the point where the boundary layer flow leaves the pipe wall there is an indication of the action of false diffusion. The locally increased thermal diffusivity increases the volume of cooled water in the region where the boundary layer leaves the wall and moves diagonally across the grid. This will tend to drag the boundary layer further down the pipe. Once the flow is moving horizontally, the flow is aligned with the grid and therefore there is no false diffusion. False diffusion is therefore responsible for making it appear that the boundary layer turns abruptly through 90° when leaving the pipe wall. This effect may be responsible for the variation in the height of the bottom of the main convection cell with grid density; the effect will be more significant with coarser grids (compare figure 5.7a and 5.7c).

5.2.2 **Validation Tests**

These tests were carried out to compare the predictions of flow field and freezing time with the experimental results obtained predominately by Tavner[5]. With the exception of the boundary layer velocities which were measured in the prototype rig, the experimental results were obtained in Tavner's final rig. This was a 100mm (4") diameter stainless steel pipe, 1m long which was placed above a tank to simulate the thermal mass of a length of pipeline. The jacket was 200mm (8") long and located 0.4m above the tank.

The numerical model of the prototype rig used the 56x81 grid used in the previous tests, giving a grid spacing of 1mm (0.04") in the radial direction and a grid spacing of 8mm (0.32") in the vertical direction. The model of the longer final rig used the same grid spacing in the radial direction; the vertical grid spacing inside the freezing zone was 8mm (0.32"), with a coarser 10mm (0.4") spacing used away from the freezing zone. The jacket was located 223mm (8.9") above the bottom of the domain. This resulted in a grid with dimensions 56x81 to model 630mm (25.2") length of pipe and 56x82 to model 654mm (26.16") length of pipe.

The following validation tests were defined to compare the experimental results with the predicted results.

1. Freezing times for initial temperatures from 0°C to 40°C.
2. Velocity in boundary layer at vertical mid-point of the jacket during freeze of water initially at 18°C (comparison with experimental results obtained in prototype pipe rig.)
3. Bulk water temperature inside the freezing zone throughout the freeze.
4. Plug profiles.

The model was run with initial water temperatures of 8°C, 18°C, 26°C and 40°C. The first three were values of initial temperature for which Tavner had performed instrumented freezes. In each case, the model was run until the ice plug had reached the centre of the pipe (ie. freeze-off); the temperature and velocity distributions were stored on the computer at the end of every 30 seconds of predicted time.

These results were presented at Eurotherm 30: Heat Transfer in Phase-Change Processes: Melting and Solidification. This paper is included in Appendix V.

5.2.2.1 Results

The results from this series of four runs were analysed using the comparison tests in order to investigate how well the model predicted the pipe freezing process. The experimental data obtained by Tavner were mainly used for comparison but some comparison with the results obtained by Burton was also carried out. The results are described in the following sections.

Freezing Times

The predicted and measured freezing times are plotted against initial temperature in figure 5.15, together with the experimental results obtained by Burton[1] and by Tavner[5].

The freeze times recorded by Burton with and without the tank are the same at 20°C but as the initial temperature increases the time to freeze increases more rapidly when the tank is included into the rig. The freeze times recorded by Tavner increase in the same way as those obtained by Burton using a tank but are consistently longer due to the differences in the jackets.

The predicted freeze times agree with Tavner's results at temperatures below 25°C because the boundary condition was established specifically for Tavner's jacket. Above 25°C, the predicted freeze times obtained when convection was included increase slightly more rapidly than those predicted when convection was ignored but much less rapidly than the measured freeze times obtained using a tank. The predicted freeze times increase with the initial temperature in the same way as those recorded by Burton when the tank was not used.

Boundary Layer Velocities

The variation of boundary layer velocity during the freeze is plotted in figure 5.16, together with the measured velocity data from Tavner[5], showing excellent agreement with the predicted velocities, with the predicted and measured velocities lying within 1mm/sec of each other.

Bulk Temperature

The bulk temperature was obtained from the experimental data by taking the temperature data at locations which lay away from the ice and the thermal boundary layer. Tavner simply averaged these temperatures; weighting the temperatures with the radius at which they were measured in order to obtain a volumetric average temperature did not affect the value significantly. These values are plotted in figure 5.17 for the 8°C, 18°C and 26°C

freezes. The predicted bulk temperatures were calculated using the temperatures at all the control volumes which lay away from the thermal boundary layer ($\Sigma(T\Delta V)/\Sigma(\Delta V)$) and also plotted on figure 5.17.

Comparison of predicted and measured bulk temperature shows that the predicted values decayed more rapidly than the measured temperature.

Plug Profiles

The predicted ice plugs are plotted in figures 5.18a-d. The ice plugs grew slightly more rapidly near the bottom of the jacket at the beginning of the freeze but appeared to be roughly symmetric by the end of the freeze. There was no great difference between the predicted profiles for the four freezes. This agrees with the observation made by Burton that the ice plugs formed in a short closed pipe are symmetric about the vertical centre of jacket.

Description of Plug Formation and Flow Field

In figures 5.18a-d, the velocity and temperature distributions during the freeze are plotted for the four freezes. The plug formation and flow field are similar in all four freezes, with the plug growing more slowly at the higher initial temperatures. The development of the flow field and the plug is first described for the 18°C freeze and then the differences in the 40°C freeze are described.

The water next to the cold wall is cooled and moves down the wall. At some point below the freezing zone, the flow leaves the wall and flows inwards across the pipe. The temperature of this flow is still lower than that of the water in the bottom of the pipe which remains at the initial water temperature. Some of the flow turns to drop down the centre of the pipe. The remainder turns and flows up the centre of the pipe. Thus two recirculation regions are established, one on top of the other. The temperature of the core flow decreased more rapidly than the temperature in the lower part of the pipe. The upper region occasionally extended into the lower section and the temperature distribution below the plug was extremely complicated. This agrees with Tavner's observations of the presence of a complex mixing zone.

Later in the freeze (at 15 minutes) a separate recirculation region can be seen above the plug neck which agrees with the three stage plug development theory postulated by Burton. However by this time, the bulk temperature has decayed significantly (and faster than measured during the experiments by Tavner and by Burton) and the flow subsides.

In the 40°C freeze, similar processes take place but the plug formation is initially much slower over the first 10 minutes and does not become significant until the bulk

temperature inside the pipe has dropped to around 10°C. The flows in the lower recirculation region are more vigorous than those for the lower temperature freezes.

The angle formed between the ice interface and the grid is approx 30° after 15 minutes in the 18°C freeze and therefore it is possible that the solution at the bottom of the plug will become affected by false diffusion. However, over this period the bulk temperature dropped to approximately 7°C and therefore convection decreased and the flow field became increasingly affected by the density inversion.

5.2.2.2 **Discussion**

The bulk temperature decay inside the freezing zone is caused by the boundary layer flow cooling the upward core flow into the freezing zone. The predicted bulk temperature decays more rapidly than the measured temperature because a smaller mass of water is cooled in the model. In the experiments with the tank, the mixing region could extend downwards to occupy a greater volume than in the model; in addition, the temperature inside the tank was maintained using heaters. The predictions agree more closely with the experimental results obtained by Burton when a tank was not included.

At higher values of initial temperature the heat transfer takes place over a longer length of pipe. The plots show that the flow falls further below the bottom of the freezing zone in the 40°C freeze than the 18°C freeze. Therefore in the higher temperature freezes the length of the domain will become more important.

No significant effects caused by false diffusion at the top and bottom of the plug were noted because the development of a significant angle between the plug and grid coincided with a significant decrease in the bulk temperature inside the freezing zone. Under the conditions where false diffusion would be expected, convection and therefore the flow field subsides.

On the basis of these results it was clear that the model was predicting convection and solidification well in a closed length of pipe and to that extent the model had been validated. However, the length of the domain which was used was inadequate to predict the plug formation at higher initial water temperatures because the bottom of the domain affected the development of the flow field.

5.3 CONCLUSIONS

A simple model of plug formation was defined using measurements of wall temperature as the boundary condition and ignoring convection. The agreement between the predictions of freezing time, temperature distribution and plug development and the experimental results was excellent at initial water temperatures below 26°C. This validated the solidification model under pipe freezing conditions.

A relationship between the wall temperature and heat flux was developed to simulate the boiling nitrogen in the jacket.

The full model of convection and freezing with a temperature dependent heat flux boundary condition was validated against the experimental results obtained by Tavner and by Burton. The agreement between the predicted and measured boundary layer velocities obtained at lower temperatures gave confidence in the convection and solidification modelling routines. At initial temperatures up to 25°C, the agreement between the predicted and measured results was excellent with the exception that the predicted bulk temperature decayed more rapidly than the measured temperature. Above 25°C, the model failed to predict the characteristic rapid increase of freezing time and predicted roughly symmetric plug profiles rather than the highly asymmetric plugs formed in the experiments. Comparison with the experimental results obtained by Burton in a closed pipe and in an open pipe placed on top of a tank showed that the problem lay in the length of pipe modelled. The pipe length modelled was too short and therefore the entire contents of the pipe were cooled and the freezing rate was increased.

There were no indications of false diffusion in the results, however it was noted that the point at which false diffusion would become important (ie. when the ice growth had caused a significant angle between the flow direction and the grid), the effect of convection had decreased because the bulk temperature had decayed.

It was therefore concluded that the numerical model was predicting convection and solidification well in a closed length of pipe but the length of the domain was found to have a significant effect on the plug formation, especially at higher initial water temperatures. This was noted in the experimental results, in which the problem was addressed by increasing the length of pipe below the freezing zone and placing the pipe above a tank in which the water temperature was maintained.

6. RESULTS

When the predictions of the flow development during solidification were examined in the previous chapter, an interesting and unexpected behaviour was observed. The cooled boundary layer ran down the wall and became warmer; however, while it was still cooler than the surrounding fluid, it became detached from the wall and turned to flow inwards. The outer layer continued to fall down the pipe, away from the pipe wall and the rest turned to flow up the centre of the pipe, decreasing the bulk temperature inside the freezing zone. Thus a recirculation cell was established with cooler and therefore more dense fluid apparently supported above warmer, less dense fluid. This flow structure remained throughout the freeze, although the size of the convection cells and flow pattern within them was observed to vary.

In this chapter, the development of this flow field is investigated and the mechanisms which control it are discussed (section 6.1). In section 6.2, the interaction between the flow field and plug formation is investigated for different initial water temperatures, different lengths of pipe and with different boundary conditions (this forms the main bulk of the results of this thesis). The results obtained when flow was allowed across the bottom boundary of the numerical domain are described in section 6.3. The understanding of the processes involved in pipe freezing obtained from the analytical model are employed to define a 'map' of the recommended modelling method over a range of pipe sizes and initial water temperatures. This is described in section 6.4 and the results from the chapter are summarised in section 6.5.

6.1 STUDY OF NATURAL CONVECTION WITH NO FREEZING

In order to investigate the factors which control this flow pattern, the model was simplified. The freezing process was not included and the wall was removed from the domain, with an adiabatic boundary condition imposed above and below the jacket position. The jacket was simplified to an isothermal 0°C wall section. The top and bottom of the domain were assumed to be isothermal at the initial temperature.

The same flow pattern was observed in this simplified situation, showing that it was unrelated to the solidification process. The model was run for a series of conditions to investigate the effect of pipe diameter, length and initial water temperature on the convection patterns. (Simulations were also carried out for a rectangular vertical duct with a cooled section of wall and similar results were obtained, showing that the flow pattern is not restricted to the radial geometry.)

6.1.1 Description of Flow Field

The underlying processes are discussed for convection in a 100mm (4") diameter pipe containing water initially at 20°C with a 200mm (8") section of cooled wall (referred to as the 'jacket'). This is used as the 'standard' and the variations on this caused by diameter, length and initial temperature are described in the following sections.

6.1.1.1 Development of the Flow Field

The predicted flow in a 100mm (4") diameter pipe containing water initially at 20°C is shown in figures 6.1a-d. The development of the flow over the first 2 minutes at 5 second intervals is shown in figures 6.1a,b and the flow structure at half minute intervals over a 10 minute period is shown in figures 6.1c,d. The development of the velocity and temperature distributions is described in the following paragraphs.

This flow development appears to be a complex interaction of various transient processes, which are described in detail below. This description represents the Author's current understanding of the process. In an attempt to make the description clearer, key points are highlighted using *italics*.

By imposing 0°C on the wall, a small flow was induced and a convection cell established. Over the first 15 seconds this cell becomes distorted; it stretches downwards as the velocities increase and becomes distorted at the top in order to feed the flow as it accelerates down the wall and the centre of recirculation drops down the cell. The flowrates increase over the time period, especially below the cooled zone where the thickening of the layer of downwards flowing water causes a corresponding increase in upwards flow.

The velocity, streamline and temperature distributions at 15 seconds are shown in more detail in figure 6.2a, where the area of interest has been expanded. In the isotherm plot, the thickening of the thermal boundary layer down the 'jacket' is clearly visible. The average temperature in the boundary layer when it leaves the wall is approximately 18°C. The boundary layer flow is sandwiched between the pipe wall on its outer face and the core flow moving in the opposite direction on its inner face. The shear at the interface between the boundary layer and the core flow decelerates the boundary layer flow and opposes the buoyancy forces, making the boundary layer turn off the wall *before it has warmed up to the initial temperature*. There appears to be a maximum thickness for both layers, when an increase in the thickness of one layer will reduce that of the other, which forces a large

increase in the velocity in that layer to maintain the flowrate and therefore increases the shear at the interface between the two flows. The maximum thickness of the boundary layer (in these results) is approximately 16mm, 32% of the pipe radius.

Closer inspection of the flow field at 1 second intervals (not included here) shows that the temperature of the flow leaving the wall decreases gradually. Over the next 5 seconds the cell stretches further downwards and a separate recirculation region forms below the point at which the boundary layer leaves the pipe wall (note the upwards flow at the wall at 20 seconds in figure 6.2a). This is formed because the water immediately below the main convection cell is cooled (by the cooled water leaving the wall) and drops, causing an up-flow next to the pipe wall. *This up-flow pushes the boundary layer flow off the wall,* augmenting the shear effect and pushing the boundary layer inwards. As time goes on the temperature of the boundary layer when it leaves the wall decreases further (all these processes develop gradually and therefore the decrease in temperature is not sudden) and this therefore drives the separate recirculation region further. *The separate region gradually increases in size, pushing the diverted boundary layer towards the centre of the pipe. This effectively decreases the pipe diameter and therefore 'chokes' the boundary layer flow.* A portion of the flow, consisting of the cooler, outer part of the boundary layer, continues to move downwards, forming a secondary region; this is balanced by a return flow moving rapidly up the centre of the pipe. The remainder of the boundary layer, which is still below the initial bulk temperature, is turned to move back up the pipe to the freezing zone, *causing the bulk temperature to decay.*

The early stages of this development are visible at 25 seconds (figure 6.2b). Complex flow patterns form within the main convection cell which interfere with and destroy the thickening of the down-flowing layer below the cooled zone. Although the thickening of the boundary layer was initially responsible for the development of the separate region, once the separate region is established it is stable.

The secondary region gradually (approximately linearly) stretches down the pipe, together with the separate region. The height of the bottom of the main convection cell levels out over the second minute (see figure 6.1b) and the bulk temperature inside the freezing zone decays. When the secondary region reaches the bottom of the domain (at 120 seconds), it breaks off the main region and falls down the pipe, separating the two regions. The lower region slowly stabilises, stratified, with the cooler cell dropping to the bottom. At around 4 minutes, the flow in this region has subsided and the cooled flow from the main convection cell starts to extend into the lower region again. There is therefore a periodic motion, with the secondary region forming, dropping to the bottom, and breaking off. The height of the

bottom of the main cell varies as the flow patterns change, moving upwards when the regions are separate and dropping down as the secondary section reforms.

When the main cell is separate, the rate of bulk temperature decay in the cooled zone increases. When the secondary region reforms the decay rate decreases. In the closed length of pipe modelled here the lower region is cooled and so the decay rate is greater than it would be if the pipe was infinitely long.

In summary, the development of the flow can be described in three stages, depicted in figure 6.3. During the first stage a convection cell is established which stretches downwards as the velocities increase. The thickness of the down-flowing layer increases and reaches a critical size when interference between the down-flow and up-flow occurs. This marks the beginning of the second stage. The shear between the boundary layer and the core flow opposes the movement in the boundary layer, with the result that the boundary layer turns and moves upwards when it is still cooler than the initial temperature. This sets up a separate recirculation region immediately below the position at which the boundary layer leaves the wall, causing an up-flow at the pipe wall which forces the boundary layer off the pipe wall. The boundary layer is diverted around this new separate region, which continues to grow and partially blocks the pipe. The outer cooler part of the boundary layer continues to fall down the pipe (forming the secondary region), returning to the freezing zone as a relatively fast, 'hot' core flow. The inner part of the boundary layer turns to move up the pipe to the freezing zone, resulting in a decay in the bulk temperature inside the freezing zone. In the case of water initially at 20°C in a 100mm (4") diameter pipe, the point at which the boundary layer leaves the wall stabilises. The secondary section stretches down the pipe and when it reaches the bottom (stage 2a in figure 6.3) it breaks off from the main cell and falls down the pipe. During the third stage, the top region is separate from the bottom and the flow in the lower part of the pipe slowly subsides. The bulk temperature decays more rapidly. The second and third stages then repeat with the secondary section reforming, stretching down the pipe and dropping off. Throughout the process, the temperature inside the pipe and especially in the cooled zone decreases and therefore convection subsides and the stages become less distinct.

6.1.1.2 Comparison with Predictions from PHOENICS and Flow-3D

These results were compared with the predictions of the flow development obtained using two general purpose commercial CFD packages; PHOENICS-1.4 (shareware version of the 1987 PHOENICS code) and Flow-3D. These packages were both used to model natural

convection inside a pipe with a cooled section of the boundary. The flow development over the first 30 seconds was modelled for a 100mm (4") diameter pipe containing water initially at 20°C. The resulting flows developed in the same way as those described above. These results are described in more detail in Appendix III.

6.1.1.3 Effect of Pipe Diameter on Flow Development

In the description of the flow development above, two controlling mechanisms were isolated: shear between the boundary layer and the core flow, and a choking effect, with the separate cell reducing the working area of the pipe and turning cooled water back up the pipe to the freezing zone. Both effects will become weaker in larger diameter pipes although shear between the boundary and the core flow will become significant in the freezing zone when the plug reaches a critical size. The following study of the effect of varying the pipe diameter on the flow development is split into two: firstly, the flow development over the initial minute was studied to confirm that these effects become weaker in larger pipes and secondly, the flow development and bulk temperature decay over 5 minutes are described.

Initial Flow Development

The flow development was predicted in pipes of diameter 50mm (2"), 100mm (4"), 150mm (6") and 200mm (8") using a constant cooled wall length of 200mm (8") to give similar conditions in the boundary layer. The cooled wall length was fixed rather than scaled with the pipe diameter in order to investigate the effect of the pipe diameter on the flow development without varying the conditions in the boundary layer. The results were plotted at four points in time which approximately spanned the time at which the second stage started. Two criteria were used to select this point: the point at which an up-flow first appeared next to the outer boundary and secondly, the point at which water at below 19°C started to move upwards in the core flow. The velocity, isotherm and streamline plots are shown in figures 6.4a-c. Several key points can be extracted from these plots; the second stage can be seen to start earlier in smaller pipes and the length of the convection cell at this point is correspondingly smaller. The velocity of the core flow is greater in the smaller pipes (as expected) and the boundary layer thickness when the second stage starts is approximately one third of the pipe radius in all cases. Comparison of the velocity (and streamline) plots and the isotherm plots (figures 6.4a-c) show that the appearance of the lower separate recirculation cell has less effect on the temperature distribution in the larger pipes; for instance, at the point

(16 seconds) at which an up-flow becomes visible in the 50mm (2") diameter results, the temperature of water moving up the centre of the pipe is in the range 16-20°C and is decreasing steadily; at the equivalent point in the flow development in the 200mm (8") diameter pipe the water temperature in the core is greater than (approx.) 18.5°C. These results are drawn together in figure 6.5, showing the height of the bottom of the main convection cell against time for the four pipe sizes, together with the temperature in the boundary layer when it leaves the wall. In the 50mm (2") diameter pipe, the bottom of the main convection cell levels out and there is a significant decrease in the temperature of the water leaving the wall (by 30 seconds the temperature is 7°C below the initial temperature). The effect is still significant in the 100mm (4"); by 30 seconds the temperature of the water leaving the wall is 3½°C below the initial temperature and over the next minute the main convection cell gradually levels out. As the pipe diameter increases, the effect both on the position of the convection cell and on the temperature of the water leaving the pipe wall decreases and it can be concluded that in pipes above 200mm (8") in diameter, the separate cell will form but will have little effect on the resulting velocity and temperature distributions.

In summary, the boundary layer thickness increases rapidly until the shear between the core up-flow and the boundary layer becomes significant; this takes place slightly later in larger pipes giving a corresponding increase in the length of the convection cell. Once this has happened, a separate cell forms below the main cell which diverts the boundary layer from the wall. In a small pipe, this occupies a significant proportion of the pipe and therefore starts to block the pipe and forces most of the boundary layer to turn and move up the pipe; the height of the bottom of the main cell levels out. In larger pipes, the separate region exists but has a weaker effect on the velocity and temperature distributions, so that the main cell continues to fall down the pipe and there is less decay in bulk temperature. It appears that in pipes greater than 200mm (8") in diameter (with 200mm (8") cooled wall) the effect on the conditions in the freezing zone will be negligible.

Flow Development over 5 minutes

The effect on the flow development over a longer term was also investigated under the realistic conditions of scaling the jacket length with the pipe diameter. This is normal pipe freezing practice and the length of the jackets used in the experimental programme were twice the diameter of the pipe. In order to investigate the flow patterns inside different diameters of pipe, the cooled wall length was scaled accordingly. The flow development was predicted over a 5 minute time interval using pipe diameters of 50mm (2"), 150mm (6") and 200mm

(8"); the length of the domain was defined so that the length of pipe below the jacket was constant and the same as that used in the predictions obtained for the 100mm (4") diameter pipe.

Figure 6.6a shows the development of the flow pattern over 5 minutes in the 50mm (2") diameter pipe containing water initially at 20°C. The development of the flow patterns is similar to that in the 100mm (4") pipe, but the height of the main convection cell levels out higher than that in the 100mm pipe (approximately 120mm (4.8") below the jacket bottom compared to 170mm (6.8") in the 100mm (4") diameter pipe) and the bottom of the secondary cell drops more slowly. The secondary region hits the bottom (approximately 730mm below the jacket bottom) in around 3 minutes and breaks off, reforming by 4½ minutes. The maximum thickness of the down-flowing layer is 8mm at 10-15secs (32% of the pipe radius).

Figure 6.6b shows the development of the flow pattern in a 150mm (6") diameter pipe. The flow pattern is similar but the secondary region reaches the bottom of the pipe before the height of the main convection cell stabilises. The maximum thickness of the down-flowing layer is 25mm (at 20-25 seconds), 33% of the pipe radius. It is interesting to note that the flow does not reach the bottom of the domain until sometime between 2 and 2½ minutes, later than in the 100mm (4") diameter pipe. This is discussed below.

The flow development in the 200mm (8") diameter pipe is plotted in figure 6.6c and is similar to that in the 150mm (6") pipe. The height of the bottom of the main convection cell does not stabilise before the flow reaches the bottom of the domain (again between 2 and 2½ minutes). The maximum thickness of the down-flowing boundary layer is 33.5mm at 30secs (33.5% of the pipe radius).

The bulk temperature decays more rapidly in smaller pipes. In figure 6.7, the average temperature in the cooled region (away from the boundary layer) is plotted against time for the 50mm (2"), 100mm (4"), 150mm (6") and 200mm (8") diameter pipes for the time prior to the flow reaching the bottom of the domain. The trend of bulk temperature decay from measurements for Tavner's instrumented 19.7°C freeze is also plotted. This demonstrates that in pipes of 150mm (6") diameter and above there is very little decay in bulk temperature and also shows good agreement between the predicted and measured temperatures in the 100mm (4") diameter pipe over the first 2 minutes, at which point the secondary region reaches the bottom of the domain.

The length of time for the flow to reach the bottom of the domain is controlled by the rate at which the main convection cell drops down the pipe and the rate at which the secondary region drops down the pipe. In the 50mm (2") and 100mm (4") diameter pipes, the bottom of the main convection cell levels out and the extension of the mixing region is

determined by the secondary region. The main region levels out higher in the smaller pipe (in addition, the velocities are lower because the cooled wall length is shorter) and therefore the flow takes longer to reach the bottom of the domain. The length of time for the flow to reach the bottom of the domain in the 150mm (6") and 200mm (8") diameter pipes is primarily controlled by the main region, which stretches down the pipe relatively slowly. It therefore appears that the case of the 100mm (4") pipe diameter is a maximum for the rate at which the flow drops down the pipe.

In summary, the maximum thickness of the down-flowing layer was approximately one third of the pipe radius when the initial water temperature is 20°C. The 'choking' effect is greater in smaller diameter pipes, where the main convection cell stabilises at a higher level and the bulk temperature decays more rapidly. Above 150mm (6"), the effect is not sufficiently strong to stabilise the height of the main convection cell.

6.1.1.4 Effect of Initial Temperature on Flow Development

The flow patterns in the 100mm (4") diameter pipe were predicted for initial temperatures of 10°C and 30°C. These velocity and streamline plots are shown in figures 6.8a,b.

The maximum thickness of the boundary layer decreases with the water temperature; 18mm, (36% of the pipe radius) at 10°C, 16mm (32%) at 20°C and 13mm (26%) at 30°C. The higher velocities at higher temperatures result in increased shear between the two layers and therefore decrease the critical boundary layer thickness.

The variation of height of the bottom of the main convection cell with time for different initial temperatures is shown in figure 6.9. As the temperature increases, the buoyancy forces increase causing the main convection cell to drop further down the pipe. When the initial temperature was above 30°C, the height of the bottom of the main cell did not appear to level out before the secondary region reached the bottom of the domain.

The distances between the bottom of the jacket and the tank used by Burton and by Tavner are also marked on figure 6.9. As a result of positioning the tank at different distances from the freezing zone, the bulk temperatures inside the freezing zone decayed at different rates. To quote Tavner[5] "the results from Burton's work show that bulk temperatures in the earlier rig were well maintained by heat exchange with the reservoir" (Burton's coldest freeze using the tank was 20°C) and (from Tavner's work) "...it appeared that the mixing region was not extending as far as the tank at temperatures below about 30°C". This is explained by the

predicted flow development. The break-point at which the main region would enter the tank is slightly above 20°C in Burton's rig compared to somewhere between 25°C and 30°C in Tavner's rig. Similar trends are noted when the freezing times obtained in the two sets of experiments are compared; Tavner's measurements start to increase more rapidly above around 25°C, slightly higher than the temperature at which Burton's freeze times start to increase more rapidly.

The bulk temperature inside the cooled zone initially decays more rapidly for higher initial temperatures. The heat flux from the water to the cooled wall is proportional to the temperature difference between the water and the cooled wall and therefore the temperature decay rate is higher for higher initial temperatures. This agrees with the predictions obtained using the simple analytical flow model described in chapter 3.

6.1.1.5 Effect of Pipe Length on Flow Development

The importance of the pipe length is linked to the effect of the secondary section hitting the bottom of the pipe. When this happens the bulk temperature both in the cooled region and in the lower section of pipe decays more rapidly. There is a rapid drop in bulk temperature when the secondary region reaches the bottom of the pipe because the main region becomes isolated from the water below.

If the pipe length is so short that the main cell reaches the bottom during the first stage then the convection cell occupies all the pipe and the water inside the pipe stratifies, cooling the entire contents of the pipe. If the pipe length is such that the bottom of the main cell is only a few pipe diameters above the bottom of the pipe when the secondary section forms then the secondary section reaches the bottom of the pipe quickly and breaks off from the main region giving a single recirculation region in the lower region. The secondary region does not reform.

The situations in which the domain lengths modelled here would be sufficient to model an infinite length are those with temperatures below 20°C in the 100mm (4") diameter pipe (with a slightly larger temperature range in the 50mm (2") diameter pipe and a smaller range in larger pipes). In these situations, the flow will not reach the bottom of the pipe over a large proportion, if not all, of the freeze time. Therefore in situations conditions where convection has a significant effect on freezing, the conditions below the freezing zone are important.

6.1.1.6 Implications to the Analytical Model

The predictions obtained from the numerical model have shown that, in pipes less than 200mm (8") diameter, the flow development is affected by a 'choking' mechanism which increases the bulk temperature decay. The analytical model (chapter 3) was developed without including this flow development; this will be responsible for the poor agreement between the analytical and experimental results. In addition, Tavner's[5] inference of the length of the mixing region, which was used to estimate this heat transfer, was not correct because he judged that it was not possible for the secondary region to enter the tank if the bulk temperature decayed.

The predicted flow development in a 100mm (4") diameter pipe is more complex than that assumed in the analytical model. The mixing processes (and effect of diameter and initial temperature) would be very difficult to formulate into the analytical model. However, if the main interest lies in larger pipes, the results from studying the flow development show that the bulk temperature decay will decrease in the larger pipes and therefore the analytical model which assumed a maintained bulk temperature (section 3.1) would provide a reasonable estimate of the freezing behaviour, subject to the limitations described in full in chapter 3.

6.1.1.7 Comparison with Experimental Results

There are no experimental results which directly confirm the predicted flow field, however, there is indirect corroboration for these results, as follows:

The height at which the bottom of the main convection cell levels out in a 100mm (4") diameter pipe at different initial temperatures can be correlated against the effect of varying the location of the tank on the bulk temperature. This was described in detail in section 6.1.1.4.

The predicted development of the flow field limits the heat transfer with the water away from the freezing zone, increasing the decay in bulk temperature in the freezing zone. The predictions agreed with the experimental results up until the flow reached the bottom of the pipe (in the predictions). This was shown in figure 5.17.

To obtain experimental confirmation of these results, the flow and/or temperature in the mixing region below the freezing zone must be monitored using flow visualisation techniques such as those applied by Tavner[5] to the flow in the freezing zone. The fast core up-flow could not have been noted by Tavner because he observed the flow across a

horizontal chord located away from the perspex plate (it is also possible that the presence of the perspex front plate may have altered the flow pattern).

Both Burton and Tavner measured the temperature inside the freezing zone using an array of thermocouples and therefore their results were examined to see whether there were signs of a warmer core flow. Burton located the tank close to the freezing zone and therefore the boundary layer would have entered the tank, destroying the 'choking' mechanism. Examination of Tavner's data shows that the column of thermocouples near the centre of the pipe consistently read between 0.5 and 1°C greater than those at the neighbouring locations, however, the proximity to the front perspex plate and the possible effect of this on the local flow makes it difficult to draw definite conclusions.

6.1.2 **Boundary Layer: Comparison with Integral Solution**

The predicted boundary layer velocities and the heat transfer coefficients were extracted from the results obtained for the flow development in a 100mm (4") diameter pipe at the mid-point of the jacket and compared with the values predicted using the integral solution for convection over a flat plate by Bejan[29] (see Appendix I). This analytical solution was derived assuming that the fluid properties (ρ, β, υ, k, c) were constant which is not true for water; the values of velocity and of heat transfer coefficients were calculated using the properties halfway between the initial temperature and the cooled wall temperature (0°C).

A difference between the numerical predictions and integral solution for boundary layer velocity was anticipated due to the difference in conditions at the top of the jacket in the two models. The flat plate solution assumes that the boundary layer velocity is zero at the top of the cooled plate (or at the bottom of the heated plate), which is not the case for convection inside small diameter pipes. The numerical model predicted a fast core flow in a 100mm (4") diameter pipe which continues (slowing down) above the freezing zone; this causes a corresponding flow down the outside of the pipe, with the result that the water above the top of the jacket is not static. The boundary layer velocity will be slightly greater than the integral solution. The core flow and therefore the velocity at the top of the jacket will decrease in larger pipes. Figure 6.10 shows the relationship between the maximum boundary layer velocity and the bulk temperature. The velocities predicted by the numerical model are slightly greater (approximately 2mm/s) than the analytical solution but lower than those predicted using the fluid properties at the bulk temperature.

The heat transfer coefficient was calculated from the numerical predictions of the

temperature distribution, assuming a linear temperature profile. Figure 6.11 plots the heat transfer coefficient against bulk temperature; the values obtained by Tavner[5] are also included in the figure. The numerical predictions lie within the scatter of the experimental results at bulk temperatures below 18°C, rising to approximately 50% greater than the experimental values at 26°C.

The integral solution for the heat transfer coefficient fits the relationship given in equation 6.1.

$$\textit{flat plate:}\quad h(z) = 25.880\ T_b^{0.680}\ z^{-0.25} \tag{6.1}$$

The heat transfer coefficient obtained from the numerical data obtained in a 100mm (4") diameter pipe fits the following relationship (see Appendix I). (This was based on the assumption that the relationship between heat transfer and cooled wall length is the same as the flat plate theory.)

$$\textit{numerical:}\quad h(z) = 18.594\ T_b^{0.707}\ z^{-0.25} \tag{6.2}$$

The 'numerical' heat transfer coefficient is approximately 72% of the 'flat plate' value. This is probably due to the density inversion at 4°C which decreases the velocity immediately next to the ice and therefore decreases the heat transfer. The 'numerical' heat transfer coefficient at the centre of the jacket is approximately equal to the 'flat plate' value at the bottom of the jacket.

Repeating the calculation for maximum temperature (chapter 3) with this relationship for heat transfer coefficient gives a maximum temperature of 70°C with the neck at the bottom of the jacket (A_h=1) and 63°C (A_h=½) in a 100mm (4") diameter pipe. The former moves the position at which the 'critical effective heat flux' crosses the line defined by critical Grashof number to a smaller pipe diameter (approximately 75mm (3")), subject to the limitations imposed by neck migration.

6.1.3 **Conclusions**

The development of the flow field has been investigated and three stages in the process have been described. The controlling factors have been isolated and the effect of the pipe diameter and length investigated.

A mechanism has been isolated which limits the size of the main convection cell; this is caused by the formation of a separate convection cell below the main cell which partially blocks the pipe. This alters the flow field such that the cooled flow leaves the wall and flows back up the centre of the pipe, resulting in a temperature decay in the cooled zone. The cooler outer part of the boundary layer continues to fall down the pipe diverted by the separate region, and a secondary region forms which quickly stretches down the pipe. The separate convection cell supports the main cell by providing a flow up the wall. When the secondary region reaches the bottom of the domain (with zero inflow boundary condition), it becomes separated from the main cell and falls down the pipe. The flow field in the lower region gradually stabilises. When the flow has subsided, the secondary region reforms and the process repeats itself periodically. The temperature in the cooled zone decays more rapidly when the two regions are isolated than when the secondary region exists, because there is mixing with the bulk of water below the main region. The temperature in the lower region gradually decays and therefore all the water inside the pipe is cooled.

The same flow development was predicted using two general purpose CFD computer packages (PHOENICS and Flow-3D); this is described in more detail in Appendix III.

Increasing the pipe diameter reduces the 'choking' effect; the separate recirculation region forms but has less effect on the subsequent flow development. The predictions imply that these processes will have negligible effect on the flow development in pipes above 200mm (8") in diameter; in such conditions the boundary layer will continue to fall down the pipe until the temperature is near ambient (initial). Any decay in bulk temperature under these conditions will be due to heat loss from the core flow to the boundary layer flow, which will also decrease in larger pipes (where the boundary layer is less significant).

An increase in the initial water temperature will increase the buoyancy forces which drive the flow development and therefore will increase the size of the main convection cell.

The numerical predictions showed that the flow development is complex and varies with temperature and pipe diameter. Attempting to include this in an analytical model would be difficult.

6.2 STUDY OF FREEZING WITH NATURAL CONVECTION IN A CLOSED PIPE

In this section, the effect of including plug formation was studied. The processes involved in the plug formation were studied and the effect of varying the values of the key parameters was investigated. The factors which were considered to be important were the pipe diameter and length, the initial water temperature, and the boundary condition on the outside of the pipe inside the freezing jacket and above and below the jacket. The parameters selected for this study were the pipe length, initial water temperature and the boundary condition inside the jacket.

The effect of increasing the pipe diameter was not investigated. This had been studied in the absence of solidification and it was shown that the convection cell stretched further down the pipe in larger pipes. This, combined with the proportional increase in jacket size, meant that there would be a substantial increase in the size of the numerical domain and it was decided that this was not possible given the computer power available. The effect of varying the boundary condition above and below the jacket, in order to model heat transfer with the surroundings, was not investigated in depth. The heat fluxes involved with heat transfer with air are low; Simonson[63] indicates heat transfer coefficients of approximately 1.6 W/m^2K for a 100mm (4") diameter pipe in air at 20°C, giving maximum heat fluxes of around 32 W/m^2 under these conditions compared to around 20 kW/m^2 to the liquid nitrogen. In the following investigations, the pipe was assumed to be perfectly lagged above and below the freezing zone.

Values of initial water temperatures between 8°C and 40°C were used. The results for initial temperatures of 8°C, 18°C, 26°C and 40°C had been obtained as part of the validation procedure (chapter 5) and these four values of temperature were used in the other parametric tests.

The predictions of the flow field detailed above (chapter 5 and section 6.1) indicated that the length of pipe was important to the freezing process because of its effect on the bulk temperature of the water in the freezing zone. The effect of increasing the length of pipe below the jacket was investigated. Several domain lengths and grid sizes were used throughout the development of the model, however, the results which are presented here were obtained using two lengths of pipe.

The final parameter which was studied was the definition of the boundary condition which simulated the liquid nitrogen boiling inside the jacket. The predictions of freezing described in the previous chapter (chapter 5) applied the boundary condition which had been

developed to simulate Tavner's freezing jacket. For comparison, the effect of applying an isothermal (-196°C) boundary condition was investigated. This was a 'best case' to describe a highly efficient jacket design.

6.2.1 Effect of Initial Temperature and Domain Length

The effect on the velocity and temperature distributions of varying the initial water temperature and the pipe length were investigated applying the heat flux correlation described in chapter 5 as the boundary condition. Four values of temperature and two pipe lengths were used, giving eight sets of results. The plug formation and flow field in the short (654mm long) pipe were available from the validation exercise (chapter 5). The models were redefined to describe a longer pipe length (1094mm) and used to predict the plug formation with the same four values of initial temperature.

The resulting distributions were examined in three ways, studying the development of the flow field during the freeze and also the interface position and bulk temperature inside the freezing zone away from the interface.

6.2.1.1 Temperature and Domain Length: Effect on the Flow Field

In the preceding sections the flow pattern induced by convection in the pipe without freezing was studied. The existence of a mechanism which acts to keep the cooled water in the area of the freezing zone was discovered and investigated. The effect of the initial water temperature and the pipe diameter was found to be important in determining the volume of water which is cooled. Some differences between the no freezing and freezing situations were expected, partly because of the slight difference in the boundary condition and also due to the distortion of the shape of the water region by the forming plug. However, in general it was expected that the results of varying the initial temperature, pipe diameter and pipe length obtained for the no freeze situation would be equally applicable to the situation with freezing.

The flow and plug development predicted using the short pipe length are shown in figures 5.18a-d (chapter 5). The results obtained in the longer pipe length are shown in figures 6.12a-d. In order to make the results clearer and to allow direct comparison with the results obtained in the short pipe length, the results in the top section of the pipe (corresponding to the domain of the short pipe model) were plotted in figures 6.13a-d. These figures contain a

large amount of information concerning the development of the flow field, temperature distribution and plug formation.

There are similarities between all the results obtained, with the general flow development following the three stage scheme described above (section 6.1.1.1). The time at which the different stages began varied with the different pipe lengths and initial temperatures. The results from the eight sets of data are summarised in the following table.

	8°C		18°C		26°C		40°C	
Time at :	Short	Long	Short	Long	Short	Long	Short	Long
End of stage 1 (mins)	2	2	1	1	1	1	1	1
End of stage 2 (mins)	7 (5½)[1]	12½ (11)[1]	2	3½	2	2½	1½	2
End of stage 3 (mins)	7½	(16½)[2]	4	9½	3½	5	SEP[3]	SEP[3]
Repetitions 2-3? (YES/NO)	YES	NO[2]	YES	YES	YES	YES	NO	NO
Dist. between btm of main cell to btm of jacket (mm)	84	84	116	100	124	116	156	140
$r_{neck} \leq 45mm$ (mins)	3	3	4	4½	6	8	9½	15
T_{bulk} @$r_{neck} \leq 45mm$ (°C)	8	8	14	14	16	16	16	19
Time to freeze (mins)	19½	19½	22	23½	24	28½	28½	37

The superscripted numbers refer to the following notes :

1. The number in brackets is the time at which the flow reached the bottom of the pipe. In all other cases, this coincided with the end of the second stage.
2. In the 8°C simulations, the flow field developed in a different way after one cycle was completed. In addition, sub-cells appeared next to the ice plug where the temperature was below 4°C.
3. In the 40°C simulations, the flow in the lower region did not subside and the two regions remained separate after the flow reached the bottom of the pipe for the duration of the freeze.

The flow field development and the plug formation were similar irrespective of initial temperature and pipe length. The flow field developed through the three stages and was accompanied by a bulk temperature decay. When the temperature in the freezing zone dropped to around 15°C, the layer of ice on the wall became noticeable. The flow subsided more rapidly in the shorter length than in the longer length, partly because the bulk temperature inside the freezing zone decayed more rapidly in the shorter pipe and partly because the secondary region, which provided a temporary relatively warm core flow, did not reform as often in the shorter pipe as in the longer pipe length. The main convection cell dropped slightly further in the short pipe length.

As the plug forms, the main recirculation region becomes distorted and as the water flows through the neck of the plug, interference between the up flow and down-flow takes place, forming subcells inside the main region above and below the plug neck. The water above the plug neck becomes increasingly isolated from the water below the neck and the temperature drops. After freeze-off, the recirculation at the top of the plug subsides giving stratified layers above the plug in the temperature range below 4°C and recirculation above that. Immediately below the plug in the water at 0-4°C the recirculation persists.

The flow field development was similar to that observed in the absence of freezing with the exception that there was a significant difference in the height at which the convection cell levelled out. This was higher with freezing than without to the extent that, even when the initial temperature was 40°C, the main convection cell levelled out above the position of the tank in Burton's and Tavner's experimental rigs. A possible reason for this is discussed in section 6.2.4.

6.2.1.2 Temperature and Domain Length: Effect on the Freezing Time

The freezing times obtained with the four values of initial temperature (8°C, 18°C, 26°C and 40°C) and the two domain lengths (654mm and 1094mm) are plotted in figure 6.14. The freezing times recorded by Tavner are also plotted. There is little or no difference in the freezing times at low initial temperature (8°C) but as the initial temperature is increased the freeze time in the longer pipe increases more rapidly than that in the shorter pipe, rising to nearly 10 minutes difference at 40°C.

There are therefore two effects; increasing freeze time with increasing length of pipe and increasing difference in freeze time between the two pipe lengths with initial temperature. The first is due to the fact that the bulk temperature inside the freezing zone drops more rapidly in a shorter pipe, thus giving faster freezing for the same value of initial temperature. The difference between the two values of predicted freeze times increases with initial temperature due to the increasing importance of convection at higher temperatures.

The experimental results indicate that there is a rapid rise in freezing time with increasing initial water temperature above 25-30°C. The numerical predictions, with both pipe lengths, failed to duplicate this behaviour because the water temperature in the freezing zone dropped more rapidly in the numerical simulation than in the experiments. This was partly due to the fact that the numerical model used a closed length of pipe and therefore included a smaller mass of water. The measured freezing times may also over-estimate the freezing time in an infinite pipe by including a tank in the rig and maintaining the temperature of the water in the tank using heaters.

6.2.1.3 Temperature and Domain Length: Effect on the Freezing Rate

In figures 6.13a-d, it was noted that the plug formation was slow until the bulk temperature had dropped below 15°C. In order to investigate this in more detail, the minimum radius of the ice plug (the neck radius) was plotted against the bulk temperature inside the freezing zone (figure 6.15) for the eight combinations of initial temperature and domain length. With the exception of the 8°C results, all the results followed one curve, showing that the freezing rate was slow at temperatures above 20°C and increased rapidly when the temperature dropped below 20°C. For initial temperatures of 18°C and 26°C, the plug grew until it reached the radius dictated by the bulk temperature, after which it followed the same curve as the 40°C results. Because 8°C is below the critical temperature of approximately

15°C, the plug growth took place with very little variation in bulk temperature. There was very little difference between the short and long pipe results for all values of initial temperature. Thus it appeared that the plug growth was controlled entirely by the bulk temperature. This implied that the plug formation proceeded as a series of steady state temperature distributions and that the ice only grows because the bulk temperature decays.

Tavner measured the position of the interface and the bulk temperature during two separate sets of experiments. There were two values of initial temperature for which there were both sets of results (18°C and 23°C) and there were values of bulk temperature available from the 8°C freeze and interface positions from a 6°C freeze. These values were included (using linear interpolation to obtain the interface positions at the same times as those at which the bulk temperature was calculated) in figure 6.15. This showed that the ice formation in the experiment was much less dependent on the bulk temperature than predicted by the numerical model. The ice formation is slightly more temperature dependent at 23°C than at 6°C and 18°C, indicating a similar trend to the predicted results but with a large offset in the temperature range at which it occurred.

This difference could be attributed either to over-prediction of the heat flux from the water to the ice front or under-estimation of the heat flux into the boiling nitrogen, therefore making the heat flux from the water proportionately more important. The peak boundary layer velocities at the plug neck during the freeze were extracted from the data and plotted in figure 6.16 together with the predicted velocities obtained without freezing. The values predicted during freezing were found to vary with bulk temperature in much the same way as the values obtained without freezing, with slight differences becoming apparent below 15°C, where the values predicted during freezing were slightly greater (maximum of about 4mm/s) than those predicted without freezing. It was therefore concluded that the problem lay in the definition of the heat flux into the liquid nitrogen; this is investigated in more detail in the following section.

6.2.2 **Effect of Varying the Jacket Boundary Condition**

In the previous section, the effect of varying the initial water temperature and the pipe length were investigated using a temperature dependent heat flux as the boundary condition inside the jacket. This relationship was set up to predict the wall temperature data measured by Tavner during a series of instrumented freezes. This allowed a finite cool-down period which was necessary because it was noted from Tavner's measurements of wall temperature

that cooling the wall to near -196°C required a significant proportion of the freezing time. Tavner's freezing jacket was welded onto the outside of the pipe, thereby creating two cooled fins (ie. forming localised regions with high rates of heat transfer out of the pipe). The boundary condition used in the previous section was established using temperature measurements taken in the centre of the jacket and did not include the 'cooled fin' effect and therefore under-estimated the heat transfer to the liquid nitrogen. (Tavner's design was not realistic; jackets are not welded onto the pipe in practice.)

The boundary condition was changed so that the temperature on the outside of the pipe inside the jacket was assumed be -196°C throughout the freeze after the first 2 minutes. This was effectively a 'best case' scenario describing the limiting behaviour with a perfectly efficient jacket design. A fill time of 2 minutes was still applied, with the condition above the liquid nitrogen level (which rose linearly from 0 at the beginning of the freeze to 200mm at 2 minutes) assumed to be adiabatic.

The model was defined to use the long (1094mm) pipe length and was run with initial temperatures of 18°C, 26°C and 40°C.

6.2.2.1 Jacket Boundary Condition: Effect on the Flow Field

The main effect of changing the jacket boundary condition was that the freezing rate increased and therefore the time scale over which the plug formed was shortened in relation to the time scale of the flow field development. The bulk temperature was higher for a given ice thickness and therefore the effect of convection was more significant. This changes the flow field, having a more significant effect at the higher initial temperatures.

Figures 6.17a-c show the development of the plug and flow field for the 18°C, 26°C and 40°C freezes. The area of interest has been enlarged in the black and white plots shown in figures 6.18a-c.

When the results from the 18°C freeze, obtained using the two boundary conditions, were considered with respect to the plug size rather than time, it was noted that there were very few differences in the development of the flow field. The bottom of the main convection cell levelled out higher up the pipe when the isothermal boundary condition was used.

In the 26°C freeze, there were several qualitative effects of the change in boundary condition. Firstly, there is a significant ice layer after 2 minutes, when the bulk temperature is around 20°C. At 4 minutes, a subcell forms inside the main cell half way up the plug. The plug forms first near the bottom of the jacket, due to imposing a fill-time, but because the

regions above and below the plug neck become increasingly isolated during the freeze, the water above the neck cools more rapidly which increases the ice formation in this region causing the plug to freeze off nearer the top of the plug. This agrees with the flow field described by both Burton and Tavner.

In the 40°C freeze, there is a significant amount of ice at 2 minutes, with a corresponding bulk temperature of around 26°C. Between 2 and 4 minutes the flow field changes from its normal form and the boundary layer flowing down over the ice becomes detached from the ice at the bottom of the plug and continues to fall down the pipe. After this, the flow inside the freezing zone subsides, with the only significant movement taking place below the plug. The vertical asymmetry of the plug is pronounced.

In all cases, the final position of the main convection cell was higher than when the heat flux boundary condition was used and the height of the cell in both of the freezing cases was higher than in the 'no freezing' case. This was attributed to false diffusion[6.1] increasing the thickness of the boundary layer at the bottom of the plug. This decreases the distance over which the boundary layer falls before the shear between the core flow and the boundary layer becomes significant and ultimately caused the bottom of the convection cell to level out higher than in the no-freeze situation. This effect was greater using the isothermal boundary condition because the initial plug growth at the bottom of the jacket was faster, causing a larger angle between the flow and the grid at the bottom of the plug early in the freeze. This would slightly decrease the accuracy of the predictions by causing a small increase in the bulk temperature decay because the size of the main convection cell was under-predicted.

6.2.2.2 Jacket Boundary Condition: Effect on the Freezing Time

Increasing the rate of heat removal reduced the freezing time by more than 50% at lower values of initial temperature. The reduction in freezing time when the initial temperature was 40°C was more dramatic (65%). This appears to be caused by the change in the flow pattern (at 2-4 minutes) and the resulting decrease in convection in the freezing zone.

[6.1]The thermal diffusivity (and to a lesser extent the momentum diffusivity) is artificially increased in regions where the flow direction is not aligned with the grid orientation (described in more detail in section 5.2.1.4).

6.2.2.3 Jacket Boundary Condition: Effect on the Freezing Rate

In the descriptions of the flow field, it was noted that there was significant ice growth when the bulk temperature was higher than 15°C. This is shown in figure 6.19 which plots includes the data for the plug growth and bulk temperature obtained using both boundary conditions. Despite using an isothermal boundary condition, the experimental results were not replicated and the predicted freezing rates were less than the experimental results. This implied that the heat flux from water to the ice front was over-predicted in the numerical model. As before, the peak velocities in the boundary layer at the centre of the jacket throughout the freeze were extracted from the four sets of data. These are plotted against the bulk temperature in figure 6.20, together with the values obtained in the absence of freezing. This shows that when the isothermal (-196°C) boundary condition was used much higher values of boundary layer velocity were obtained. There was, in effect, forced convection in these freezes which decreased the freezing rate. It was noted that these high velocities and corresponding heat fluxes were limited to the initial part of the freeze, with decreasing effect as the plug formed. Given the complexity of the flow field, it was difficult to determine the cause of the problem but the fact that the high velocities appeared under conditions which included both significant plug formation and convection indicated that it could be a result of false diffusion. Until this point it had been assumed that false diffusion would cause localised inaccuracies in the temperature and velocity distributions near the top and bottom of the plug, together with a small increase in the bulk temperature decay rate. These results implied that the effects were more extensive. It is possible that the artificially thickened boundary layer above and below the plug neck increases the velocity in these regions and drives more flow through the plug neck. This results in forced convection over the ice surface and causes lower freezing rates.

6.2.4 Discussion

In this section the main results of the investigation into the effect of initial temperature, pipe length and boundary condition on pipe freezing in a closed pipe are discussed.

The flow field forms in such a way that a proportion of the cooled down-flow is returned to the freezing zone up the centre of the pipe. The flow which continues to drop down the pipe (the secondary region) does so away from the pipe wall; it turns from the wall,

flows inwards and then continues to drop down the pipe. This causes a flow which moves up the centre of the pipe and therefore brings relatively warmer water into the freezing zone from below the main convection cell. The bulk temperature inside the freezing zone drops and therefore the heat supplied to the ice front decreases, with corresponding increase in freezing rate. When the secondary region reaches the bottom of the pipe it breaks off from the main region, leaving two separate regions. This causes the bulk temperature inside the freezing zone to decay more rapidly. When (if) the secondary region reforms there is an increase in bulk temperature. Repeated reforming and separation of the two regions causes occasional jets of warmer water up the centre of the pipe. In the numerical model, a closed length of pipe was used and therefore the bulk temperature inside the freezing zone decreased more rapidly than it would in an infinite pipe length.

The flow field is affected by the pipe diameter, with the cooled flow falling further down the pipe in larger pipes leading to a lower temperature decay. These geometric aspects are important when considering a freezing site; a tank or junction onto a horizontal pipe below the freezing zone will destroy the mechanism which causes the bulk temperature decay if the main convection cell falls into it, but should have a minimal effect if it lies below the lowest point that the cell will reach. The location of the lowest position is dependent on the pipe radius and the initial temperature. All these factors must be taken into account when trying to predict the time to carry out a particular freeze.

The rate at which heat can be removed from the pipe partly determines the rate of ice formation. The plug growth is controlled by the balance between the heat flux arriving at the ice/water interface and the rate at which heat is removed from the interface through the ice. In order to predict the plug growth (and therefore freezing time) the heat flux out of the pipe must be quantified. The rate at which the heat is removed to the boiling nitrogen depends on a large number of factors; in this investigation two methods were used. The bulk of the results used a temperature dependant heat flux which cooled the outside of the wall gradually. In addition, faster cooling was obtained by imposing -196°C on the outside of the pipe wall. Using the first boundary condition, the freezing rate was strongly dependent on the initial temperature, to the extent that plug formation was not significant until the bulk temperature had dropped below 15°C. With the isothermal (-196°C) boundary condition, freezing took place much more quickly, being significant for bulk temperatures of over 30°C. This demonstrated that increasing the rate at which heat is removed from the pipe leads to a decrease in the importance of the heat flux arriving at the interface.

As stated above, an accurate prediction of the plug formation depends both on predicting the rate at which the heat is removed from the pipe and also the rate at which the

heat arrives at the ice-water interface. In modelling a closed length of pipe, the bulk temperature, and therefore the heat flux arriving at the interface, decayed more rapidly than it would in an infinite length of pipe. Comparison with the experimental results obtained by Tavner showed that using the heat flux boundary condition gave good agreement in freezing time for initial temperatures of 8°C, 18°C and 26°C. However, the bulk temperature decay in the 18°C and 26°C freezes was more rapid than in the experiments and the predicted freezing rates were more dependent on the bulk temperature than those observed in the experiments. The isothermal boundary condition increased the rate at which heat was removed from the pipe, leading to lower freezing times than those recorded in the experiments. Because this higher heat flux matched the higher decay in bulk temperature in the predictions, the shape of the plugs was more realistic than those obtained applying the heat flux boundary condition. In addition, separation of the boundary layer from the ice was noted in the 40°C freeze, which is a phenomenon observed in practice (both by Burton[1] and by Tavner[5]).

There is doubt over the accuracy of the convection model when the isothermal -196°C boundary condition was used. The magnitude of the boundary layer velocities at the beginning of the 26°C and 40°C freezes were higher than expected. This disappeared later in the freeze when the bulk temperature decayed and was not significant when the heat flux boundary condition was used. This implies that the combination of plug formation and a relatively high bulk temperature (more than 25°C) gives rise to problems in the flow prediction. This was attributed to the effect of false diffusion which increases the mass of liquid which is cooled and therefore increases the boundary layer velocity. In addition, the bottom of the main convection cell was closer to the bottom of the jacket with the isothermal -196°C boundary condition than with the heat flux boundary condition. This was attributed to the fact that a thicker boundary layer will result in increased shear between the core up-flow and the down-flow which increases the 'choking' effect and slows the boundary layer flow more rapidly.

6.3 DEVELOPMENT OF AN OPEN BOTTOM MODEL OF PIPE FREEZING

The results obtained modelling convection and freezing in a closed length of pipe are limited because the convection cell drops rapidly down the pipe, especially in large diameter pipes and at high water temperatures, and cools the entire contents of the pipe. Using a closed pipe it is possible to freeze water at any initial temperature and therefore the model cannot be used to study freezing in long pipes at high temperatures. Increasing the length of the pipe which is modelled is not a satisfactory solution because it places an exorbitant demand on computer requirements. A large number of control volumes were required to model even a short length of pipe because a high grid refinement is required to resolve the boundary layer next to the ice and the complex flow field below the freezing zone.

In order to develop the numerical model further, an open bottom model was proposed. The bottom of the domain was located a short distance below the bottom of the freezing jacket and flow was allowed across the boundary. The temperature of the core flow and therefore the bulk temperature inside the freezing zone was controlled. By excluding the mixing region, inaccuracies are introduced to the predicted velocity and temperature distributions inside the freezing zone; in particular, the fast core flow caused by the boundary layer being diverted towards the centre of the pipe will not be predicted. These inaccuracies are offset against the great savings in solution times and memory requirements. The open bottom model offers great improvements in modelling larger diameter pipes when the 'choking' effect is less significant and therefore the flow field will be more accurate and the bulk temperature can be maintained. In addition, by using an open bottom model, the effect of false diffusion in a simplified flow field can be investigated.

6.3.1 'Open' Boundary Condition

The open boundary condition required radial and vertical components of velocity and pressure on the boundary which were compatible with the solution inside the domain to avoid turning the flow at the boundary (ie. as a result of limiting the flow across the boundary) but without making the velocities higher than necessary, which would cause increased convection. Continuity is enforced throughout the domain and so, with the boundary velocities included as unknowns in the solution, the resulting velocity distribution will exhibit equal flowrates into and out of the domain. The normal method of modelling an outflow boundary condition

is by specifying the outlet pressure distribution (usually constant); inlet conditions are normally specified by fixing the velocity distribution. A brief survey of the literature describing the formulations of open or 'pseudo' boundary conditions (for instance, Nakamura et al[64] and Kakaç[65]) showed that either the pressure and one component of velocity (the value or the gradient in the respective direction) could be set, with the other velocity component calculated via continuity, or both components of velocity (or gradients in respective directions) could be set, in which case the pressure would drop out of the equations.

Several methods of formulating the boundary condition were used. The results described in the following sections were obtained by fixing the pressure on the boundary (constant across the pipe) and setting the gradient of radial velocity in the radial direction to zero; the vertical velocity was calculated during the solution procedure from continuity. An alternative approach of fixing the both radial velocity and the gradient of vertical velocity (in the vertical direction) equal to zero was used to produce the results which were presented at the Tenth International Heat Transfer Conference and included in Appendix V. This method was found to be very sensitive to the location of the boundary with respect to the bottom of the freezing jacket.

The temperature boundary condition was split in two; in the outer region where the water was flowing out of the domain, the gradient of temperature in the vertical direction was zero; in the inner region, over which the water flows upwards, an isothermal boundary condition was used.

The open boundary condition causes problems in the prediction of the flow development over the initial minute, when the convection cell forms and stretches down the pipe; at the point when the bottom of the cell reaches the boundary, the assumptions concerning the pressure and radial velocities were not valid. In addition, there will be a step change in the temperature of the upwards core flow when the bottom of the convection cell drops through the bottom of the numerical domain. Attempts to try to predict the transient flow development in the pipe resulted in a failure to converge early in the solution. An alternative approach was taken. The freezing jacket was replaced by an isothermal (0°C) wall condition and the model run to predict the resulting steady state velocity distribution (using heavy under-relaxation, large time step and a maximum number of iterations per time step). Once a steady state flow distribution was obtained, the freezing boundary condition was introduced and, from that point on, the transient freezing and convection problem was solved. This is slightly inaccurate at low initial temperatures when there is significant plug growth during the period over which the flow field develops. This should become less important in

higher initial water temperature when the plug growth is initially slow. The prediction of the steady state velocity distribution also allowed validation of the model (checking that the open boundary condition would not cause divergence). The peak boundary layer velocities were compared with those predicted in a closed pipe without freezing.

6.3.2 Convection in an Open Bottom Pipe

The open bottom model predicted convection and solidification using a 56x52 grid to model a 384mm (15.36") length of 100mm (4") diameter pipe. The bottom of the jacket was 42mm (1.68") from the bottom of the domain.

The steady state velocity, temperature and pressure distributions were predicted for initial and core flow temperatures of 10°C, 20°C, 30°C and 40°C. An infinite number of velocity distributions exist which satisfy the velocity and continuity equations for this problem: the further condition of no change over successive 'time' steps was imposed to obtain the steady state solution. The convergence to the steady state was slow and required a large number of iterations. These steady state velocity, streamline and temperature distributions are plotted in figures 6.21a,b, showing increasing boundary layer velocities and thinner boundary layers with increasing temperature.

In addition to obtaining the starting distributions for the freezing simulations, the model was also run with a minimal wall thickness to obtain the boundary layer velocities for comparison with the closed pipe - no freezing results. The resulting values of peak boundary layer velocity at the centre of the jacket are shown in figure 6.22; they show excellent agreement with the predicted values obtained in a long closed pipe.

6.3.3 Convection and Freezing in an Open Bottom Pipe

The plug development was predicted for an initial temperature of 20°C. The initial velocity and temperature distributions were set at the steady state results which had been obtained without including freezing. The 'jacket' freezing condition was isothermal -196°C and a fill-time of 2 minutes was used; the wall was maintained at 0°C above the liquid nitrogen level and at -196°C below the nitrogen level. The wall condition was adiabatic above and below the jacket.

The plug development is shown in figures 6.23a,b. At 4 minutes a separate

recirculation region forms above the plug neck (the neck radius is 33.5mm). After this, cooled water becomes increasingly trapped above the neck and the core flow is turned at the neck. The neck position migrates up the plug and the plug becomes increasingly asymmetric. This predicts the three stage plug formation, agreeing with the experimental observations of Burton[1], Burton and Bowen[8], and Tavner[5].

This interaction between the core flow and the boundary layer at the plug neck is controlled by the shear between the two flows and is therefore the same as that which takes place below the freezing zone causing the complex flow development. The critical plug neck radius will be greater at higher values of water temperature because, with the higher velocities, the shear between the boundary layer and the core flow will be greater. This agrees qualitatively with the experimental results of Tavner, however, the critical plug size is much larger than that observed by Burton and by Tavner. This is due to the fact that the boundary layer velocities are much higher than expected (this is discussed in more detail in the following paragraphs) and therefore the shear between the boundary layer and the core flow is increased and the critical ice thickness is lower.

After 15 minutes, the solidification rate drops off and the plug and flow field appear to have reached a steady state, implying that it is not possible to freeze water initially at 20°C when there is no bulk temperature decay even with a highly efficient jacket. This is in complete contradiction with the experimental results of Burton, who froze water at temperatures up to 45°C while maintaining the bulk temperature by including a tank in the experimental rig. However, the form of plug development, with neck migration, is similar to that noted in the experiments at higher temperatures.

The maximum predicted velocity at the bottom of the jacket was 27mm/s at 4½ minutes after the freezing condition was imposed. This is about 35% greater than that obtained without plug formation. The velocity at the bottom of the jacket levels out at 22mm/s, 10% above the steady level without solidification. The increased velocity effectively adds a forced convection component to the free convection and leads to a plug formation which resembles the experimental results obtained for higher temperature freezes.

The probable cause of these results is false diffusion. Closer examination of the temperature distribution in figure 6.23a shows that the boundary layer increases in thickness below the plug. Thus a thicker layer of water is cooled and the velocities increase. This increase in flow is initially fed by pulling more water down over the ice surface but when the ice layer is thicker than the boundary layer (at 4 minutes), it can pull water into the domain through the open bottom; the up-flow immediately below the neck increases (see figure 6.23a). False diffusion is at a maximum when the flow is at 45° to the grid direction, which

is possible at the bottom of the plug. False diffusion is also proportional to the speed of the flow and therefore has a greater effect at higher initial temperatures. In addition, this positive feedback in the system causes the velocities to increase until the convected heat flux is sufficiently large to melt the plug.

6.3.4 Conclusions

The open bottom boundary condition appears to be an acceptable method of modelling convection in a vertical pipe and will be more accurate in larger diameter pipes (200mm+), with special treatment required to predict the initial formation of the convection cell. The main difference between the open bottom condition and an infinite pipe is that there may be some bulk temperature decay in an infinitely long pipe. There are also differences in the flow field: the closed model will predict a fast core flow in smallish pipes but this will become less important in larger pipes (greater than 200mm in diameter). The open bottom pipe model predicts steady state convection inside a pipe for the case where there is no decay in bulk temperature. This is useful for modelling convection and freezing in large diameter pipes and at high temperatures where a closed pipe would predict a decay in the bulk temperature, with a resulting decrease in the level of natural convection.

The predictions of plug formation indicate clearly the interaction between convection and plug growth. Once the plug neck reaches a critical size, the core flow and boundary layer start to interfere at the plug neck causing the water above the neck to become increasingly isolated from the water below. The relatively warm core flow is turned at the plug neck to move down the ice front and the water above the neck cools rapidly, accelerating solidification and making the position of the neck move up the pipe. This agrees with the plug formation process proposed by Burton[1] and confirmed by Burton and Bowen[8] and by Tavner[5].

When freezing was introduced the predicted velocities were much higher than those predicted with an isothermal (0°C) wall section. The predicted flow was sufficiently fast to stop freezing in water initially at 20°C and produced a plug profile which resembled that observed in experiments at initial temperatures of above 40°C. In the closed pipe model the bulk temperature and velocities decayed as the plug grew and therefore the increase in convected heat flux was only obvious when the ice growth was plotted against bulk temperature. In the open bottom pipe model, the effect was far more obvious because the bulk temperature was deliberately maintained at the initial temperature.

It was established that the cause of the high velocities was false diffusion. Essentially in the regions where the flow was not aligned with the grid the thermal diffusivity was locally increased, ie. above and below the plug neck, especially at the very bottom of the plug. This caused a thicker boundary layer, a greater volume of cooled water and therefore higher velocities in the boundary layer. The combination of high angle between the flow and grid direction and the low thermal diffusivity of water, made this problem important in modelling convection and freezing in situations where the convection is significant. The problem was therefore more noticeable when the isothermal (-196°C) jacket boundary condition was used, because it resulted in more significant plug growth before the bulk temperature had decayed.

6.4 RECOMMENDATIONS FOR SELECTION OF THE MODELLING METHOD

The method of scaling the effect of convection on freezing between different sizes of pipe which was proposed in the chapter 3 was used to create a 'map' showing which type of model (ie. conduction only, convection, turbulent, analytical, open bottom, etc.) is required under which conditions (water temperature and pipe size). This is plotted in figure 6.24 and explained below.

- Neglecting convection was found to predict the freezing times adequately in a 100mm (4") diameter pipe for water temperatures less than 20°C; this will scale with 'effective heat flux' (e.h.f.) and can be extrapolated to different pipe sizes, giving the region shaded blue in figure 6.24. This is valid for pipes diameters up to around 250-300mm (10-12") where the conditions approach the transition from laminar to turbulent.
- Between 20°C and 50°C in a 100mm (4") diameter pipe laminar natural convection must be included in the model to predict the freezing process accurately. This region is shaded pink in figure 6.24.
- Above about 30°C (value taken from experimental data obtained by Burton[1] with maintained bulk temperature in the freezing zone), convection and solidification interact, changing the flow field and the plug shape. Below this point, the analytical model[6.2] can be used to provide an estimate of the freezing time. This process depends on the effect of the convective heat flux and therefore scales with e.h.f.. The area over which the analytical model can be used is shown in figure 6.24 using diagonal (//) shading. Above this temperature, the

[6.2]Developed further as suggested in chapter 8.

numerical model must be employed to describe the two-dimensional convection, conduction and solidification processes.

- The region shaded red represents the region where a turbulence model must be incorporated into the numerical model to predict freezing accurately.
- The region shaded grey indicates the region where a successful freeze is not possible.
- These observations assume that the bulk water temperature in the freezing zone remains at the initial temperature throughout freezing and are overly conservative for pipes less than 100mm (4") diameter when the bulk temperature will decay during freezing.
- In pipes greater than 200mm (8") in diameter, the bulk temperature decay can be neglected and therefore an open bottom pipe model[6.3] can be used. This area is indicated in figure 6.24 using horizontal (=) shading.
- Below 100mm (4") diameter, the bulk temperature decay will become more significant and therefore the effect of convection on freezing will become less important. The bulk temperature decay must be modelled to describe the freezing process and therefore a closed pipe model must be used. Convection is less important because the bulk temperature drops during freezing and therefore, apart from at very high temperatures, false diffusion will be less critical. The existing closed pipe model could be used to describe freezing under such conditions.
- Below 200mm (8") the open bottom model will over-estimate the freezing time and the effect of convection on freezing, and (unless a long[6.4] domain is used) closed model will under-predict the effect of convection and freezing time. The two approaches could be used to provide upper and lower bounds for freezing times.
- The formulation of the boundary condition inside the jacket is critical to the accurate prediction of the freezing time. Assuming that the outer wall temperature drops immediately to the coolant temperature provides a 'best-case' scenario for the freezing time. In the previous sections it was demonstrated that using a heat flux - wall temperature relationship which was close to published data for the boiling curve of liquid nitrogen approximately doubled the freeze time.

[6.3]Developed to reduce false diffusion.

[6.4]The length of which increases with temperature and pipe diameter.

6.5 CONCLUSIONS

An analysis of the effect of convection on pipe freezing has been described in this chapter. The results have shown that a complex flow field forms when a section of the pipe wall is cooled. This is an important new result and forms one of the main results of this thesis. This flow field initially consists of a single convection cell, however, shear between the boundary layer and the core flow slows the boundary layer flow with the result that it turns off the wall before it has warmed up to the initial (ambient) temperature. This cools the water immediately below and establishes a separate convection cell below the main cell. The water in the separate cell flows upwards next to the pipe wall and pushes the boundary layer off the pipe wall, supporting the main cell. The cooler, outer region of the boundary layer continues to drop down the pipe, diverted from the wall by the separate cell and forms a secondary region off the main recirculation cell. This water warms up and turns to flow back up the pipe to the freezing zone as a relatively warm and fast central core flow. The inner layers of the boundary layer are turned to move up the pipe, giving a two-part core flow consisting of a 'warm' fast central region and a cooler slow outer region. The principal effect of this on freezing is a decay in the bulk temperature inside the freezing zone during freezing, accelerating solidification. A three stage flow development was proposed (this is distinct from the plug-flow development process proposed by Burton[1] and modified by Burton and Bowen[8] and by Tavner[5]): in the first stage the flow field consists of a single convection cell and the second phase starts when the separate cell formed below the main cell and covered the development of the secondary region. When the flow reaches the bottom of the pipe (the third stage), it breaks off the main region and the flow in the lower section of the pipe subsides. The bulk temperature decays more rapidly in the main region which is now isolated. The second and third stages repeat, with the secondary region reforming, stretching down the pipe and breaking off, although the decaying bulk temperature makes the stages less distinct.

This flow development is dependent on the pipe diameter and the initial water temperature. The majority of the numerical simulations were carried out for a 100mm (4") diameter pipe, in which the bulk temperature decayed from 20°C to 19°C over the first 2 minutes and the height of the bottom of the main region levelled out when the initial temperatures was below 25-30°C. In smaller pipes, the boundary layer thickness formed a significant proportion of the pipe diameter and caused a more rapid decay in bulk temperature. In larger pipes the effect of the separate region was weaker and the decay in bulk temperature was lower (from the data presented here it appears that the effect is small in pipes greater than 200mm (8") in diameter). Increasing the difference between the

temperature of the water and of the cooled wall increases the buoyancy forces and also decreases the thickness of the boundary layer leaving the freezing zone. The main convection cell drops further.

A similar interaction between the boundary layer and the core flow was noted later in the freeze, when interaction between the boundary layer flowing down over the ice interacts with the core up-flow through the plug neck. The regions above and below the neck become increasingly isolated as the plug develops, causing faster solidification in the upper region and the position of the plug neck moves up the pipe. This was observed during experiments by Burton[1], Burton and Bowen[8] and Tavner[5] and was the main effect which caused the second stage in the three stages stages plug development. At higher water temperatures, the thickness of the boundary layer is lower and therefore the critical neck radius at which this happens decreases, as noted by Tavner.

The predictions of boundary layer velocity and of the heat transfer at the cooled wall were compared with the analytical flat plate solution by Bejan[29], showing that the analytical solution under-predicts the boundary layer velocity by approximately 2mm/s and over-predicts the heat transfer coefficient by approximately 39%.

When a closed length of pipe was modelled, after the flow reached the bottom of the domain, the entire contents of the pipe will be cooled and the bulk temperature inside the freezing zone decreased more rapidly than expected in an infinite length of pipe. Allowing flow across the bottom boundary allows the temperature of the return flow to be specified. In the investigations carried out, the core temperature was assumed to be maintained at the initial temperature and therefore modelled the situation where a tank of water at the initial temperature was placed a short distance below the freezing zone. This approach allowed the interaction between convection and ice formation to be observed, showing the increasing separation by the plug neck and giving good qualitative agreement with the experimental results.

The development of the flow field is affected by any change in pipe diameter. Including a tank in an experimental rig will change the flow development if the main convection cell reaches the tank but should be less significant if it stabilises above the tank. This observation was made in the experimental work performed by both Burton and Tavner from temperature measurements during pipe freezing. This agreement between the experimental and numerical results provides corroboration for the numerical results. The results indicate that the tank will have a less significant effect in larger pipes and it can be proposed that the position of the tank will be of little importance in pipes greater than 200mm (8") in diameter. The improved understanding of the flow field will be important in the design

of experimental rigs and in interpreting the results from experiments in which tanks were used.

Although the infinite pipe was used as the ideal for this model, in real situations it is more likely that there will be either an obstruction below the freezing zone, for instance a bend or valve, or that there will be a junction with a larger diameter pipe. There may be significant heat flux through the pipe wall which may affect the convection patterns, either in causing an up-flow next to the wall which disrupts the down-flow or by accelerating the flow downwards further. The predictions described above do not cover these actual conditions but they do provide an indication of the behaviour in these conditions.

The freezing process is governed by the convected heat flux from the water and the heat flux into the liquid nitrogen. Assuming a highly efficient jacket (ie. isothermal -196°C jacket boundary condition) in the closed pipe model gave an improved idea of the interaction between the plug growth and convection because plug formation took place before the bulk temperature had decayed significantly. This was made more obvious when the temperature of the core flow was deliberately maintained at the initial temperature by using the open bottom boundary condition. The distortion of the flow field by the growing plug was predicted showing that the cooled boundary layer flow mixes with the core flow at the plug neck, leading to a separate convection cell forming above the plug neck. The water above the plug neck becomes increasingly isolated and therefore cools more rapidly. The neck position moves up the plug making the predicted plug profile increasingly asymmetric. This agrees qualitatively with the experimental results but the effect of false diffusion increases the velocities, making the predicted plug profiles resemble the experimental results obtained at higher temperatures or with forced convection. It must be concluded that the model is not accurately predicting the freezing when the bulk temperature is sufficiently high to cause significant flow. However, the results confirm that the model successfully predicts the interaction between flow and plug formation noted in the experiments.

Finally, the analytical and numerical models were pulled together to define a series of criteria which show the type of model necessary to model freezing for a range of pipe diameters and initial water temperatures.

7. CONCLUSIONS

The aim of this research was to develop a numerical model of plug formation inside a pipe which could then be exercised to study the effect of varying the freezing conditions. This understanding, combined with an accurate model of the cooling process, could be used to predict whether a freeze is possible and how long it will take under certain conditions. It should be emphasised that this work, by itself, did not aim to produce such a predictive tool; this work concerned the research into the mechanisms involved in pipe freezing by developing and using a numerical model.

In this chapter, the main results from this research are presented in the context of their significance to pipe freezing and the relevance of the different modelling methods which were used in this research is discussed. The research concentrated on the effect of natural convection on freezing in vertical pipes containing water which is initially static; the freezing method was taken to be liquid nitrogen.

This chapter includes a brief review of the pertinent experimental results which formed the understanding of the process at the beginning of this work. The modelling carried out for this research is separated into analytical and numerical modelling.

7.1 EXPERIMENTAL RESULTS

The results from a detailed experimental programme at Southampton studying freezing water in vertical pipelines (Burton[1], Bowen and Burton[8] and Tavner[5]) were reviewed. These are briefly described in the following points.

- The freezing time is proportional to the cross-sectional area of the pipe (assuming constant jacket length to diameter ratio) when the initial temperature is near 0°C and increases approximately linearly with increasing initial temperature until convection becomes important. There is an intermediate region where the freezing time increase more rapidly with increasing temperature, reaching a limiting value where it is no longer possible the freeze a complete plug. This limiting temperature is lower in larger pipes.
- When the ice thickness reaches a critical size the boundary layer and core flows start to interfere at the plug neck and the water above the neck becomes increasingly isolated from that below the neck. The water temperature drops more rapidly above the neck, accelerating freezing and therefore making the position of the plug neck move up the plug. The critical neck radius increases with initial temperature (and therefore boundary layer velocity).
- It was noted that the water temperature inside the freezing zone dropped during freezing

in a 100mm (4") diameter pipe. When a tank was placed near the bottom of the freezing zone, the bulk water temperature was maintained in the freezing zone. When the distance between the freezing zone and the tank was increased, it was noted that there was a critical temperature below which the bulk temperature decayed and above which it was maintained.

7.2 ANALYTICAL MODEL

The analytical model assumed that the problem was one-dimensional and that the buoyancy-driven flows were laminar. The effect of convection was included via an analytical solution for the heat transfer coefficient for the induced flow over a heated vertical flat plate. This led to a simple finite difference formula which was solved numerically to predict the freezing time. Attempts to incorporate a simple model of the bulk temperature decay by considering the mixing between the boundary layer and core flow did not prove to be successful when the results were compared with experimental data for bulk temperature. The results obtained from the numerical model indicated that the actual mixing mechanisms were more complex than assumed in the derivation of the simple analytical model and also demonstrated that it was not strictly possible to infer the length of pipe over which mixing takes place from the bulk temperature measurements. It was therefore not possible to obtain agreement between the numerical and analytical results and a more complex description of the mixing process is required. The following discussion assumes that the bulk temperature in the freezing zone remains constant.

The analytical model provides a quick estimate of the freeze time, it can be applied to different pipe sizes, fluid temperatures, jacket lengths, cooling methods and even to different fluids and, used together with a turbulence criterion (inferred from experimental data), it produces estimates of the maximum temperature which can be frozen. The disadvantages and errors in the method can be split into two; those which over-estimate and those which under-estimate the freezing time.

- The freeze times were increased because the heat transfer coefficient for the heat flow from the water to the freezing front was greater than both the experimental and the numerical data (attributed to the fact that the coefficient was derived assuming constant fluid properties). In addition, the initial period in which the fluid starts to move from static is neglected and despite attempts to do so, no method of successfully incorporating the temperature decay of the water in the freezing zone was formulated.
- The freeze times are under-predicted if the combination of jacket length (ie. pipe diameter)

and water temperature are such that the boundary layer becomes turbulent which increases heat transfer to the ice interface. In addition, as the plug forms the flow field becomes increasingly distorted, increasing the heat flow from the water to the ice below the neck and decreasing it above the neck. The flat plate assumptions, which were used to predict the heat transfer coefficient, become increasingly inappropriate and therefore the accuracy of the analytical model decreases. This is augmented by the fact that axial conduction, which is neglected in the analytical model, increases as the plug becomes asymmetric, with the result that the freezing rate decreases.

The problems with the analytical model can therefore be split into the following areas :

- heat transfer coefficient : over-predicts for laminar flow, not formulated for turbulent flow. The laminar values were modified by making use of numerical results; further development, for instance using an empirical correlation would be required to describe turbulent heat transfer,
- bulk temperature decay : important in pipes less than 200mm (8") in diameter, and
- breakdown in similarity to convection over a flat plate. This occurs when the shear between the boundary layer and core flows through the plug neck reaches a critical level; the critical neck radius is therefore controlled by the velocity and thickness of the boundary layer (ie. water temperature and jacket length).

The first point can be improved on within the existing framework. The latter two points indicate regions where the one-dimensional approach breaks down. Neglecting bulk temperature decay will over-predict the freezing time and under-predict the maximum temperature; this may limit the application of pipe freezing in situations where it could be successful but it does provide a conservative estimate. The third point indicates the major failing in this approach; the analytical model will be over-optimistic of the success of a freeze under conditions where convection is important.

The simplicity of the analytical model led to the formulation of a method of scaling the 'effect of convection' between different pipe sizes and temperatures. This suggests that the effect of convection is proportional to the product of the radius (or diameter) and the water temperature raised to the power 0.446. Given the previous discussion, this is only applicable for conditions where convection exists but does not significantly affect freezing. The experimental data for the maximum temperature which can be frozen successfully lie on the line of equal Grashof number (equal to 2.1×10^9 based on the jacket length). This suggests that the limiting behaviour, in these results, is controlled by transition to turbulent flow. If this is the case (given that it is inferred from only three data points), this criterion should be

applicable to pipes greater than 150mm (6") diameter. Below this point, freezing may be limited by the laminar heat flux; this will be affected by the breakdown in one-dimensional behaviour.

7.3 NUMERICAL MODEL

The numerical model predicted the forming two-dimensional ice plug both without and with convection driven flows by solving the governing Navier-Stokes equations. The finite volume methodology was used with a fixed (non-transforming) grid; the SIMPLER algorithm was used to predict convection and the enthalpy method used to model the freezing process. The computer code was developed specifically for this application and was extensively validated during its development against published benchmark tests. The resulting model of convection and solidification was validated against experimental results. The numerical model was used to predict natural convection inside a pipe with no freezing, freezing in the absence of convection and, finally, freezing and convection. Most of the investigations were carried out for a long but closed length of pipe; a further development was to impose an 'open' boundary condition below the freezing zone. The results can be summarised as follows :

- the bulk temperature decay is primarily due to the formation of a complex flow field below the freezing region. This is set up by shear between the boundary layer (which becomes thicker by entrainment) and the core flow which, by a series of stages, establishes a separate recirculation region immediately below the point at which the boundary layer leaves the wall. This separate region diverts the boundary layer off the wall and effectively decreases the pipe diameter, 'choking' the flow. The cooler outer part of the boundary layer continues to fall down the pipe and warms up while the remaining part turns to flow back up the pipe to the freezing zone, causing a decay in the local bulk temperature. The height of the bottom of the main region may level out or fall slowly; further investigations using longer pipe lengths are required to determine whether the bulk temperature continues to decay. Without this information it is not possible to conclude whether or not it is possible to freeze water at any initial temperature (a turbulence flow model will be required at higher temperatures). The bulk temperature decay is controlled by the length of the main part of the convection cell and increases with water temperature; the 'choking' effect decreases with increasing pipe diameter. It is not a significant effect in pipes greater than 200mm (8") diameter.
- Interaction between the boundary layer and core flow at the plug neck, again controlled by

shear, is observed.

- Modelling a closed pipe length ultimately cools the entire contents of the pipe. This becomes important in cases where convection is significant; modelling too short a length results in the bulk temperature dropping to a point which convection is not important. Therefore, a significant length of pipe must be included below the freezing zone (for instance, 0.730m length was insufficient to model freezing in water initially at 18°C in a 100mm (4") diameter pipe). Further investigations would be necessary to determine the required pipe length.
- Modelling freezing using a fixed grid under conditions where convection is significant results in significant false diffusion. This is important below the plug neck where it increases the thickness of the layer of water cooled by the ice, increasing the boundary layer velocity and therefore increasing the flows in the pipe.
- An accurate formulation of the cooling process to required in order to compare the predictions with experimental results; this controls the relative importance of convection on the freezing process.
- The open bottom model (developed further to remove false diffusion) can be used to predict convection in cases where the bulk temperature does not decay (eg. large pipe, above tank). This method also allows a decay in bulk temperature to be specified explicitly.

7.4 RECOMMENDATIONS FOR MODELLING PIPE FREEZING

Consideration of the one-dimensional analytical model gave a method of scaling the effect of convection on freezing which was applicable while the flow remained laminar and the separation on the water above and below the plug neck did not cause neck migration. This, together with a criterion for the transition to turbulent flow, gave rise to a 'map' of the relationship between water temperature and pipe diameter with convection and turbulence. This was used to produce recommendations on the type of modelling approach which should be used for a given pipe size and initial water temperature.

It was noted that if the water temperature was less than $20x(0.05/R)^{0.446}$ (and the flow was still laminar) the freezing time could be obtained either by the analytical model or the numerical model (with or without convection).

At Grashof numbers of near $1.3x10^9$ and greater, a turbulence model will be required. At pipes greater than 300mm (12") diameter, with the exception of very low water temperatures, a turbulence model will be required irrespective of the water temperature. In

order to model the effect of convection on freezing at temperatures at which neck migration occurs, a numerical model is required. If convection is important throughout the freeze, the fixed grid approach will not be accurate[7.1]; this applies to water temperatures above 35-40°C in a 100mm (4") diameter pipe and for decreasing temperatures in larger pipes. The closed pipe-fixed grid should be applicable in pipes less than 100mm (4") in diameter because the 'choking' mechanism will naturally cause a decay in the bulk temperature. The open bottom method should be applied to model pipes greater than 200mm (8") in diameter. The intermediate region could either be modelled with a closed pipe which would increase the bulk temperature decay and therefore under-estimate the freeze time, or using the open bottom model which would over-estimate the freeze time. A compromise scheme is possible, in which the open bottom model is used, together with a estimate of the bulk temperature decay rate which is explicitly incorporated into the model.

[7.1]The required further developments to the model are discussed in more detail in the following chapter.

8. RECOMMENDED FURTHER WORK

A numerical model has been developed which predicts the plug formation and natural convection flows inside a pipe during pipe freezing. The prediction of the velocity distribution is not accurate under conditions which combine plug formation and significant buoyancy effects. In order to develop the model further, the solution method must be altered to minimize the effect of false diffusion. One method of achieving this is to improve the discretisation scheme so that it is accurate when the flow is not aligned with the grid orientation. This requires consideration of a greater number of neighbour control volumes in the discretisation scheme and therefore will result in an increase in solution time. Alternatively, the alignment between flow and grid would be improved by using a transforming grid to model the solidification process. This has the added advantage that, since the position of the interface in the computational grid is fixed, it is possible to refine the grid next to the interface without refining the entire grid. However, it is possible that there will be problems in applying a transforming grid method to a situation which would involve a high degree of grid distortion. A third option for solving the problem would be to reformulate the model using a less structured adaptive mesh, either using a completely unstructured mesh or to employ a 'block' structure grid[7.1] such as that used in the CFD package Flow-3D. This would allow extra refinement where required and an adapting mesh could maintain the orientation of the control volume faces perpendicular to the direction of the flow.

The third option requires a totally different approach to the problem and is not a realistic alternative if the model development is to continue using code written 'in-house'. This is an excellent point at which to re-assess the overall approach to modelling pipe freezing. Over the period that this research has been carried out, commercial CFD codes have developed enormously; they have become more user-friendly (mostly menu driven through graphical interfaces) and are available on a range of computers, from mainframes to Personal Computers. Such packages offer the advantage of pre-written code which has been validated and also optimised to maximise the solution speeds and also offer a range of options, such as griding methods and turbulence models. If a package was chosen which used a less structured mesh, it would be possible to locate the grid refinement only in the regions of interest, which would result in savings in the number of grid points and therefore improvements in performance. On the down side, the things that can be modelled are generally restricted by the available options and therefore it may not be possible to model, for instance, a complicated boundary condition or relationship between variables.

[7.1]Based on a topologically orthogonal grid (ie. a deformed orthogonal grid) in which areas with different grid resolutions can be used.

If the code development continues 'in-house', one way of reducing the solution times is to modify the code and change the type of computer used to exploit the faster processing capabilities offered by parallel computing methods. The solution speeds are increased by splitting up a calculation into separate processes which are farmed out to separate processors and performed in parallel. It is therefore ideal in situations where a number of calculations are carried out starting from the same data set; if a process has to wait on another process then the gain is decreased. Southampton University is at the forefront of developing such methods and well-supported hardware and software facilities are available. There are several parts of the solution process which could be carried out in parallel, for example, the calculation of equation coefficients and the 'line-by-line' solution procedure used to calculate each variable.

Savings in run-time by using a package are possible if an unstructured grid or a transforming (adaptive) grid is used however, they may still be less than the conceivable benefits from parallel processing. At this point in time, commercial packages which take advantage of parallel architecture are available but are not common. The advantages of using a package in terms of speed of developing a model must be weighed against possible increases in run-times.

Some method of increasing the solution speeds will be essential for further development of the numerical model. The possible directions in which the investigation could continue are described in the following paragraphs. These areas fall into two groups, model application and further model development.

One area which has not been covered in this research is the effect of heat flux through the wall below the freezing zone; cooling the wall would effectively accelerate the downwards flowing cooled boundary layer whereas warming the wall could cause an up-flow next to the wall which would interfere with the boundary layer. The possibility of isolating the water in the freezing zone by a convection cell formed below the freezing zone driven by a warmed section of the wall could be investigated.

Another application of the model is to investigate freezing in a vertical pipe which is joined at some point below the freezing zone to a horizontal pipe which contains flowing water. The flow at the junction between the two pipes will be fully three-dimensional and therefore either a three-dimensional model will be necessary or it may be possible to approximate the flow below the freezing zone to fit a two-dimensional model.

The effect of an upwards or downwards net flow (ie. forced or mixed convection) on plug formation is also of interest. This would be a straightforward development of the open bottom model (if the problem of false diffusion is solved) with the inlet boundary conditions

defined by fully developed isothermal pipe flow.

The majority of pipe freezing situations involve horizontal pipes. In a horizontal pipe, the flow mainly takes place in the vertical plane perpendicular to the pipe axis. Observations made during experiments show that there is also axial, rolling, flow which causes mixing with the water outside the freezing zone. Both the process of filling the freezing jacket and the effect of convection cause a fully three-dimensional plug form and flow field. The existing model can be extended to three dimensions, by including the calculation of the tangential velocity and a method of handling the singularity at the centre of the pipe. The resulting model would predict freezing in horizontal or inclined pipes but will be very demanding on computer requirements.

In order to model convection at higher temperatures and in large pipes, a method of accounting for turbulence will have to be incorporated into the model. It is not possible to predict the intricate detail of turbulent flow but the overall effects can be predicted. Such models (for example, the k-ε model) introduce extra variables which must be calculated as part of the solution procedure to estimate the effect of turbulence.

The investigation could be extended to model freezing a range of fluids; freezing hydrocarbons was investigated in the experimental work. Hydrocarbons gradually thicken as the temperature decreases and do not solidify at a discrete temperature; this could be included into the numerical model. The fluid properties are very different to those of water and therefore the flow field will develop in a different way. In particular, the highly convective nature of some hydrocarbons means that the mixing with fluid outside the freezing zone and heat flux from the environment will be important.

The analytical model could be developed further to include the effect of the flow development predicted by the numerical model. By studying the rate at which the main convection cell drops down the pipe in the numerical results for the no-freezing case (this requires a long domain) for different pipe diameters, the analytical model could be modified to give more accurate estimates of the bulk temperature decay and the freezing time. In addition, this understanding of the bulk temperature decay could be applied to the open bottom pipe model as the temperature boundary condition.

If the models are developed further to include these options, they will provide two predictive tools which can be applied to investigate freezing under a range of conditions. This will be useful both in further analysis of pipe freezing and in predicting the behaviour in specific cases of interest to pipe freezing contractors.

9. # REFERENCES

1. Burton M.J. An experimental and numerical study of plug formation in vertical pipes during pipe freezing. PhD Thesis.
Dept. of Mechanical Engineering,
University of Southampton. 1986

2. Keary A.C. The development of a numerical model of natural convection and solidification for cryogenic pipe freezing.
Internal Report No. ME/94/16
Dept. of Mechanical Engineering,
University of Southampton. 1994

3. Wigley D.A. Final report on Phase I of the Southampton University pipe freezing project.
Internal Report No. ME/85/09
Dept. of Mechanical Engineering,
University of Southampton. 1985

4. Bowen R.J. Final report on Phase 2 of the Southampton pipe freezing project.
Internal Report No. ME/91/04
Dept. of Mechanical Engineering,
University of Southampton. 1991

5. Tavner A.C.R. An experimental study of ice formation and convection during cryogenic pipe freezing. PhD Thesis.
Dept. of Mechanical Engineering,
University of Southampton. 1992

6. Wigley D.A.(editor) Guidelines to good practice in pipe freezing.
Internal Report No. ME/91/06
Dept. of Mechanical Engineering,
University of Southampton. 1991

7. Keary A.C. Numerical Investigation of the Stress Development in Pipelines during Cryogenic Pipe Freezing: Final Report: Phase III.
Internal Report No. ME/94/22
Dept. of Mechanical Engineering,
University of Southampton. 1994

8. Burton M.J. and Bowen R.J. Effect of convection on plug formation during cryogenic pipe freezing.
Second National Heat Transfer Conference
Glasgow, UK. 1988

9. Bowen R.J. Burton M.J. and Smith G.S. The effect of pipe diameter and pressure drop on the formation of ice plugs in pipelines.
9th International Heat Transfer Conference
Jerusalem, Israel. 1990

10. Lannoy A. Problèmes thermiques posés par la congélation d'un fluide dans une tuyauterie.
Revue Géneral Thermique n220, pp.311-320, 1980. (In French)
Thermal problems involved in freezing a fluid in pipework. Translation from : British Library Document Supply Centre DSC 6196.3 1990

11. Lannoy A. and Flaix B. Experimental analysis of the obturation of pipes by ice plugs.
Nuclear Engineering and Design 86. pp.305-313
Amsterdam, NL. 1985

12. Law K.M. An investigation into cryogenic pipe freezing. PhD Thesis.
Paisley College of Technology, Glasgow. 1989

13. Sparrow E.M. Ramsey J.W. and Kemink R.G. Freezing controlled by natural convection.
Trans. ASME J. Heat Transfer
Vol.101, p.578. 1979

14. Sparrow E.M. and Souza Mendes P. Natural convection heat transfer coefficients measured in experiments on freezing.
Int. J. Heat and Mass Transfer
Vol.25, n.2, pp.293-297. 1982

15. Bathelt A.G. and Viskanta R. Heat transfer at the solid-liquid interface during melting from horizontal cylinder.
Int. J. Heat and Mass Transfer
Vol.23, pp.1493-1504. 1980

16. Sparrow E.M. and Broadbent J.A. Freezing in a vertical tube.
Trans. ASME J. Heat Transfer
Vol.105, p.217. 1983

17. Boger D.V. and Westwater J.W. Effect of buoyancy on the melting and freezing processes.
Trans. ASME J. Heat Transfer
Vol.89, pp.81-89. 1967

18. Patankar S.V. Recent Developments in Computational Heat Transfer.
Trans. ASME J. Heat Transfer
Vol.110, p.1037. 1988

19. Ostrach S. Natural convection in enclosures.
Trans. ASME J. Heat Transfer
Vol.119, pp.1175-1189. 1988

20. Viskanta R. Heat transfer during melting and solidification of metals.
Trans. ASME J. Heat Transfer
Vol.110, pp.1205-1219. 1988

21. London A.L. and Seban R.A. Rate of ice formation.
Trans. ASME
Vol.65, pp.771-778. 1943

22. Luikov A.V. 'Solidification of a cylinder'.
Analytical Heat Diffusion Theory
pp.452-453
Academic Press, New York. 1968

23. Shamsundar N. Approximate calculation of multidimensional solidification by using conduction shape factors.
Trans. ASME J. Heat Transfer
Vol.104, n.1, pp.8-12. 1982

24. Zerkle R.D. and Sunderland J.E. The effect of liquid solidification in a tube upon laminar-flow heat transfer and pressure drop.
Trans. ASME
Vol.90, pp.183-190. May 1968

25. Sadeghipour M.S., Ozisik M.N. and Mulligan J.C. Transient freezing of a liquid in a convectively cooled tube.
Trans. ASME J. Heat Transfer
Vol.104, n.2, pp.316-322. 1982

26. Huang S.C. Analytical solution for the buoyancy flow during the melting of a vertical semi infinite region.
Int. J. Heat and Mass Transfer
Vol.28, n.6, pp.1231-1233. 1985

27. Bejan A. Analysis of melting by natural-convection in an enclosure.
Int. J. Heat and Mass Transfer
Vol.10, n.3, pp.245-252. 1989

28. Zhang Z.Q. and Bejan A. The problem of time-dependent natural convection melting with conduction in the solid.
Int. J. Heat and Mass Transfer
Vol.32, n.12, pp.2447-2457. 1989

29. Bejan A. Convection Heat Transfer.
John Wiley and Sons. New York, USA. 1984

30. Hirata T. and Matsuzawa H. A study of ice-formation phenomena on freezing of flowing water in a pipe.
Trans. ASME J. Heat Transfer
Vol.109, pp.965-970. 1987

31. Wiegand B. and Beer H. A numerical and experimental study of wavy ice-structure in an asymmetrically cooled parallel-plate channel.
Proc. Eurotherm Seminar 30. Heat Transfer in Phase-Change Processes Melting and Solidification. 1992

32. Albert M.R. Moving boundary step ice formation in turbulent flow.
7th Int. Conf. Numerical Methods in Thermal Problems
Pineridge Press, Swansea. 1991

33. Bellecci C. and Conti M. Phase change thermal storage - transient-behavior analysis of a solar receiver storage module using the enthalpy method.
Int. J. Heat and Mass Transfer
Vol.36, n.8, pp.2157-2163. 1993

34. Ramachandran N., Gupta J.P. and Jaluria Y. Thermal and fluid flow effects during solidification in a rectangular cavity.
Int. J. Heat and Mass Transfer
Vol.25, pp.187-194. 1982

35. Gadgil A. and Gobin D. Analysis of 2-dimensional melting in rectangular enclosures in presence of convection.
Trans. ASME J. Heat Transfer
Vol.101, n.1, pp.20-26. 1984

36. Ho J. and Viskanta R. Heat transfer during melting from an isothermal wall.
J. Heat Transfer
Vol.106, pp.12-19. 1984

37. Benard C., Gobin D. and Zanoli A. Moving boundary-problem - heat-conduction in the solid-phase of a phase-change material driven by natural-convection in the liquid.
Trans. ASME J. Heat Transfer
Vol.29, n.11, pp.1669-1691. 1986

38. Beckermann C. and Viskanta R. Effect of solid subcooling on natural convection melting of a pure metal.
Trans. ASME J. Heat Transfer
Vol.111, pp.416-424. 1989

39. de Vahl Davis G., Leonardi E., Wong P.H. and Yeoh G.H. Natural convection in a solidifying liquid.
6th Int. Conf. Numerical Methods in Thermal Problems
Pineridge Press, Swansea. 1989

40. Yoo H. and Ro S.T. Melting process with solid-liquid density change in natural-convection in a rectangular cavity.
Int. J. Heat and Mass Transfer
Vol.12, n.4, pp.365-374. 1991

41. Yao L.S. and Cherney W. Transient phase-change around a horizontal cylinder.
Int. J. Heat and Mass Transfer
Vol.24, n.12, pp.1971-1981. 1981

42. Ho C.J. and Chen S. Numerical simulation of melting of ice around a horizontal cylinder.
Int. J. Heat and Mass Transfer
Vol.29, n.9, pp.1359-1368. 1986

43. Rieger H., Projahn U., Berkiss M. and Beer H. Heat transfer during melting inside a horizontal tube.
Trans. ASME J. Heat Transfer
Vol.105, n.2, pp.226-234. 1983

44. Sparrow E.M., Patankar S.V. and Ramadhyani S. Analysis of melting in the presence of natural convection in the melt region.
Trans. ASME J. Heat Transfer
Vol.99, pp.520-526. 1977

45. Sparrow E.M. and Ohkubo Y. Numerical predictions of freezing in a vertical tube.
Numerical Heat Transfer
Vol.9, pp.79-95. 1986

46. Hibbert S.E., Markatos N.C. and Voller V.R. Computer simulation of moving-interface, convective, phase-change processes.
Int. J. Heat and Mass Transfer
Vol.31, n.8, pp.1709-1718. 1988

47. Bennon W.D. and Incropera F.P. Developing laminar mixed convection with solidification in a vertical channel.
Trans. ASME J. Heat Transfer
Vol.110, p.410-415. 1988

48. Flynn T.M., Draper J.W. and Roos J.J.
Advances in Cryogenic Engineering
Vol.7, pp.539-545. 1962

49. Mahajan R.L. and Gebhart B. An experimental determination of transition limits in a vertical natural convection flow adjacent to a surface.
J. Fluid Mech.
Vol.91, 1979, pp.131-154

50. Patankar S.V. Numerical heat and Mass transfer.
Hemisphere, New York. 1980

51. Sparrow E.M. and Ohkubo Y. Numerical analysis of transient freezing including solid-phase and tube-wall conduction and liquid-phase convection.
Numerical Heat Transfer
Vol.9, pp.59-77. 1986

52. de Vahl Davis G. and Jones I.P. Natural convection of air in a square cavity : a benchmark numerical solution.
Int. J. Numerical Method Fluids
Vol.3, pp.249-264. 1983

53. Markatos N.C. and Pericleous K.A. Laminar and turbulent natural convection in an enclosed cavity.
Int. J. Heat Mass Transfer
Vol.27, n.5, pp.755-772. 1984

54. Huang D.-Y. and Hsieh S.-S. Analysis of natural convection in a cylindrical enclosure.
Numerical Heat Transfer
Vol.12, pp.121-135. 1987

55. Voller V.R., Cross M. and Markatos N.C. An enthalpy method of convection/diffusion phase change.
Int. J. Numerical Methods in Engineering
Vol.24, pp.271-284. 1987

56. Shamsundar N. and Sparrow E.M. Analysis of multidimensional conduction phase change via the enthalpy method.
J. Heat Transfer
Vol.97, n.3, pp.333-340. 1975

57. Hill J.M. and Dewynne J.N. Heat Conduction.
Oxford : Blackwell Scientific. 1986

58. Shamsundar N. and Rooz E. 'Numerical methods for moving boundary problems'.
Handbook of Numerical Heat Transfer
Minkowycz W.J., Sparrow E.M., Schneider G.E. and Pletcher R.H.
John Wiley and Sons, Inc. 1988

59. Lee S.L. and Tzong R.Y. An enthalpy formulation of phase-change problems with a large thermal diffusivity jump across the interface.
Int. J. Heat and Mass Transfer
Vol.34, n.6, pp.1491-1502. 1991

60. Cao Y. and Faghri A. A temperature transforming model with a fixed grid methodology for phase-change problems including natural convection.
1989 Nat. Heat Transfer Conf., HTD-vol.109

61. Hanson W.B. and Richards R.J. Heat transfer to a boiling liquified gas.
Unpublished laboratory note 56-1
NBS-CEL, Boulder, Colorado 1956

62. Raithby G.D. Skew upstream differencing schemes for problems involving fluid flow.
Comp. Methods Appl. Mech. Eng.
Vol.9, p.153, 1976

63. Simonson J. An Introduction to Engineering Heat Transfer.
McGraw Hill, 1967

64. Nakamura I., Watanabe T. and Yoshida T. On the numerical outflow boundary condition of the viscous flow around a square cylinder.
Memoirs of the School of Engineering, Nagoya University
Vol.45, n.1, 1993

65. Kakaç S., Aung W. and Viskanta R. Natural Convection : Fundamentals and Applications.
Hemisphere, New York. 1985

66. Squire H.B. Integral solution published in 'Modern Developments in Fluid Dynamics, Vol.II'.
S. Goldstein, ed.
Dover, New York, 1965, pp.641-643

67. Rogers and Mayhew. Engineering Thermodynamics, Work and Heat Transfer. 3rd Edition.
Longman, London 1980

68. Ösişik M.N. Heat Transfer : a basic approach.
McGraw-Hill Inc. New York, USA. 1985

69. Kreith F. and Bohn M.S. Principles of Heat Transfer. 5th Edition
West Publishing Company, U.S.A 1993

70. Carslaw H.S. and Jaeger J.C. Conduction of Heat in Solids
Clarendon Press, 1959

Figure 1.1: Sketch Showing Plug Formation During Pipe Freezing

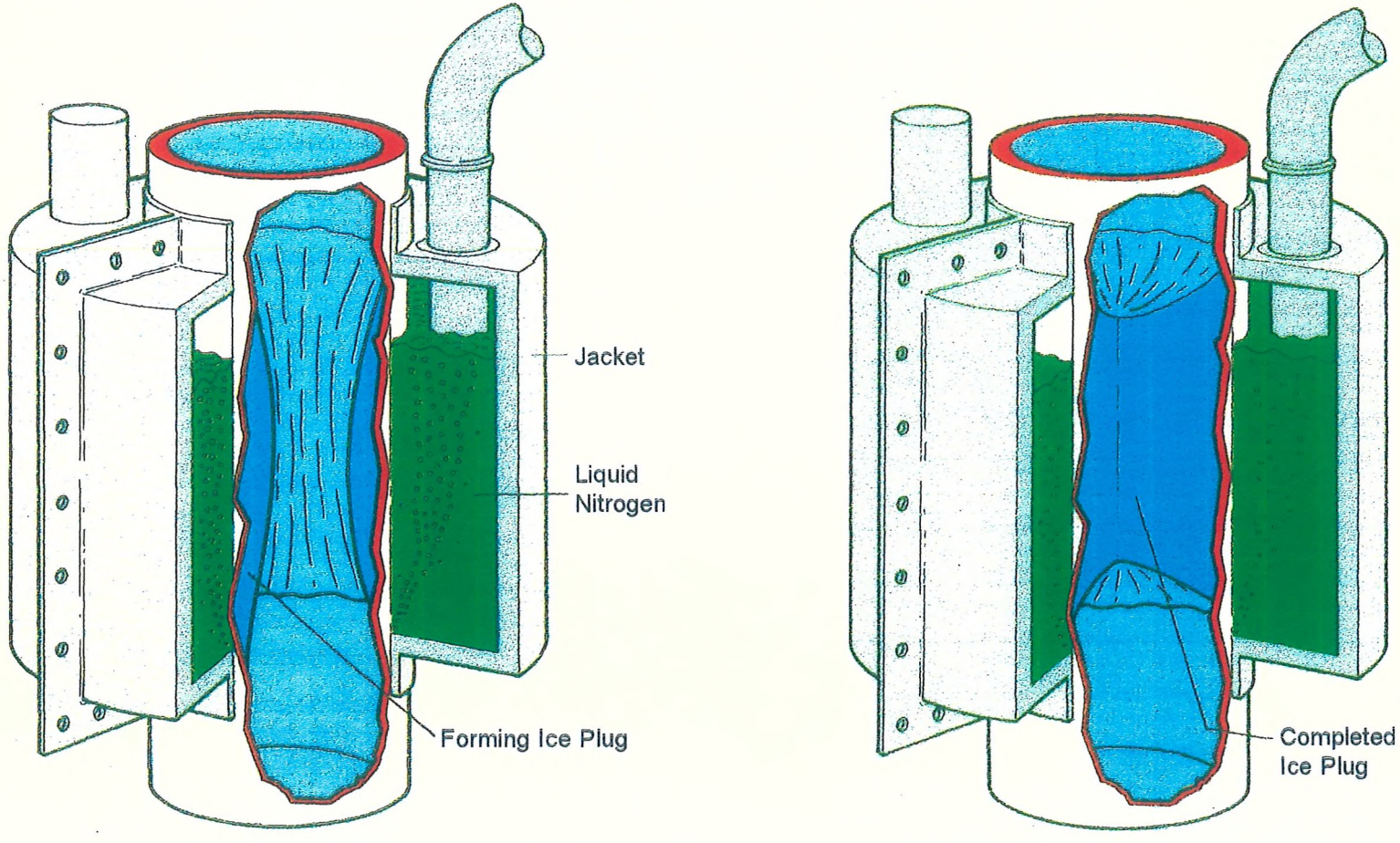

Time To Freeze Water in a Vertical Pipe

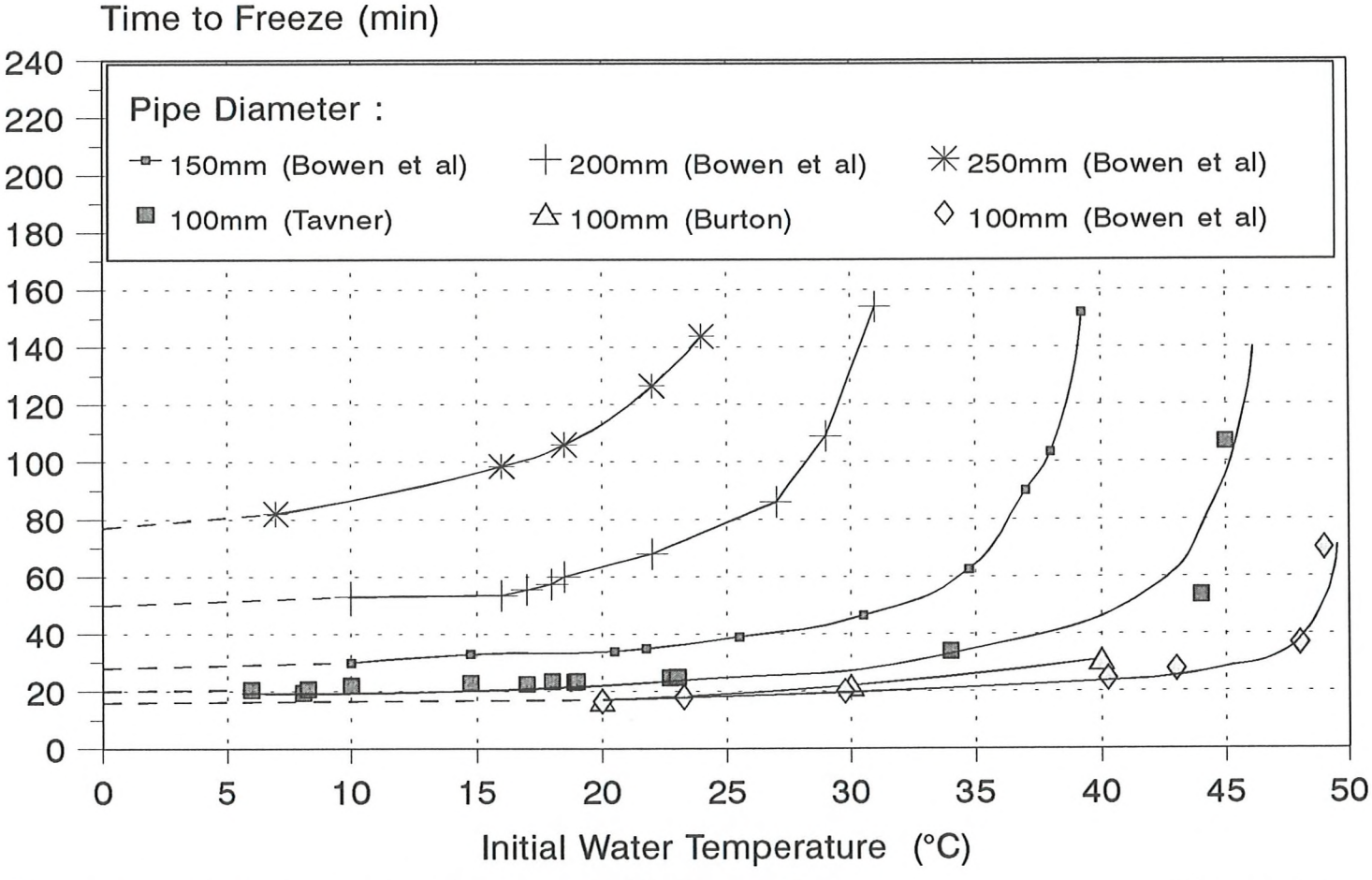

Measurements: Burton[1], Bowen et al[9], Tavner[5]

Figure 2.1

Figure 2.2: Sketch showing Three Stages of Plug Formation Proposed by Burton[1]

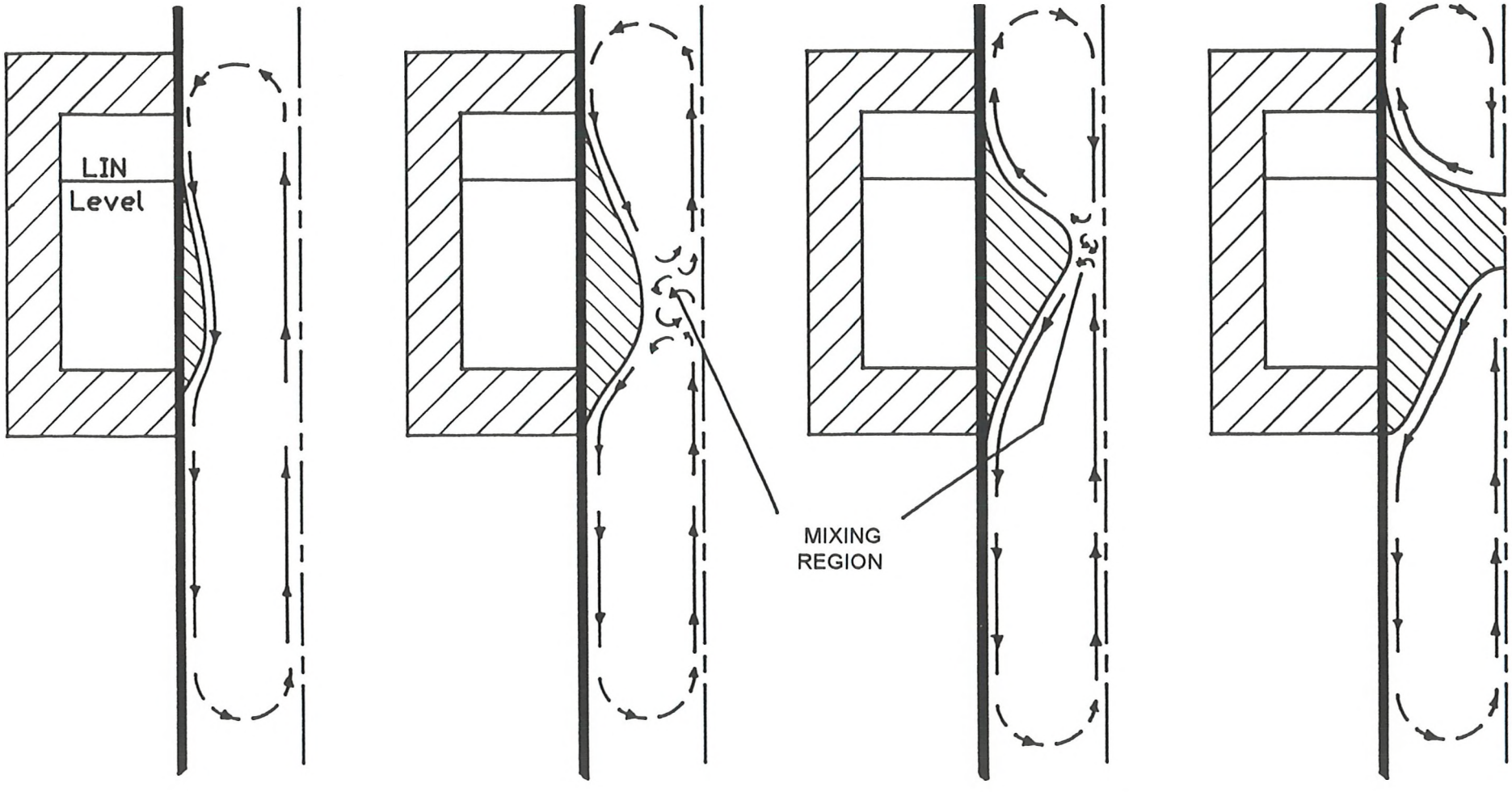

Predicted Time to Freeze

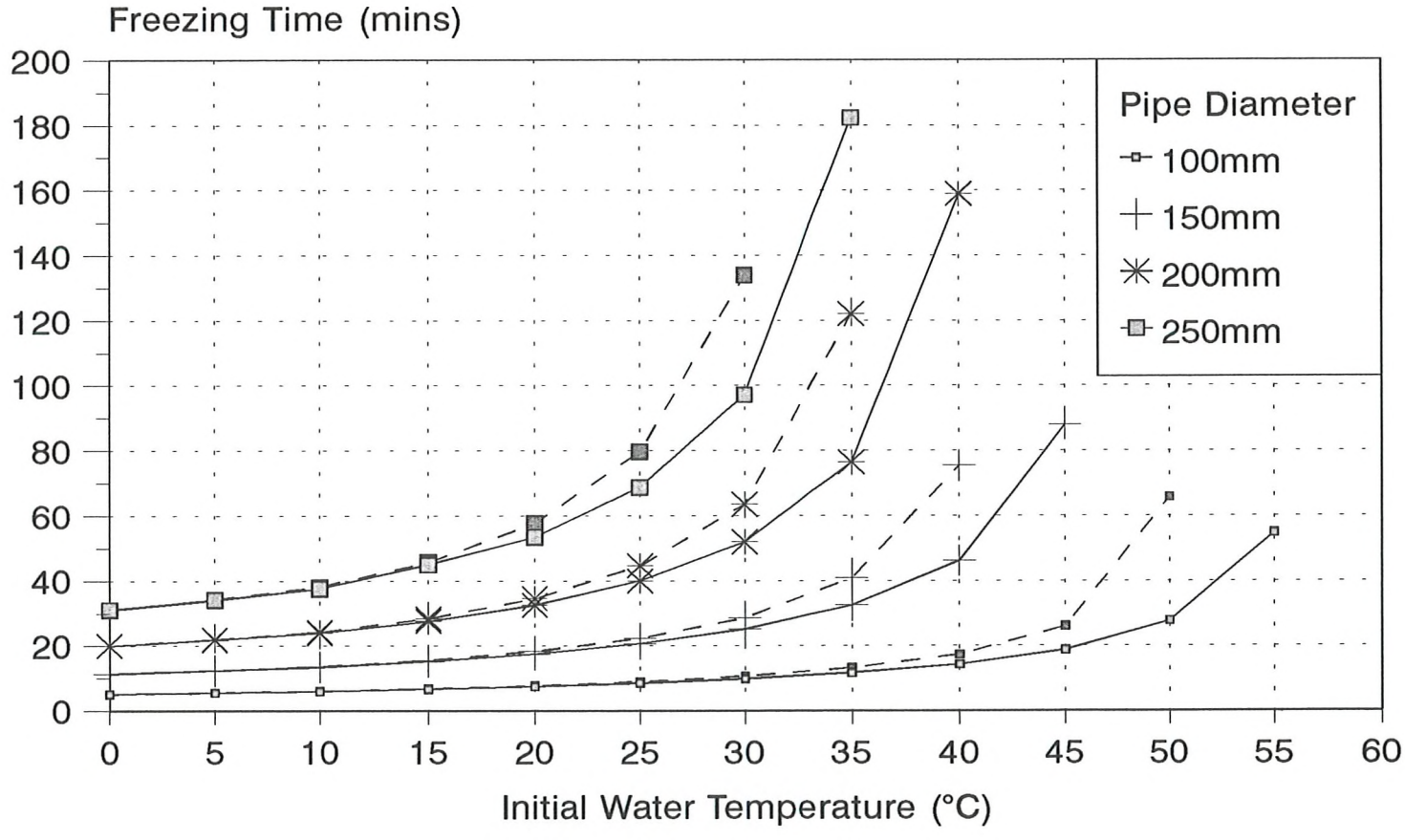

Analytical model; no bulk temperature decay
H=2xdia; T_c=-196°C; A_h=1.0 (solid lines), ½ (dashed lines); h_c=2000 W/m²K

Figure 3.1

Maximum Water Temperature for Successful Freeze
- Effect of Pipe Size -

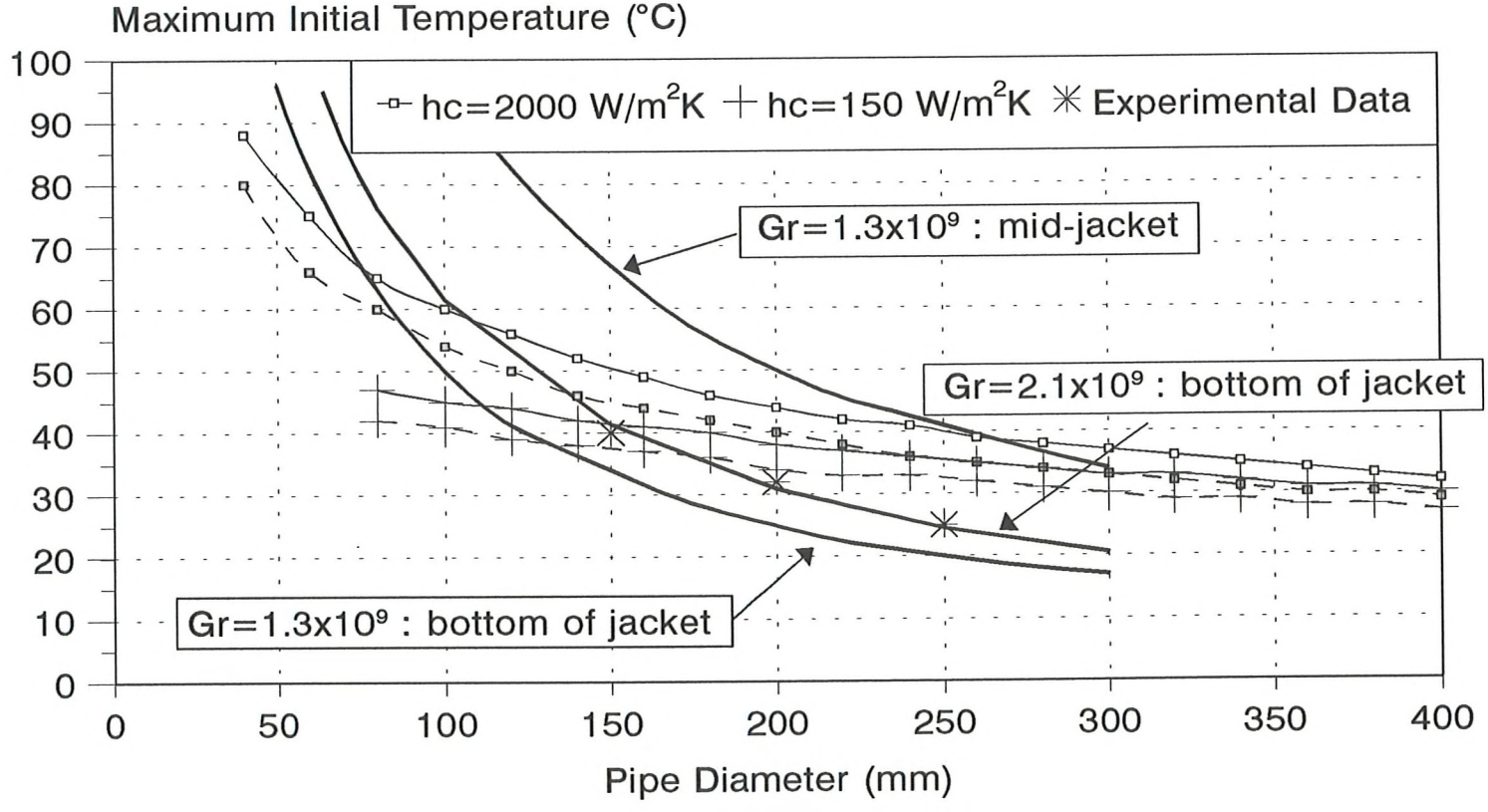

Analytical model - no bulk temperature decay; Experimental data from Bowen et al[9]
H=2xdia; T_c=-196°C; A_h=1.0 (solid lines), ½ (dashed lines)

Figure 3.2

Maximum Water Temperature for Successful Freeze
- Effect of Jacket Length -

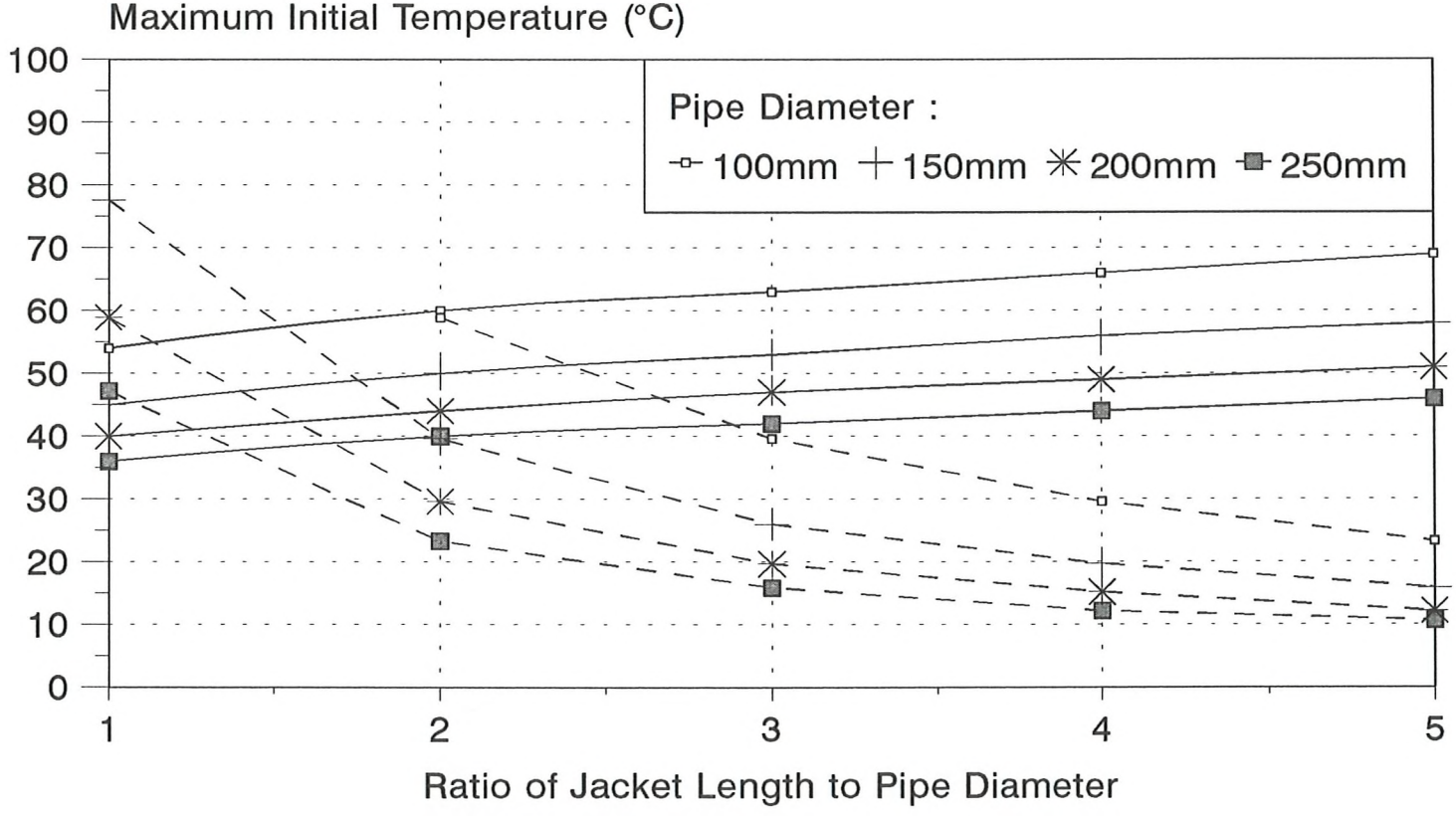

Analytical model - no bulk temperature decay; Tc=-196°C; A_h=1; h_c=2000 W/m²K
Dashed line: Gr=2.1x10⁹ at bottom of jacket

Figure 3.3

Maximum Water Temperature for Successful Freeze
- Effect of Coolant Temperature -

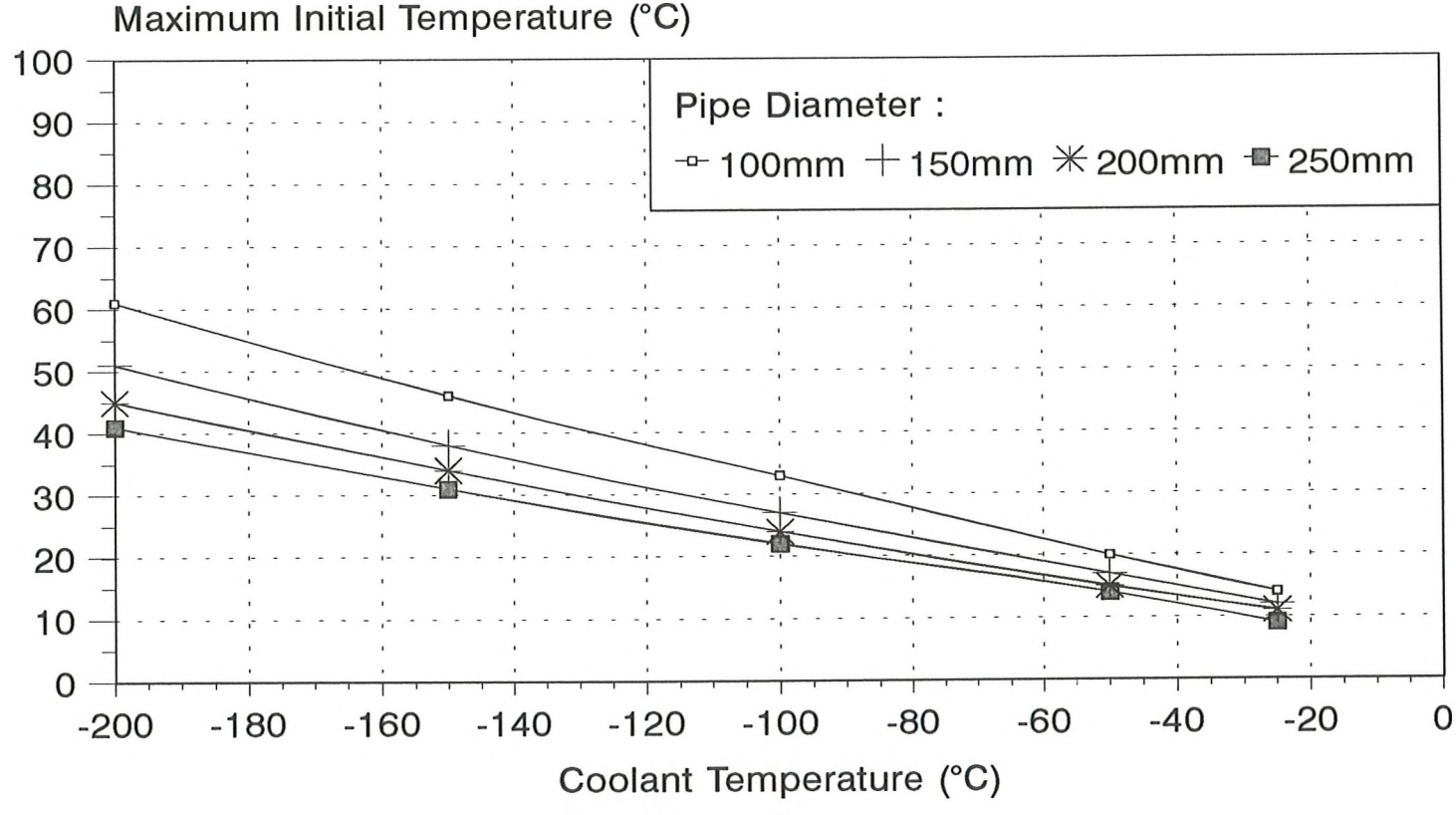

Analytical model - no bulk temperature decay
H=2xdia; A_h=1; h_c=2000 W/m^{2}K

Figure 3.4

Effect of Convection and Turbulence on Pipe Freezing

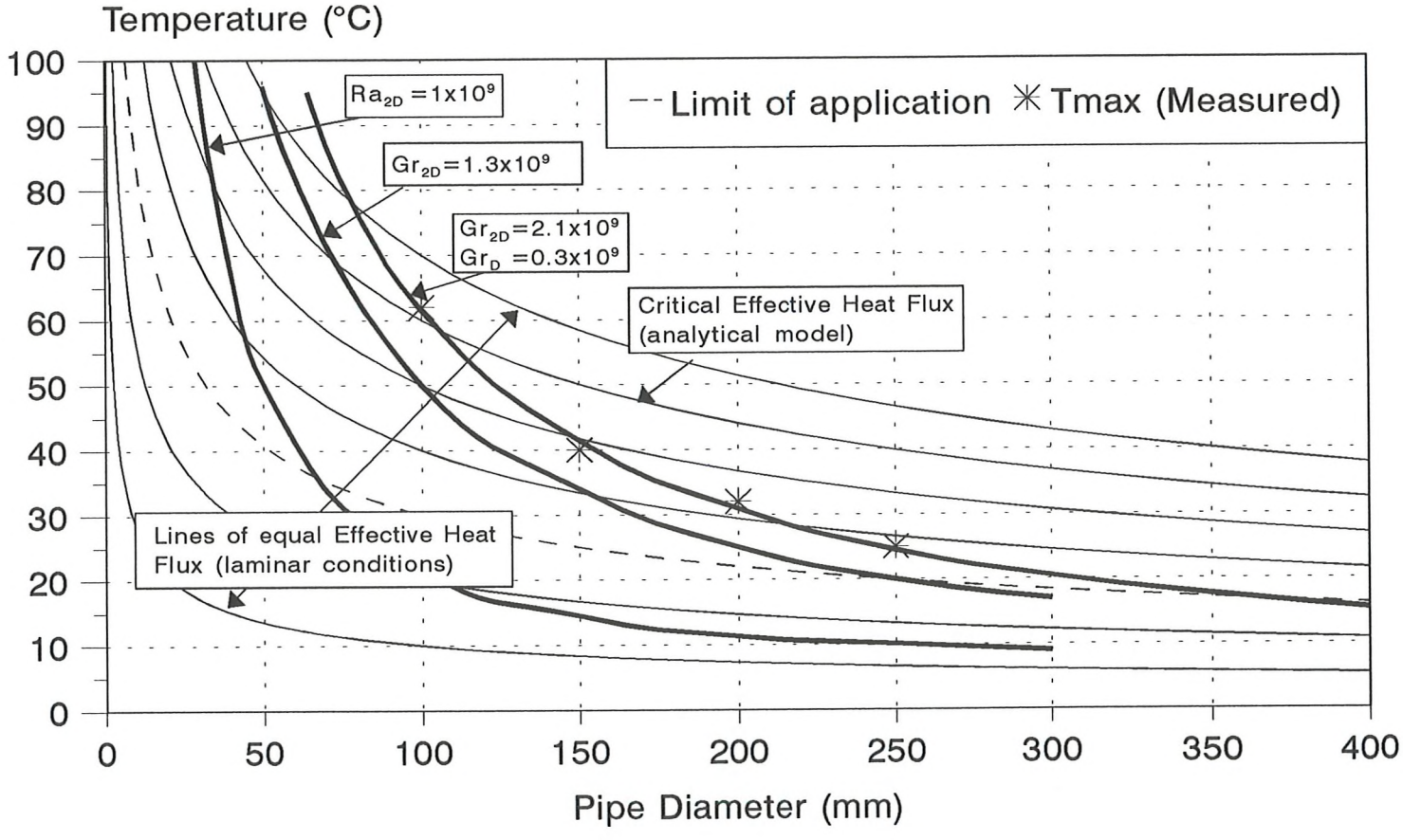

Effective Heat Flux = h.Tb.H (see 3.1.3); Measurements from Bowen et al[9]
H=2xdia; Tc=-196°C; hc=BIG

Figure 3.5

Figure 3.6: Assumed Flow Development for Analytical Flow Model

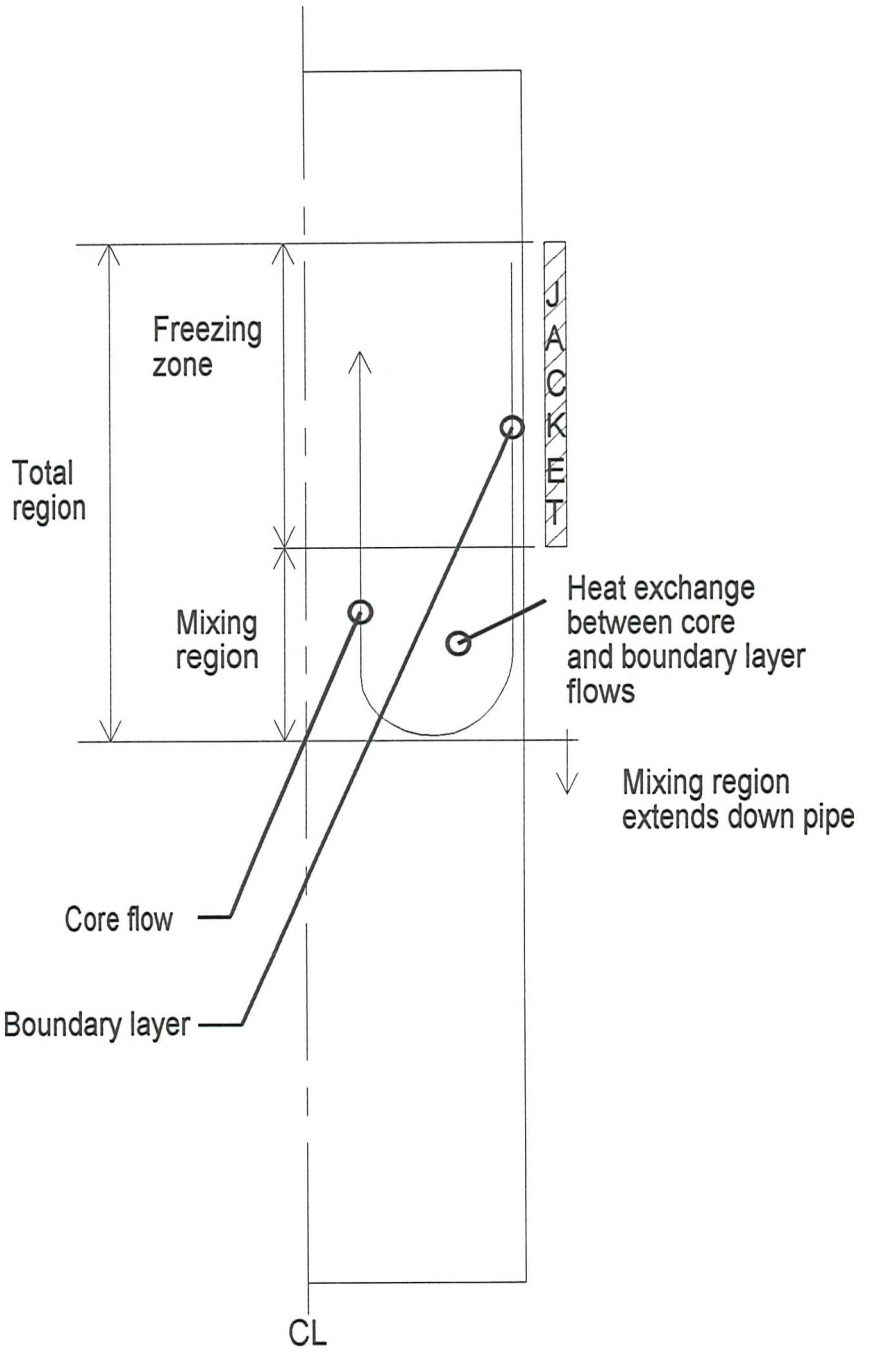

Predicted Bulk Temperature Decay and Length of Mixing Region - Analytical Model of Flow Development -

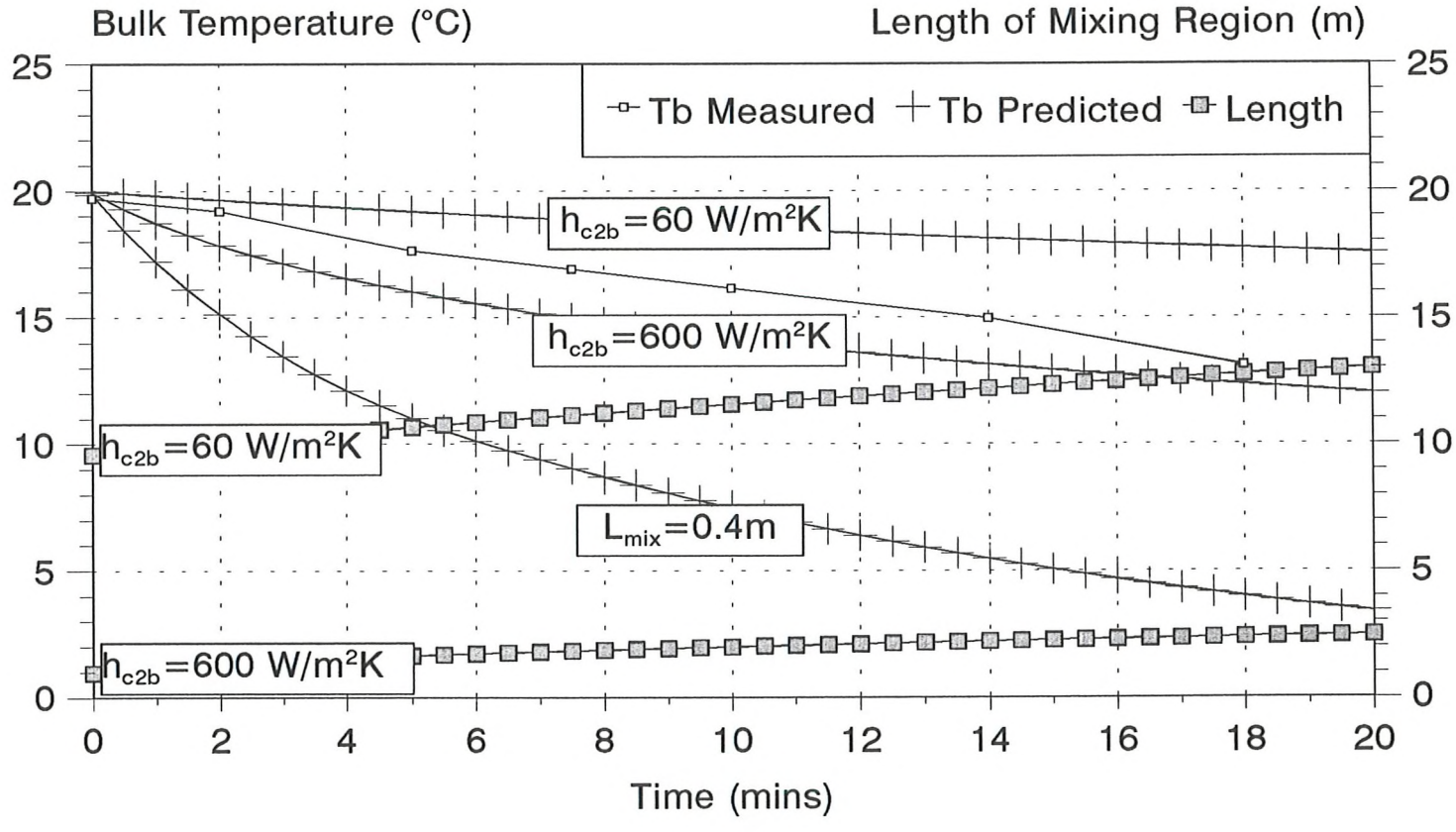

Dia=100mm; H=2xdia; Tc=0°C; Tin=20°C
Measurements from Tavner[5]

Figure 3.7

Predicted Time to Freeze
- Analytical Freezing Model with Bulk Temperature Decay -

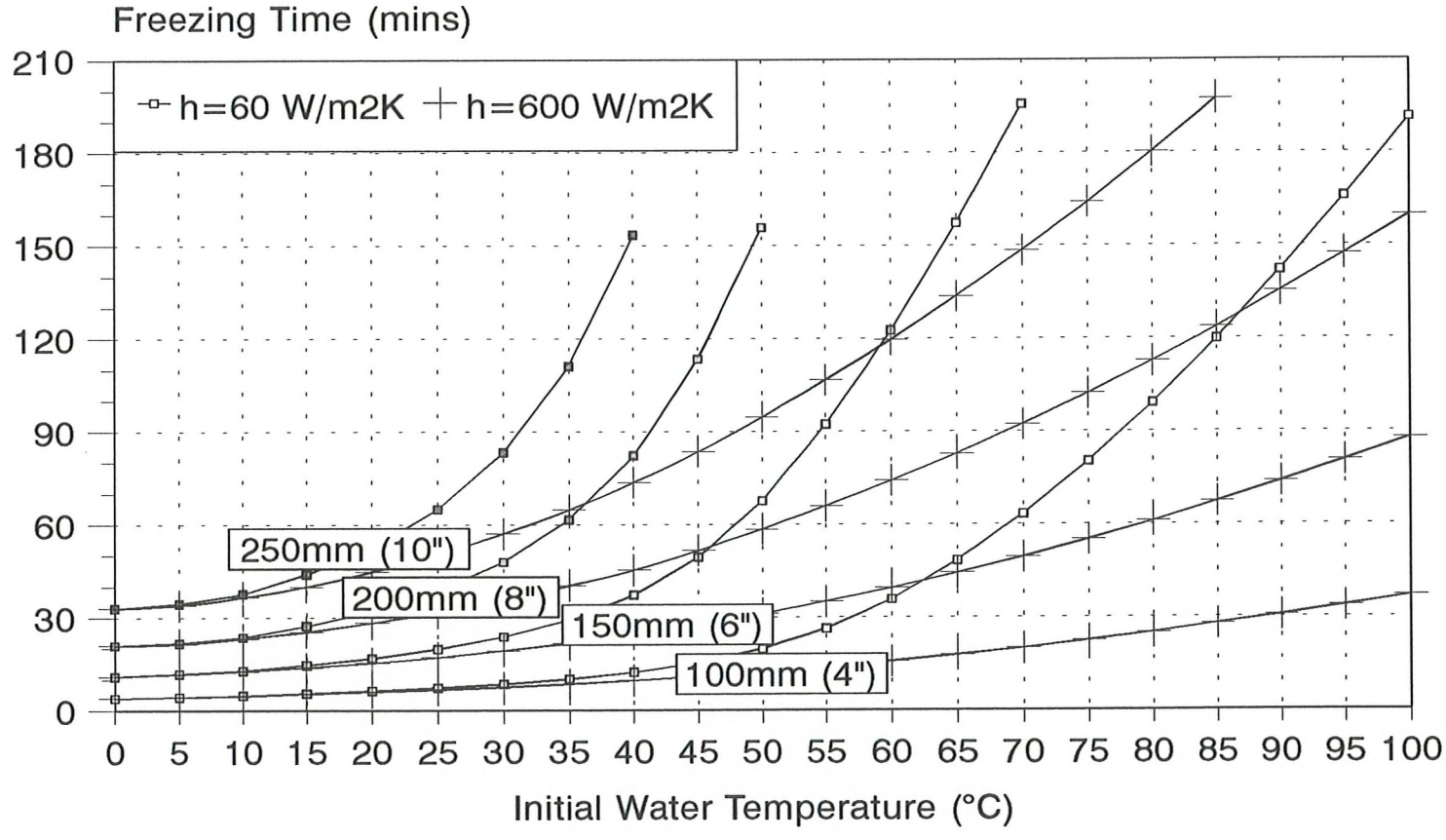

$H=2xdia$; $T_c=-196°C$; $A_h=½$

Figure 3.8

'Stepping' Movement of the Solid/Liquid Interface Predicted using the Enthalpy Method

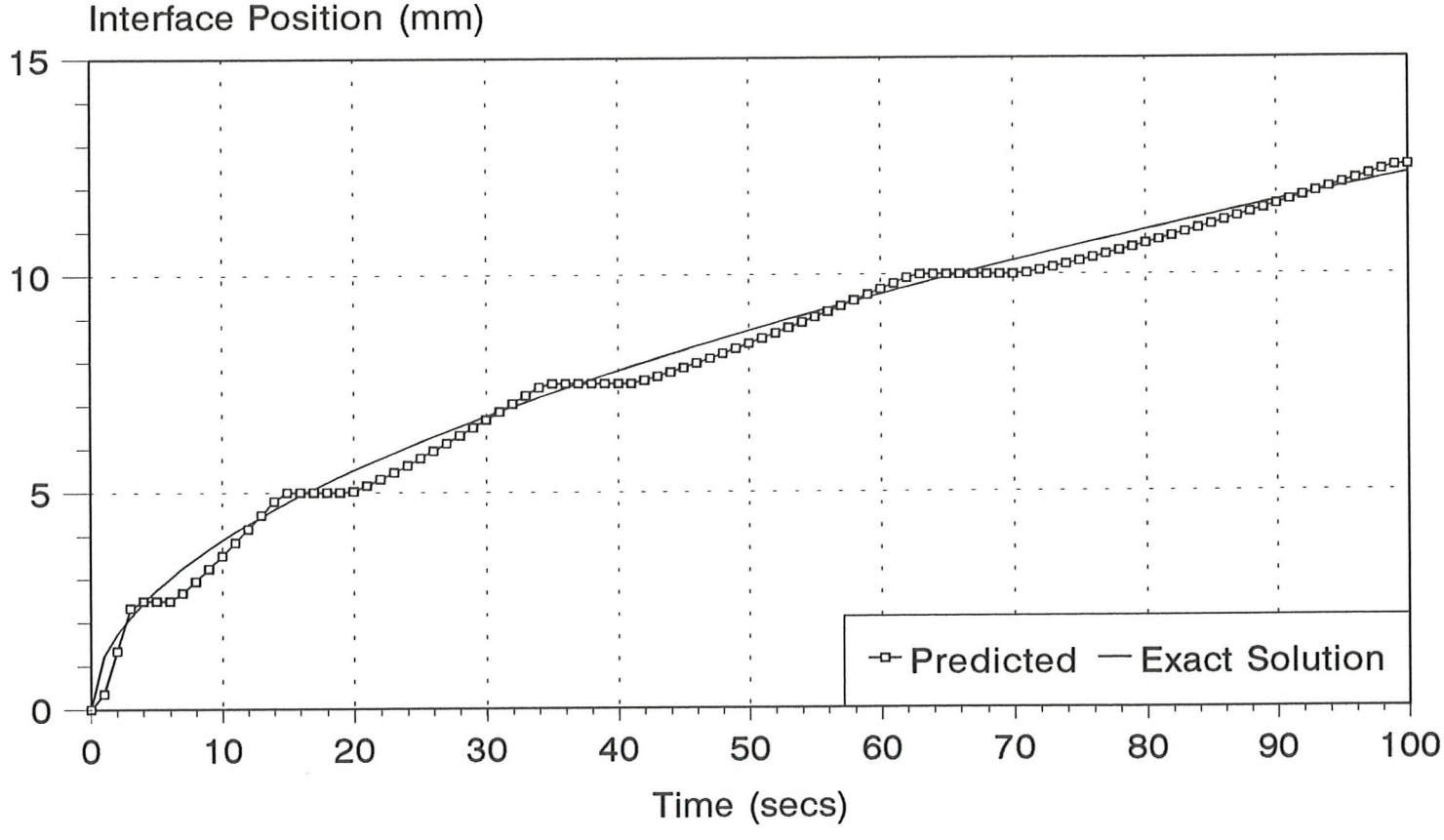

1D Neumann Problem[70]; dx=2.5mm

Figure 4.1

Comparison between Predicted and Measured Freezing Times

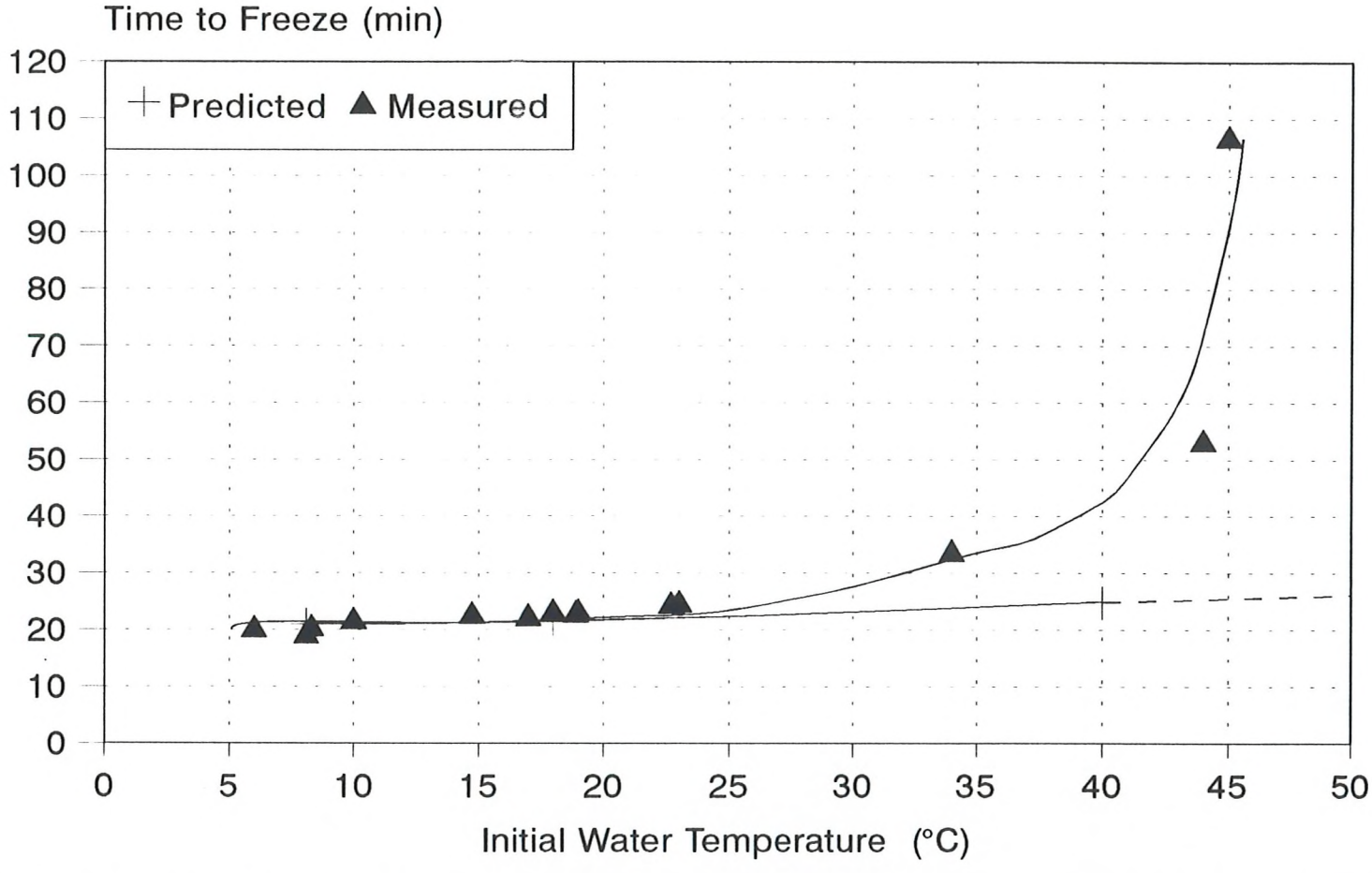

Prediction: no convection; Jacket BC : measured wall temperature from Tavner[5]

Figure 5.1

Figure 5.2a: Temperature profiles for 8°C freeze; No convection

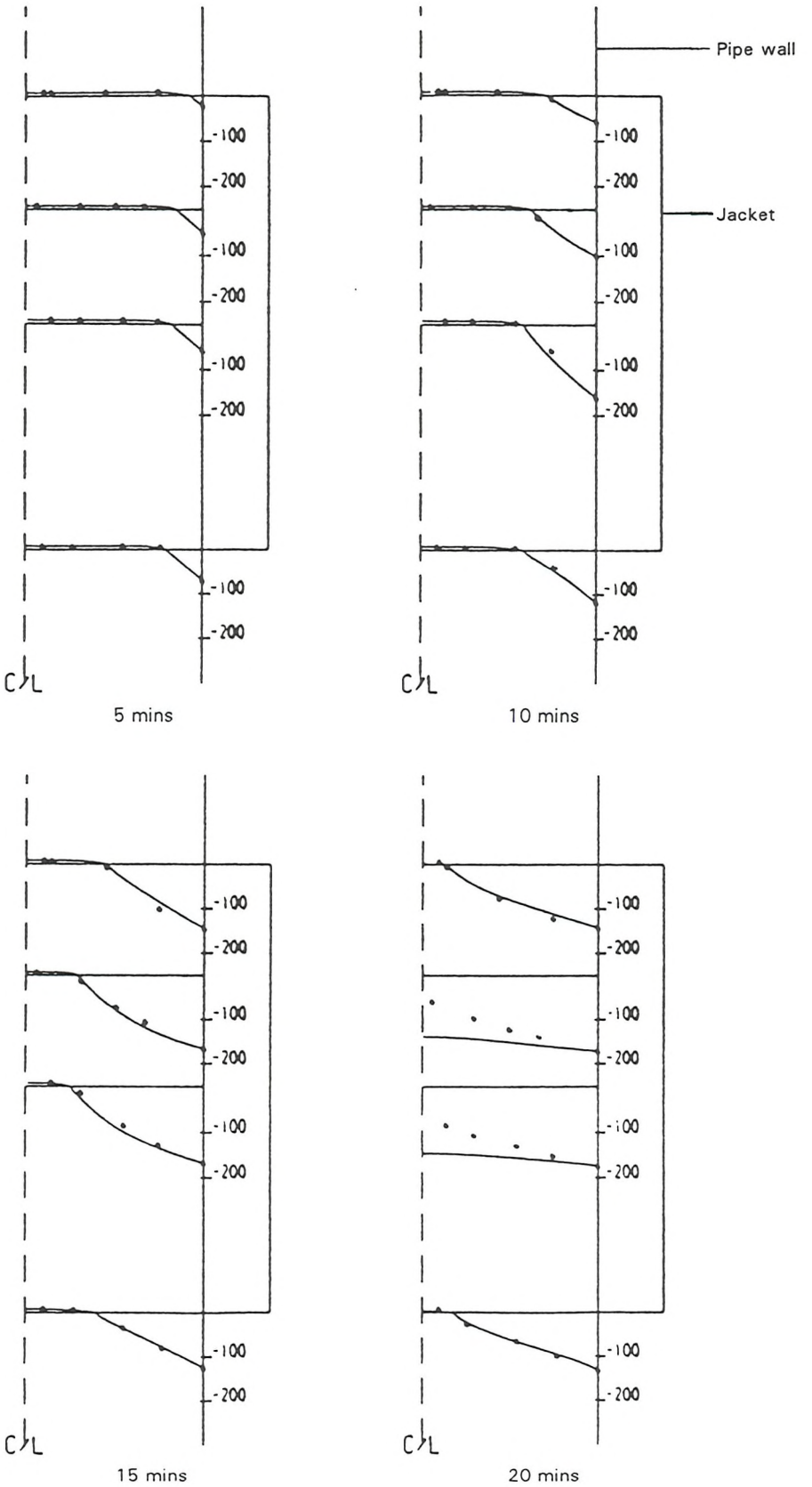

Figure 5.2b: Temperature profiles for 26°C freeze; No convection

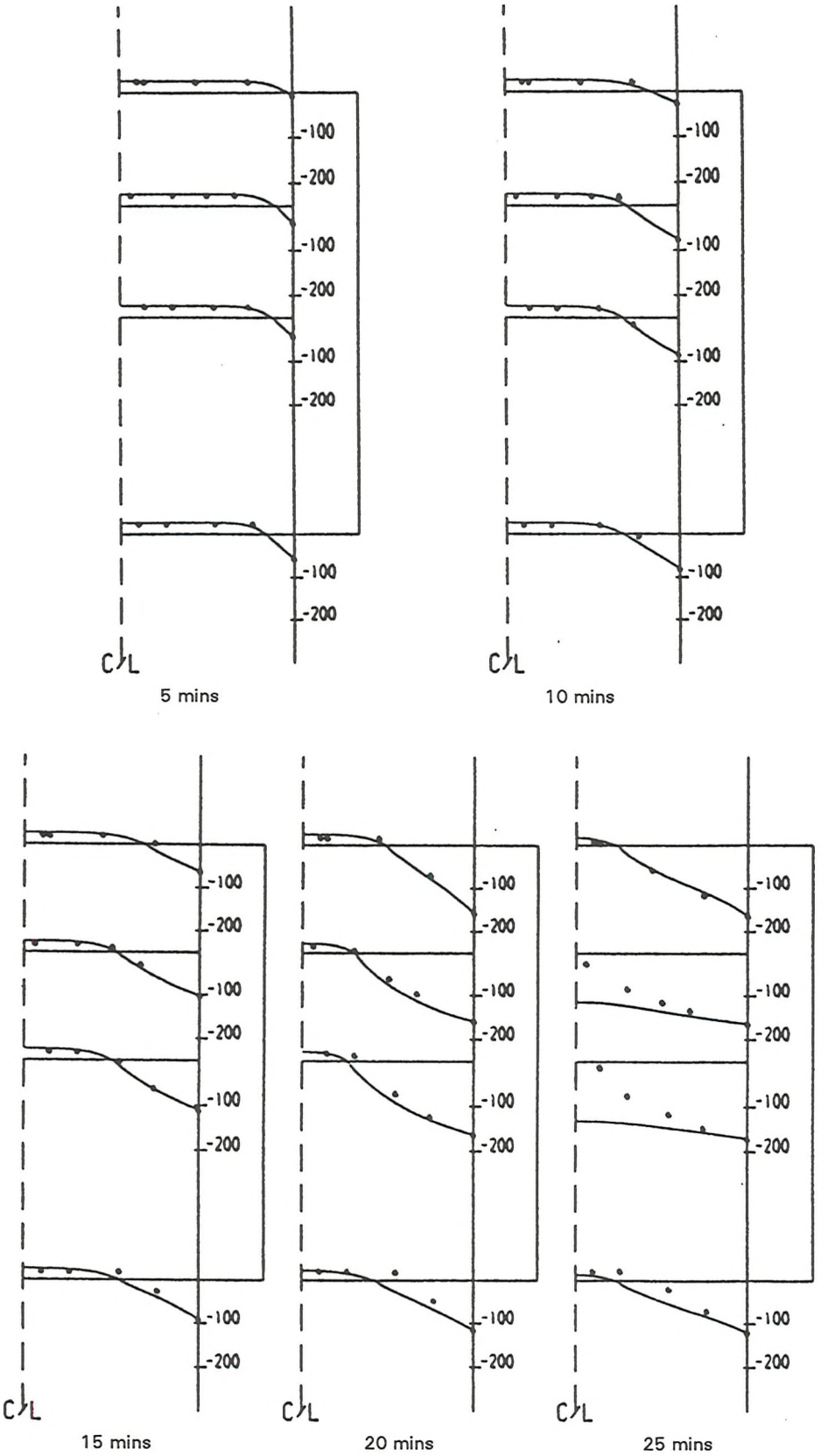

Figure 5.3: Plug profiles for 23°C freeze; No convection

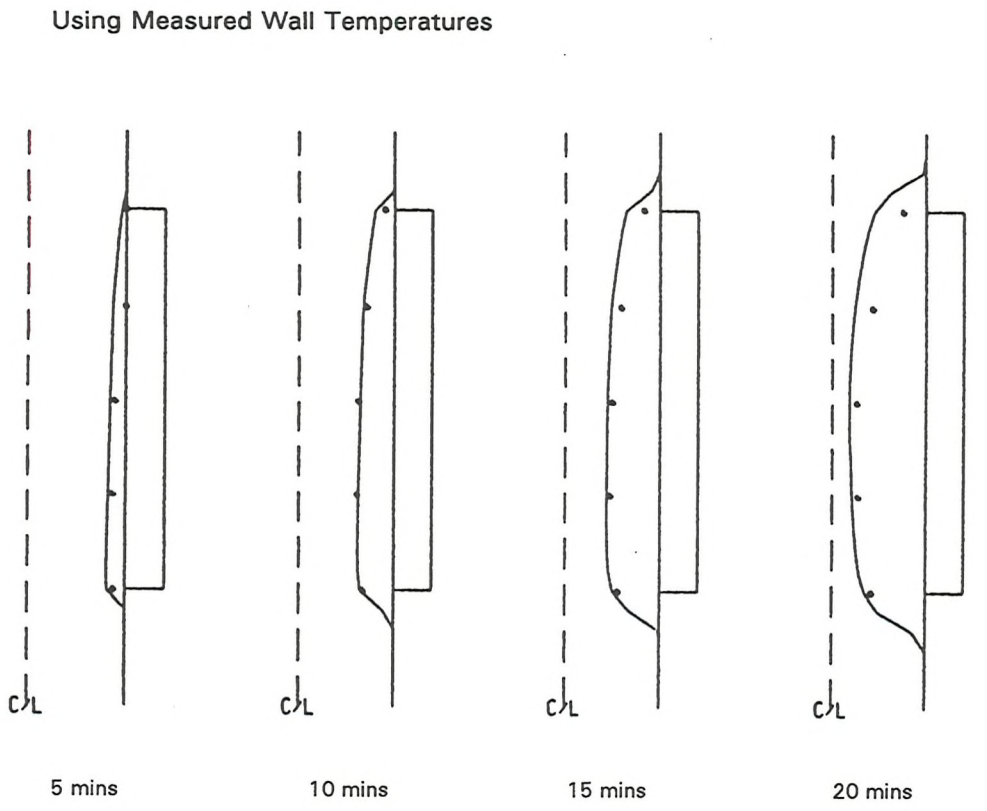

Boiling Curve for Liquid Nitrogen

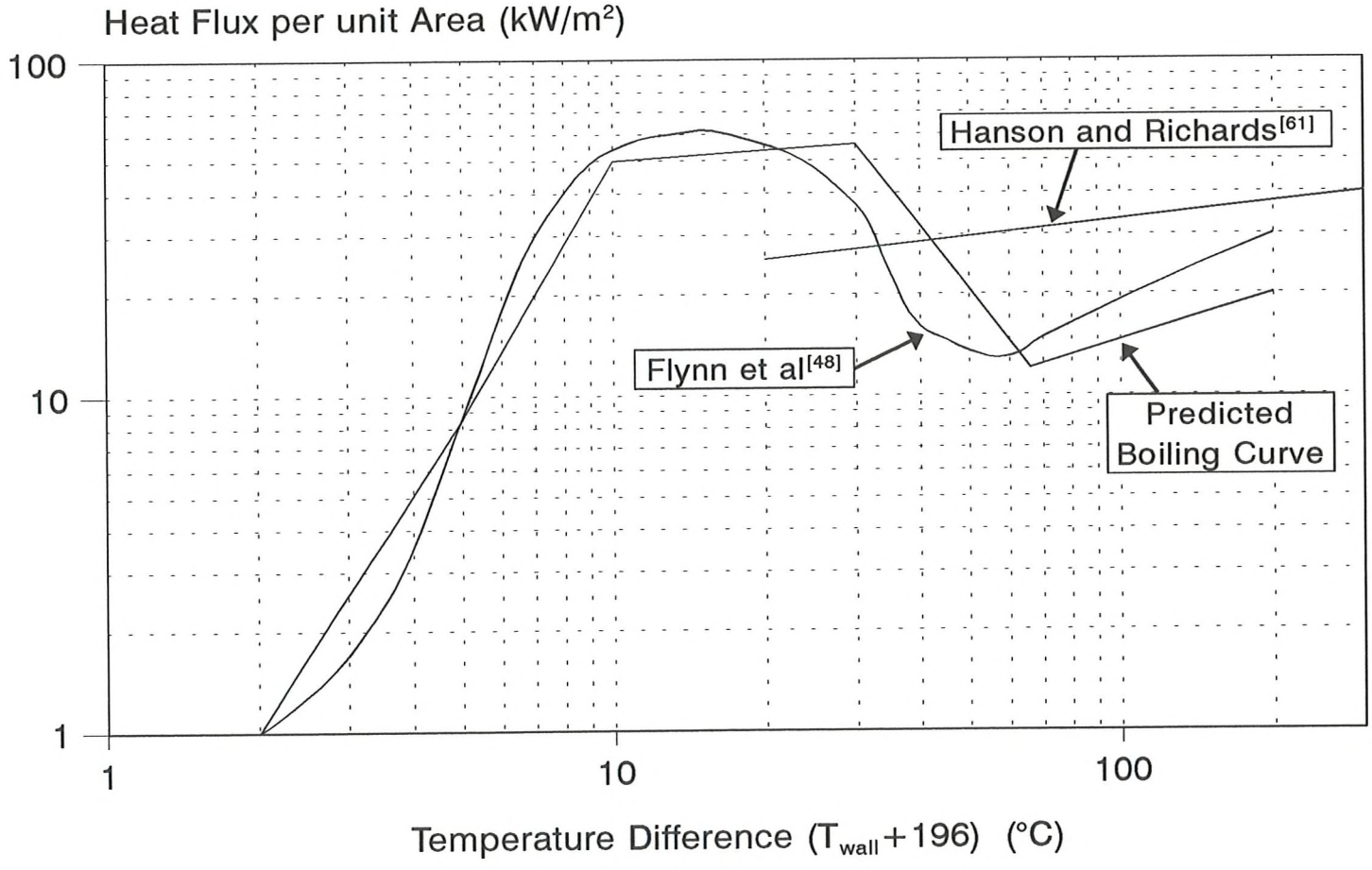

Figure 5.4

Temperature Inside the Pipe Wall at the Centre of Jacket
Comparison using 17°C Freeze Data

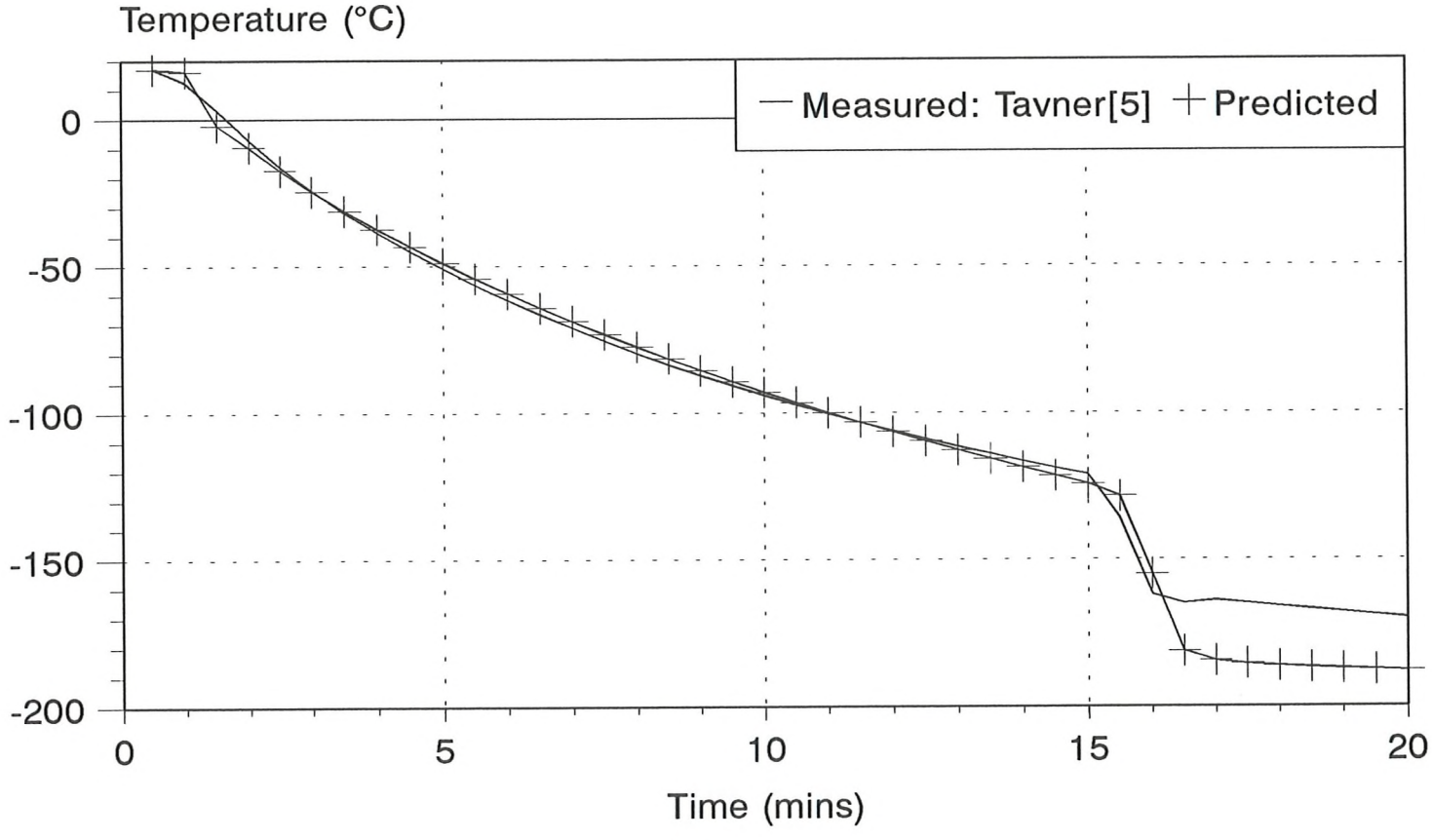

Prediction: no convection; Tin=17°C

Figure 5.5a

Temperature Inside the Pipe Wall at the Centre of Jacket
Comparison using 2°C Freeze Data

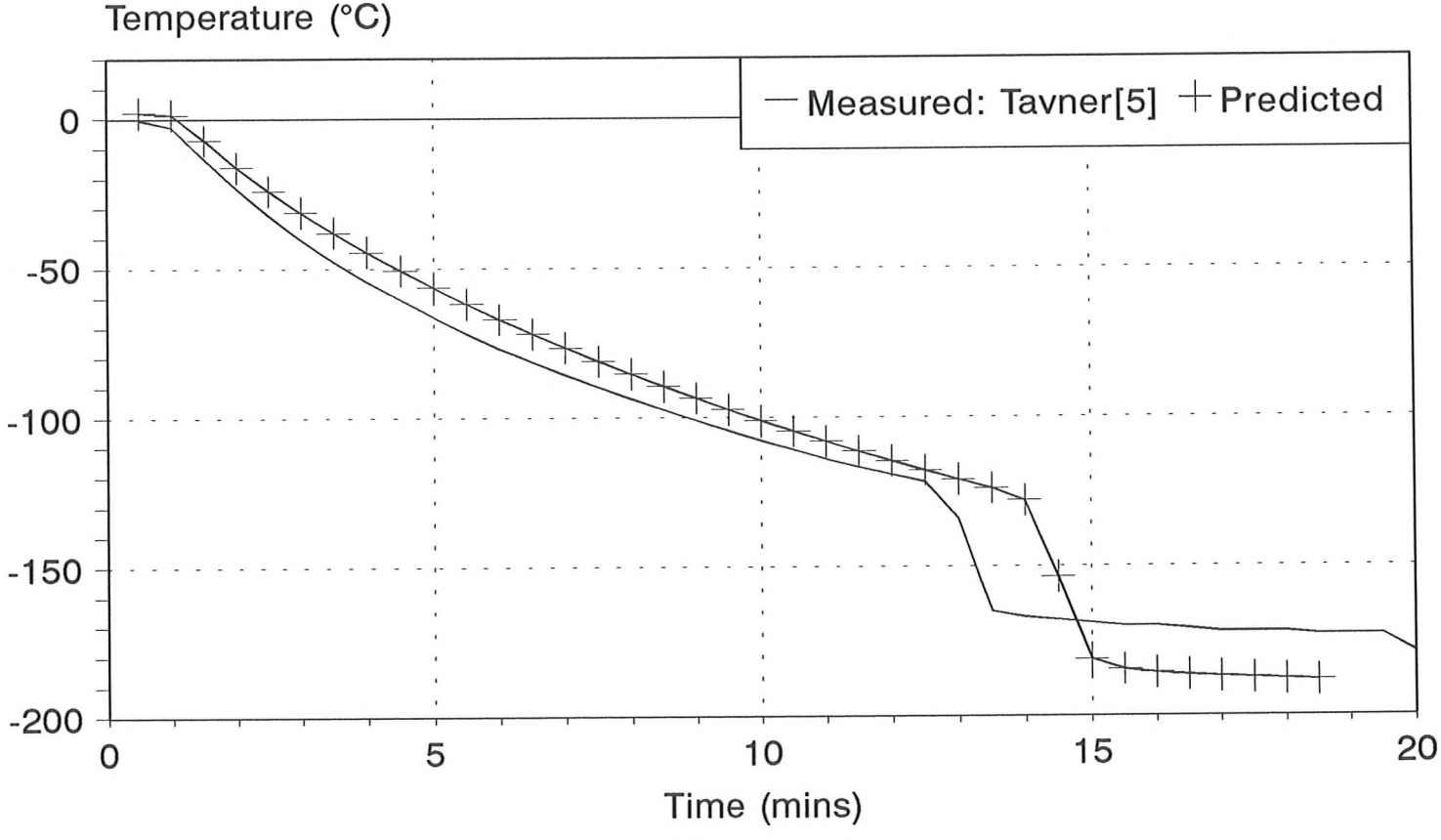

Prediction: no convection; Tin=2.1°C

Figure 5.5b

Figure 5.6: Plug profiles for 23°C freeze; No convection

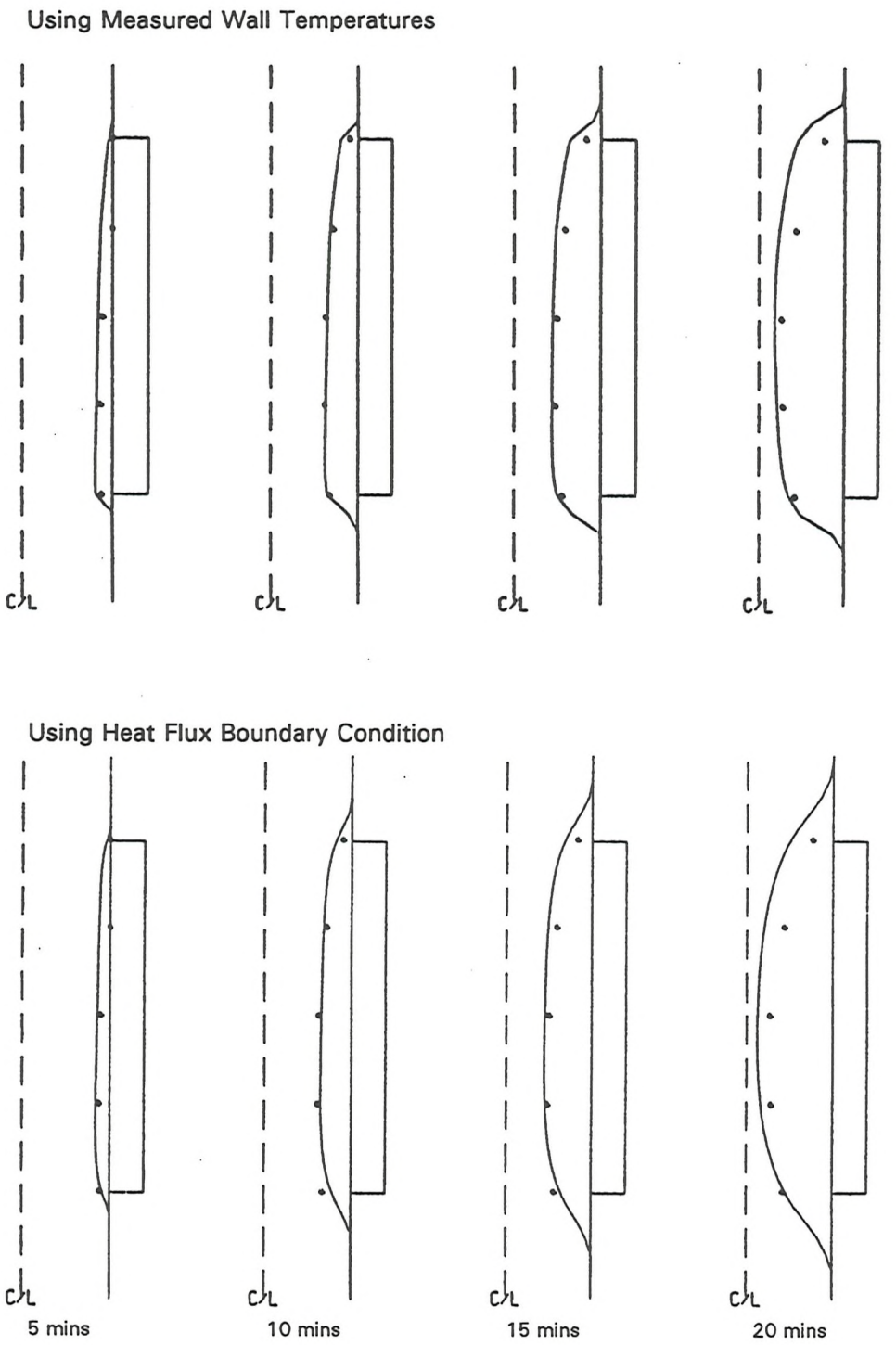

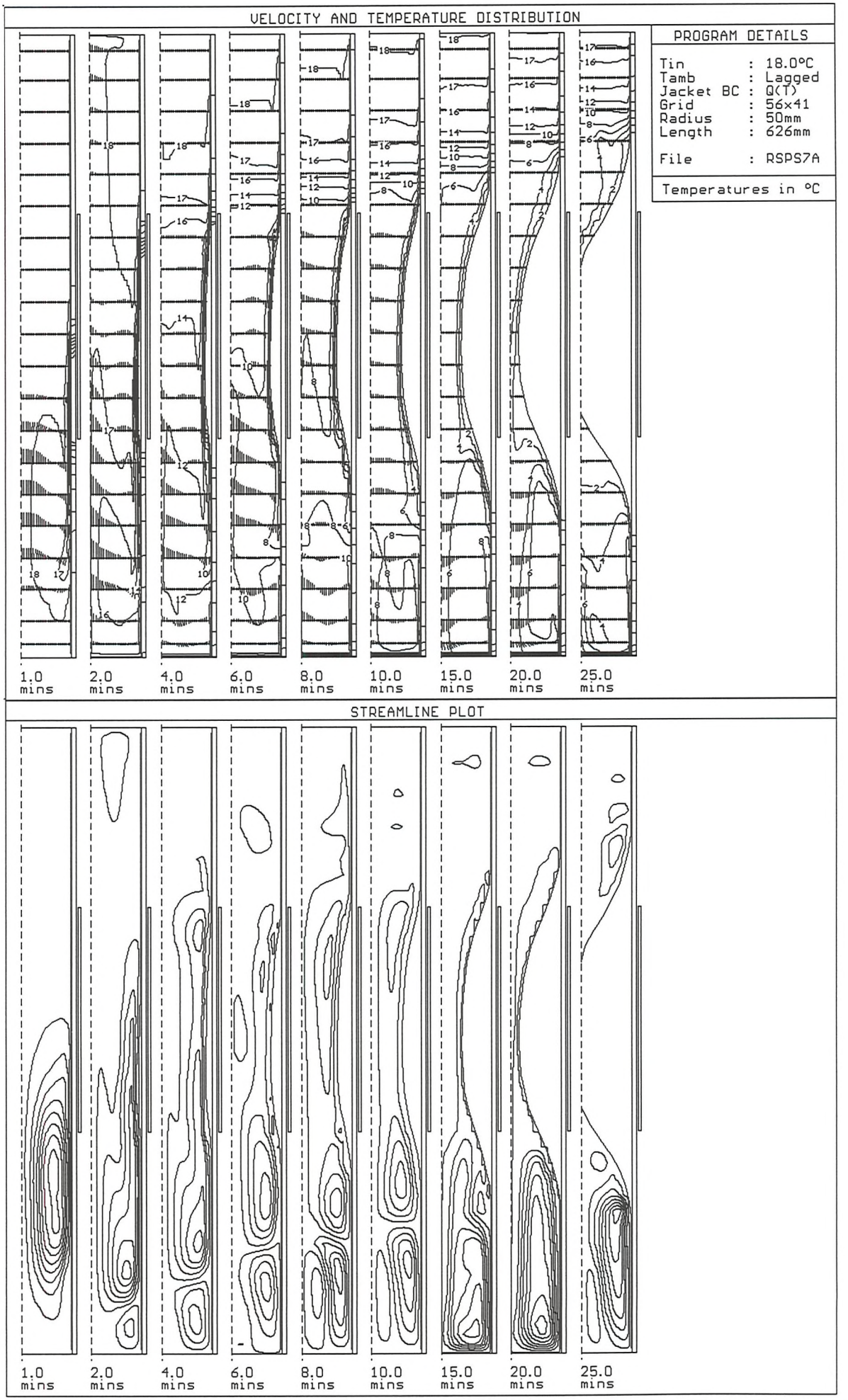

Figure 5.7a : Grid sensitivity test; 'coarse' vertical grid; 56x41; (Test case: 100mm dia.; Tin = 18°C; fv = 1E6)

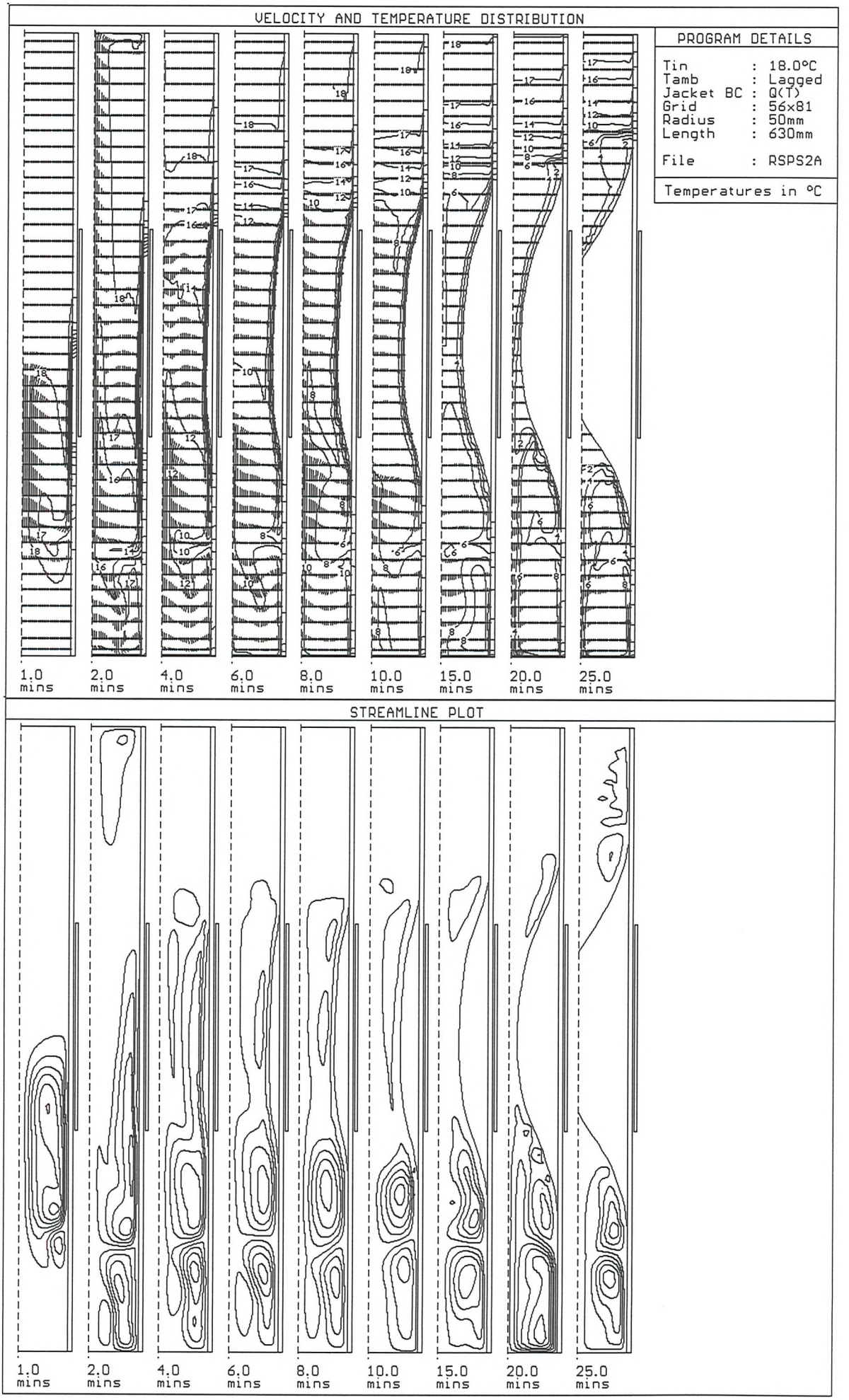

Figure 5.7b : Grid sensitivity test; 'Standard' grid; 56x81; (Test case: 100mm dia.; Tin = 18°C; fv = 1E6)

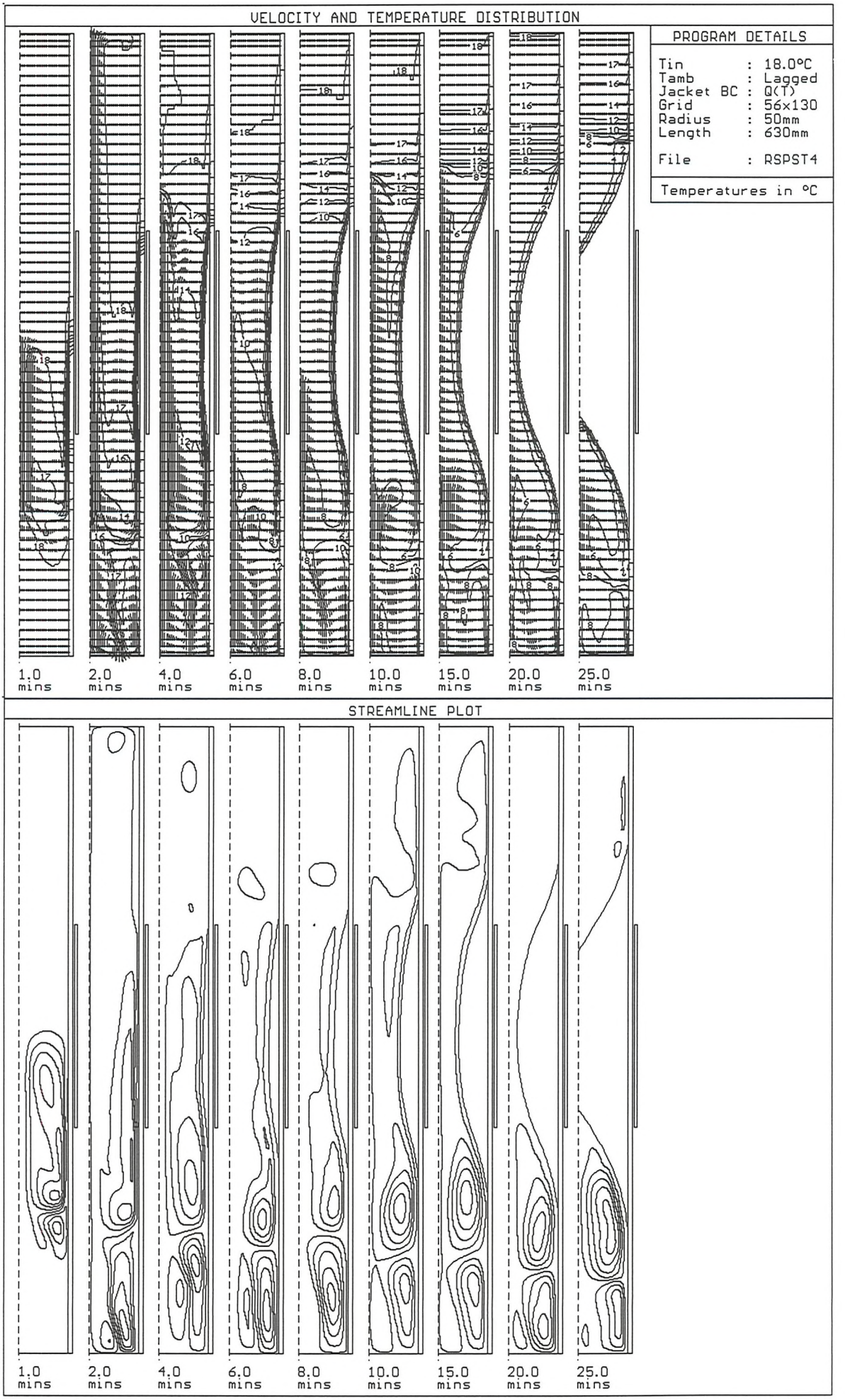

Figure 5.7c : Grid sensitivity test; 'Fine' vertical grid; 56x130; (Test case: 100mm dia.; Tin = 18°C; fv = 1E6)

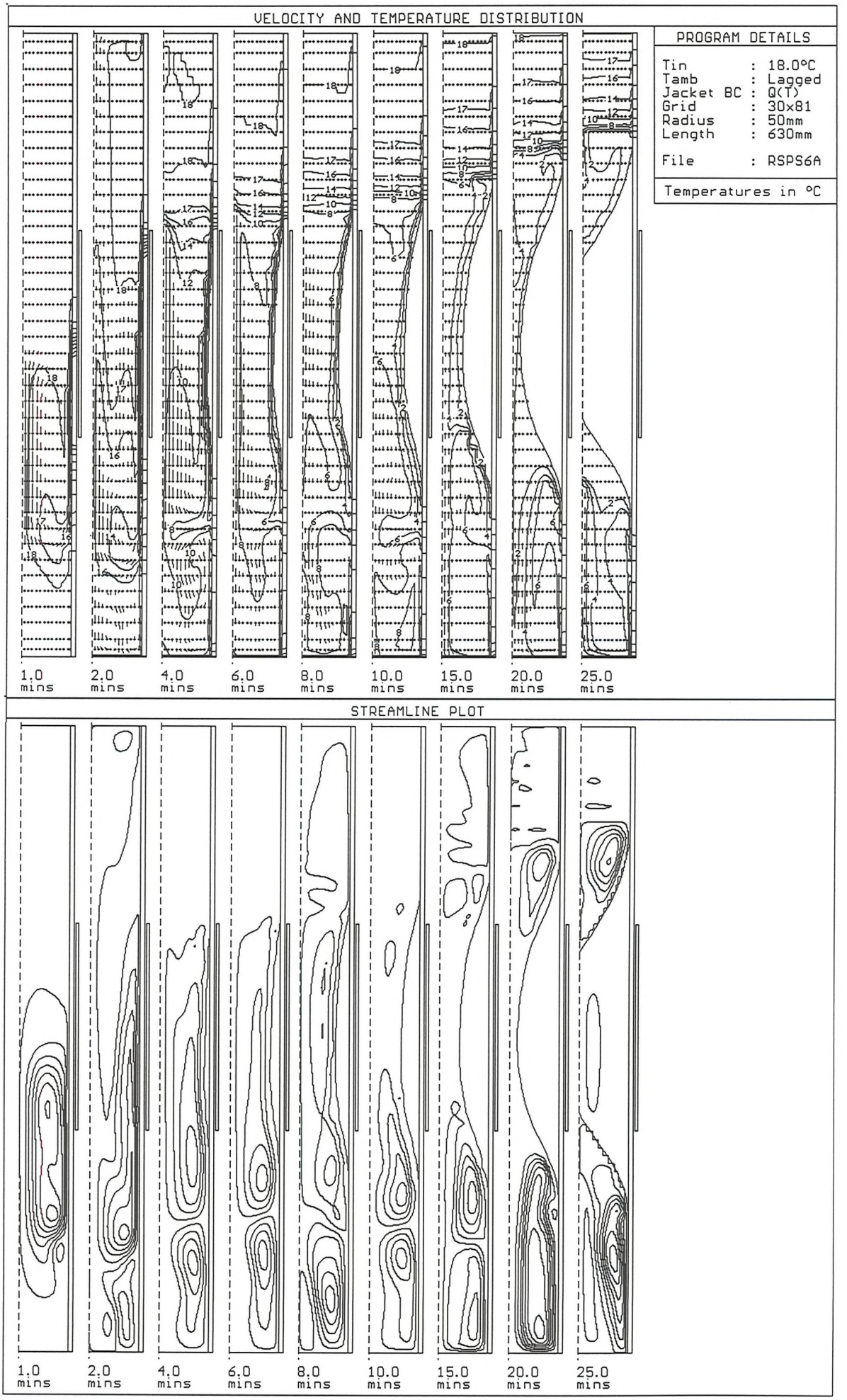

Figure 5.7d : Grid sensitivity test; 'Coarse' radial grid; 30x81; (Test case: 100mm dia.; Tin = 18°C; fv = 1E6)

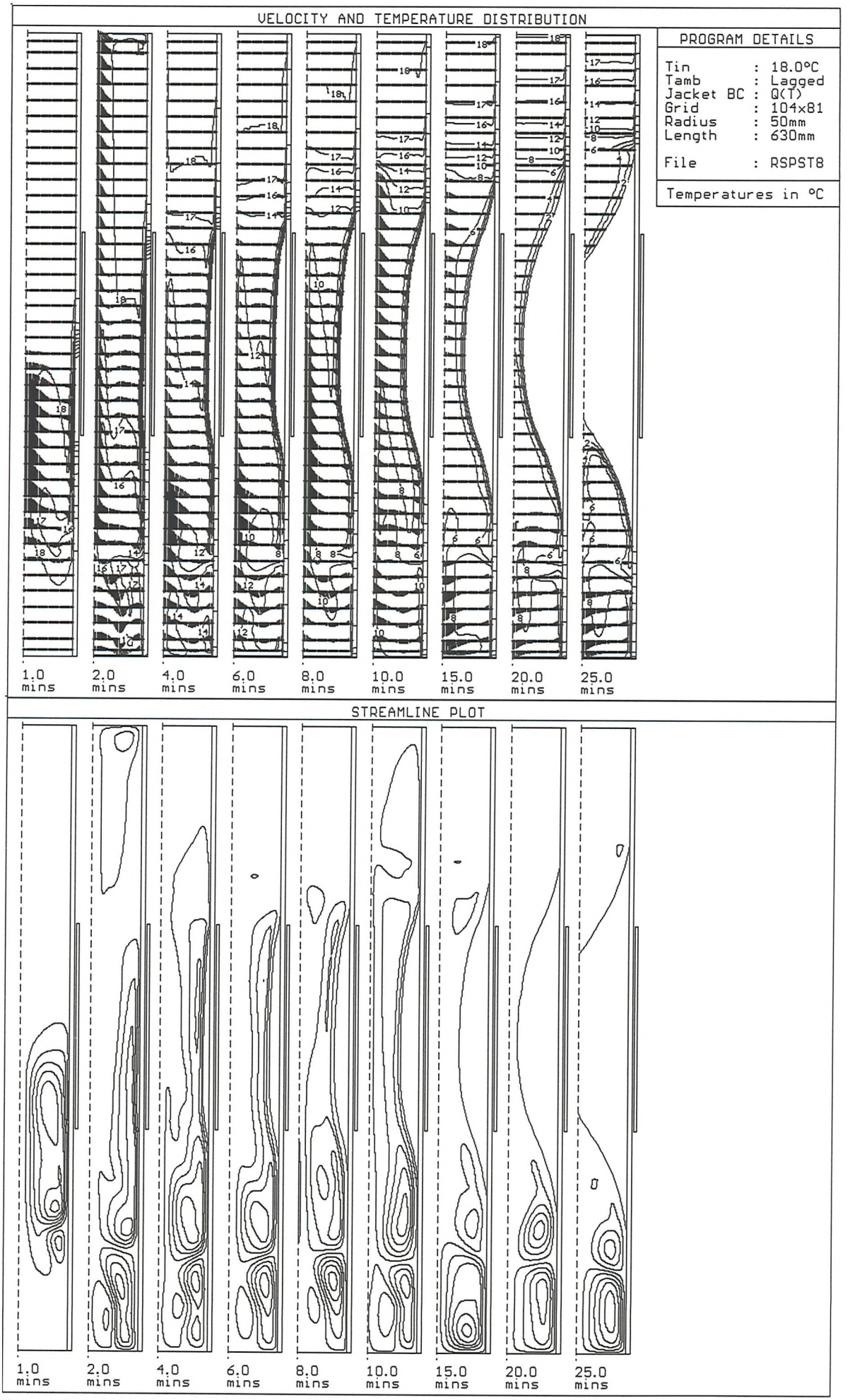

Figure 5.7e : Grid sensitivity test; 'Fine' radial grid; 104x81; (test case: 100mm dia.; Tin = 18°C; fv = 1E6)

Radial Grid Spacing Sensitivity
Boundary Layer Velocity at Centre of Jacket

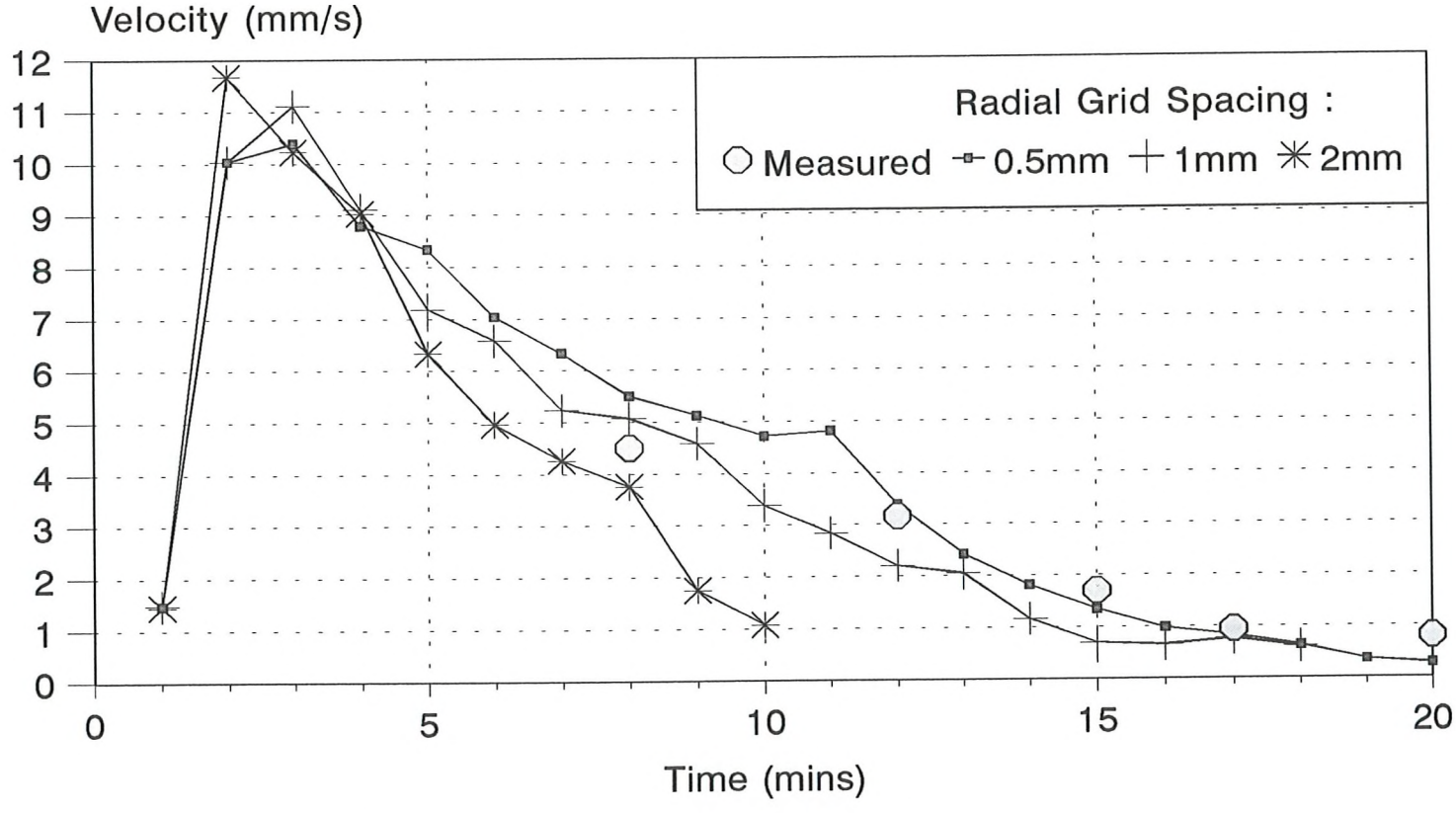

Vertical Grid Spacing 8mm; Pipe Length 630mm; Tin=18°C
Measurements from Tavner[5] (prototype rig:run M36)

Figure 5.8a

Vertical Grid Spacing Sensitivity
Boundary Layer Velocity at Centre of Jacket

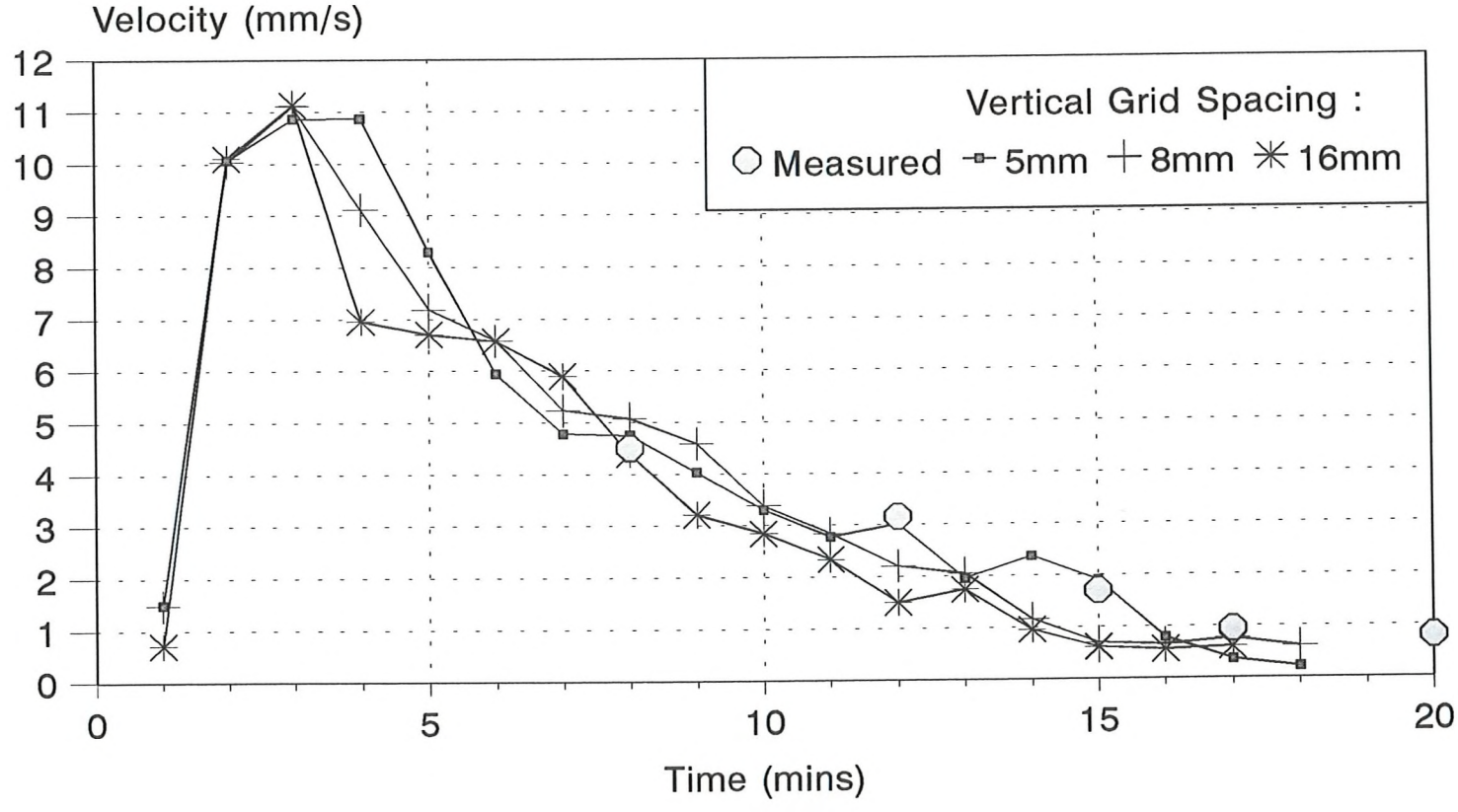

Radial Grid Spacing 1mm; Pipe Length 630mm; Tin=18°C
Measurements from Tavner[5] (prototype rig:run M36)

Figure 5.8b

Radial Grid Spacing Sensitivity
Bulk Temperature Inside Freezing Zone

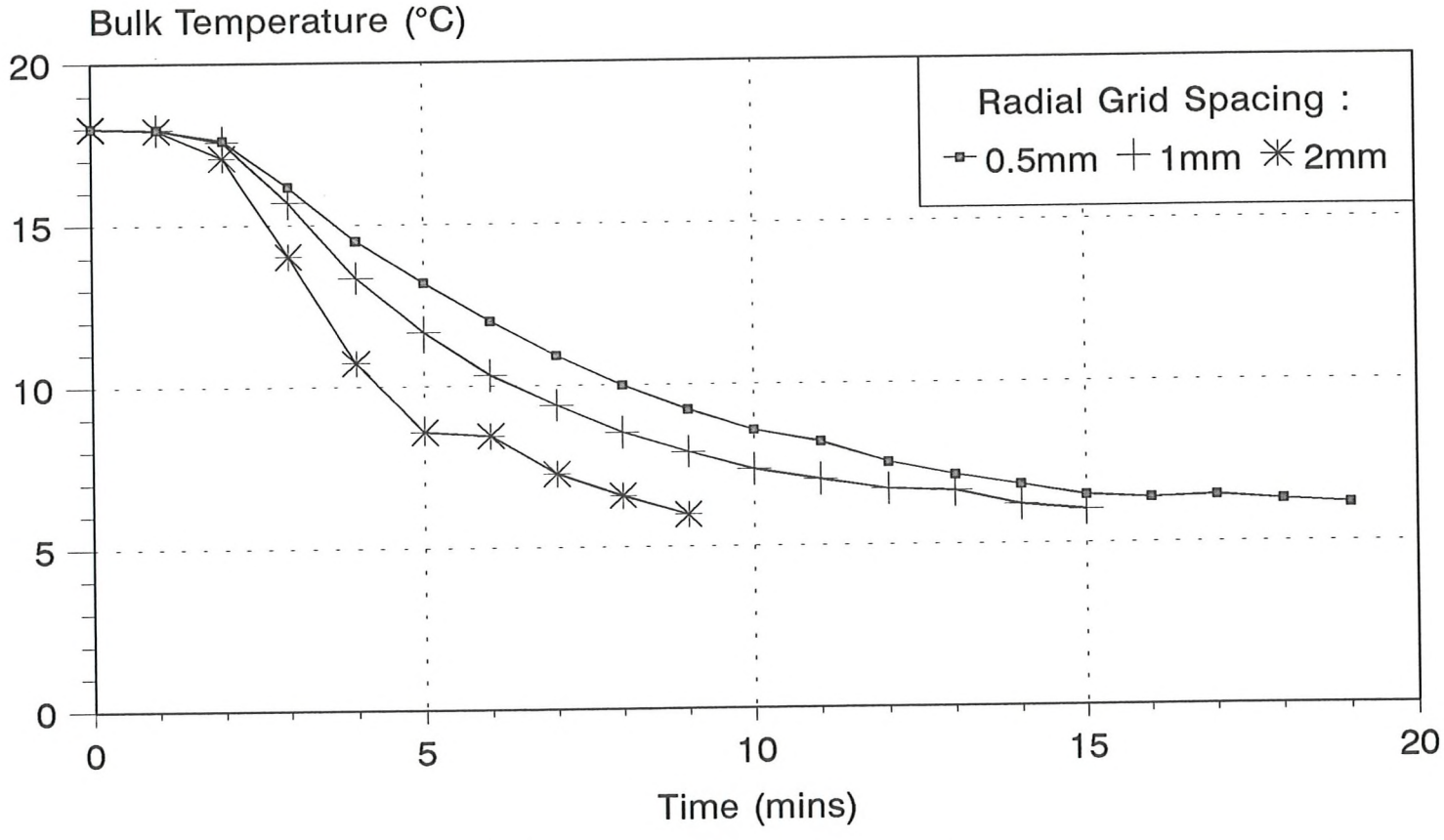

Vertical Grid Spacing 8mm; Pipe Length 630mm; Tin=18°C

Figure 5.9a

Vertical Grid Spacing Sensitivity
Bulk Temperature Inside Freezing Zone

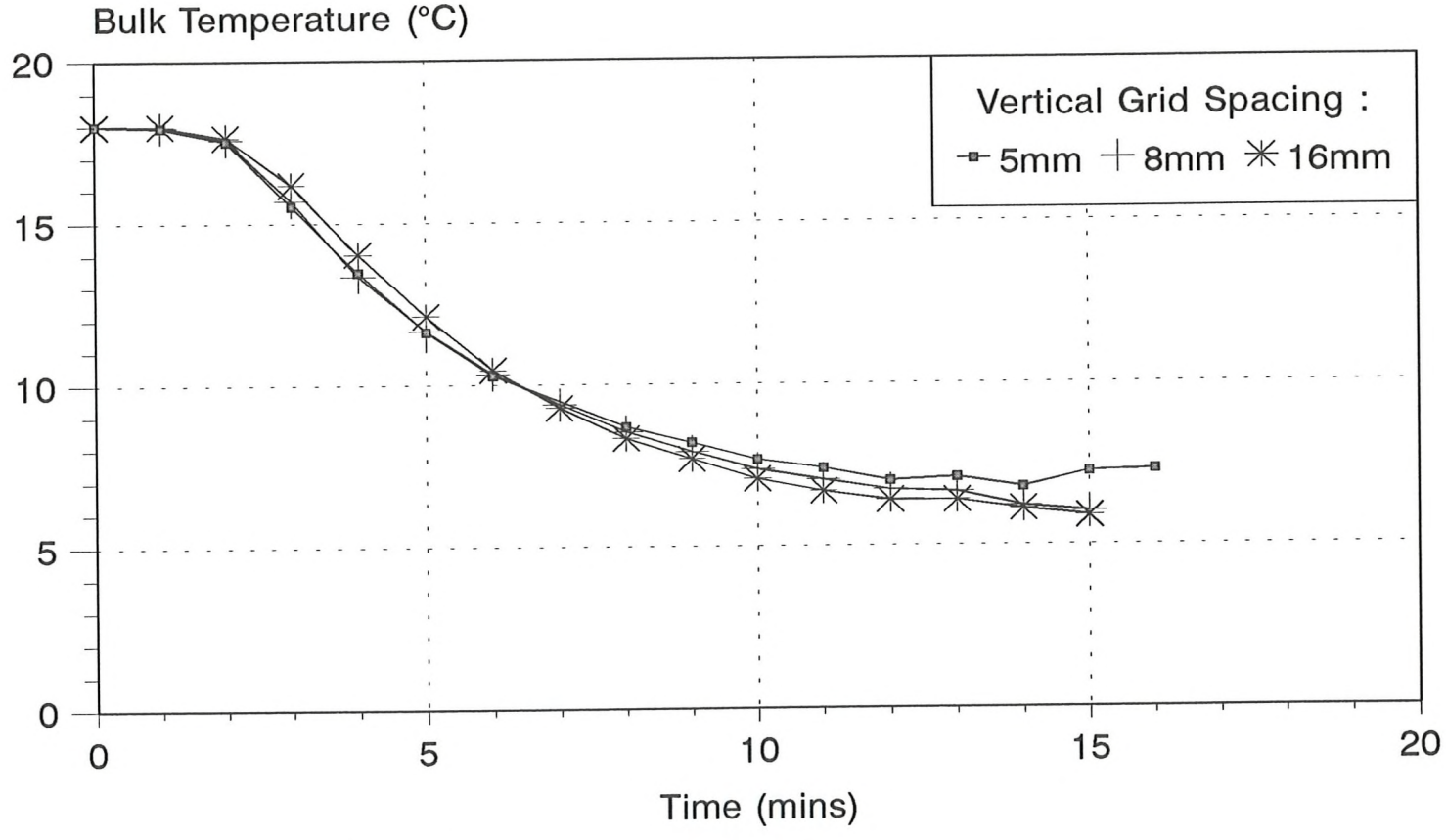

Radial Grid Spacing 1mm; Pipe Length 630mm; Tin=18°C

Figure 5.9b

Radial Grid Spacing Sensitivity
Minimum Plug Radius

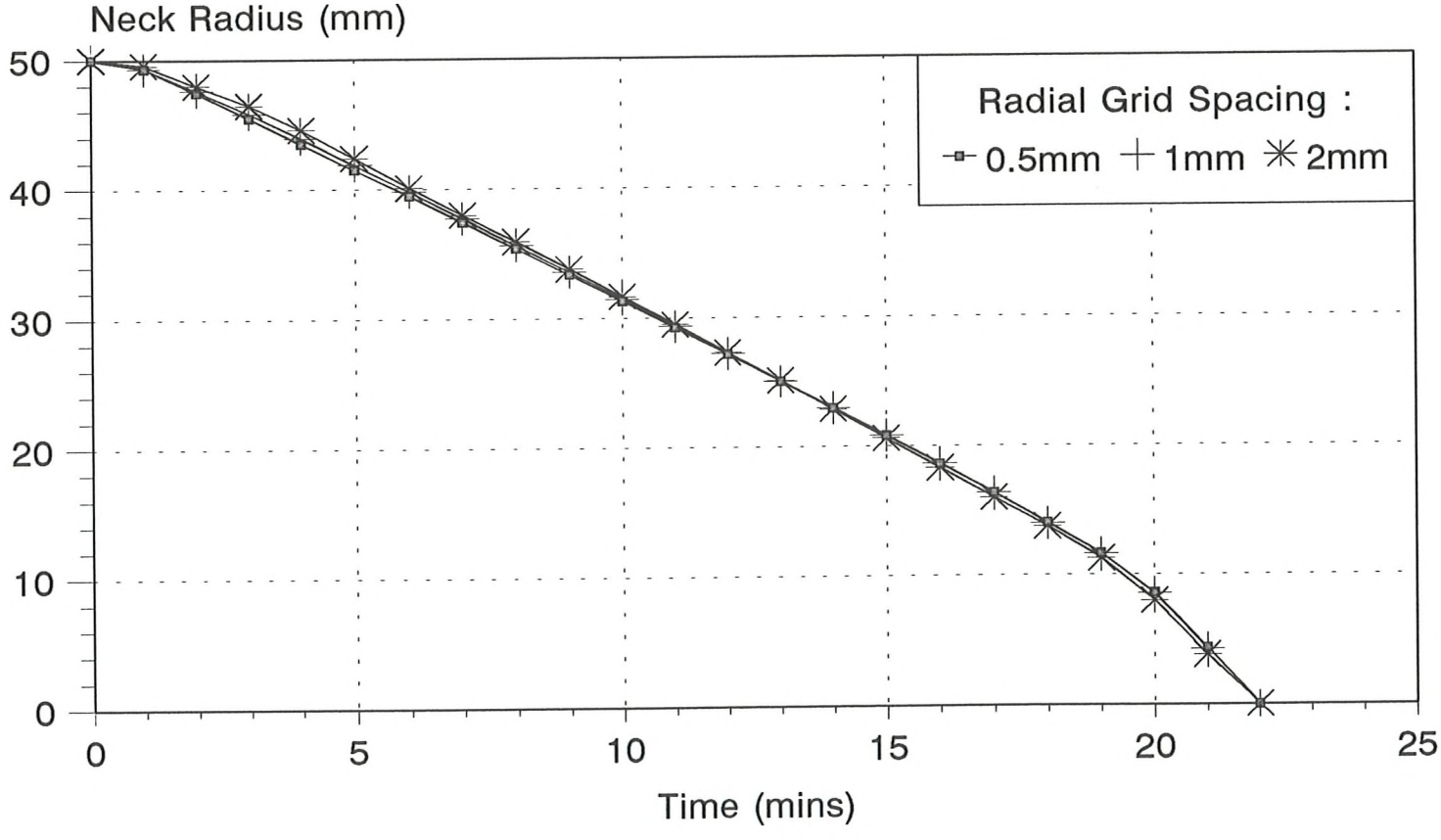

Vertical Grid Spacing 8mm; Pipe Length 630mm; Tin=18°C

Figure 5.10a

Vertical Grid Spacing Sensitivity
Minimum Plug Radius

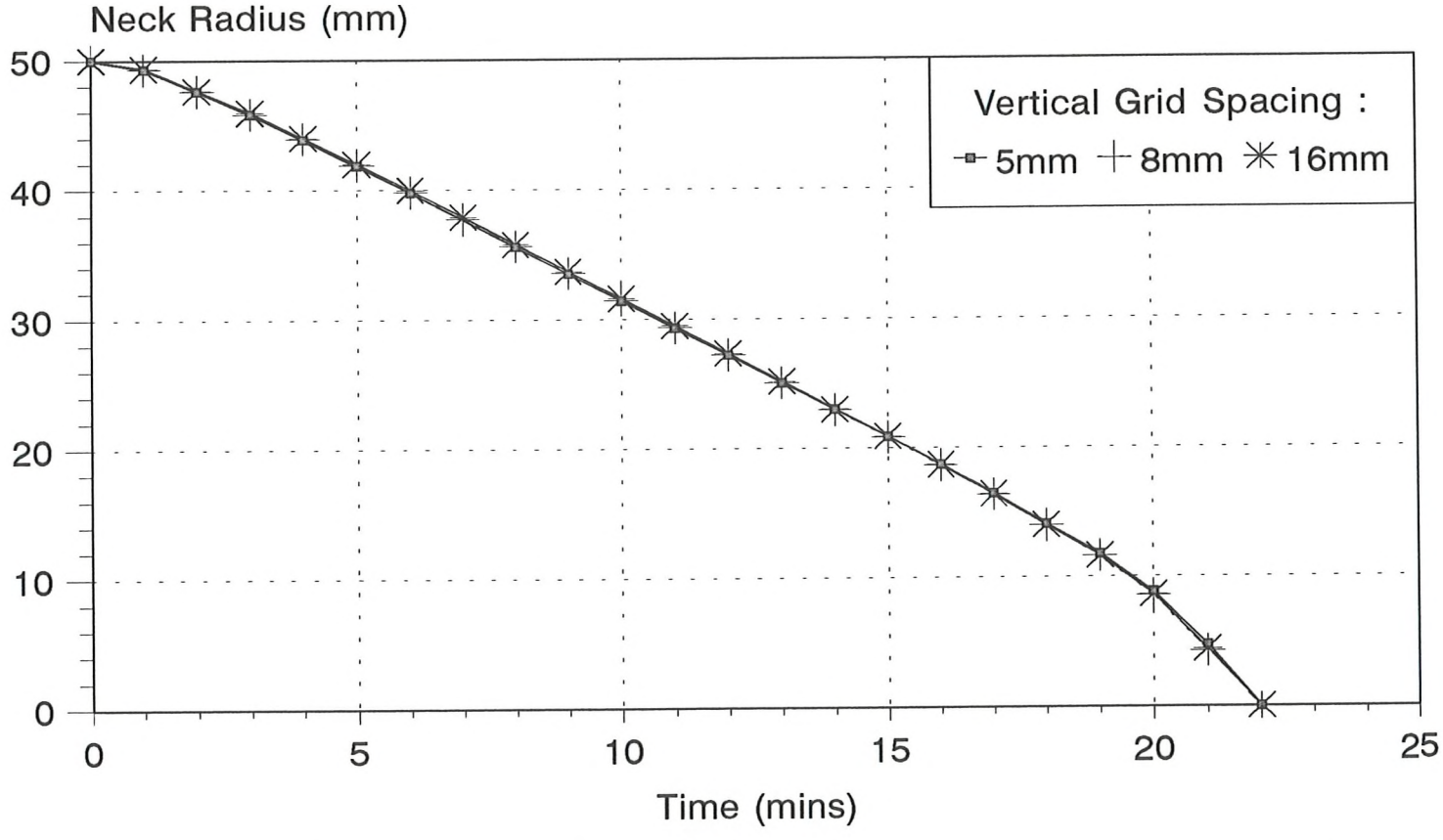

Radial Grid Spacing 1mm; Pipe Length 630mm; Tin=18°C

Figure 5.10b

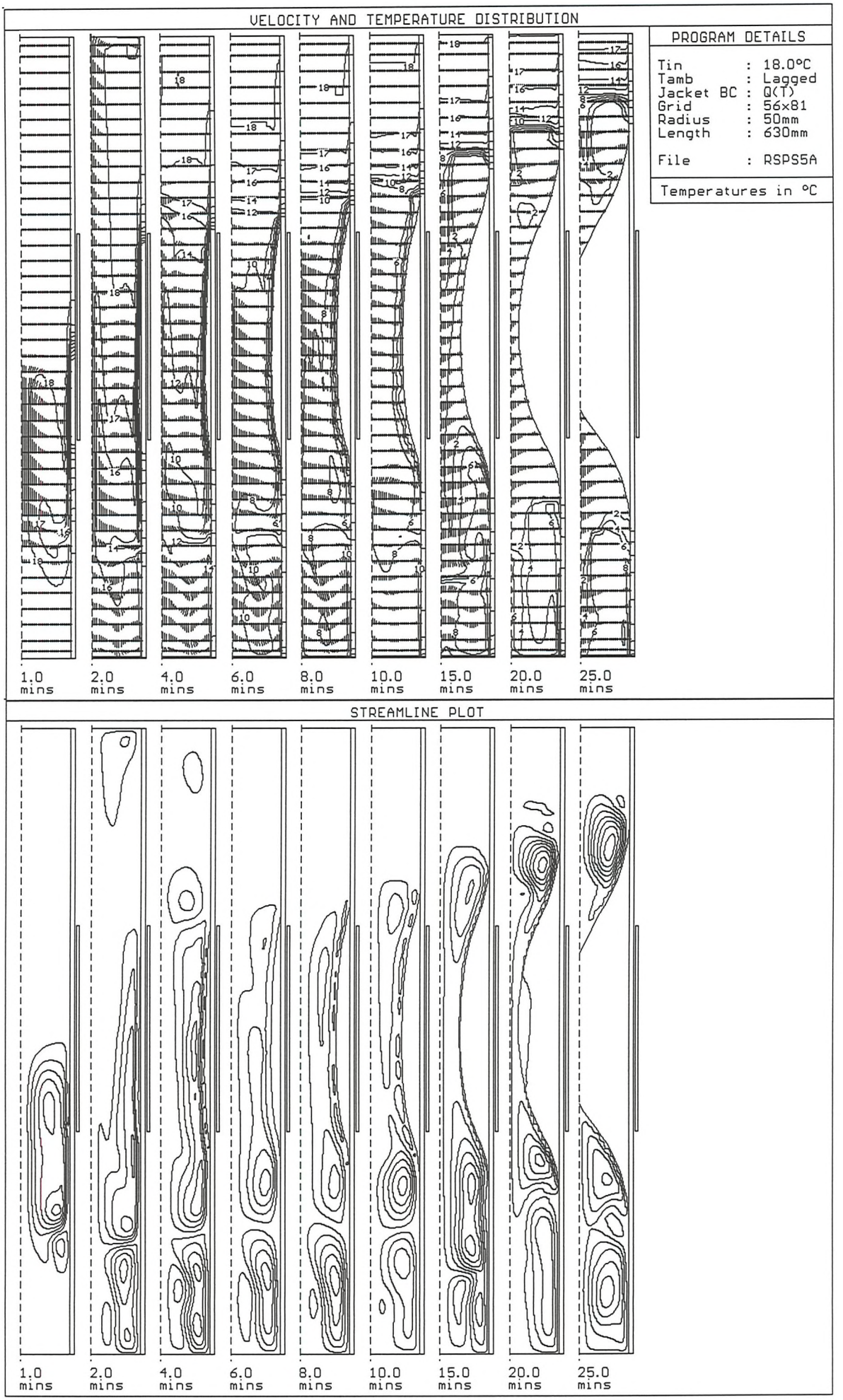

Figure 5.11a: Immobilisation factor sensitivity test; fv = 1E5; (Test case: 100mm dia; Tin = 18°C)

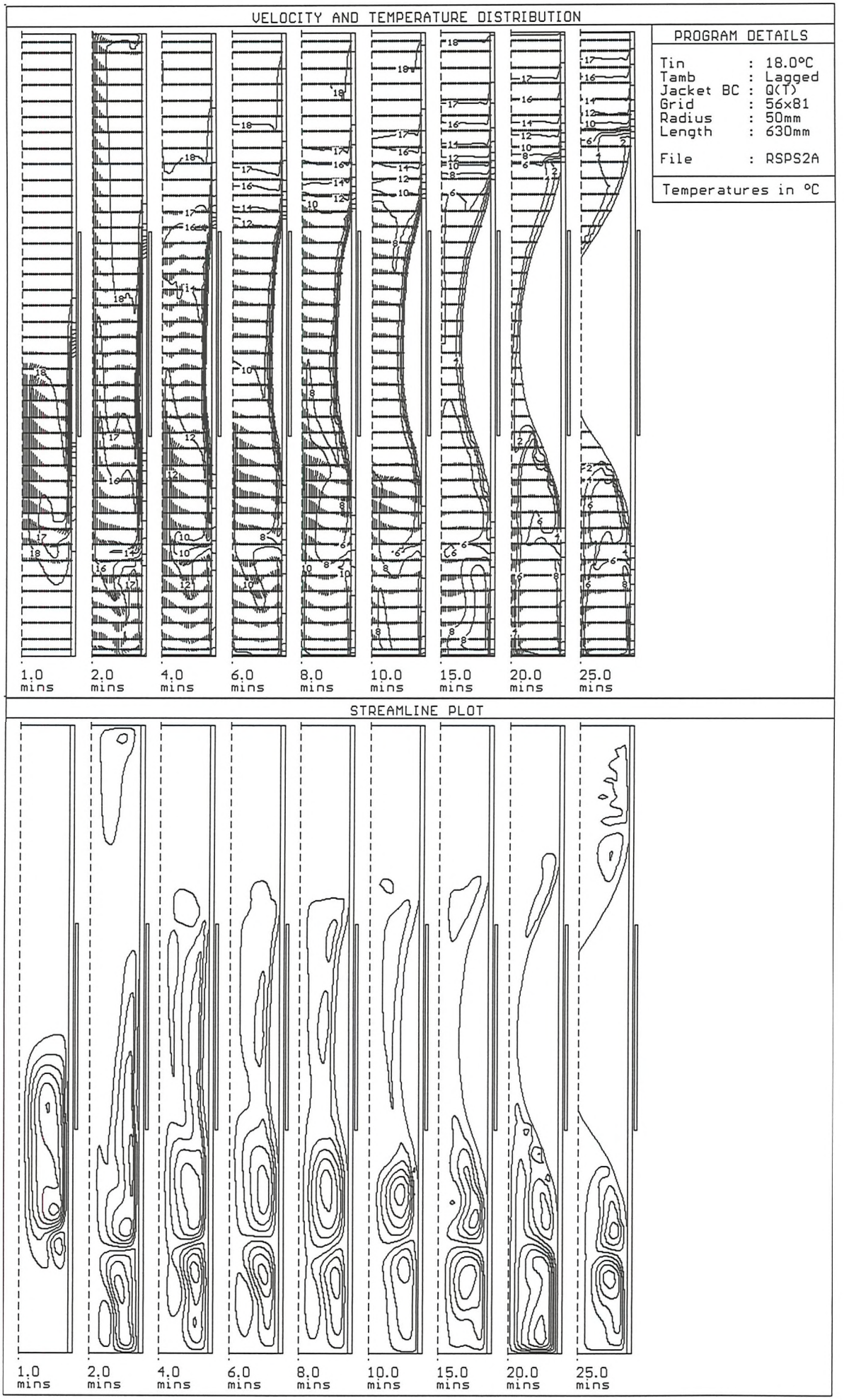

Figure 5.11b: Immobilisation factor sensitivity test; fv = 1E6; (Test case: 100mm dia; Tin = 18°C)

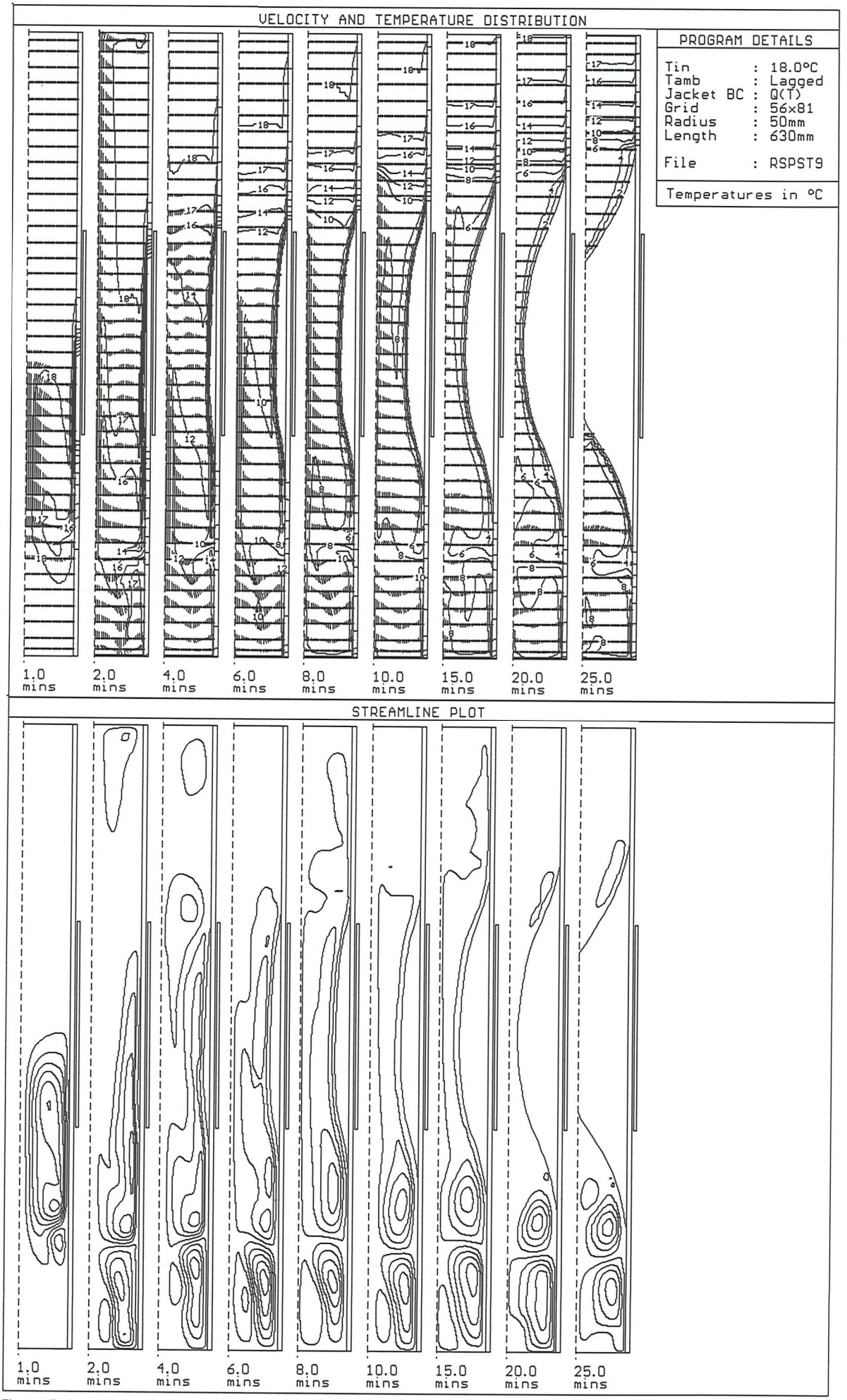

Figure 5.11c: Immobilisation factor sensitivity test; fv = 1E7; (Test case: 100mm dia.; Tin = 18°C)

Effect of Velocity Immobilisation Factor
Boundary Layer Velocity at Centre of Jacket

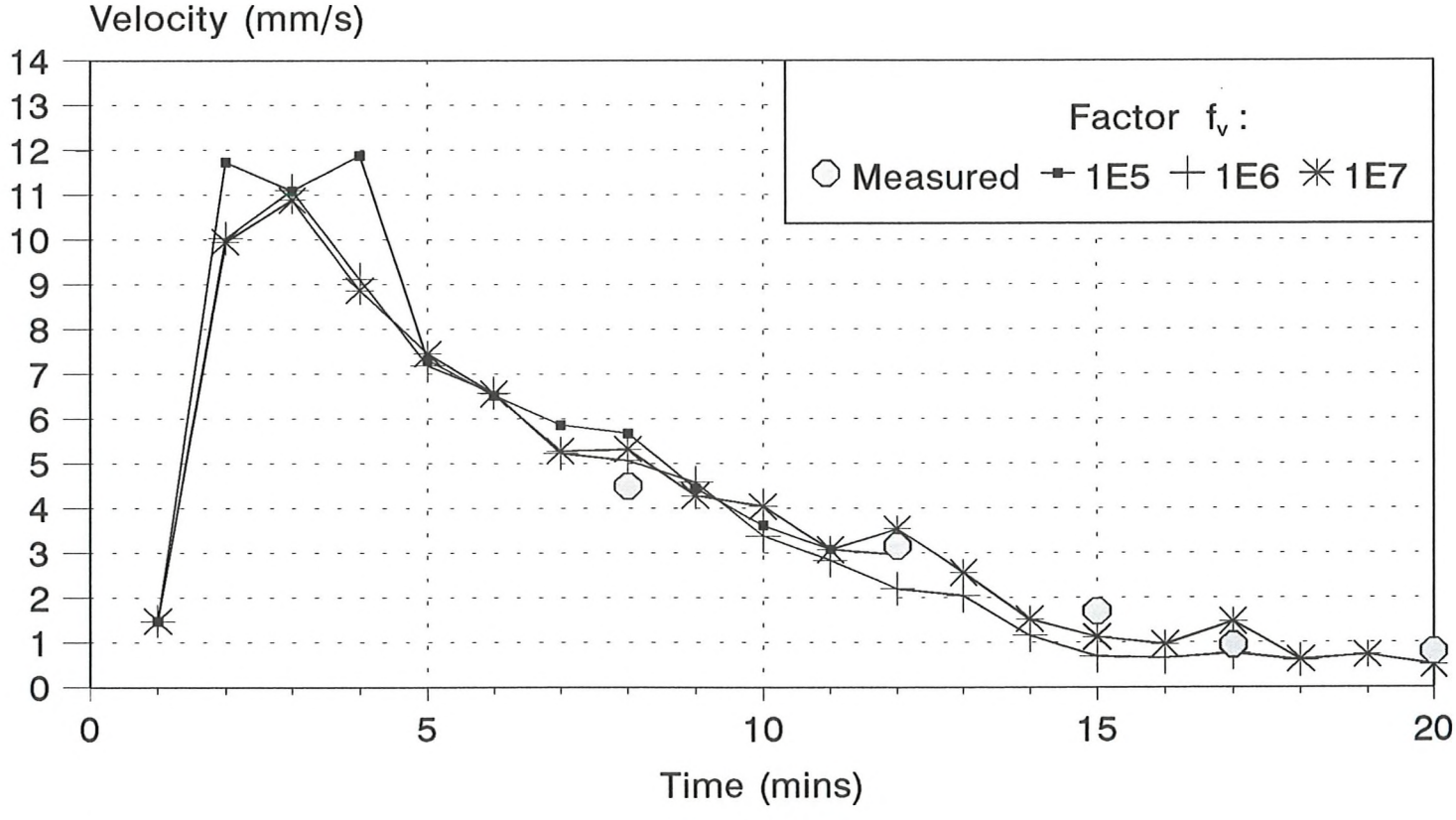

Grid Spacing: Radial 1mm, Vertical 8mm; Pipe Length 630mm; Tin=18°C
Measurements from Tavner[5] (prototype rig:run M36)

Figure 5.12

Effect of Velocity Immobilisation Factor
Bulk Temperature Inside Freezing Zone

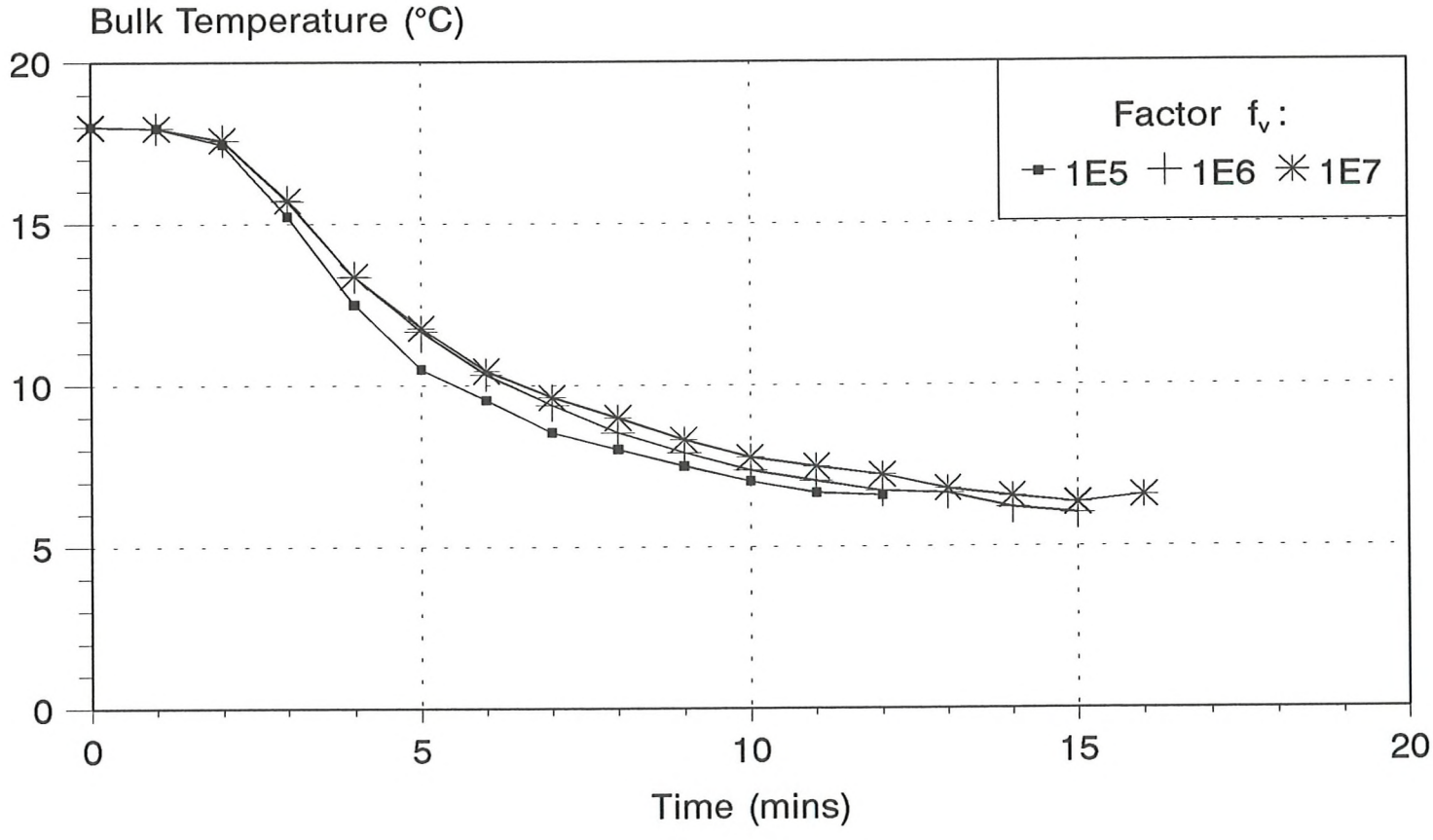

Grid Spacing: Radial 1mm, Vertical 8mm; Pipe Length 630mm; Tin=18°C

Figure 5.13

Effect of Velocity Immobilisation Factor
Interface Position

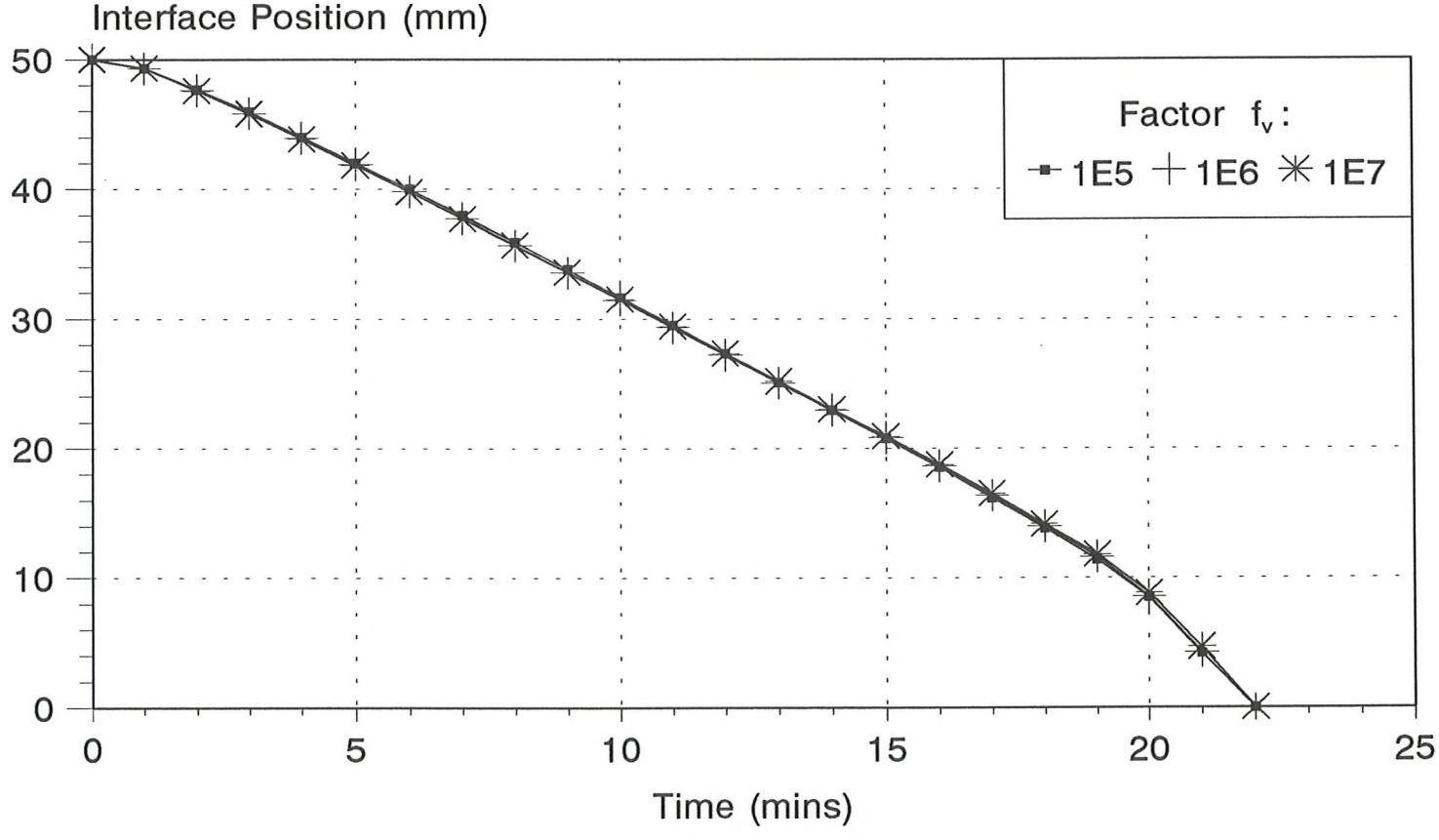

Grid Spacing: Radial 1mm, Vertical 8mm; Pipe Length 630mm; Tin=18°C

Figure 5.14

Comparison between Predicted and Measured Freezing Times

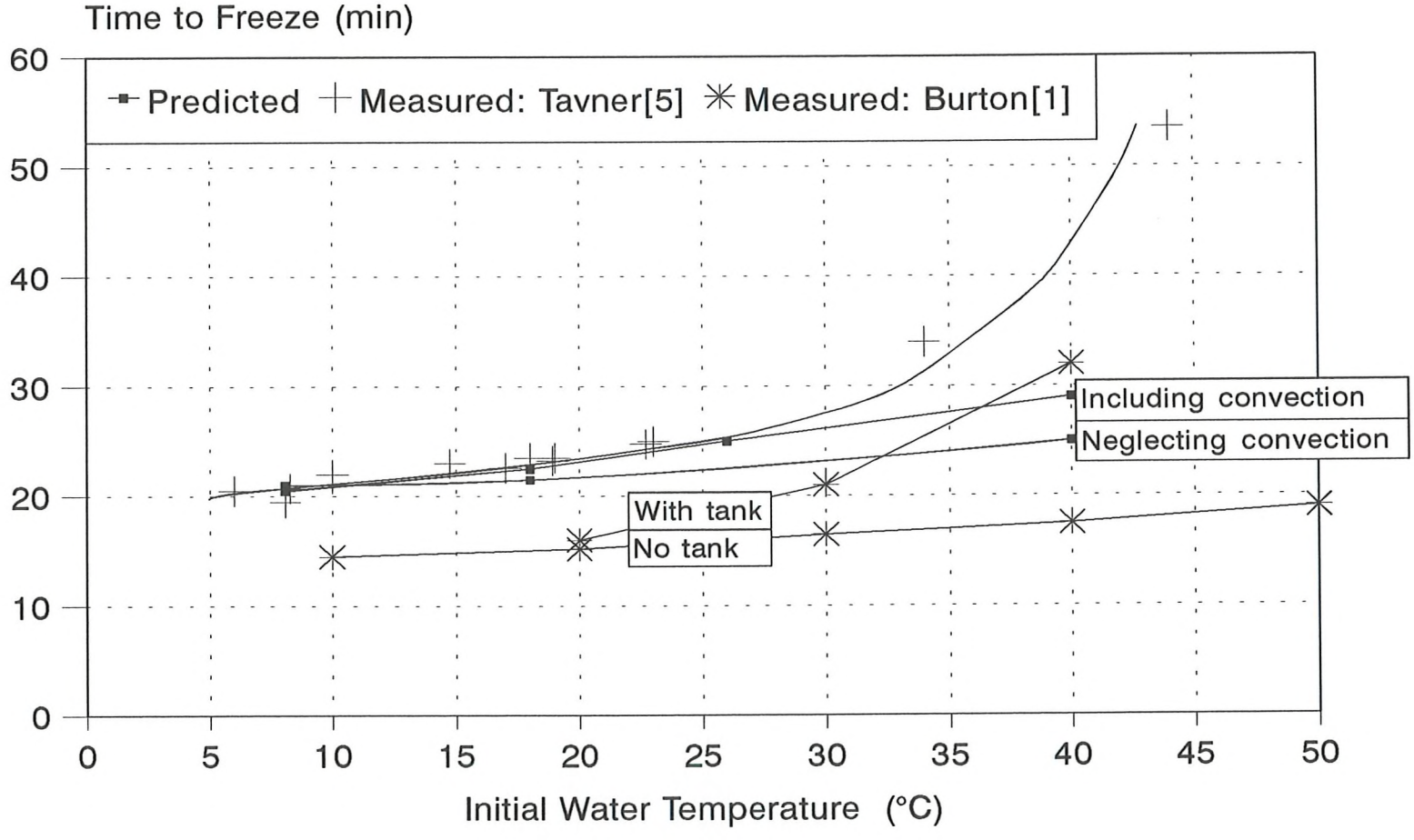

Figure 5.15

Boundary Layer Velocity at the Centre of the Jacket

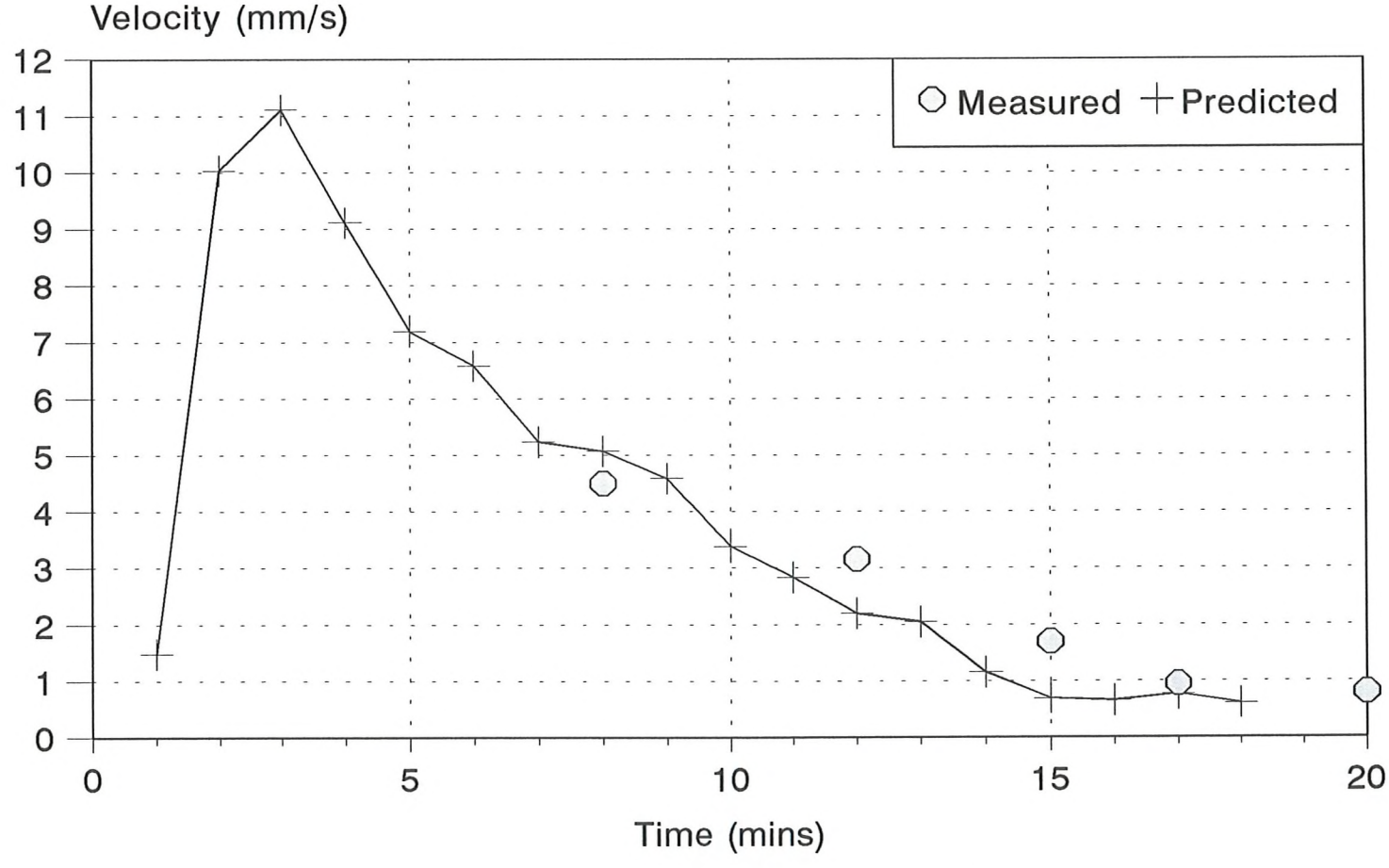

Measurements from Tavner[5] (prototype rig:run M36); Tin=18°C

Figure 5.16

Average Temperature Inside Freezing Zone

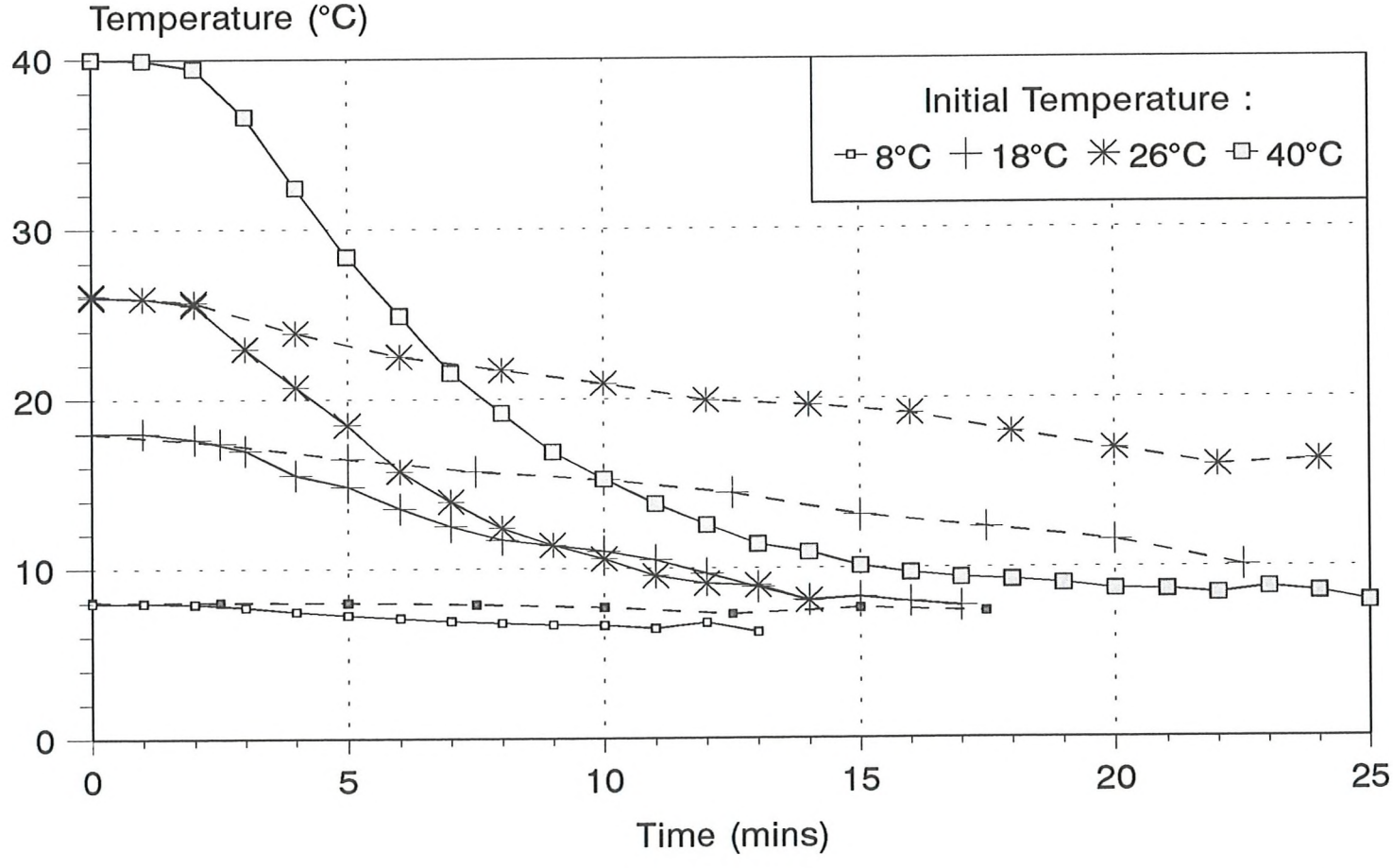

Prediction : Solid Line; Measurement : Dashed Line : from Tavner[5] Figure 5.17

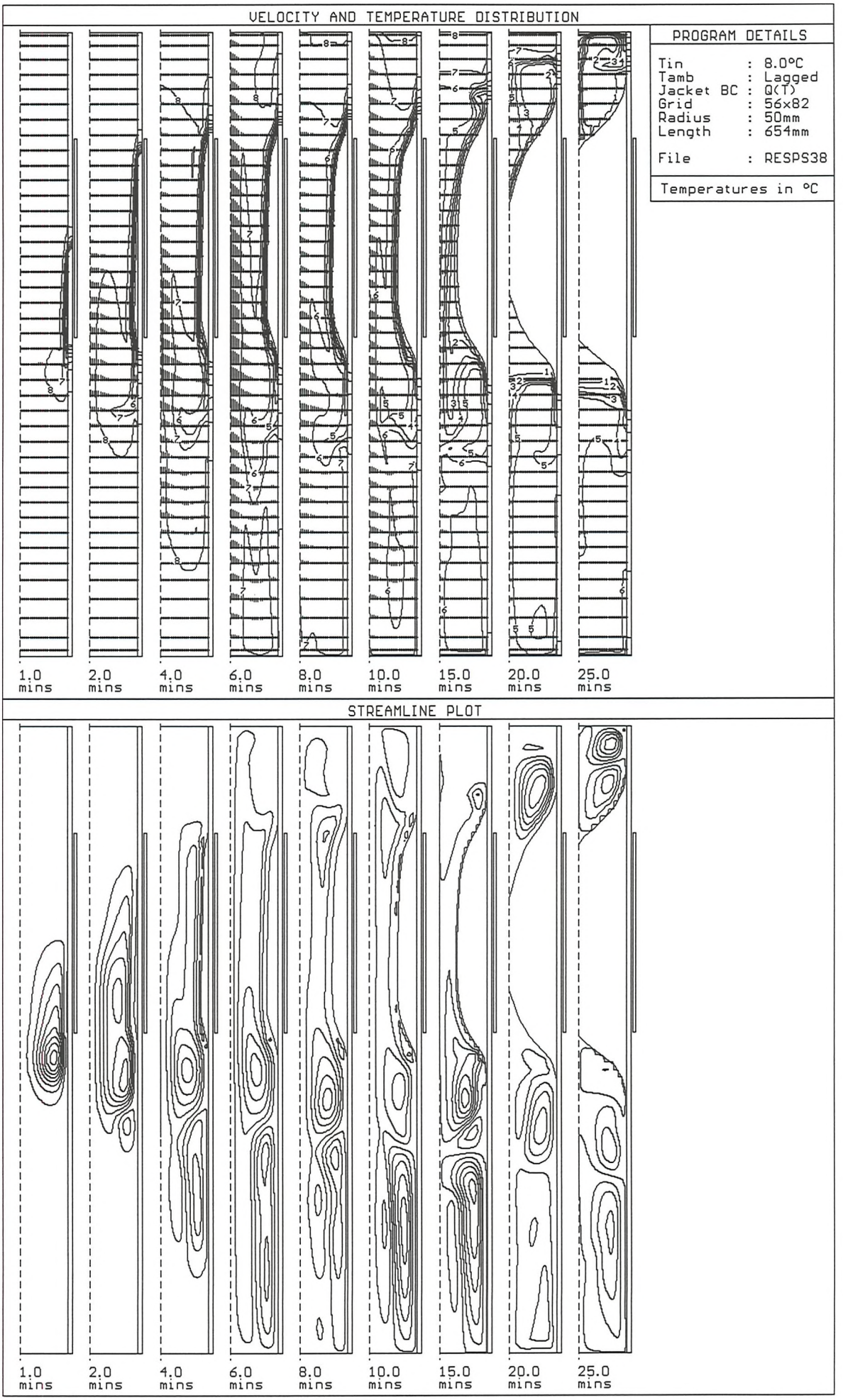

Figure 5.18a: Results from 8°C freeze; 'Short' pipe; Q(T) jacket BC

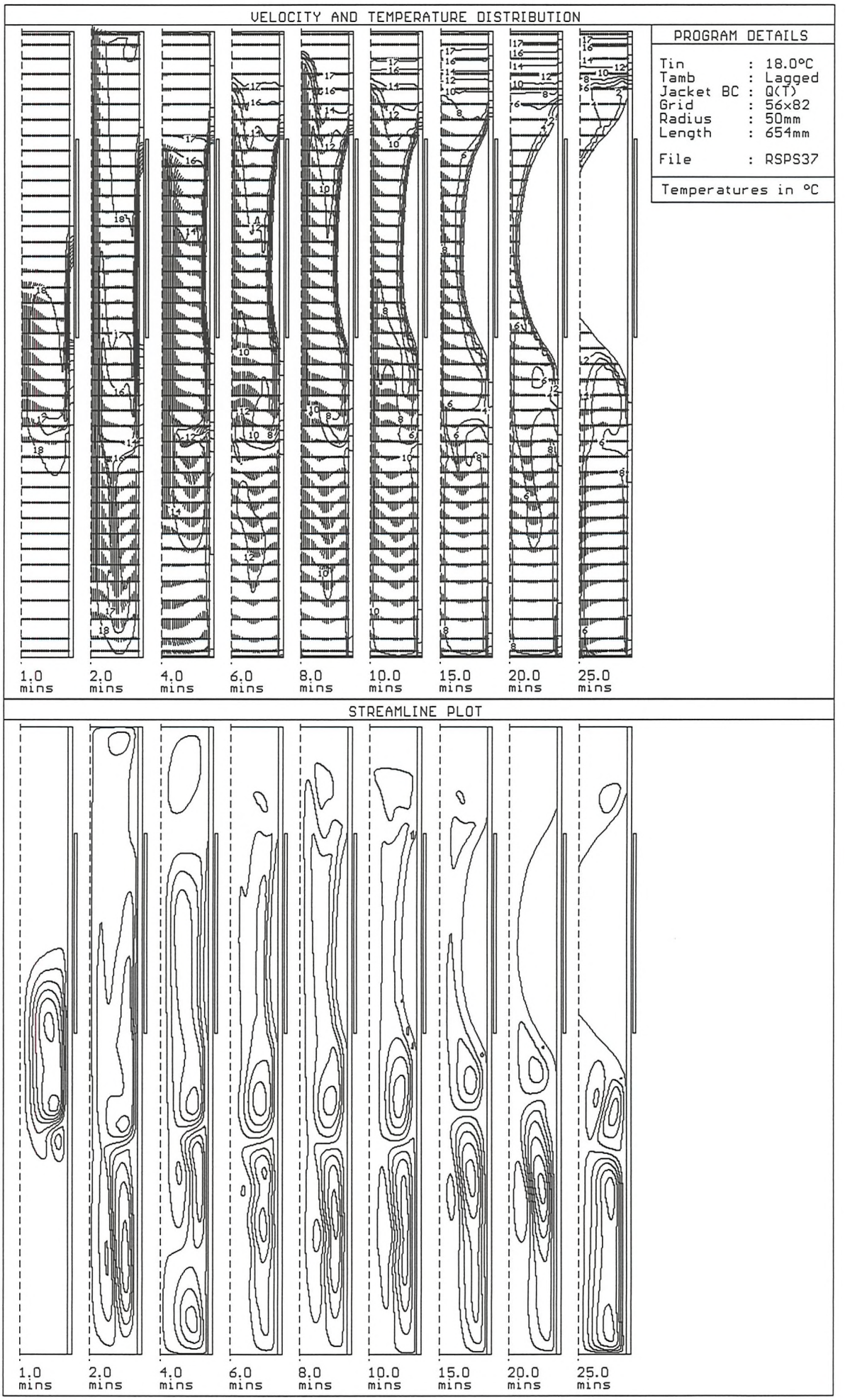

Figure 5.18b: Results from 18°C freeze; 'Short' pipe; Q(T) jacket BC

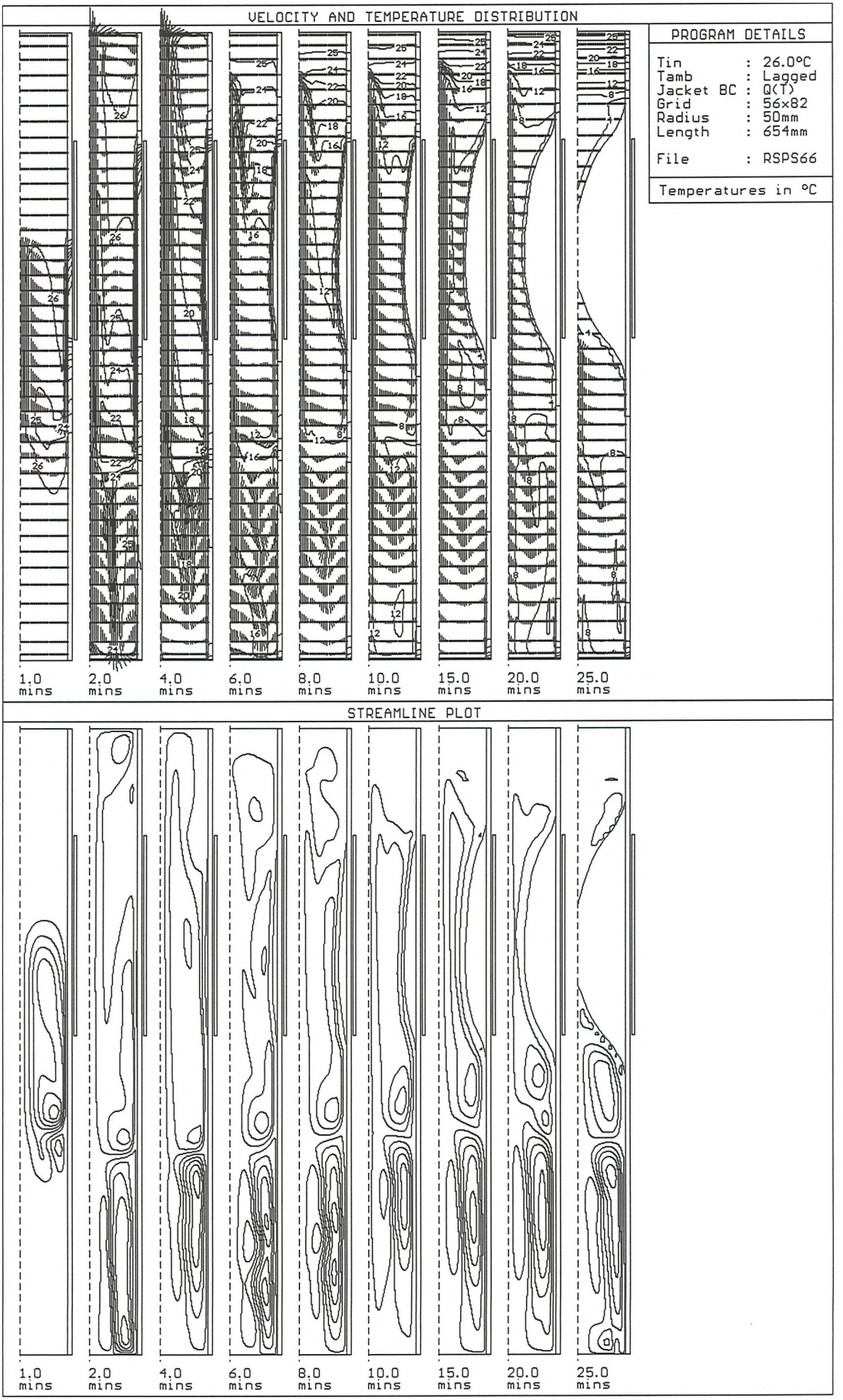

Figure 5.18c: Results from 26°C freeze; 'Short' pipe; Q(T) jacket BC

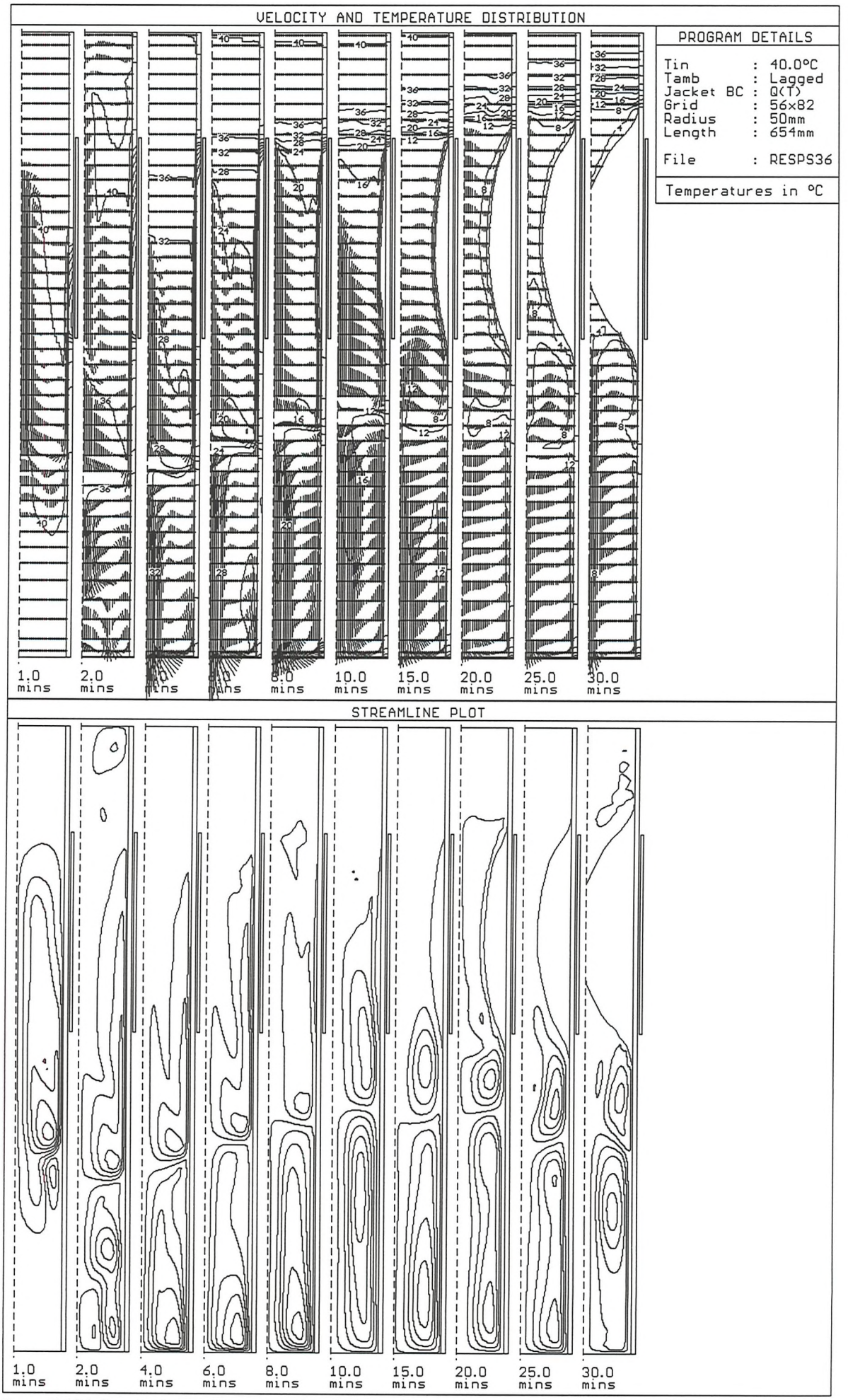

Figure 5.18d: Results from 40°C freeze; 'Short' pipe; Q(T) jacket BC

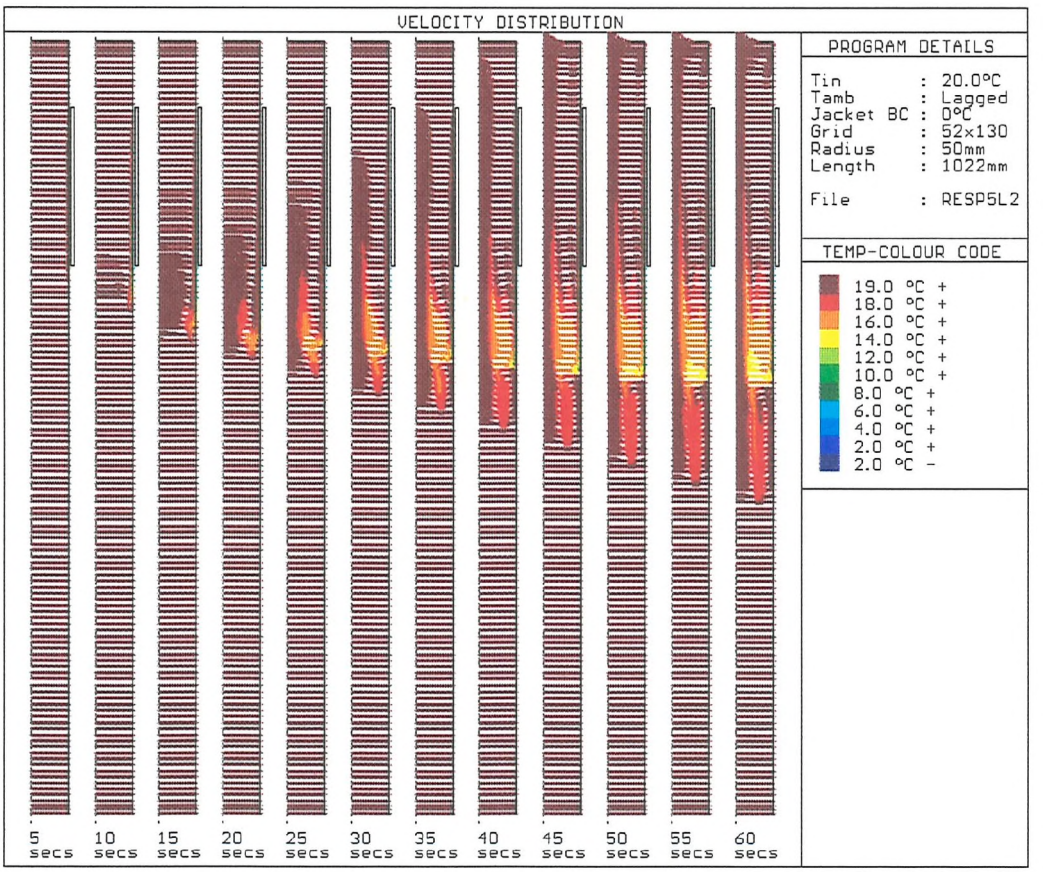

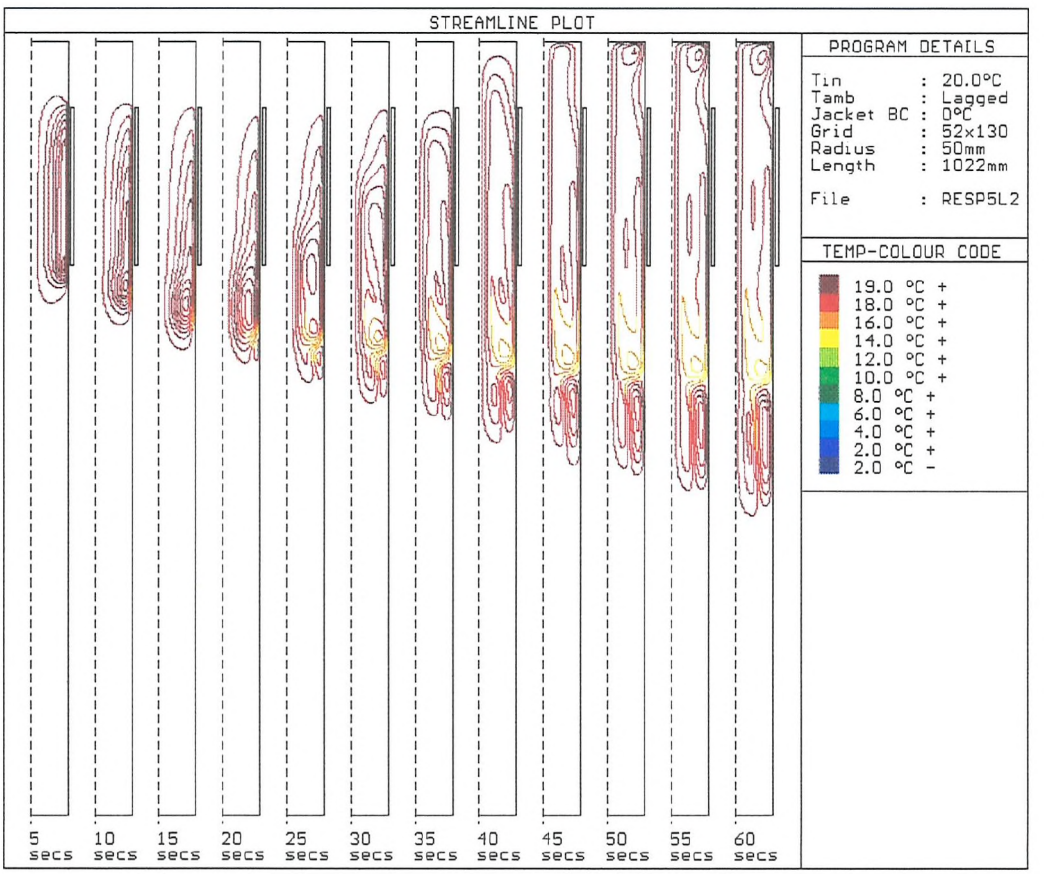

Figure 6.1a: Flow development at 5 second intervals (5..60secs); 100mm dia. pipe; Tin=20°C

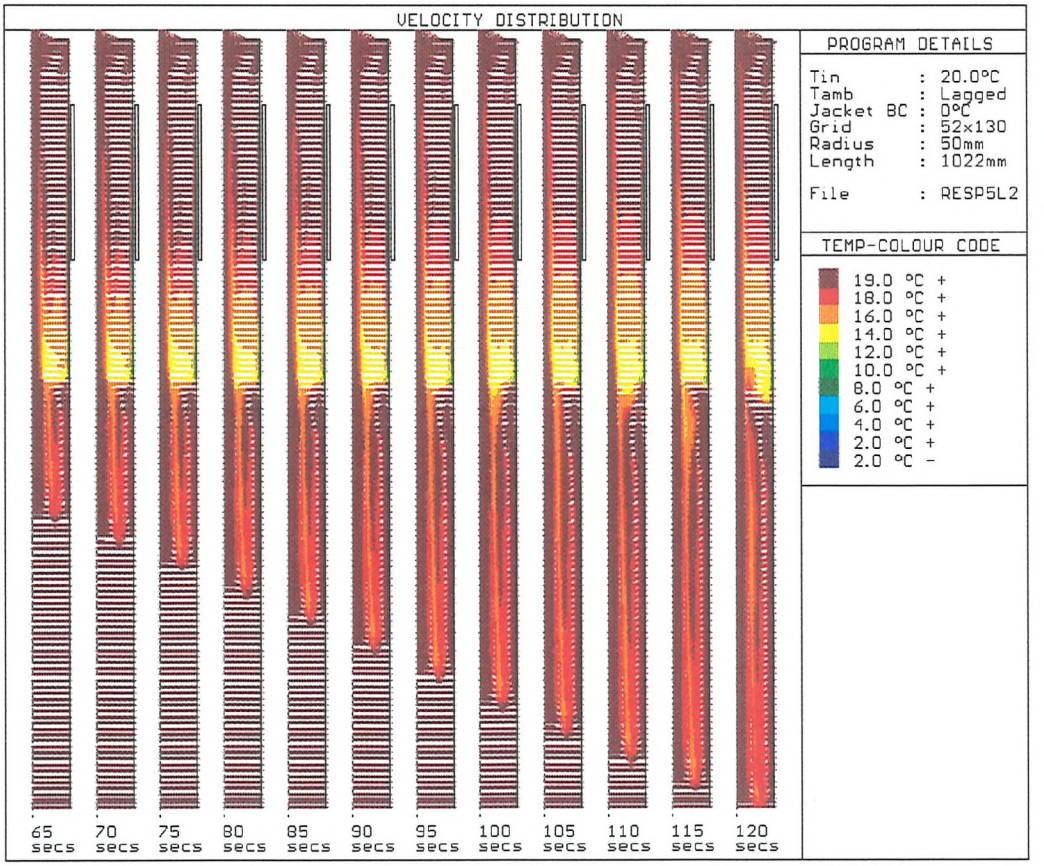

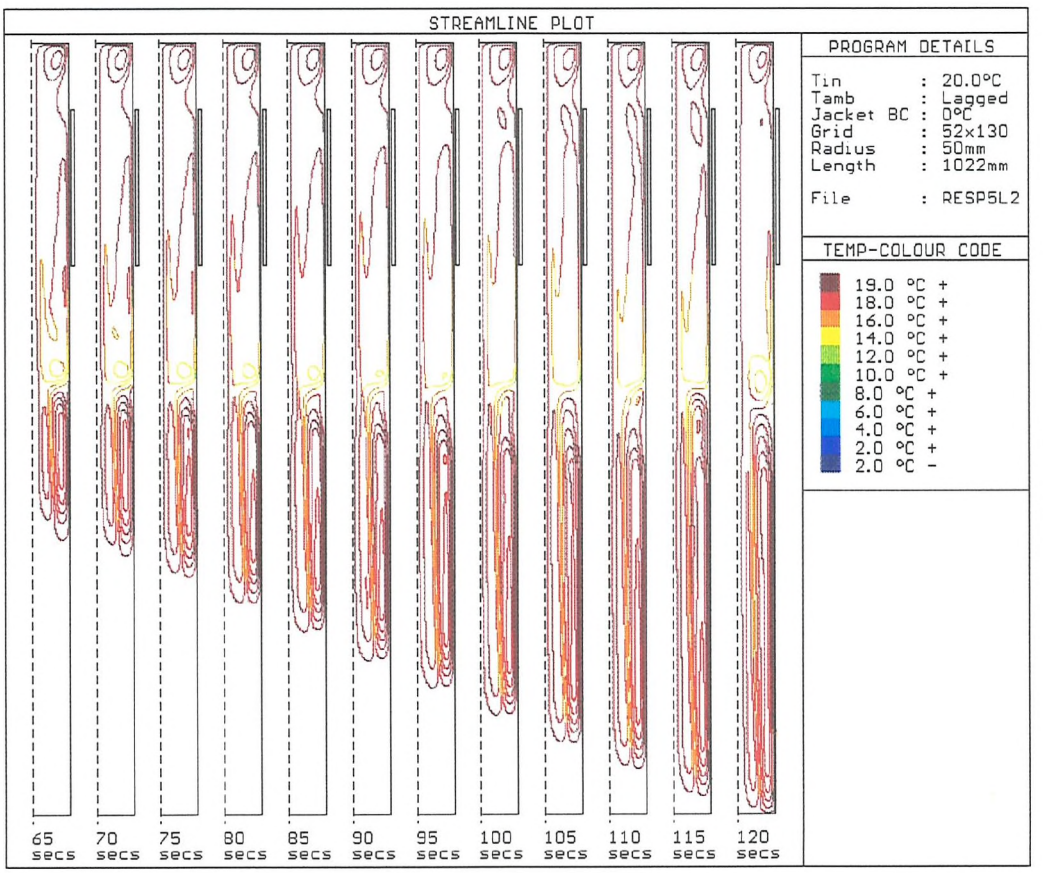

Figure 6.1b: Flow development at 5 second intervals (65..120secs); 100mm dia. pipe; Tin=20°C

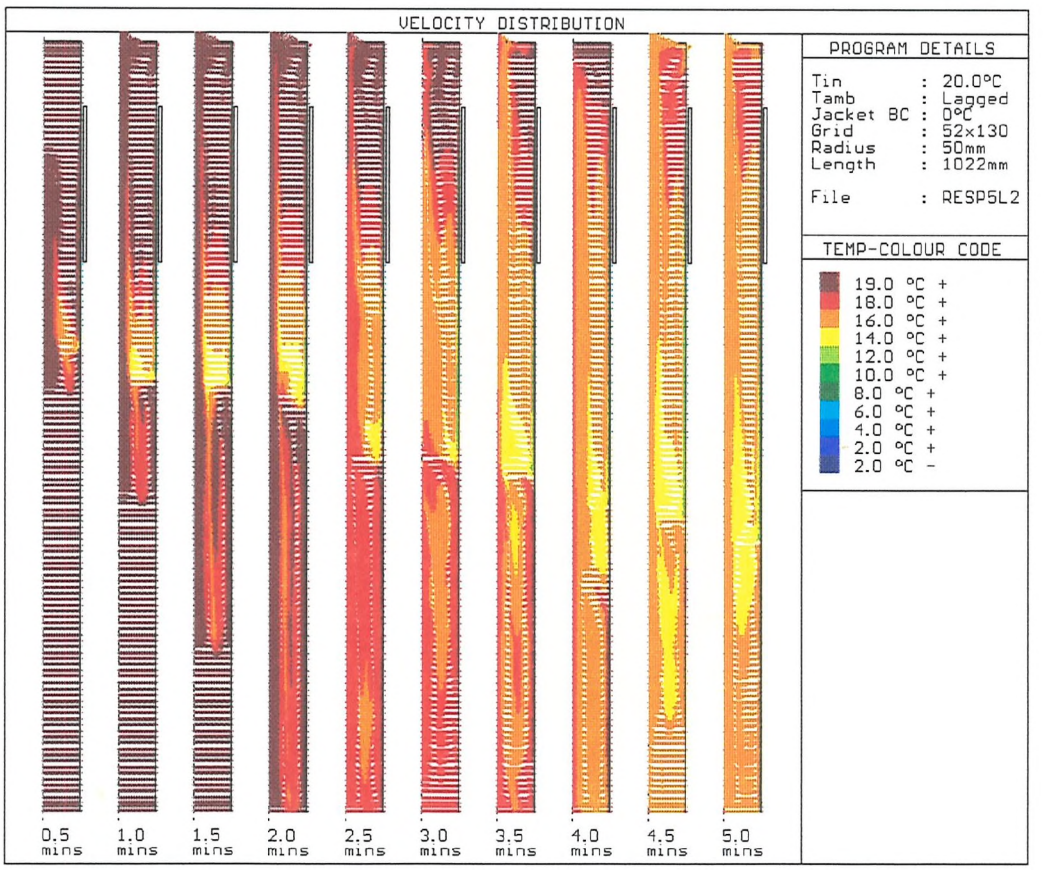

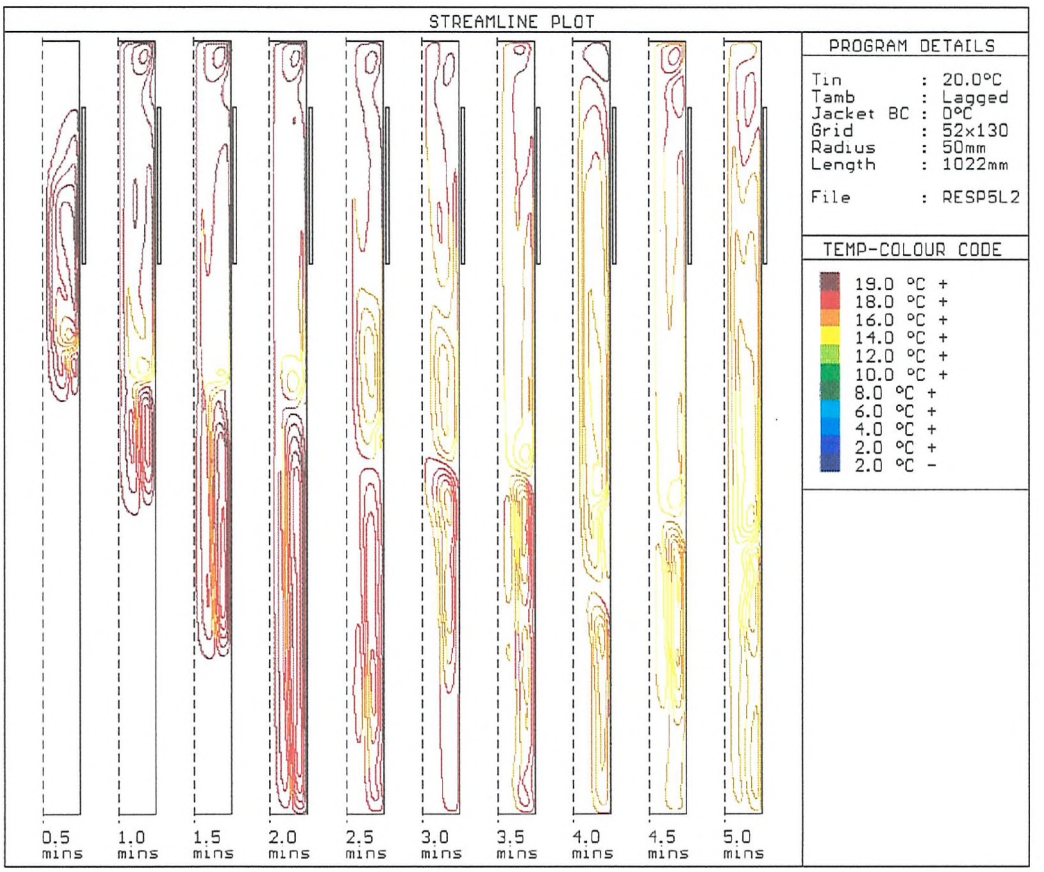

Figure 6.1c: Flow development at ½ minute intervals (½..5mins); 100mm dia. pipe; Tin=20°C

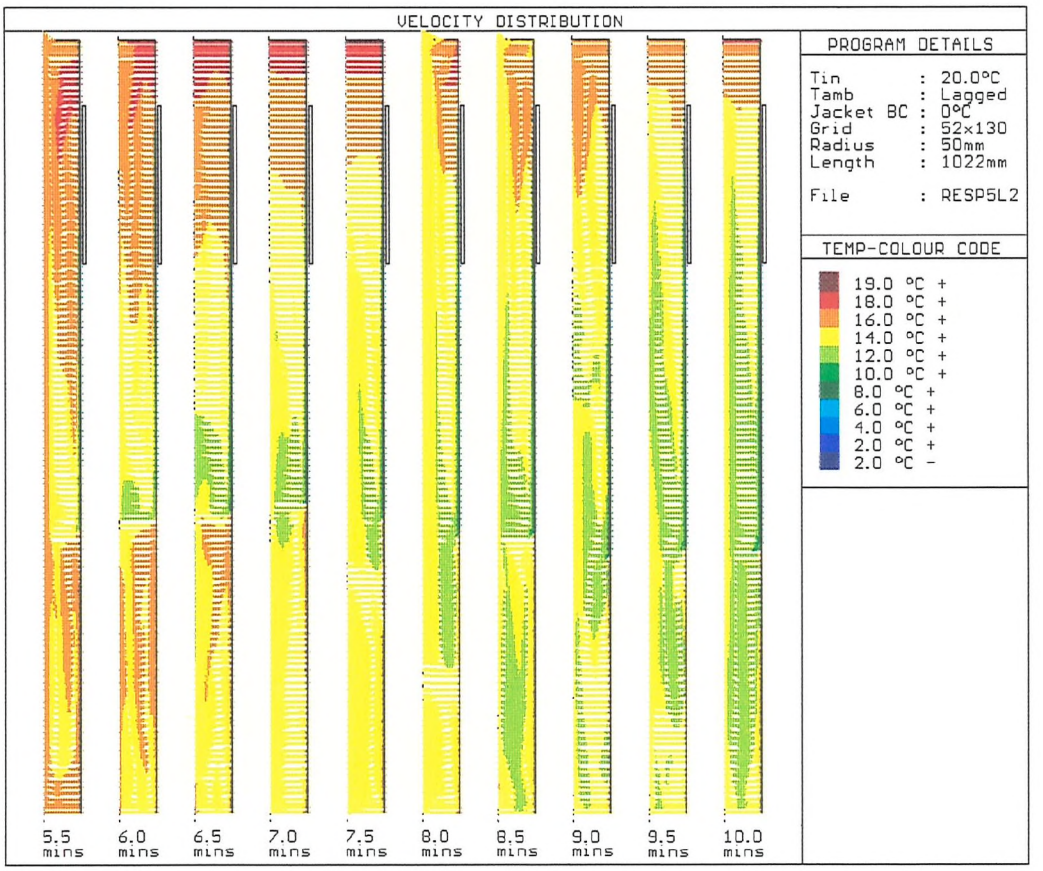

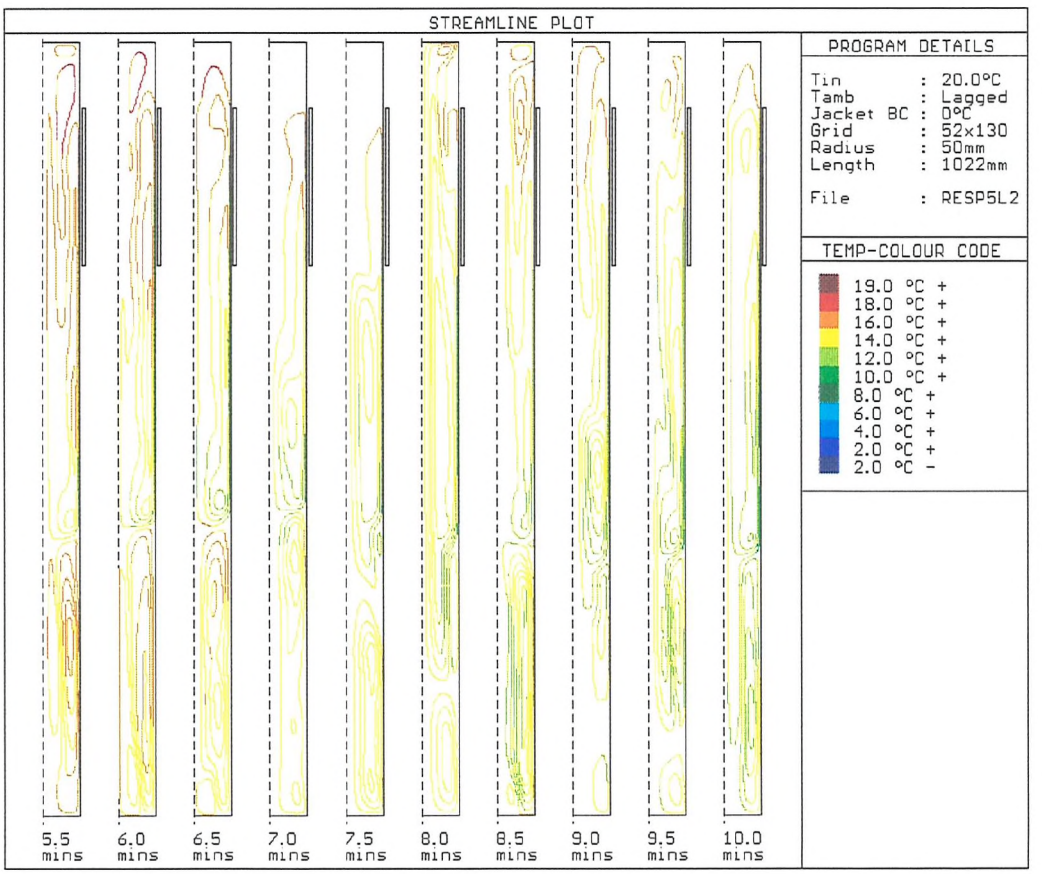

Figure 6.1d: Flow development at ½ minute intervals (5½..10mins); 100mm dia. pipe; Tin=20°C

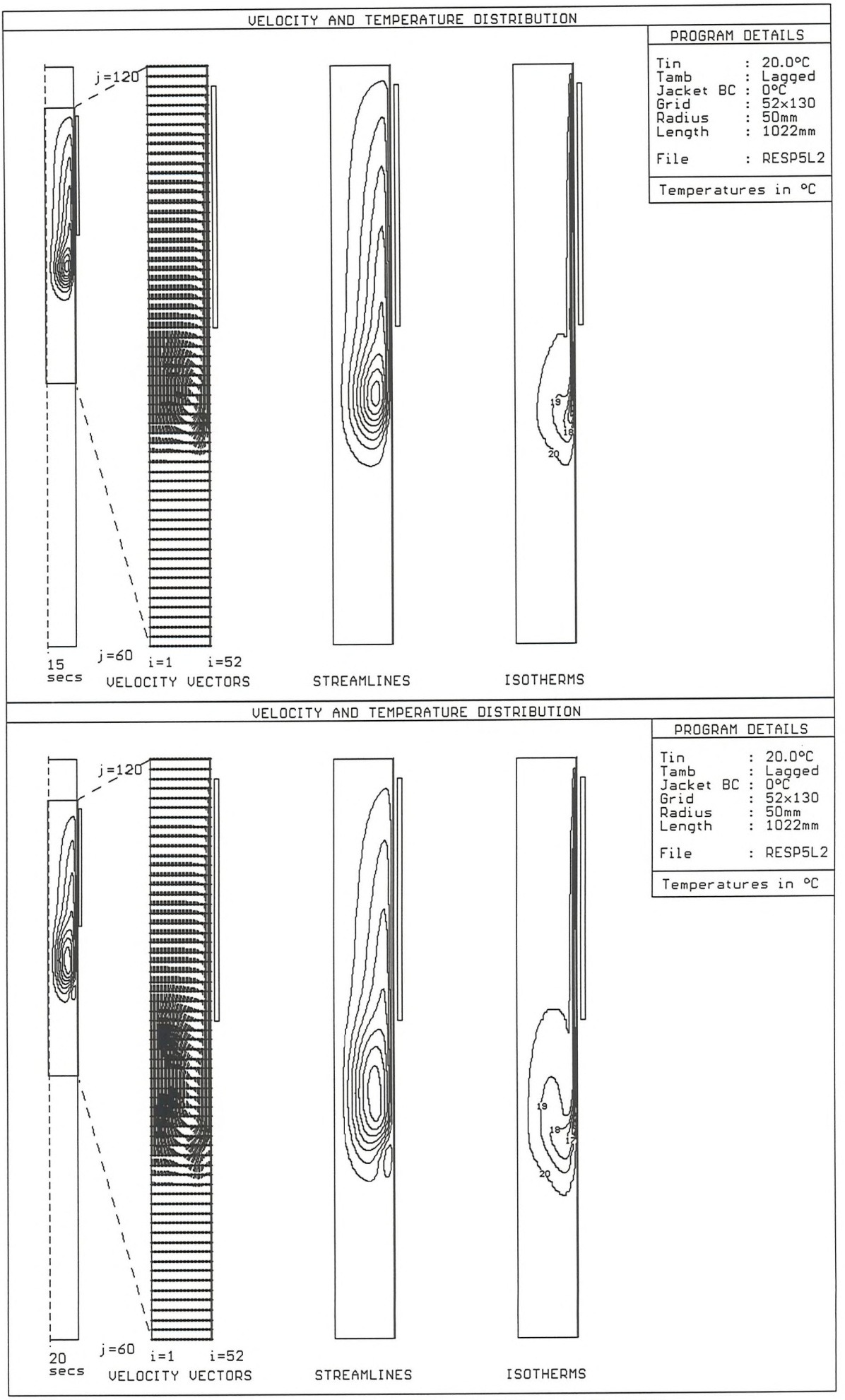

Figure 6.2a : Snapshots of flow development at 15 and 20 seconds; 100mm dia.; Tin = 20°C

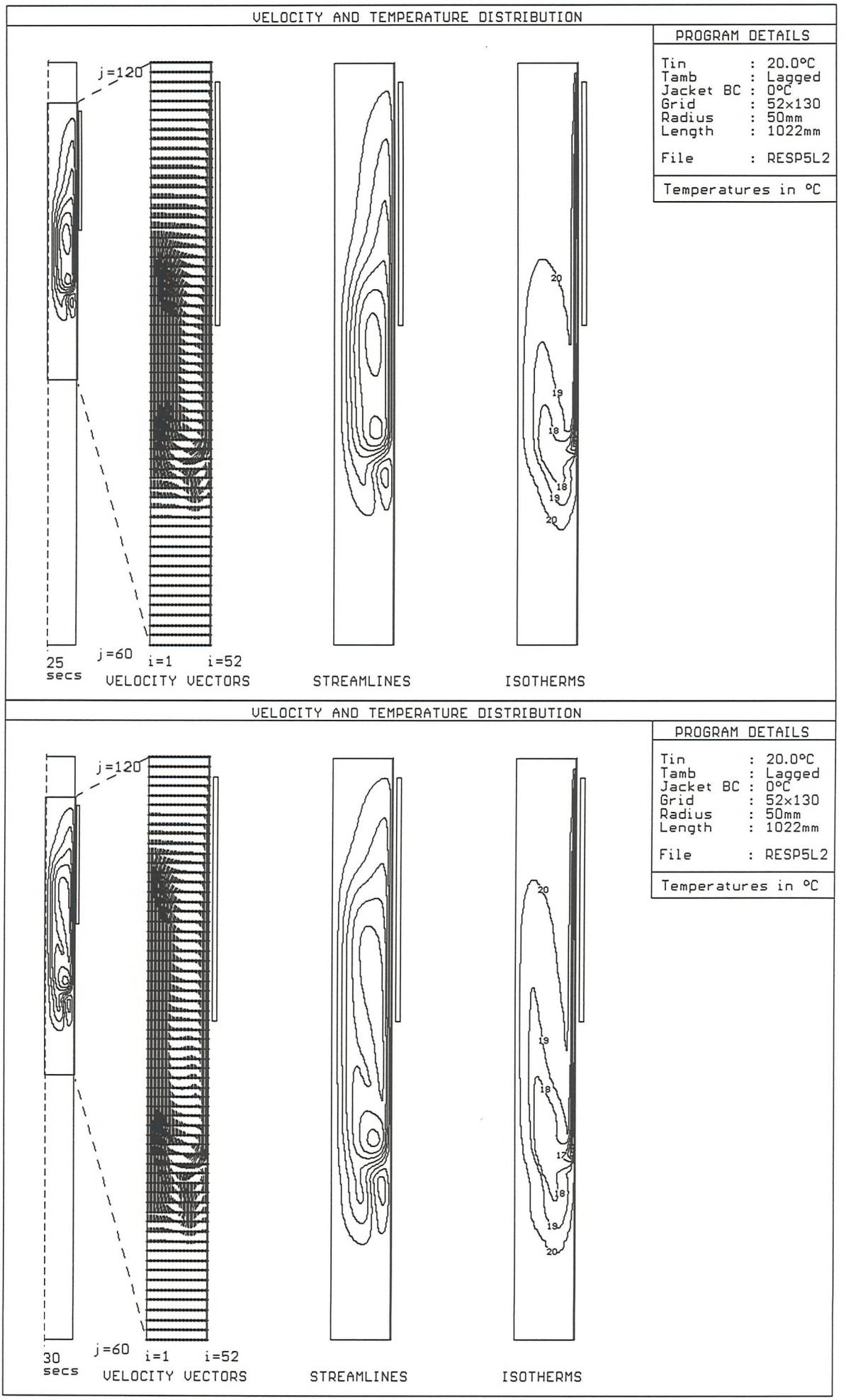

Figure 6.2b : Snapshots of flow development at 25 and 30 seconds; 100mm dia.; Tin = 20°C

Figure 6.3: Sketch showing Development of Flow Field

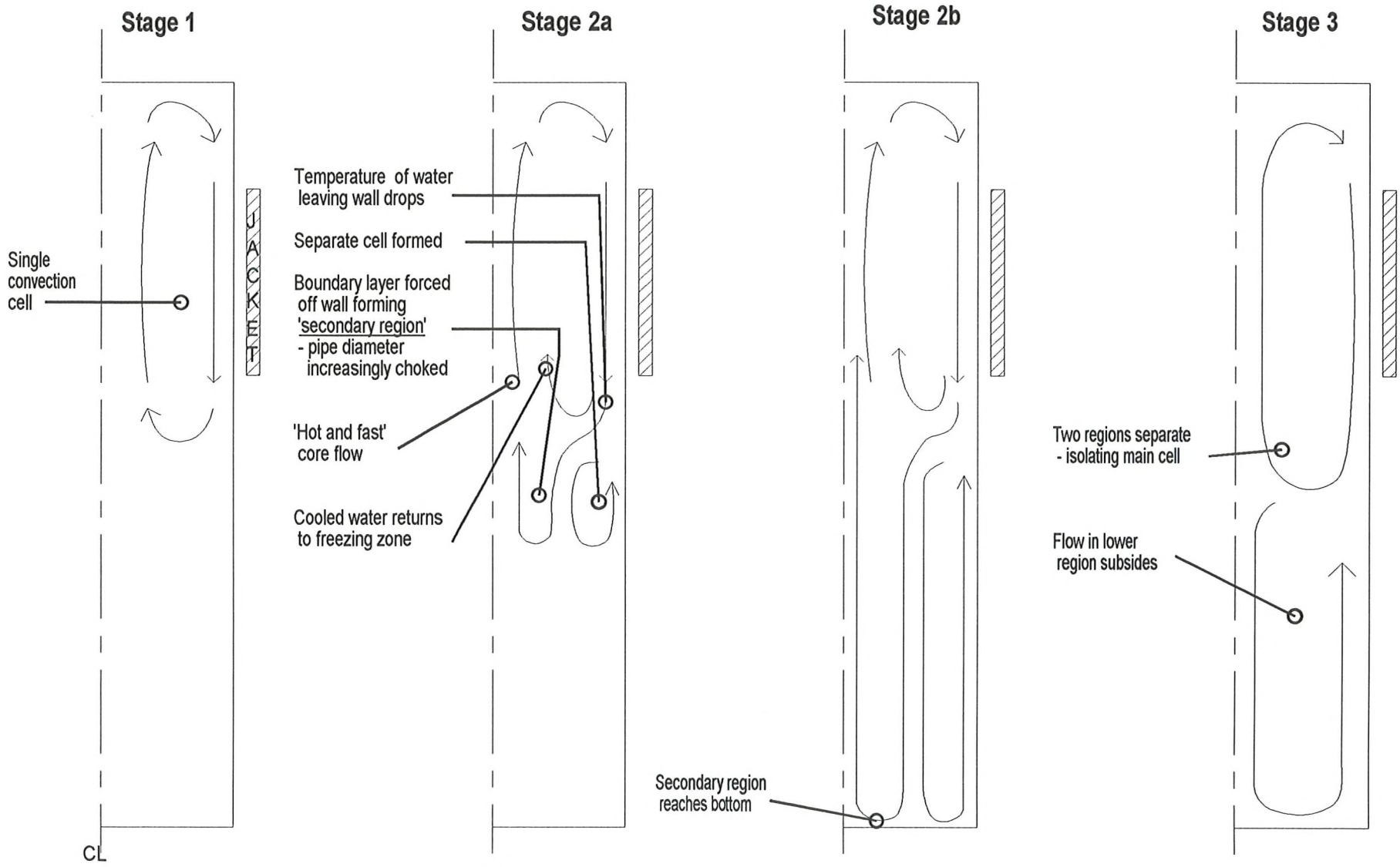

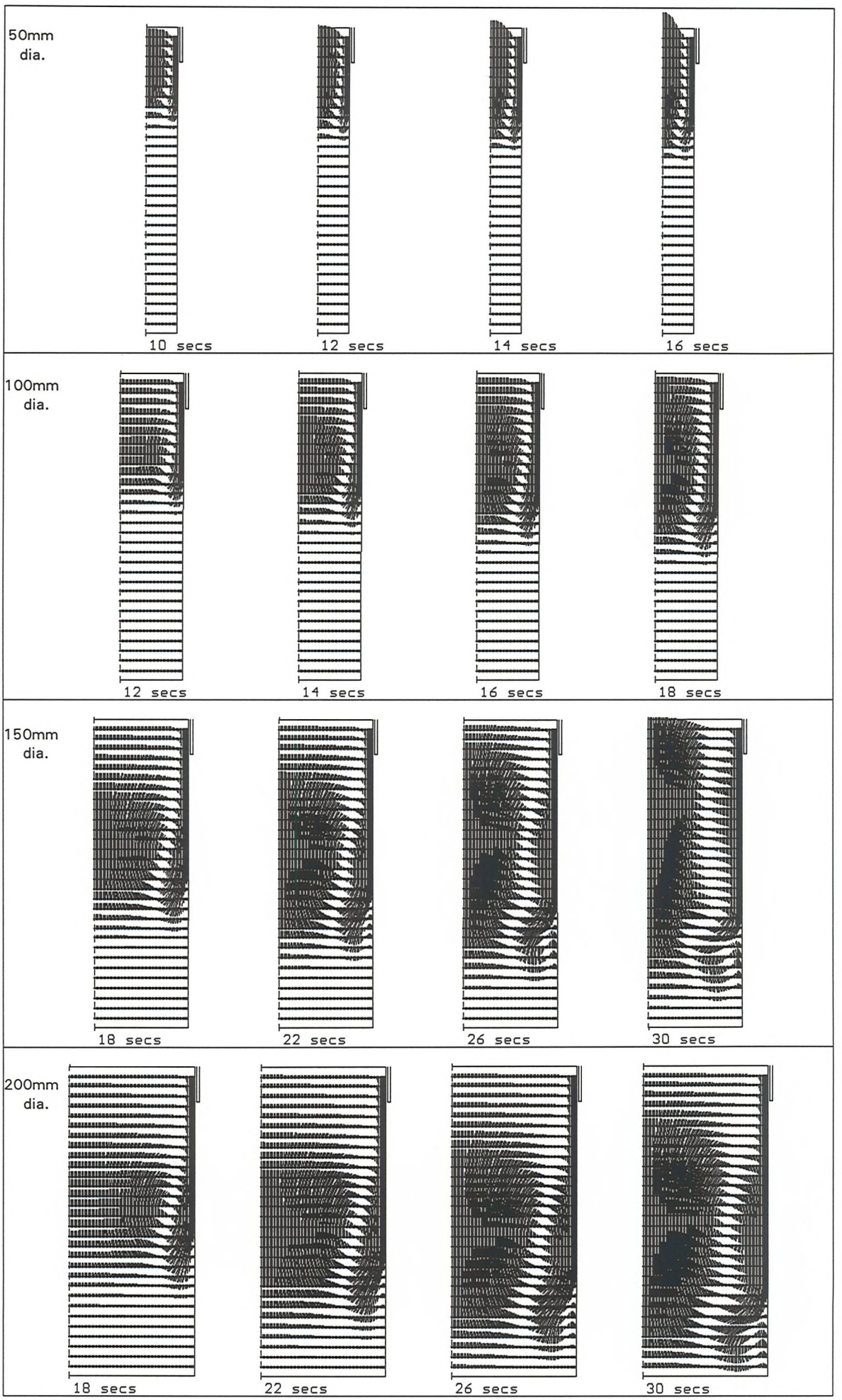

Figure 6.4a : Velocity Distribution in 50-200mm dia. pipes. Jckt 200mm long; Tin = 20°C; Zoom Plot

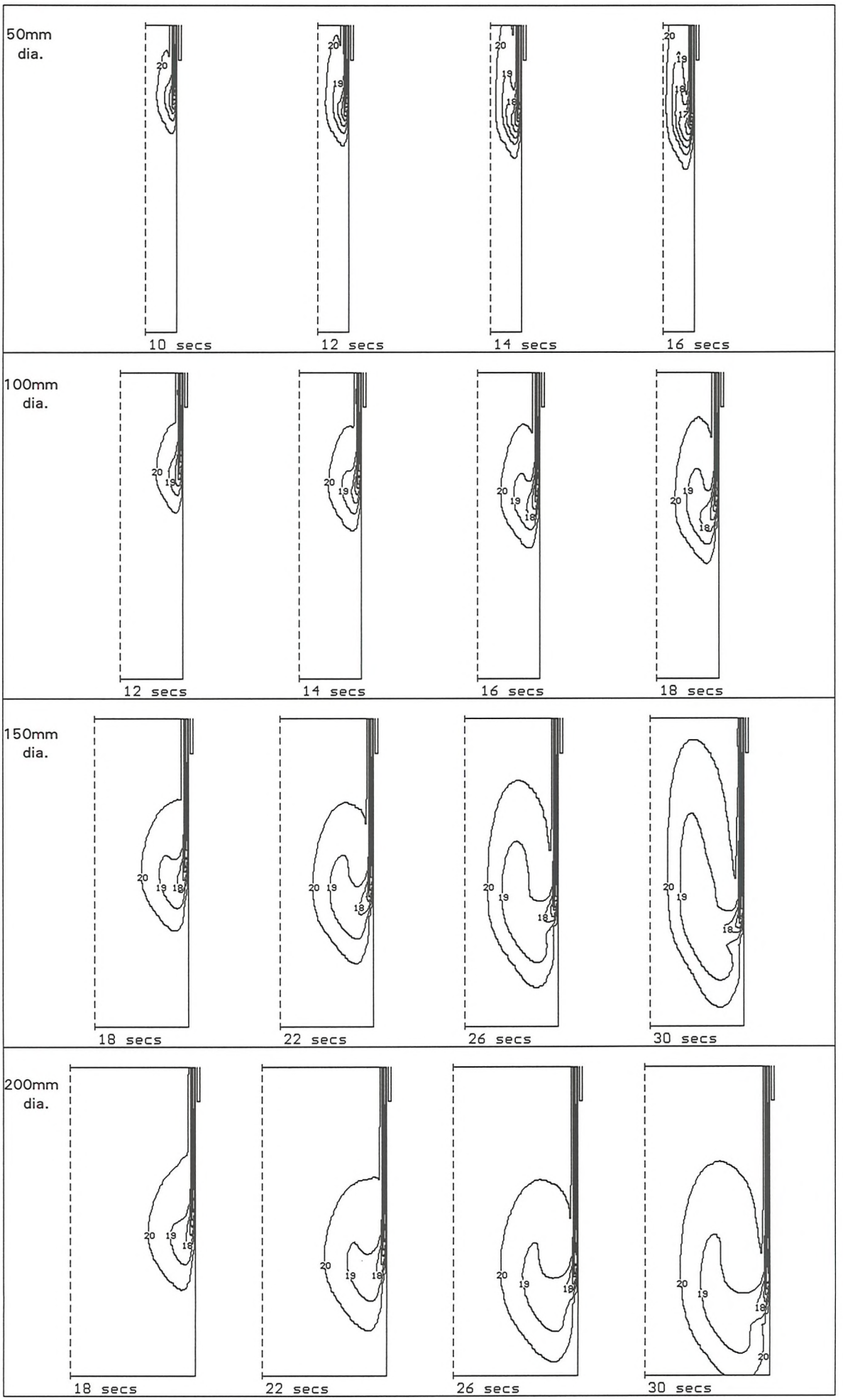

Figure 6.4b : Temperature Distribution in 50-200mm dia. pipes; Jckt 200mm long; Tin = 20°C; Zoom Plot

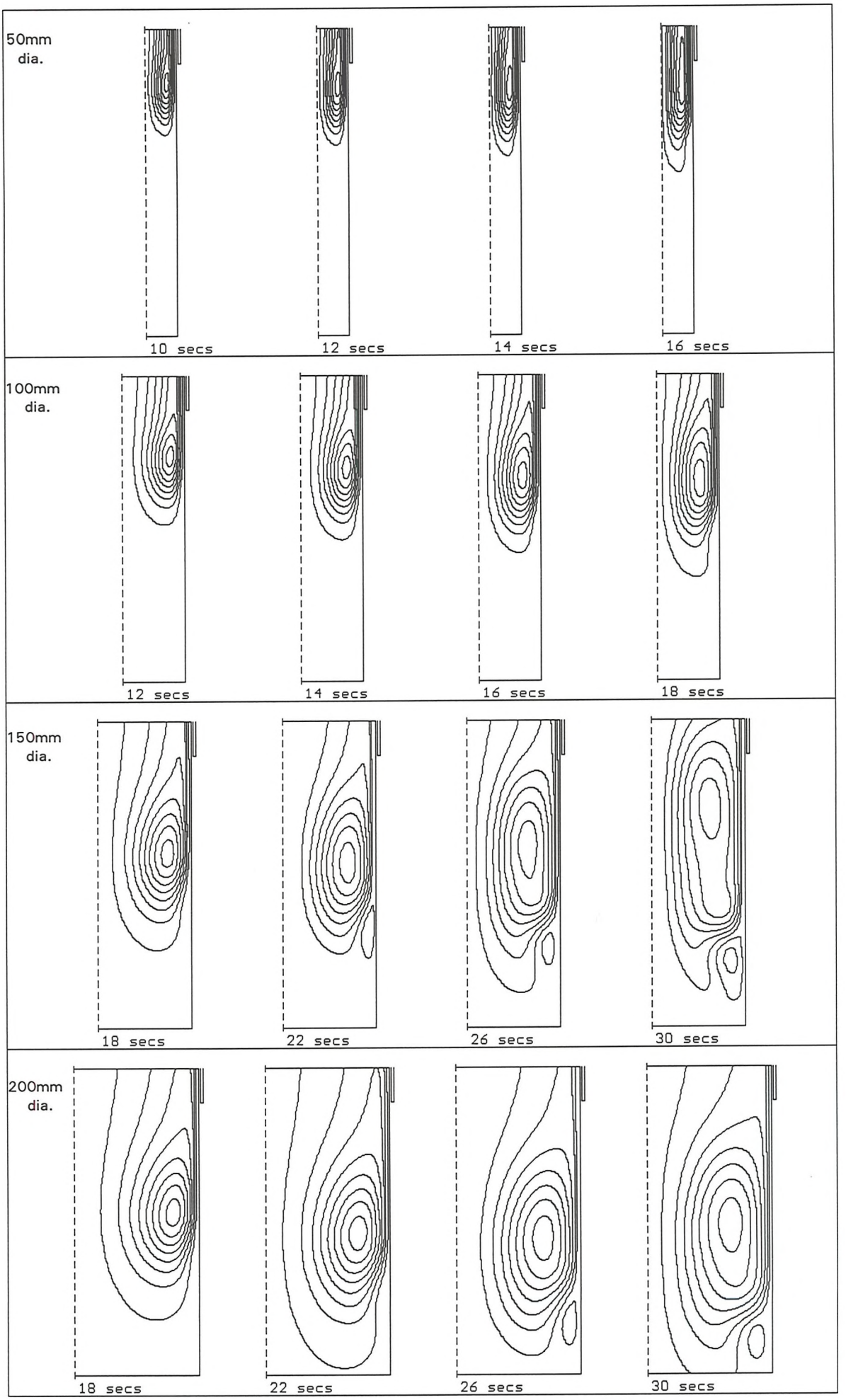

Figure 6.4c : Streamline Dist. in 50-200mm dia. pipes; Jckt 200mm long; Tin = 20°C; Zoom Plot

Height of Bottom of Main Convection Cell
Effect of Pipe Diameter

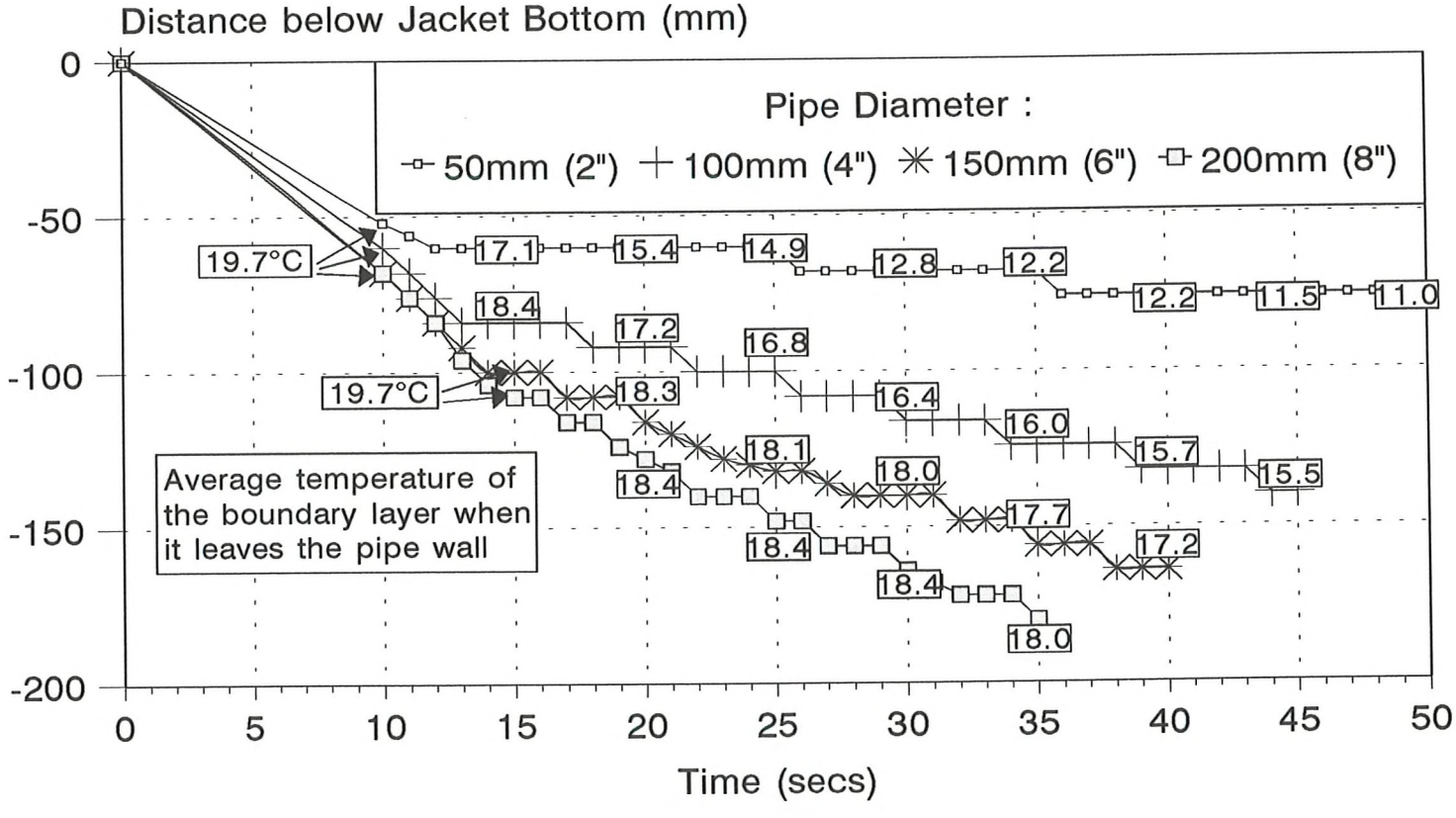

Tin=20°C; convection - no solidification; no wall; Twall=0°C in Jacket (0.2m long)
- Results extracted before flow reached bottom of domain -

Figure 6.5

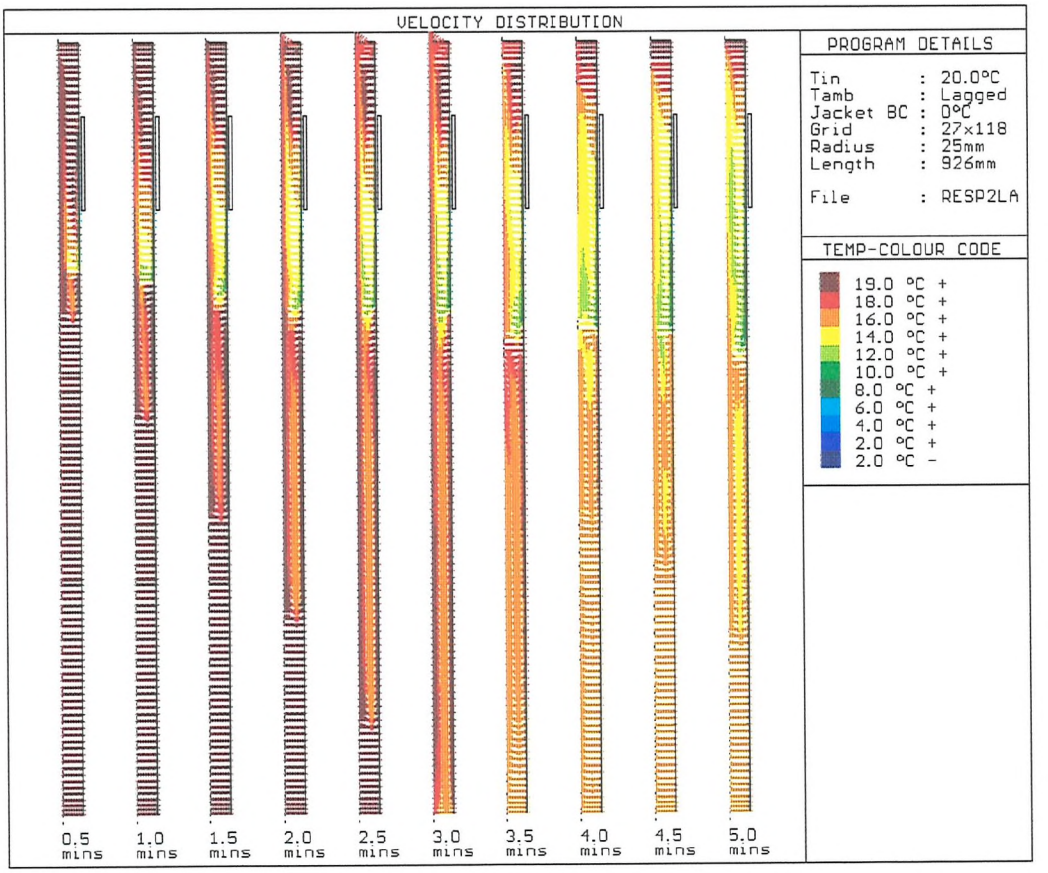

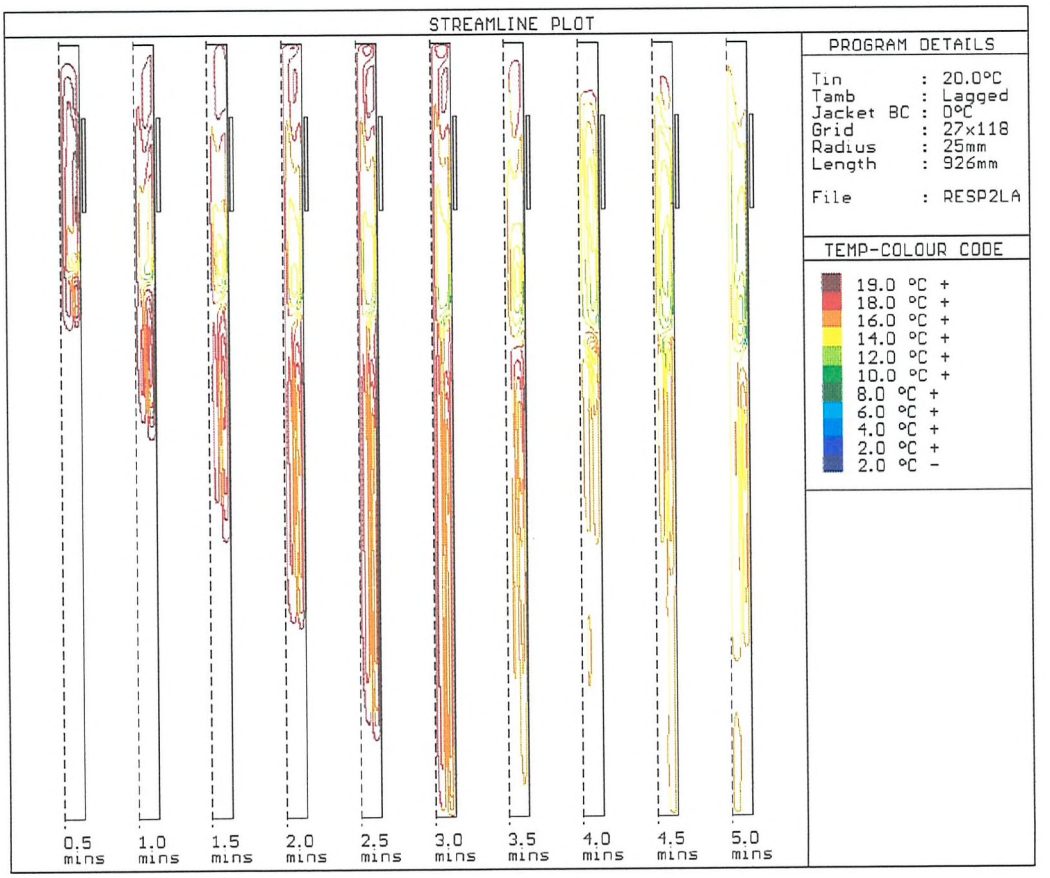

Figure 6.6a: Flow development at ½ minute intervals (½..5mins); 50mm dia. pipe; Tin=20°C

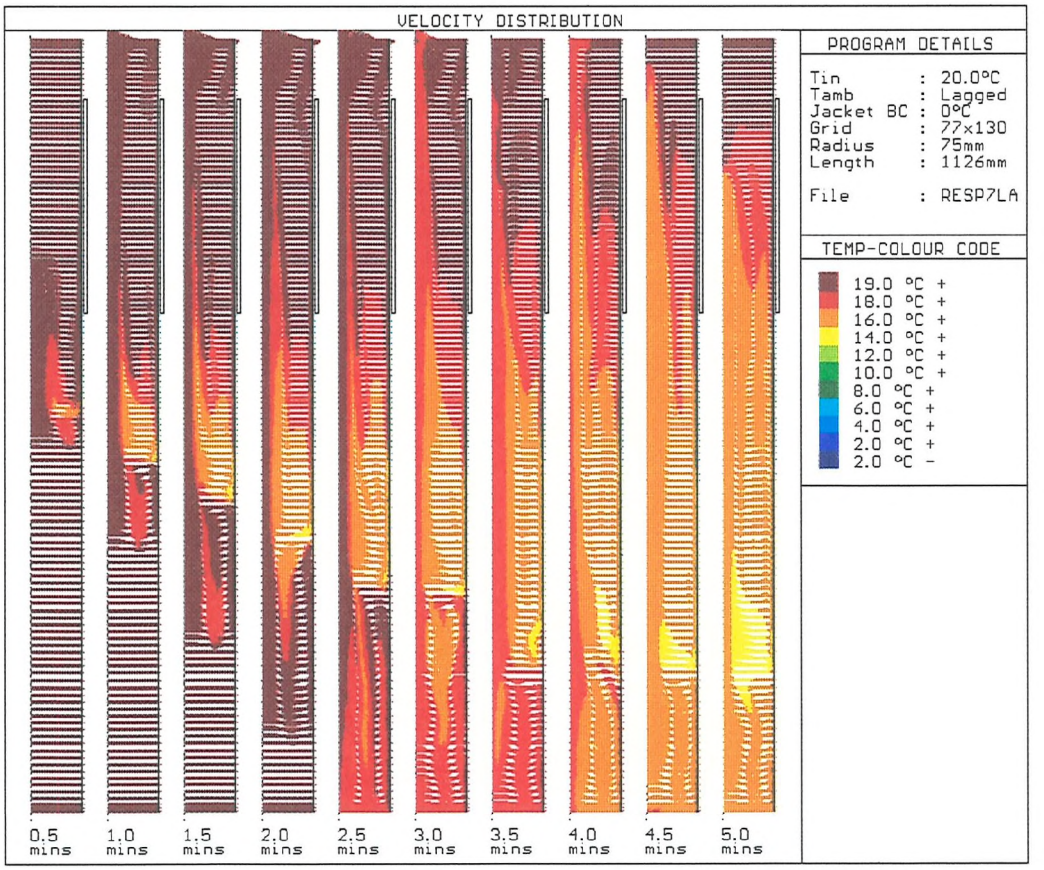

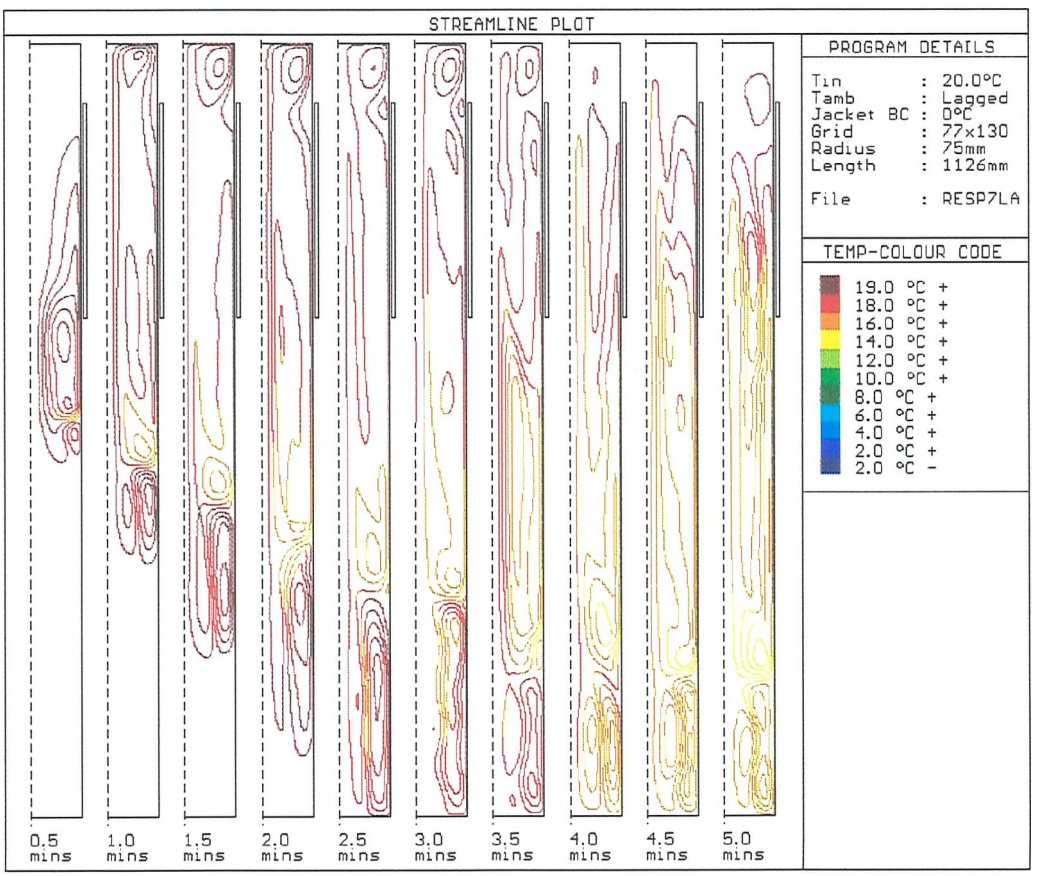

Figure 6.6b: Flow development at ½ minute intervals (½..5mins); 150mm dia. pipe; Tin=20°C

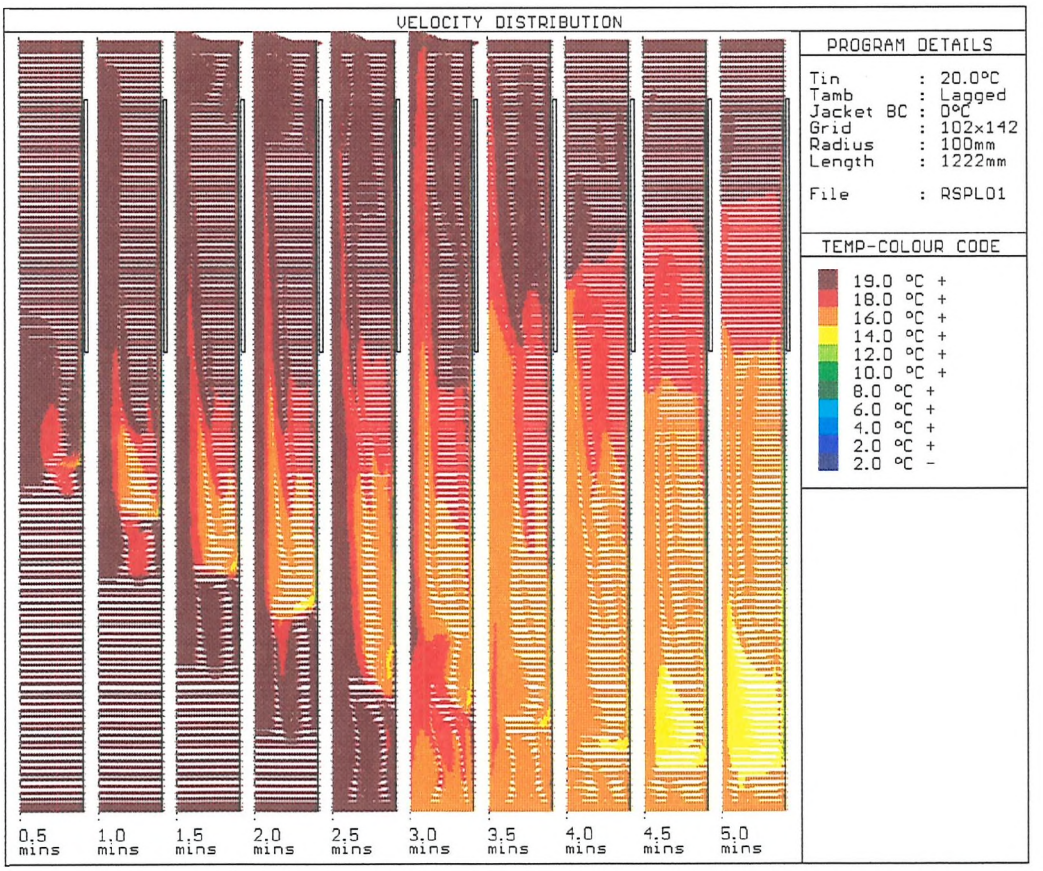

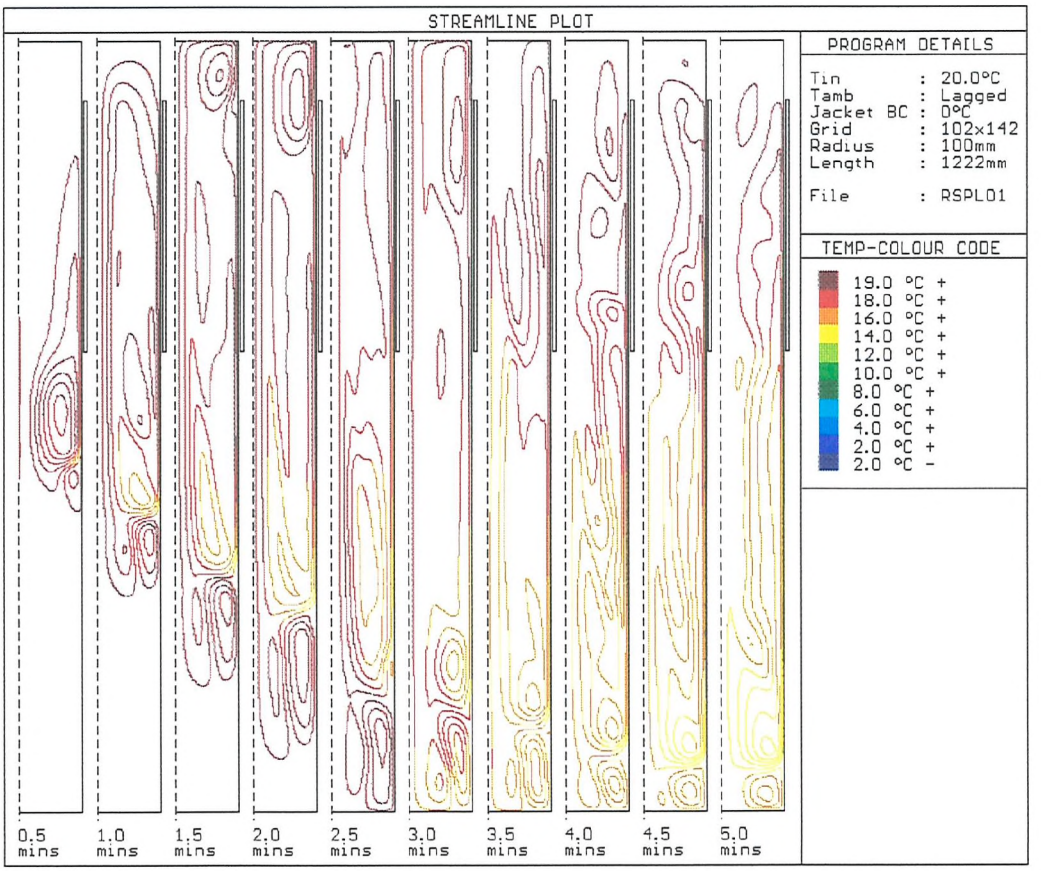

Figure 6.6c: Flow development at ½ minute intervals (½..5mins); 200mm dia. pipe; Tin=20°C

Bulk Temperature Decay

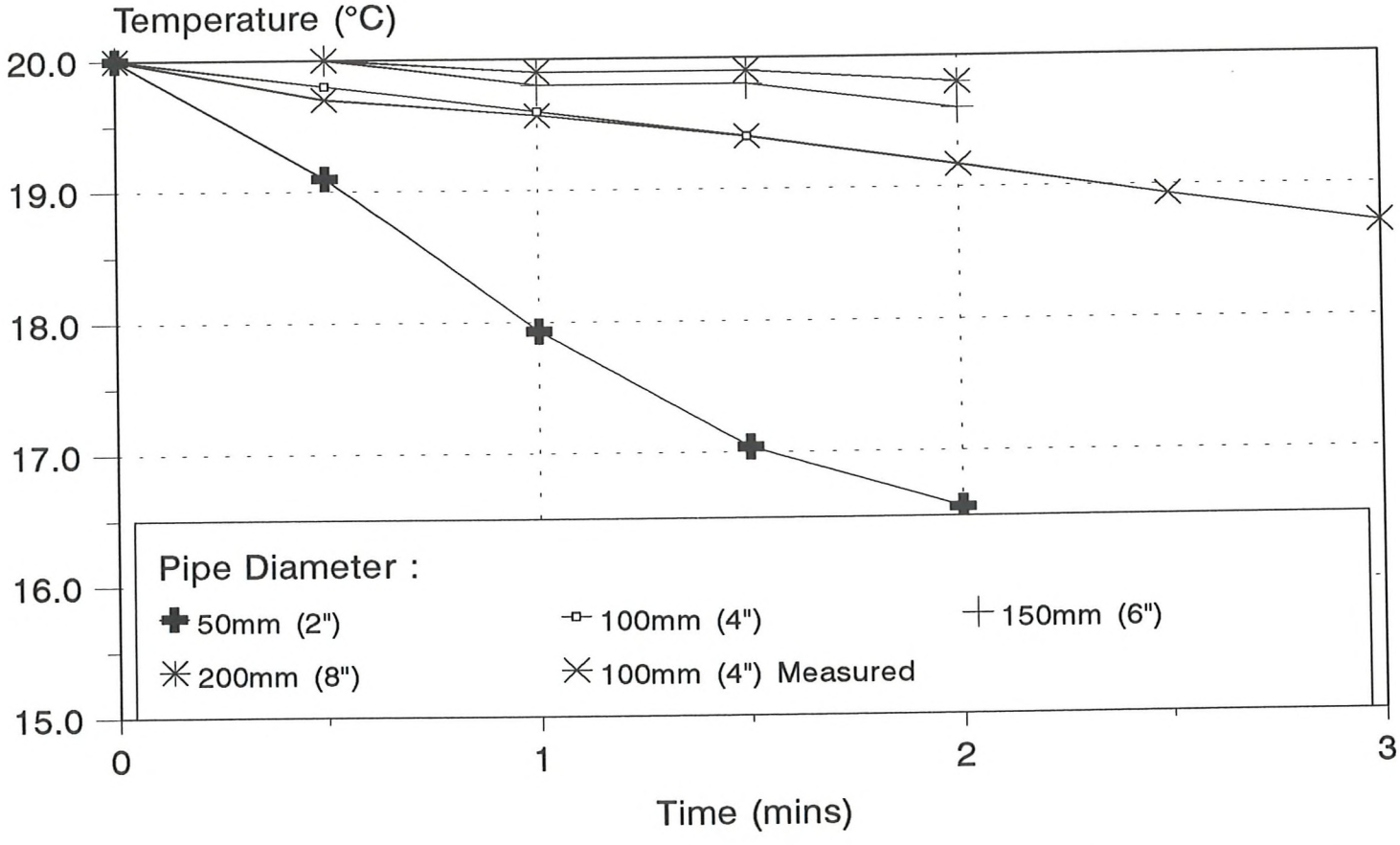

Initial Temperature=20°C; convection - no solidification; no wall; Twall=0°C in 'Jacket' (2D long)
Measurements from Tavner[5] -Results extracted before flow reached bottom of domain- Figure 6.7

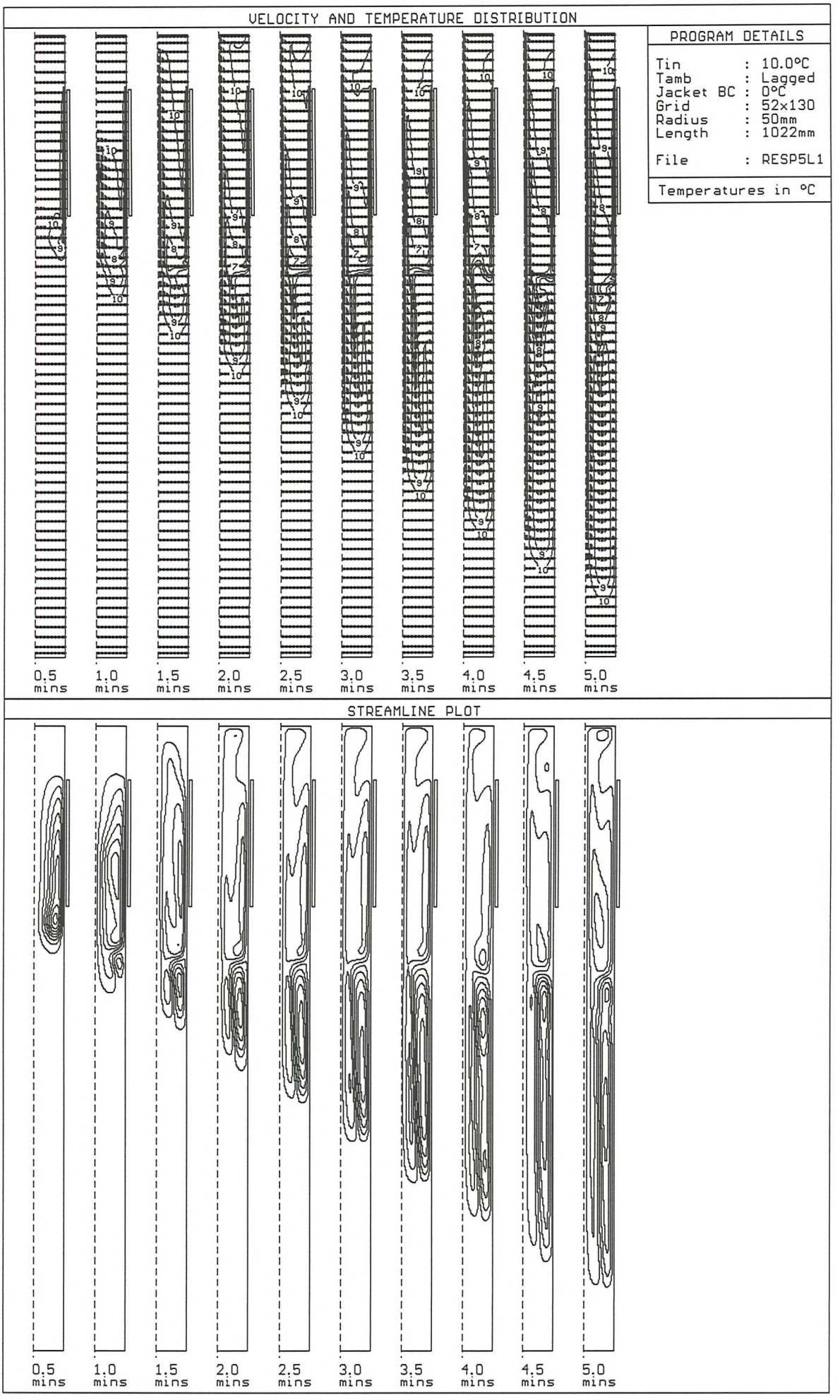

Figure 6.8a : Flow development at ½ minute intervals (½..5mins); 100mm dia. pipe; Tin = 10°C

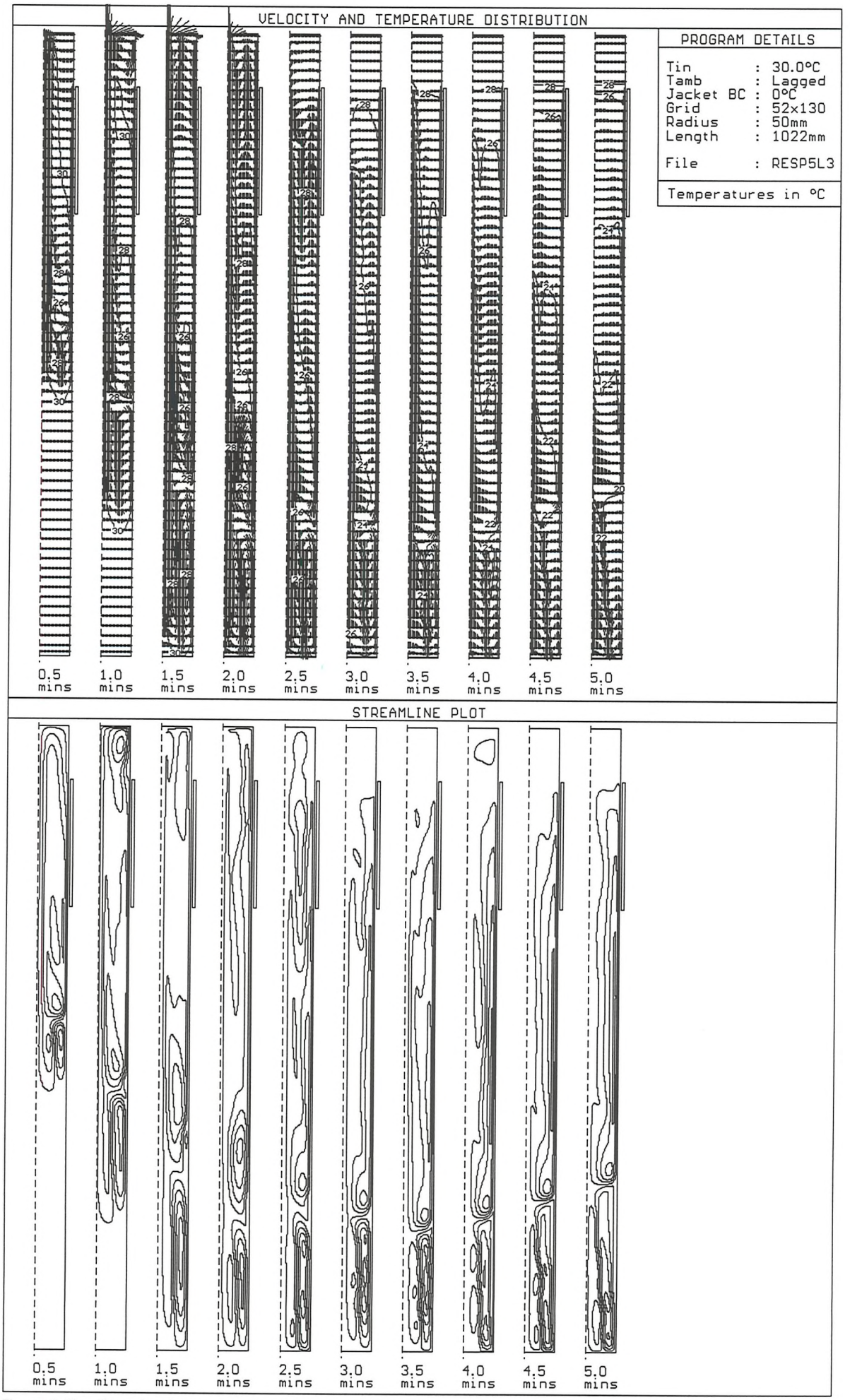

Figure 6.8b : Flow development at ½ minute intervals (½..5mins); 100mm dia. pipe; Tin = 30°C

Height of Bottom of Main Convection Cell

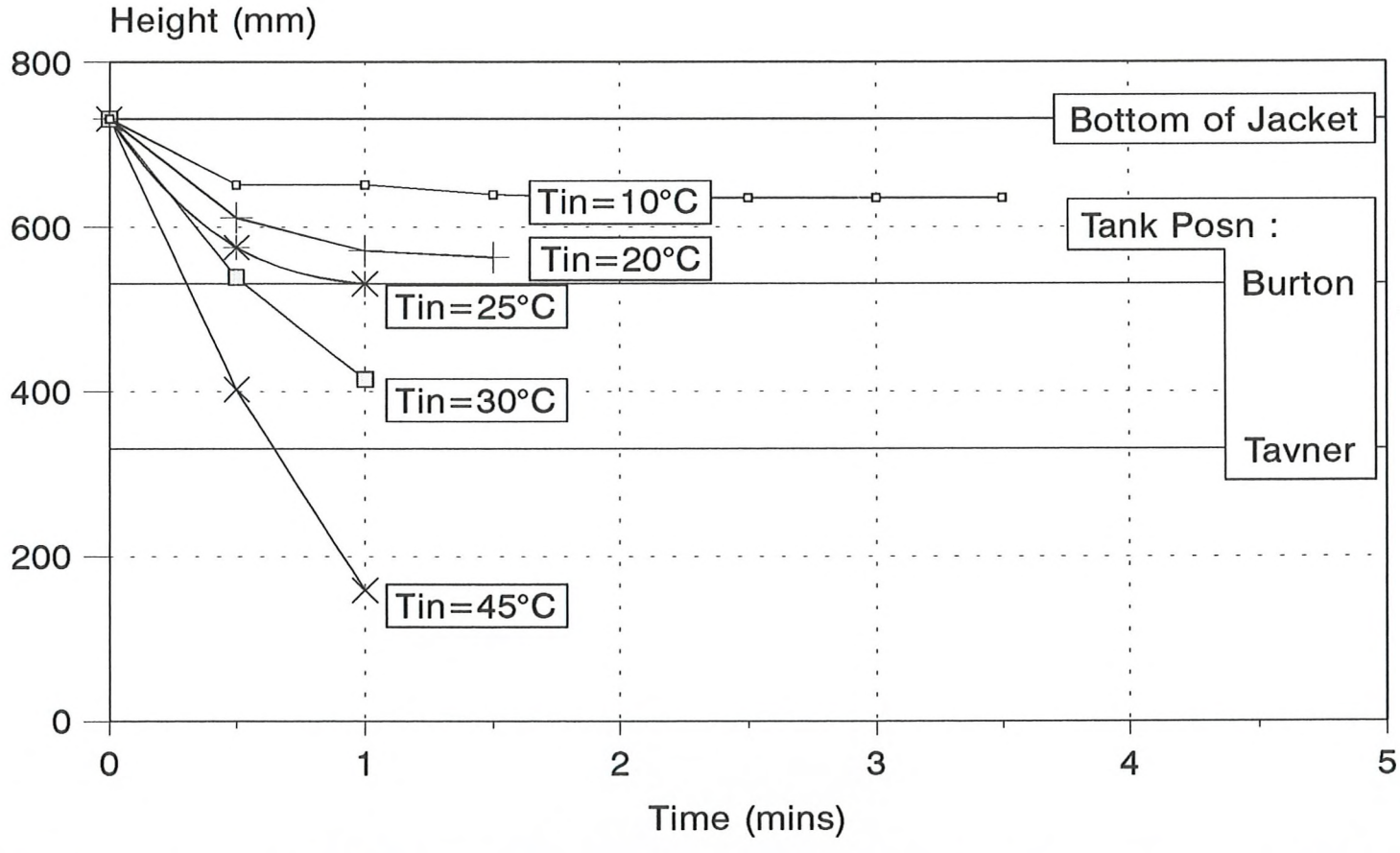

Radius 50mm; convection - no solidification; no wall; Twall=0°C in 'Jacket' (0.2m long)
- Predicted velocities extracted before flow reached bottom of domain - Figure 6.9

Boundary Layer Velocity
Comparison with Integral Solution from Bejan[29]

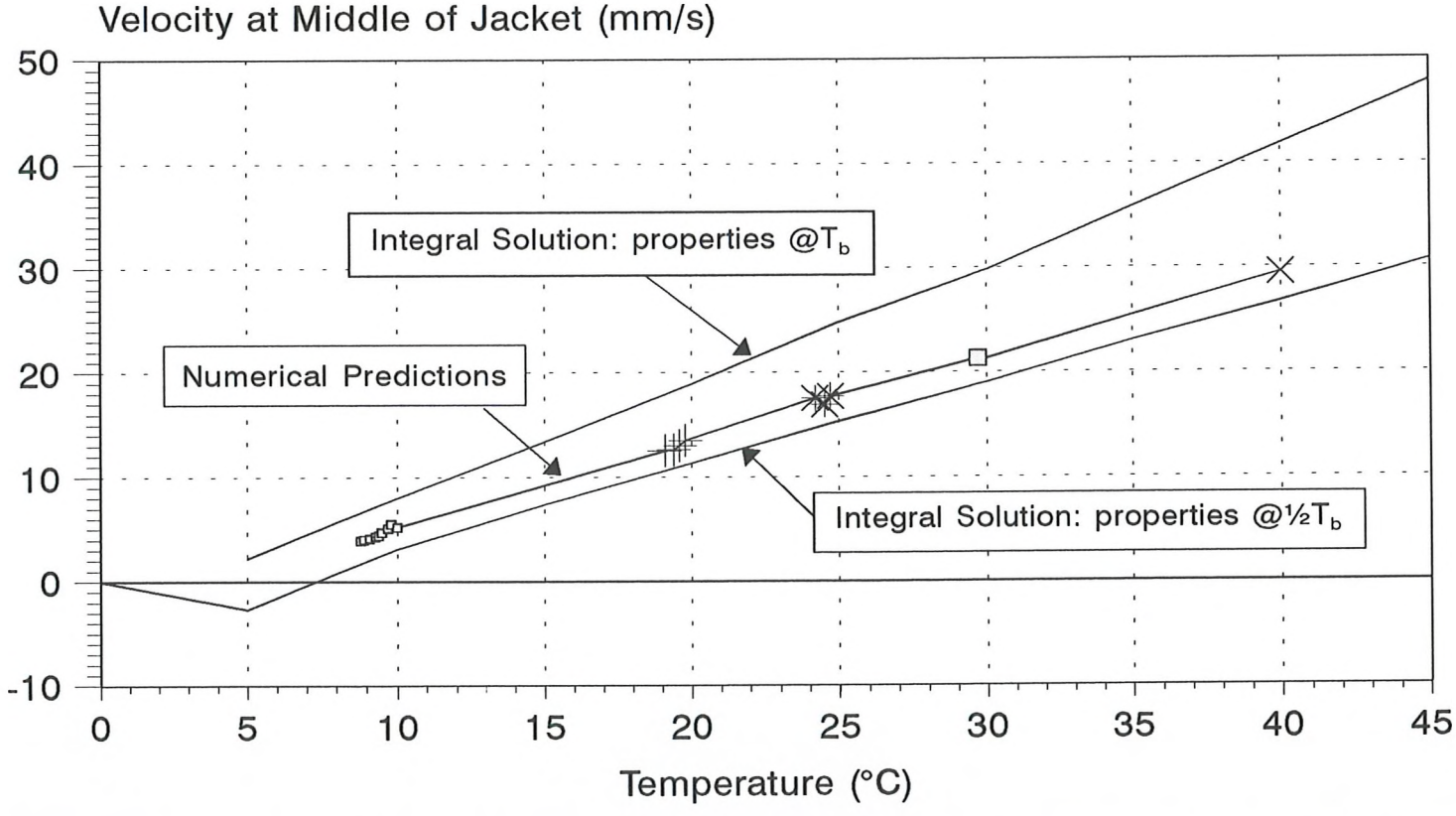

Radius 50mm; convection - no solidification; no wall; Twall=0°C in 'Jacket' (0.2m long)
- Predicted velocities extracted before flow reached bottom of domain - Figure 6.10

Heat Transfer Coefficent at the Centre of the Jacket

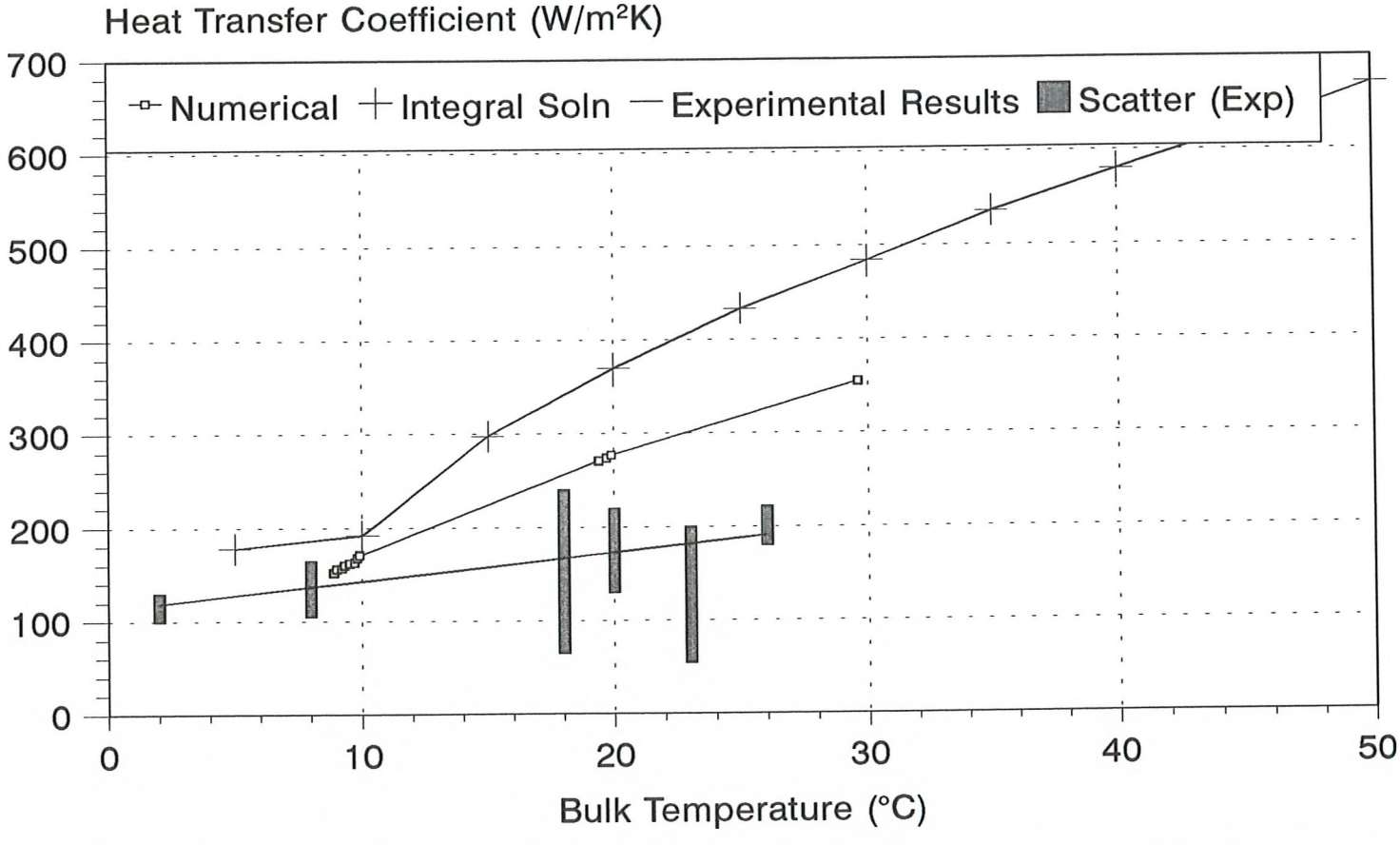

Numerical results: no freezing, no wall; Results extracted before flow reached bottom of domain
Integral solution from Bejan[29] (properties @½Tb); Experimental results from Tavner[5] Figure 6.11

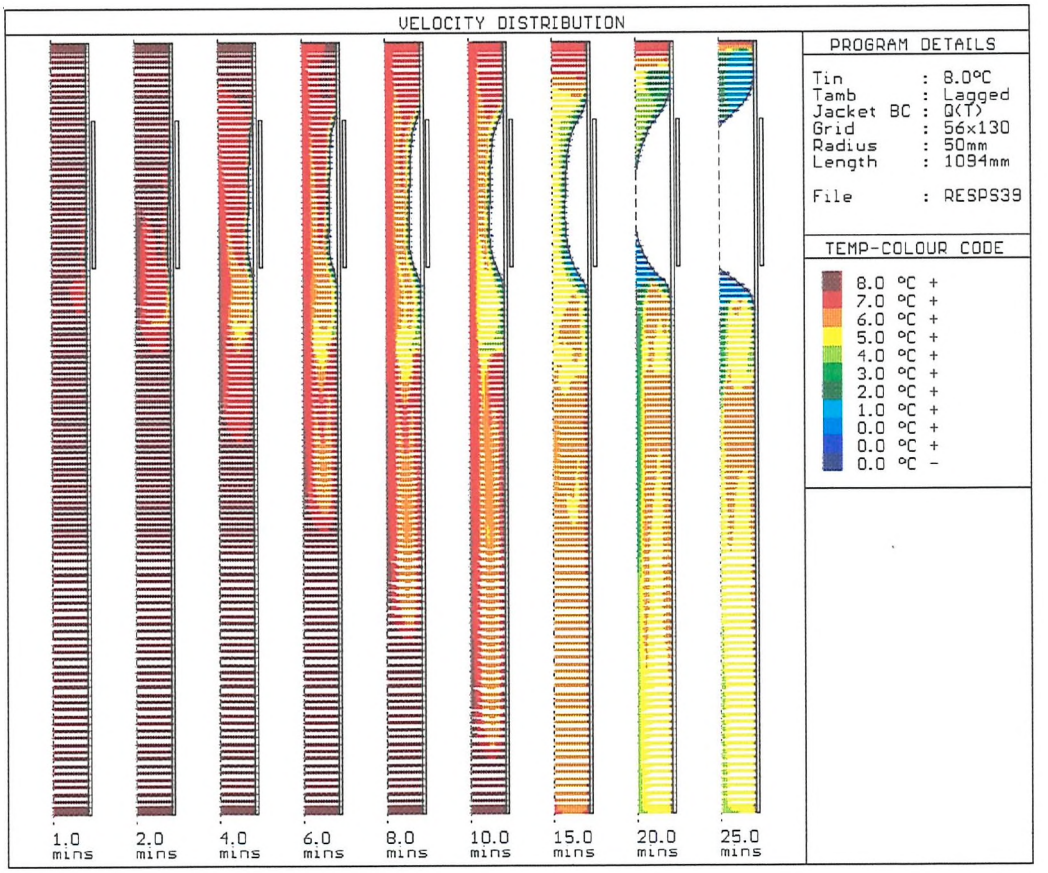

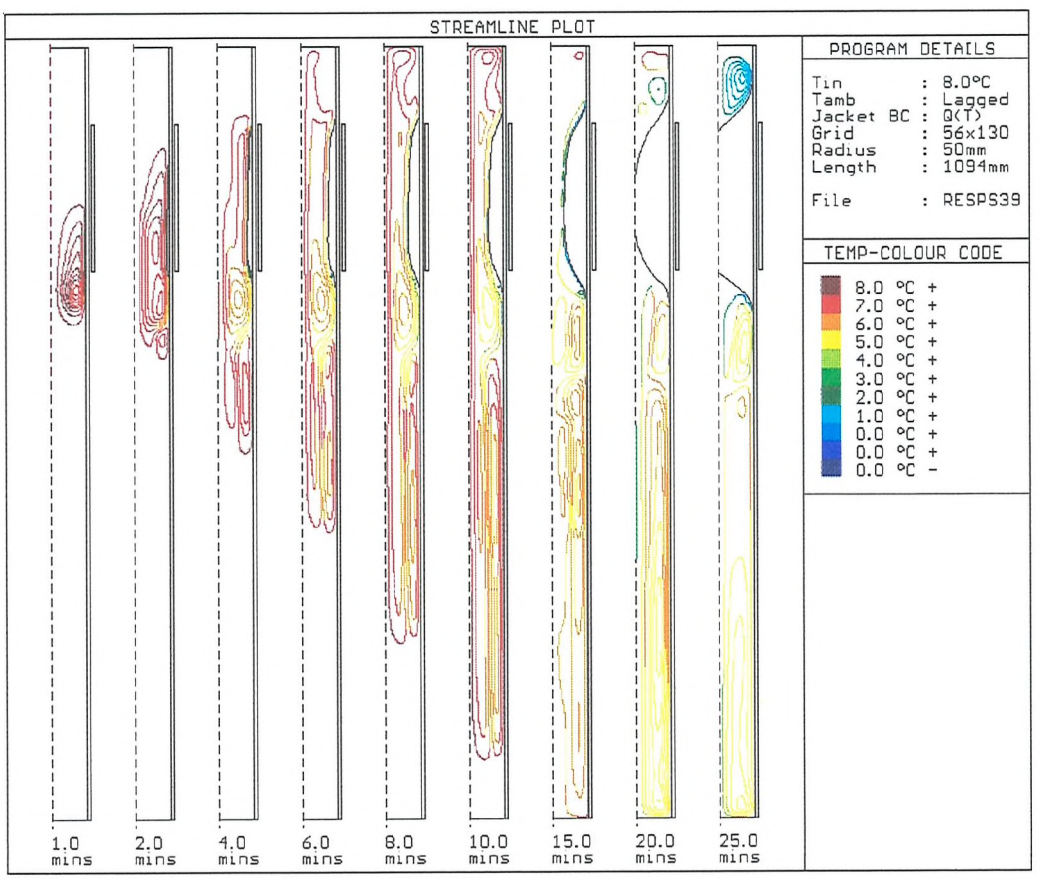

Figure 6.12a: Results from 8°C freeze; 'Long' domain; Heat flux BC

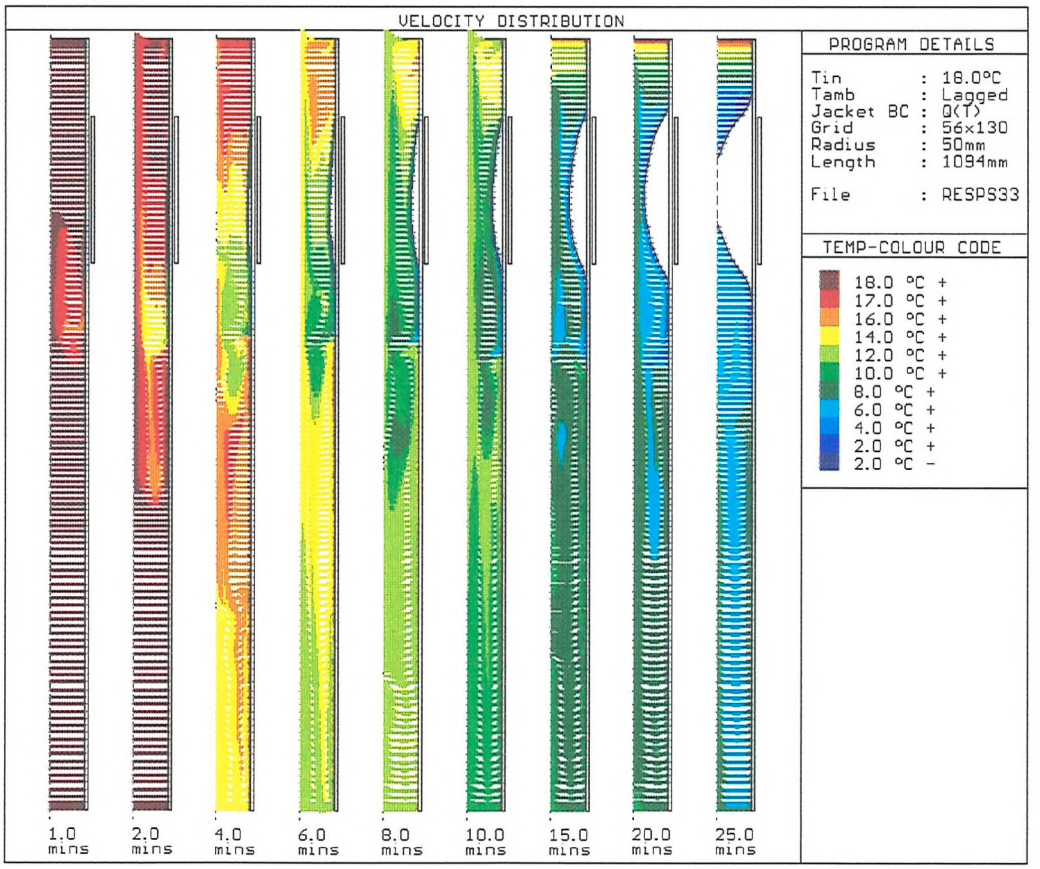

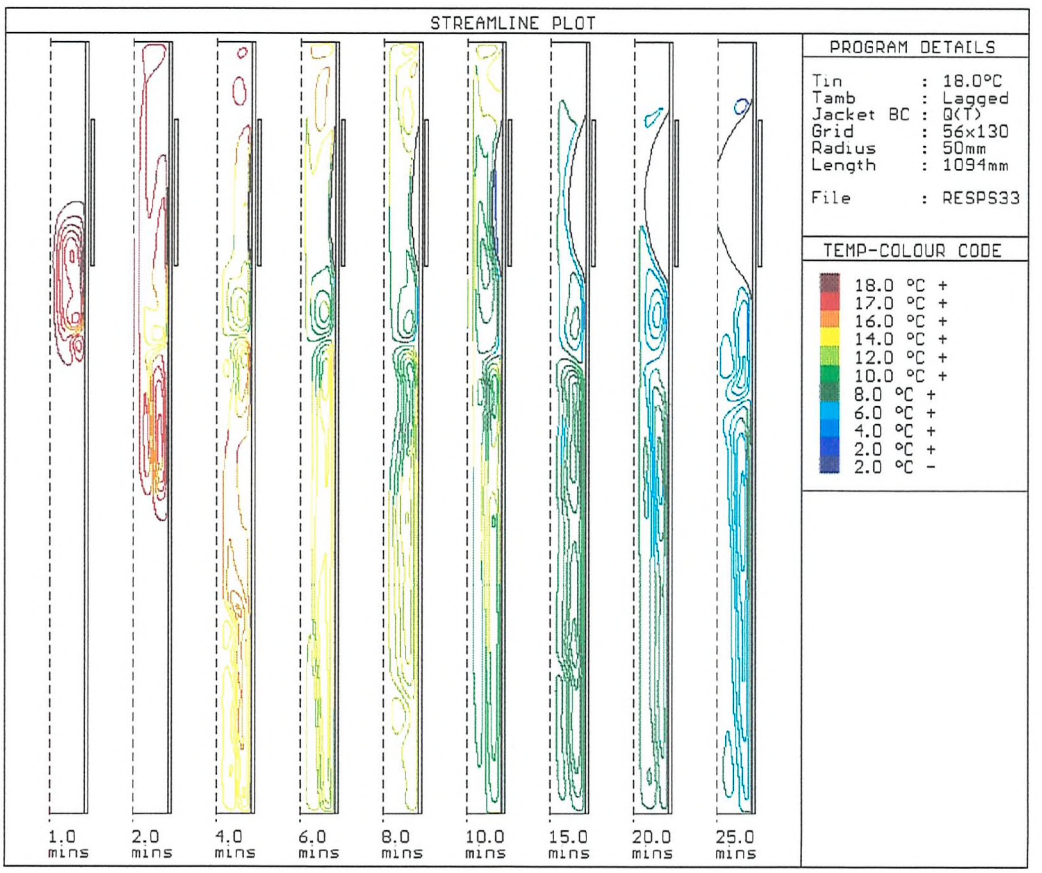

Figure 6.12b: Results from 18°C freeze; 'Long' domain; Heat flux BC

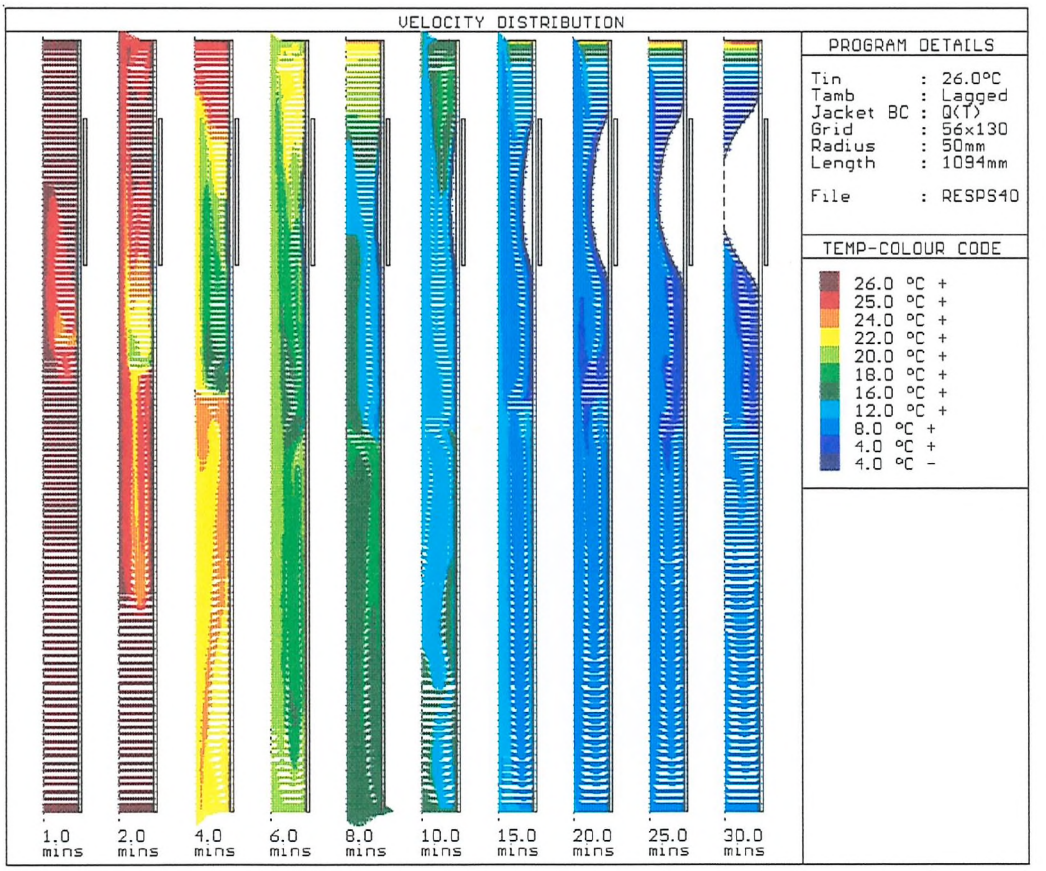

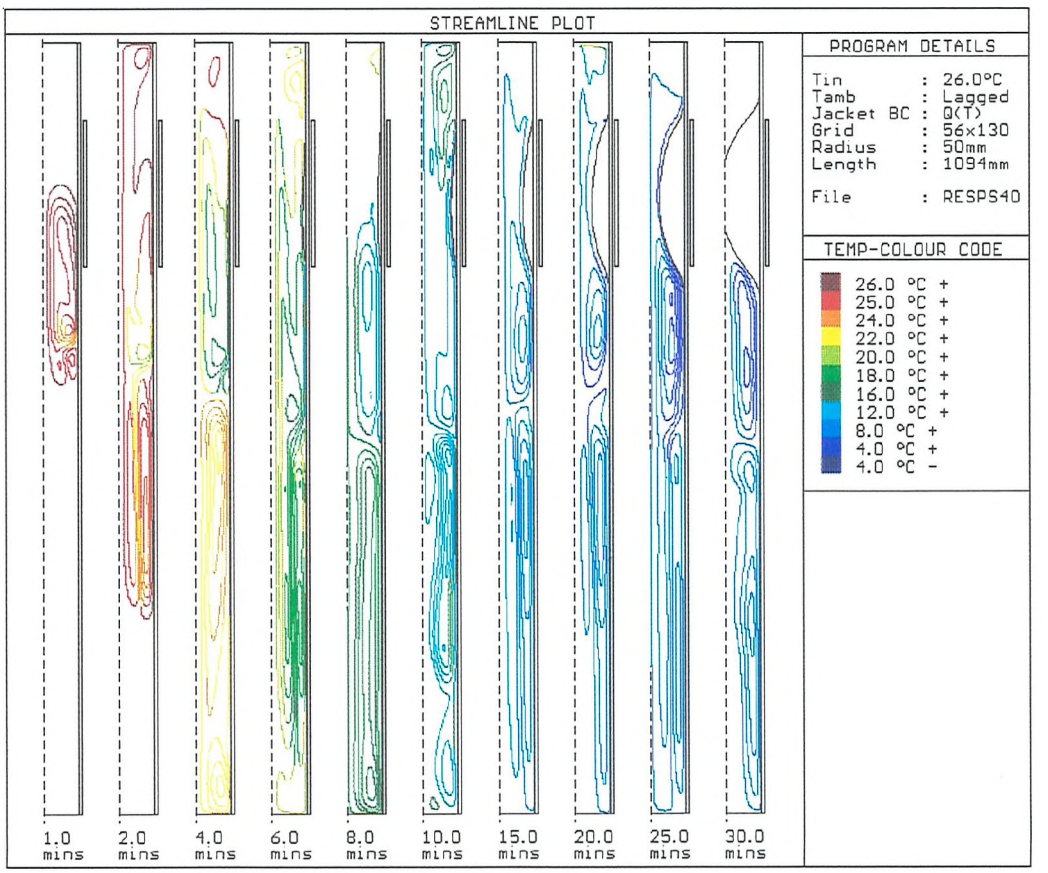

Figure 6.12c: Results from 26°C freeze; 'Long' domain; Heat flux BC

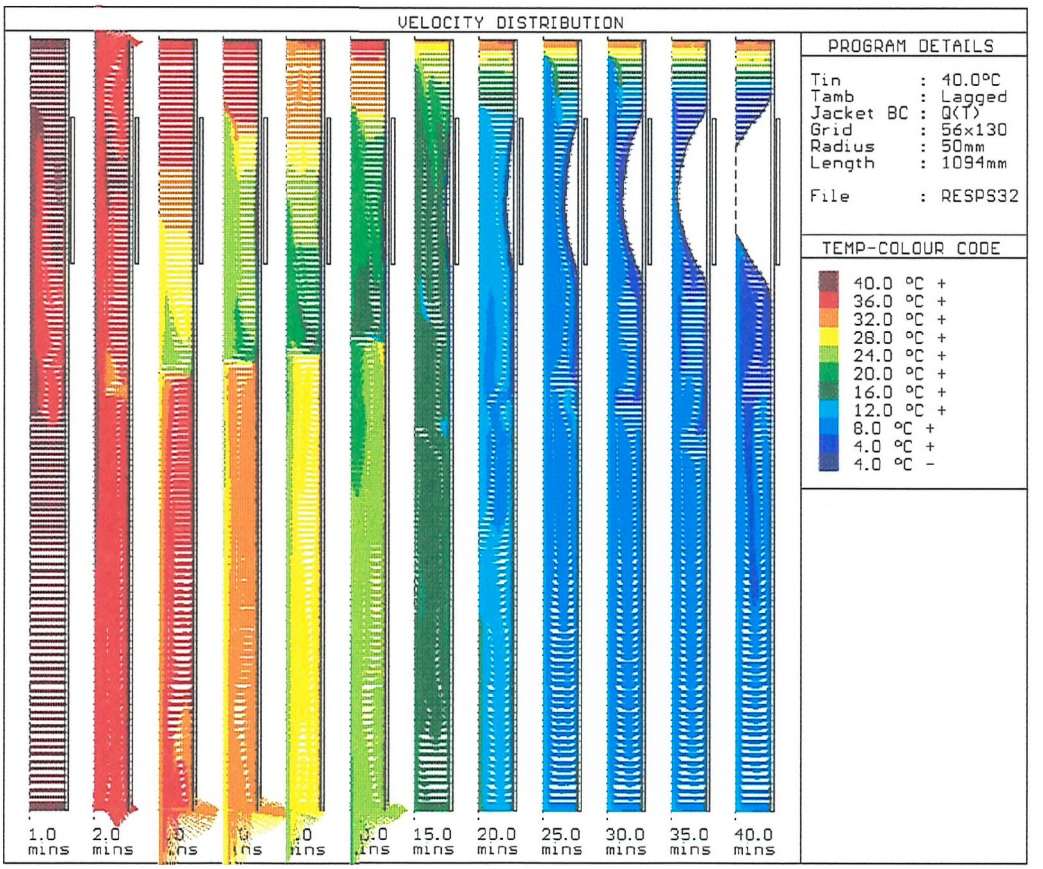

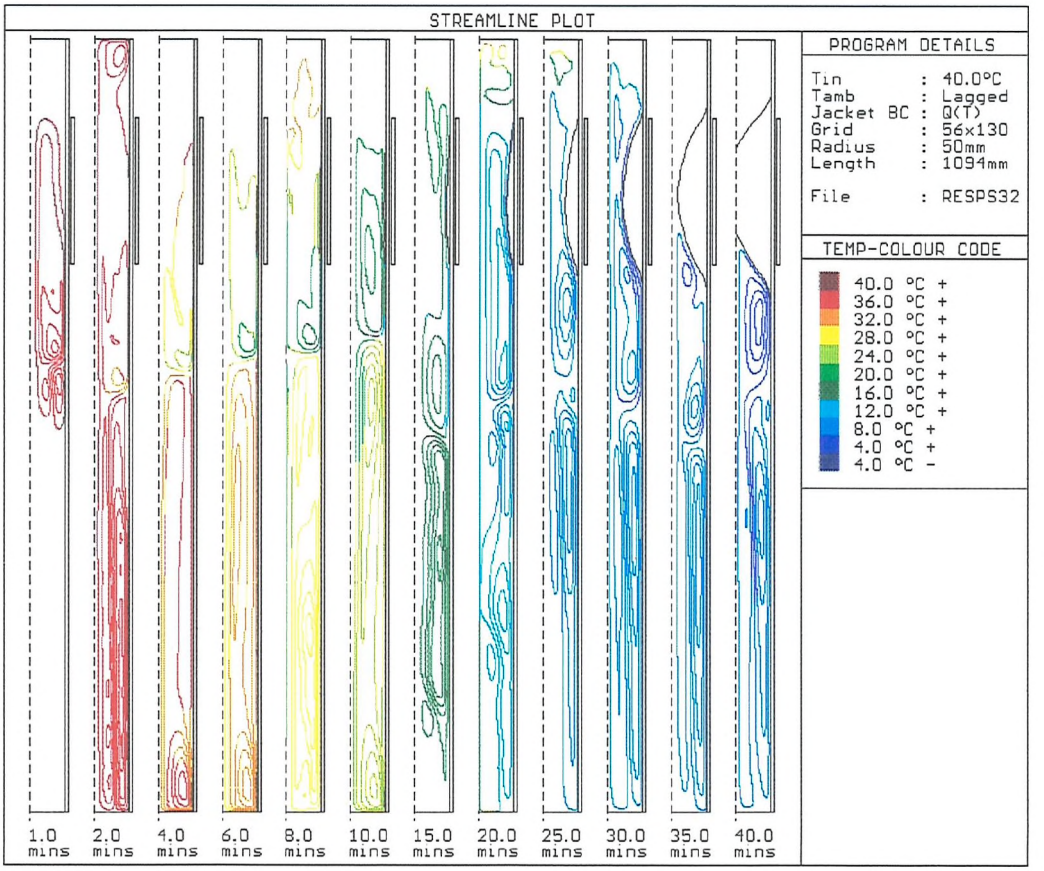

Figure 6.12d: Results from 40°C freeze; 'Long' domain; Heat flux BC

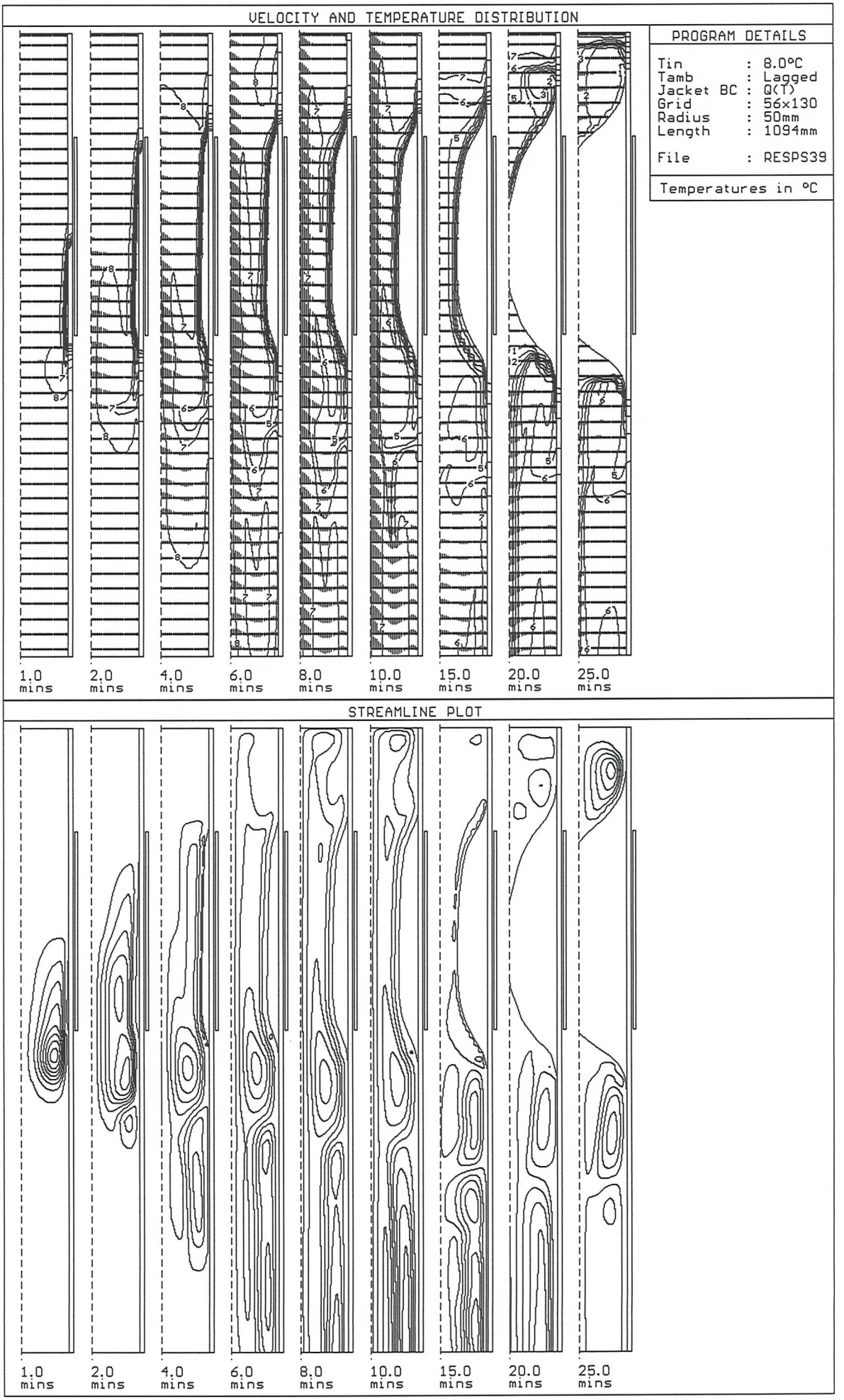

Figure 6.13a: Results from 8°C freeze; 'Long' pipe; Q(T) jacket BC; Zoom on 'short' pipe domain

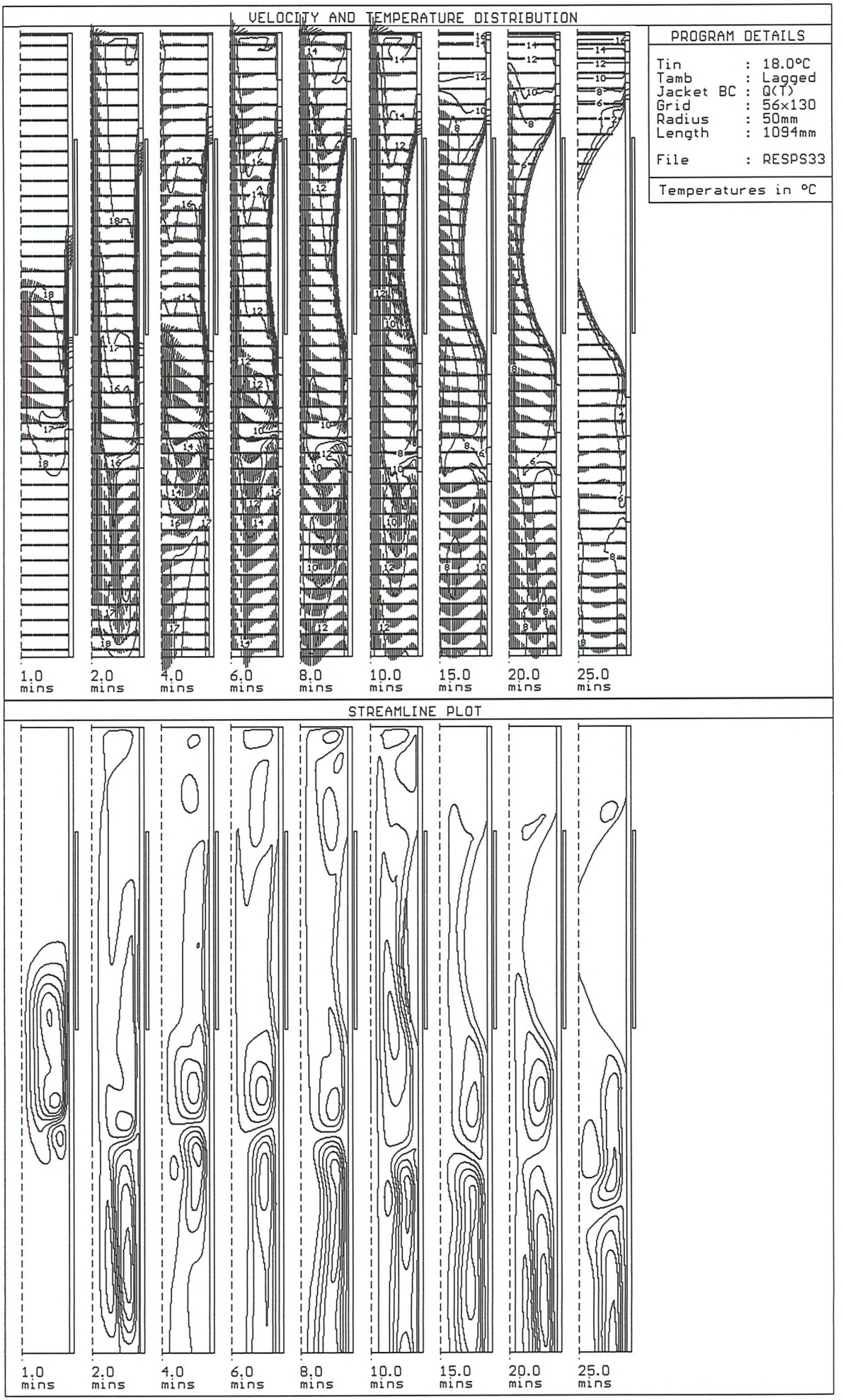

Figure 6.13b: Results from 18°C freeze; 'Long' pipe; Q(T) jacket BC; Zoom on 'short' pipe domain

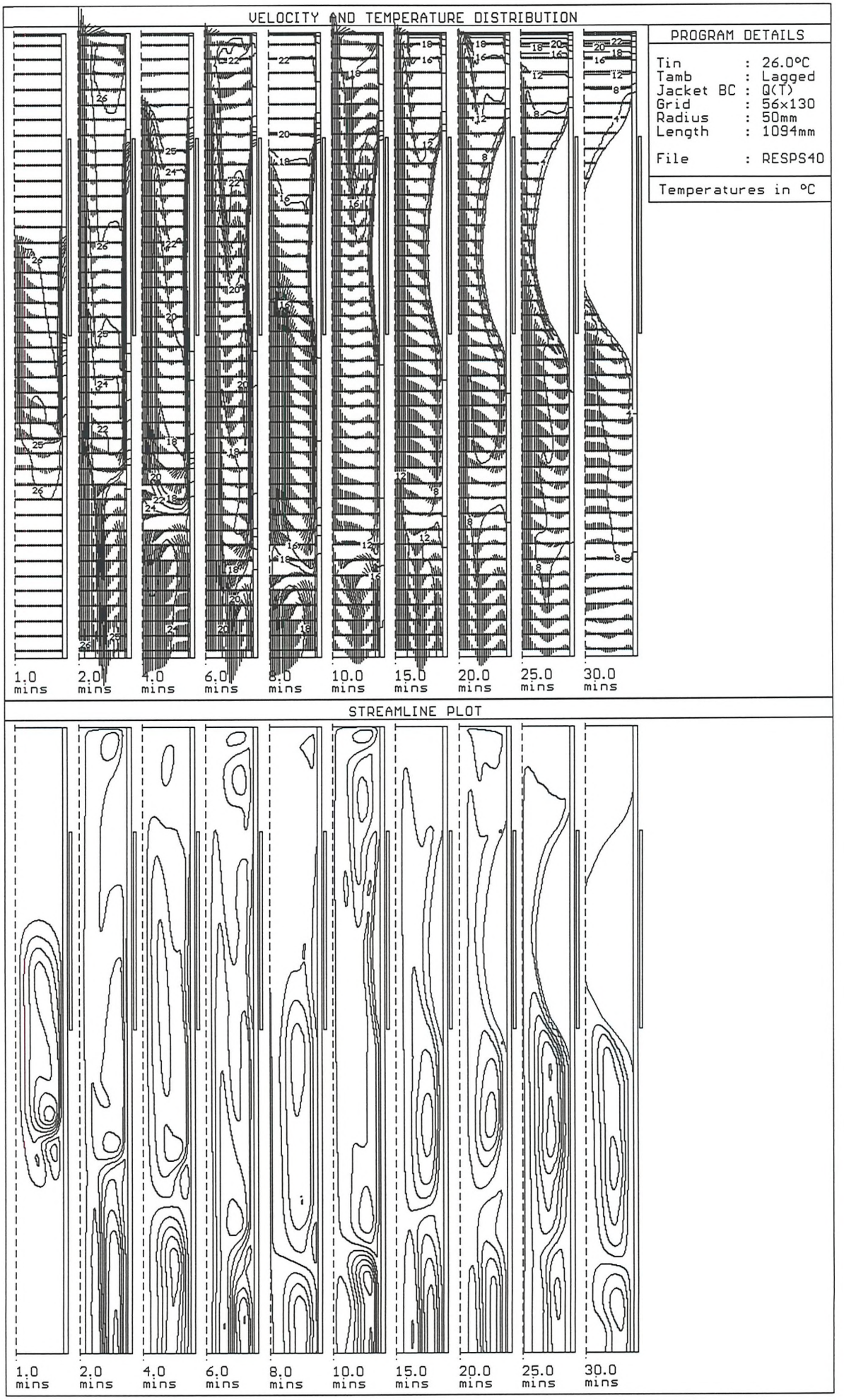

Figure 6.13c: Results from 26°C freeze; 'Long' pipe; Q(T) jacket BC; Zoom on 'short' pipe domain

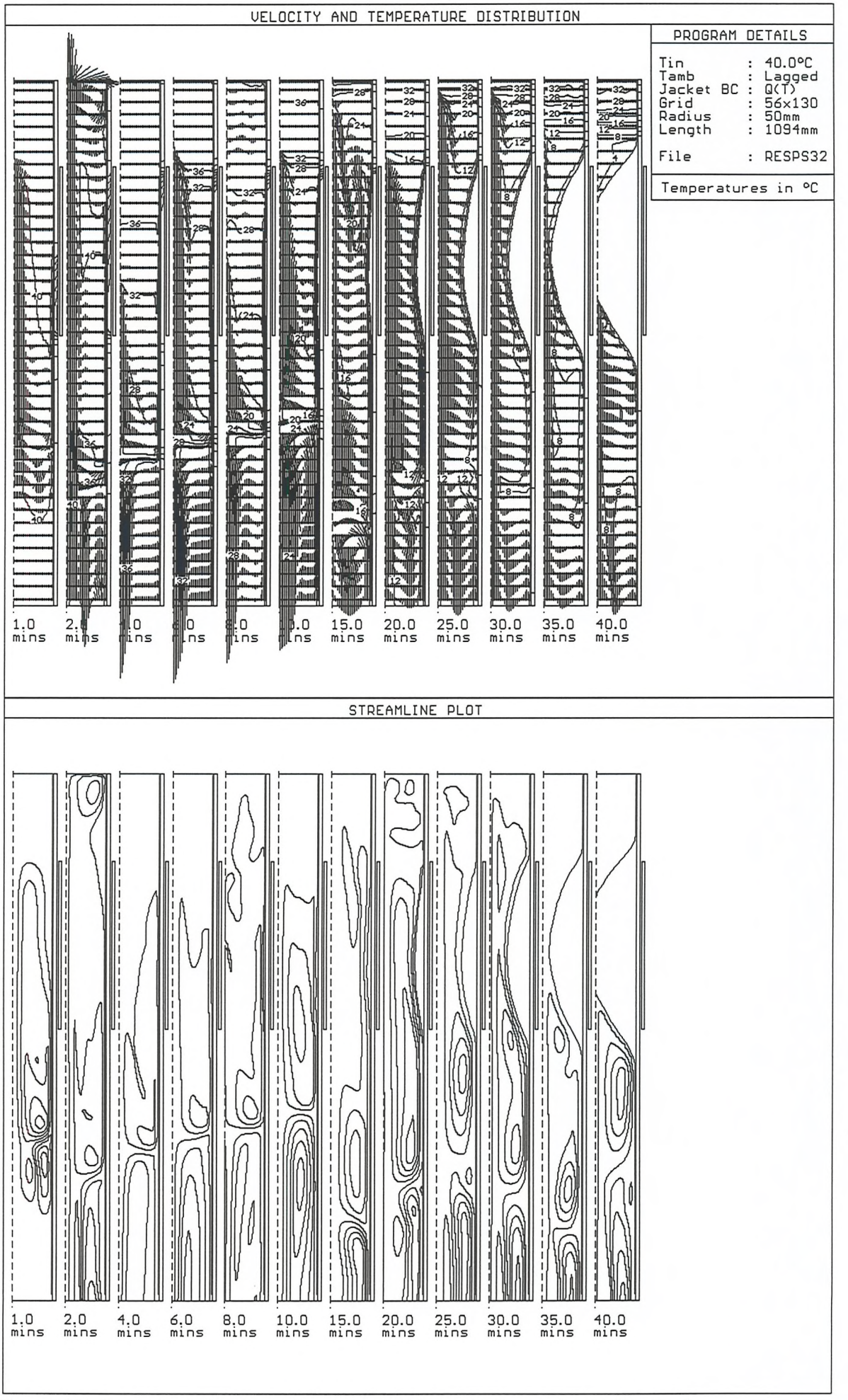

Figure 6.13d: Results form 40°C freeze; 'Long' pipe; Q(T) jacket BC; Zoom on 'short' pipe domain

Effect of Domain Length on Freezing Time

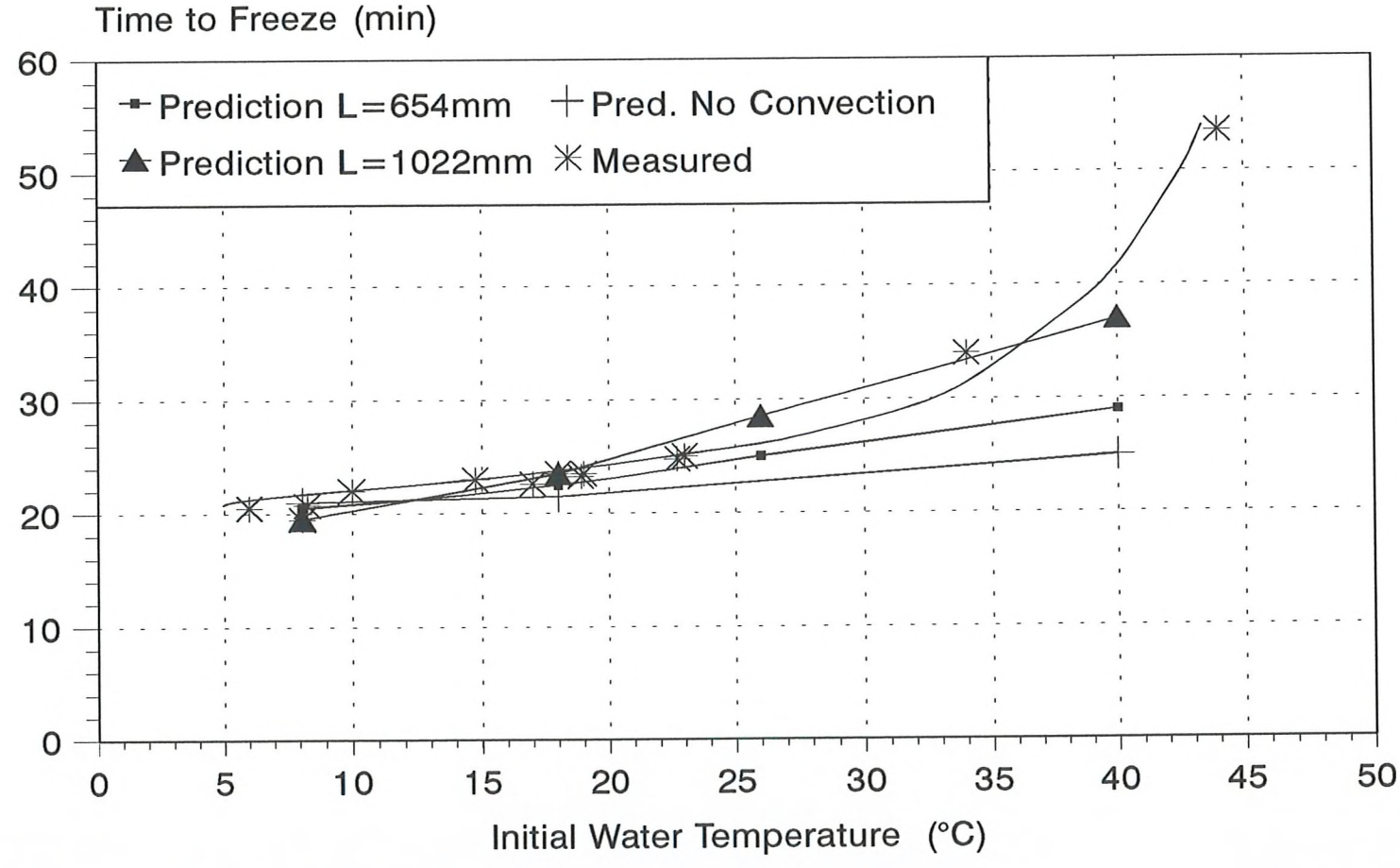

Heat Flux Boundary Condition; Measurements from Tavner[5]

Figure 6.14

Relationship between Plug Neck Radius and Bulk Water Temperature

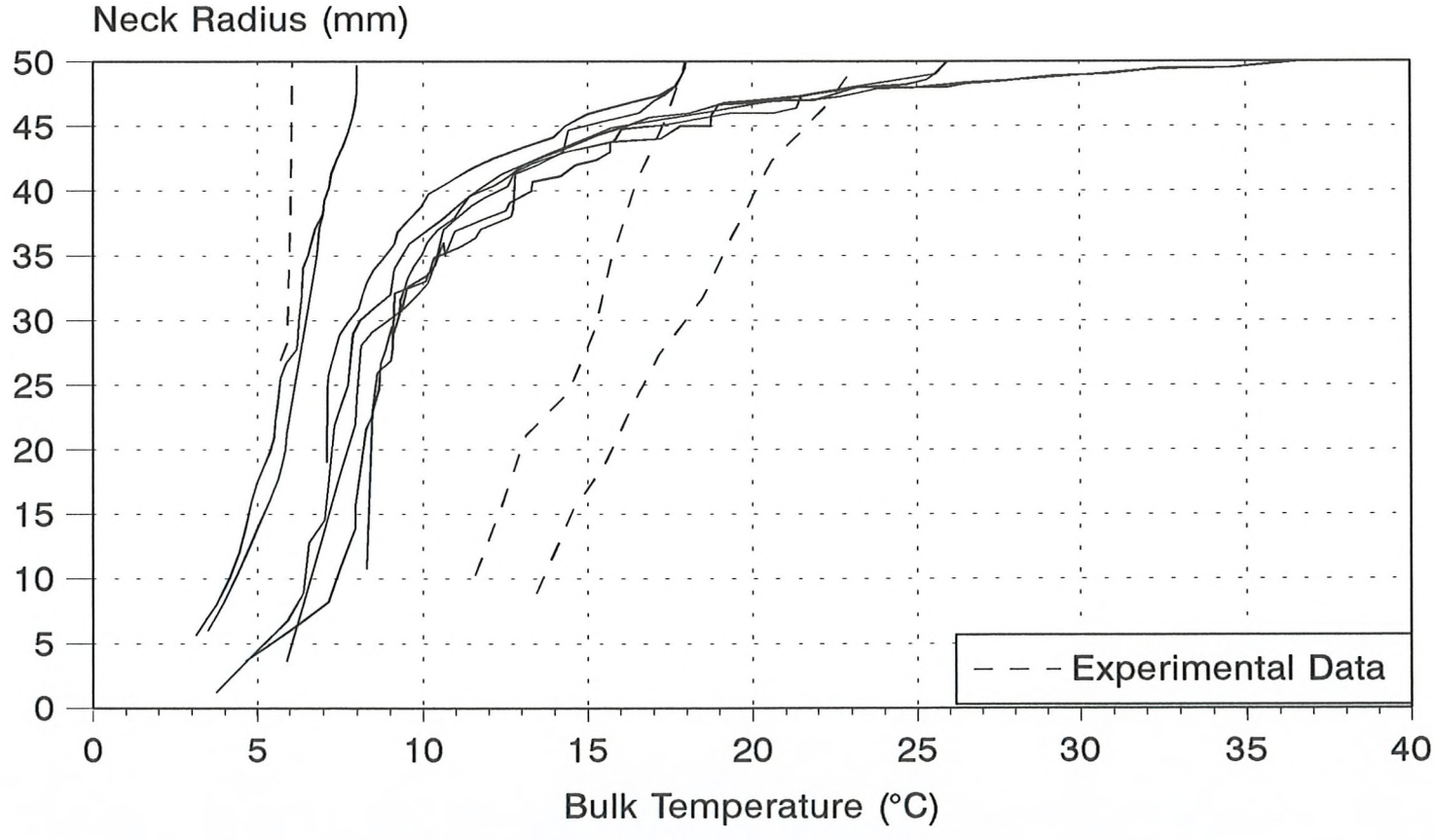

Tbulk evaluated away from ice; Q(T) Jacket BC; Measurements from Tavner[5] Figure 6.15

Predicted Boundary Layer Velocities During Freezing Heat Flux Jacket Boundary Condition

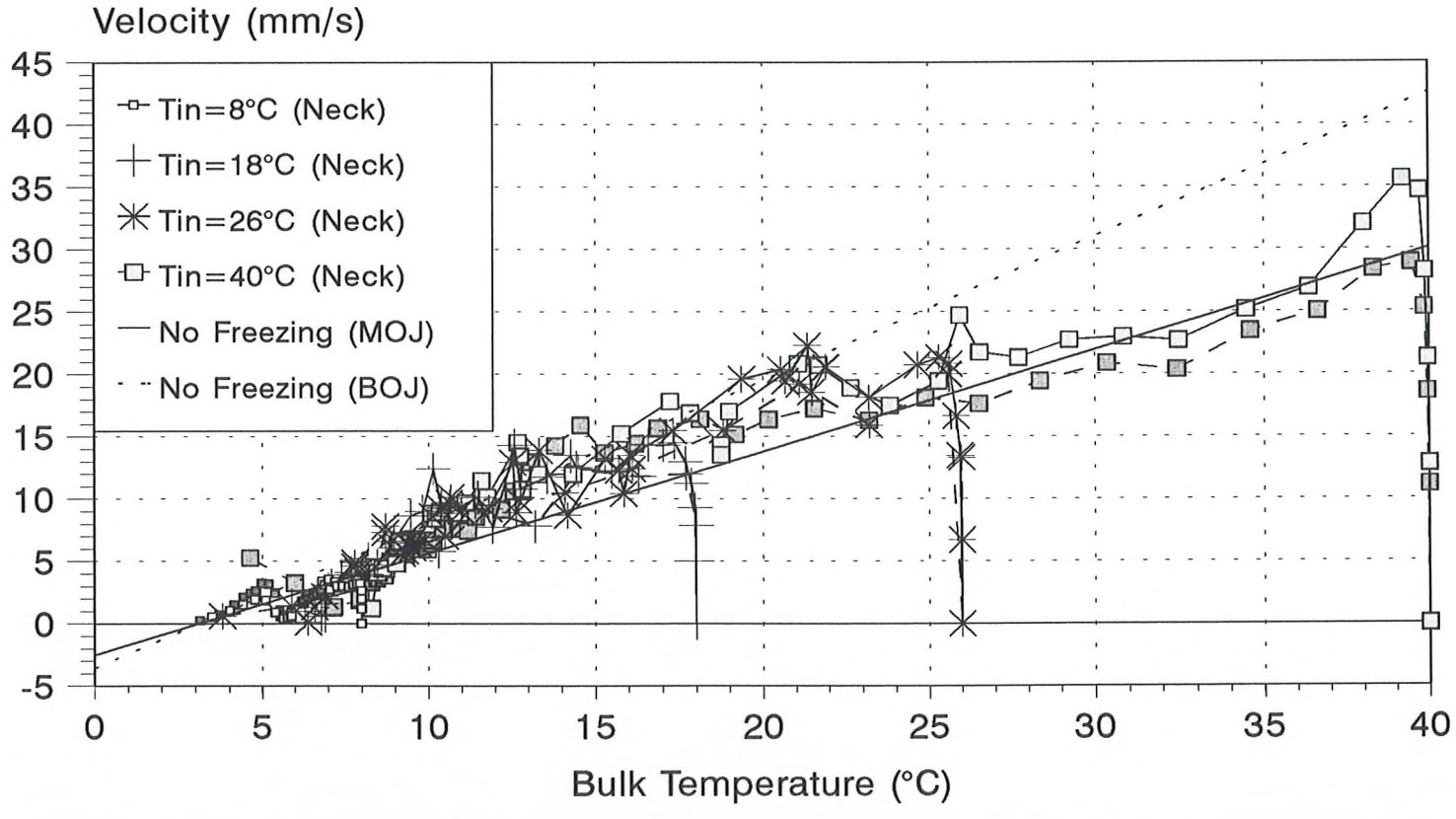

Solid line : 'Long' domain (L=1022mm); Dashed Line : 'Short' domain (L=654mm)
(MOJ:Middle of jacket; BOJ:Bottom of Jacket)

Figure 6.16

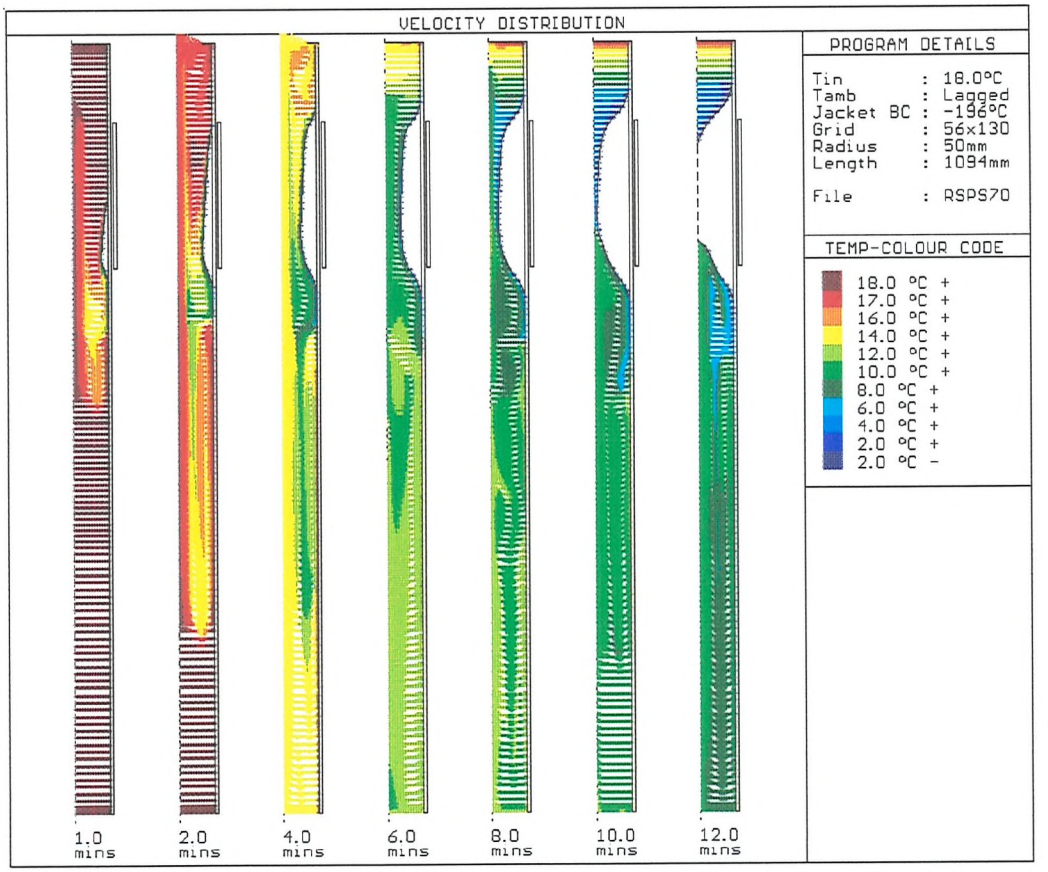

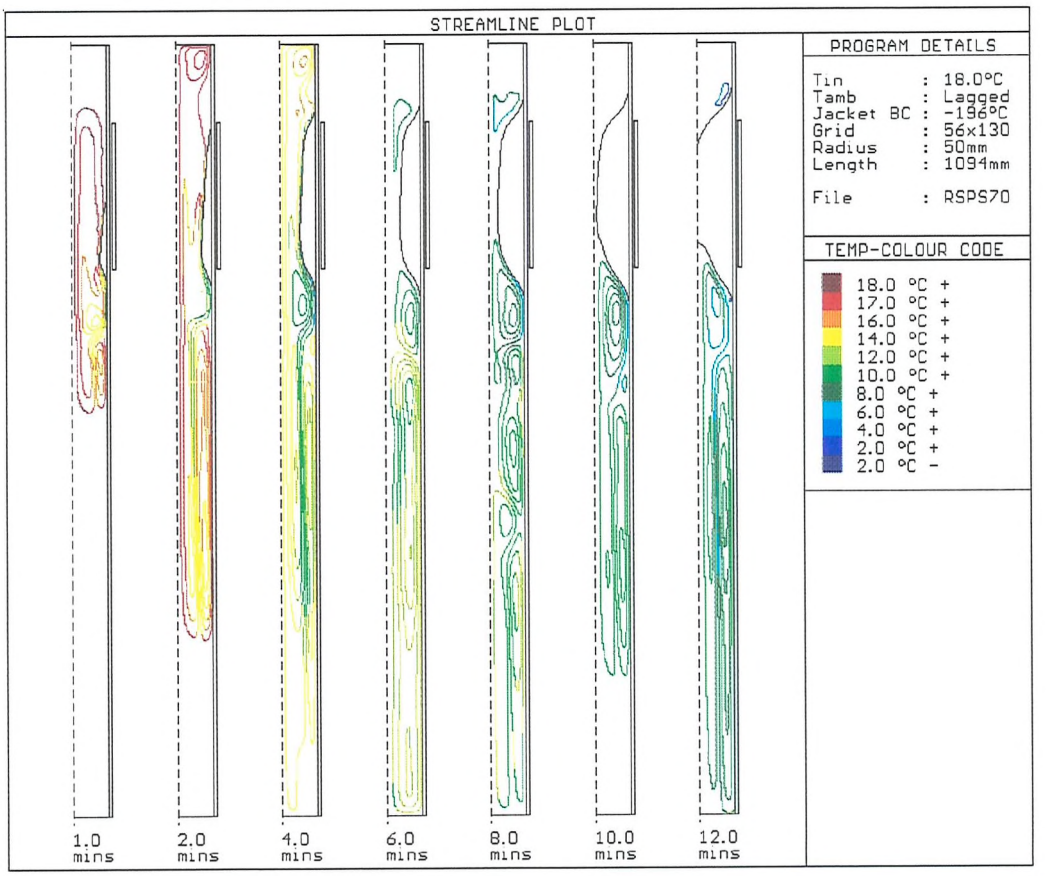

Figure 6.17a: Results from 18°C freeze; 'Long' domain; -196°C jacket BC

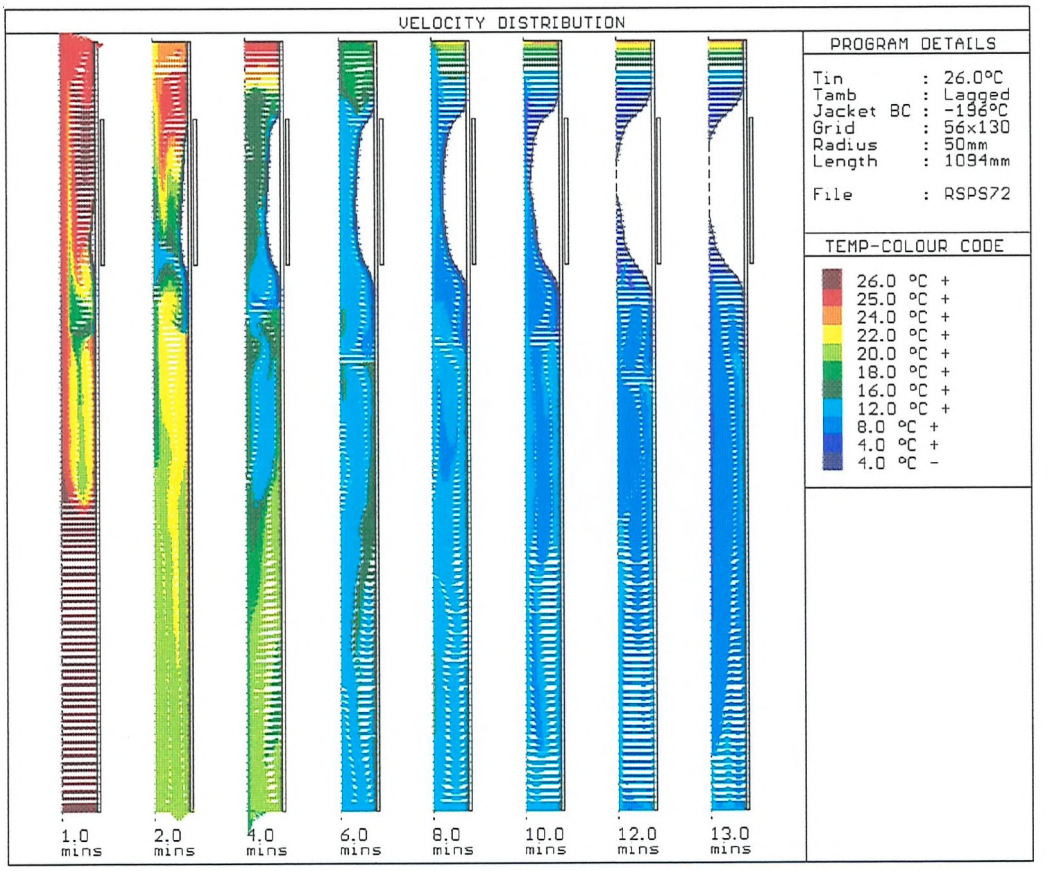

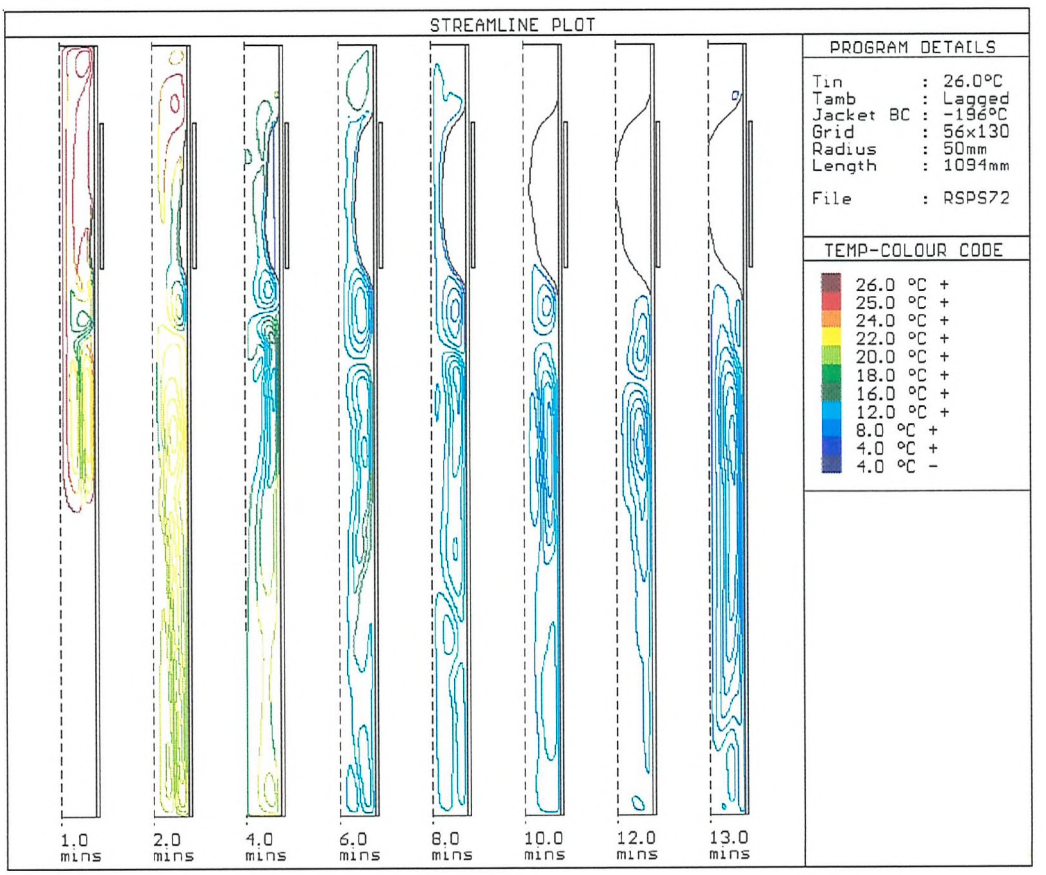

Figure 6.17b: Results from 26°C freeze; 'Long' domain; -196°C jacket BC

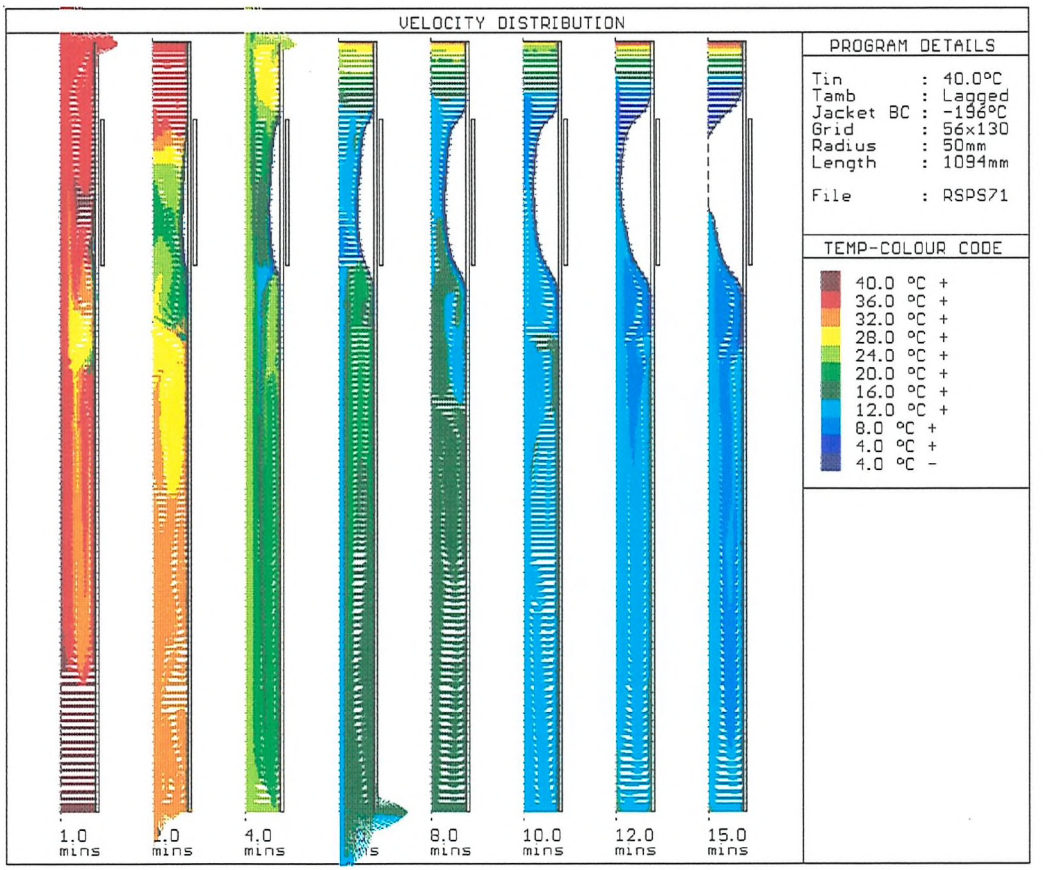

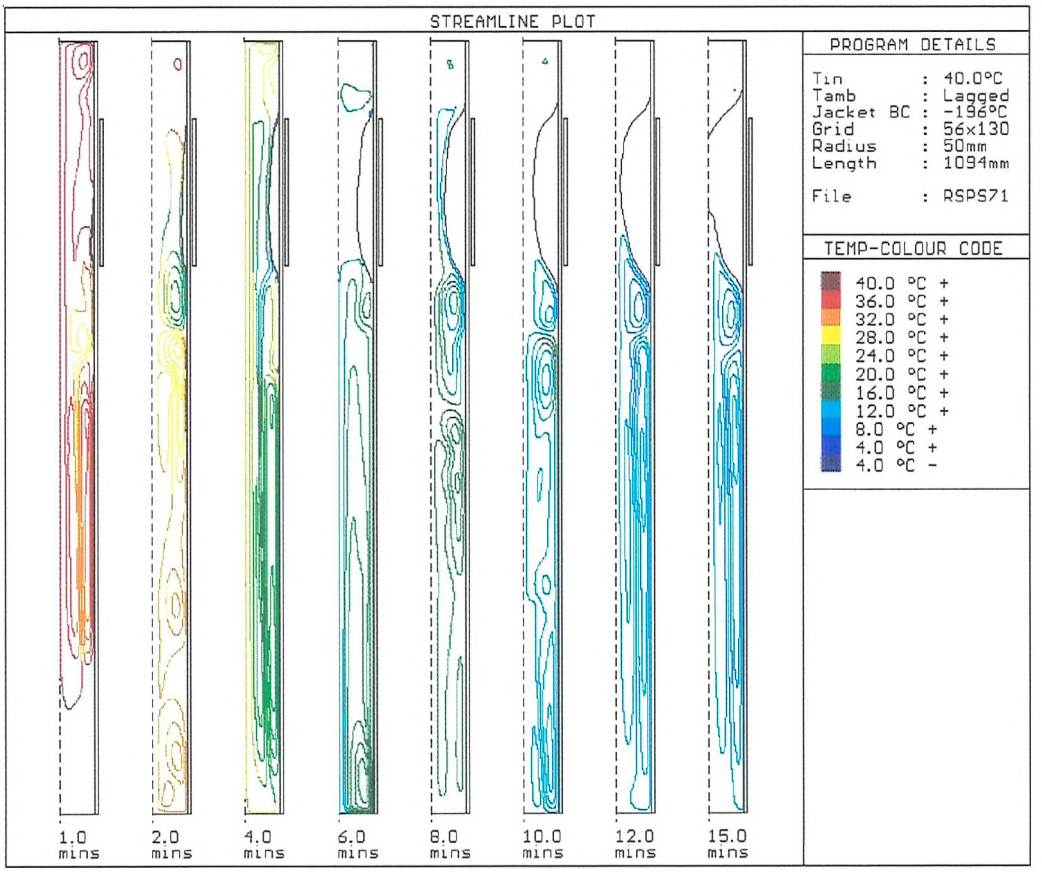

Figure 6.17c: Results from 40°C freeze; 'Long' domain; -196°C jacket BC

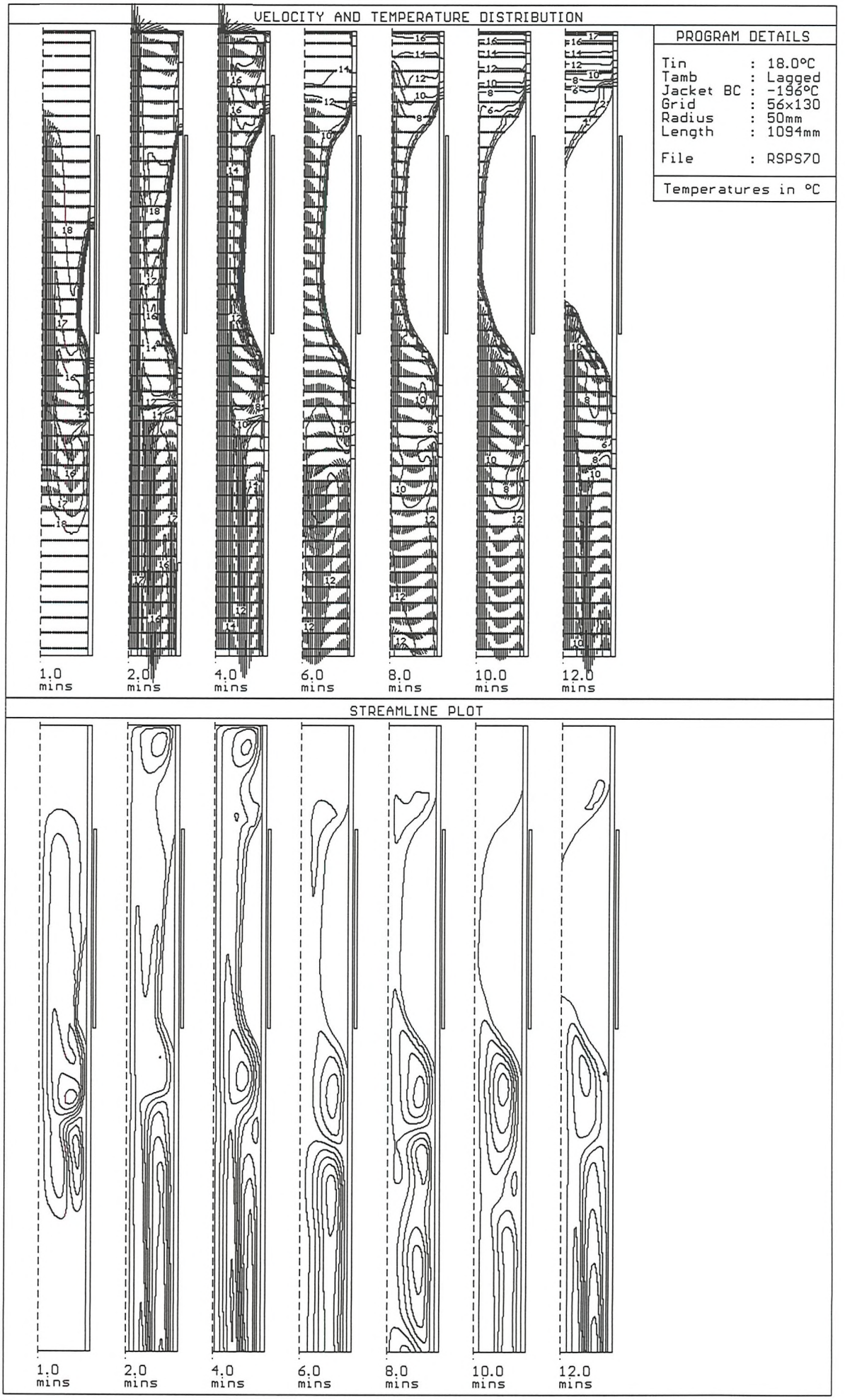

Figure 6.18a: Results from 18°C freeze; 'Long' pipe; -196°C jacket BC; Zoom on 'short' pipe domain

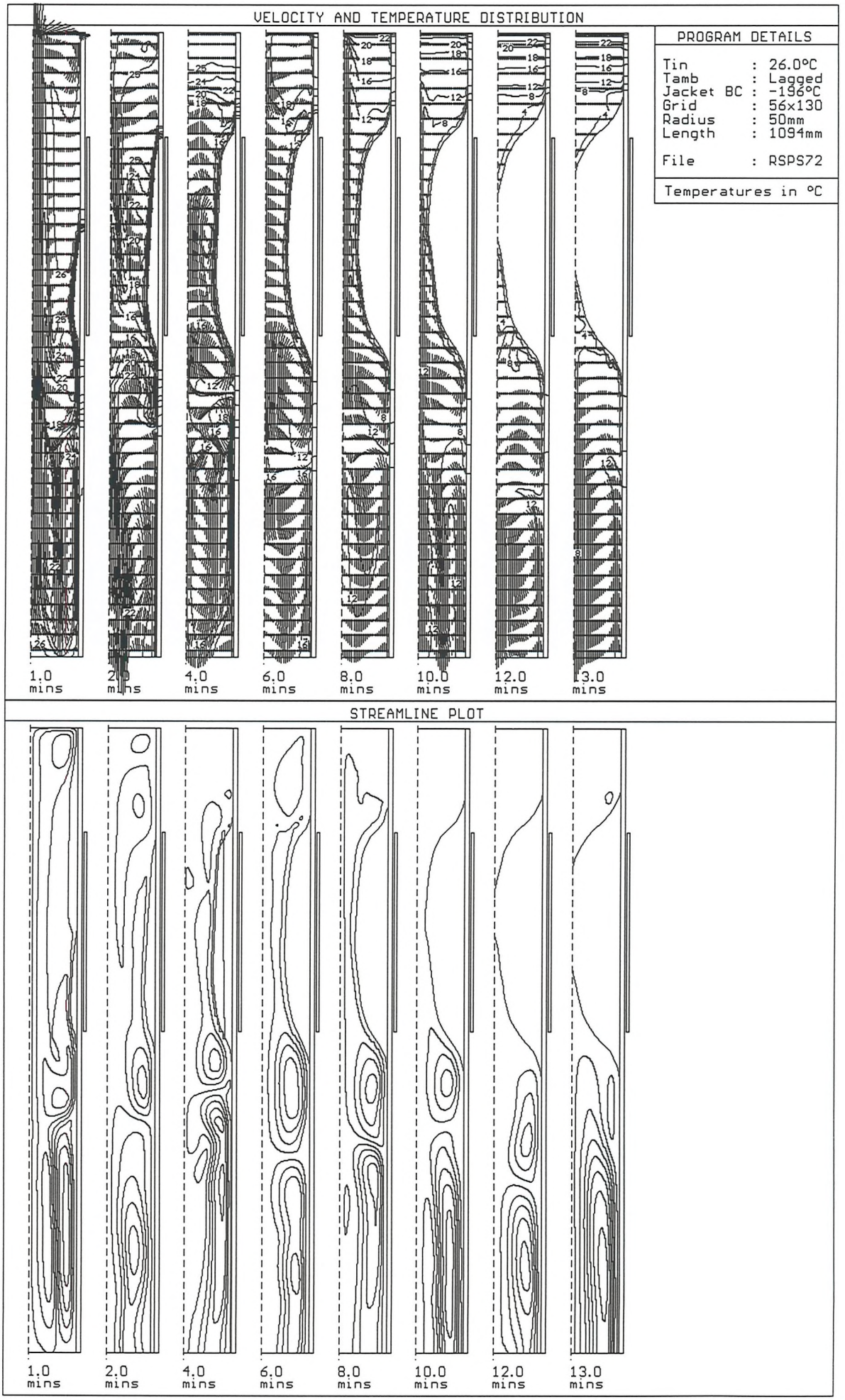

Figure 6.18b: Results from 26°C freeze; 'Long' pipe; -196°C jacket BC; Zoom on 'short' pipe domain

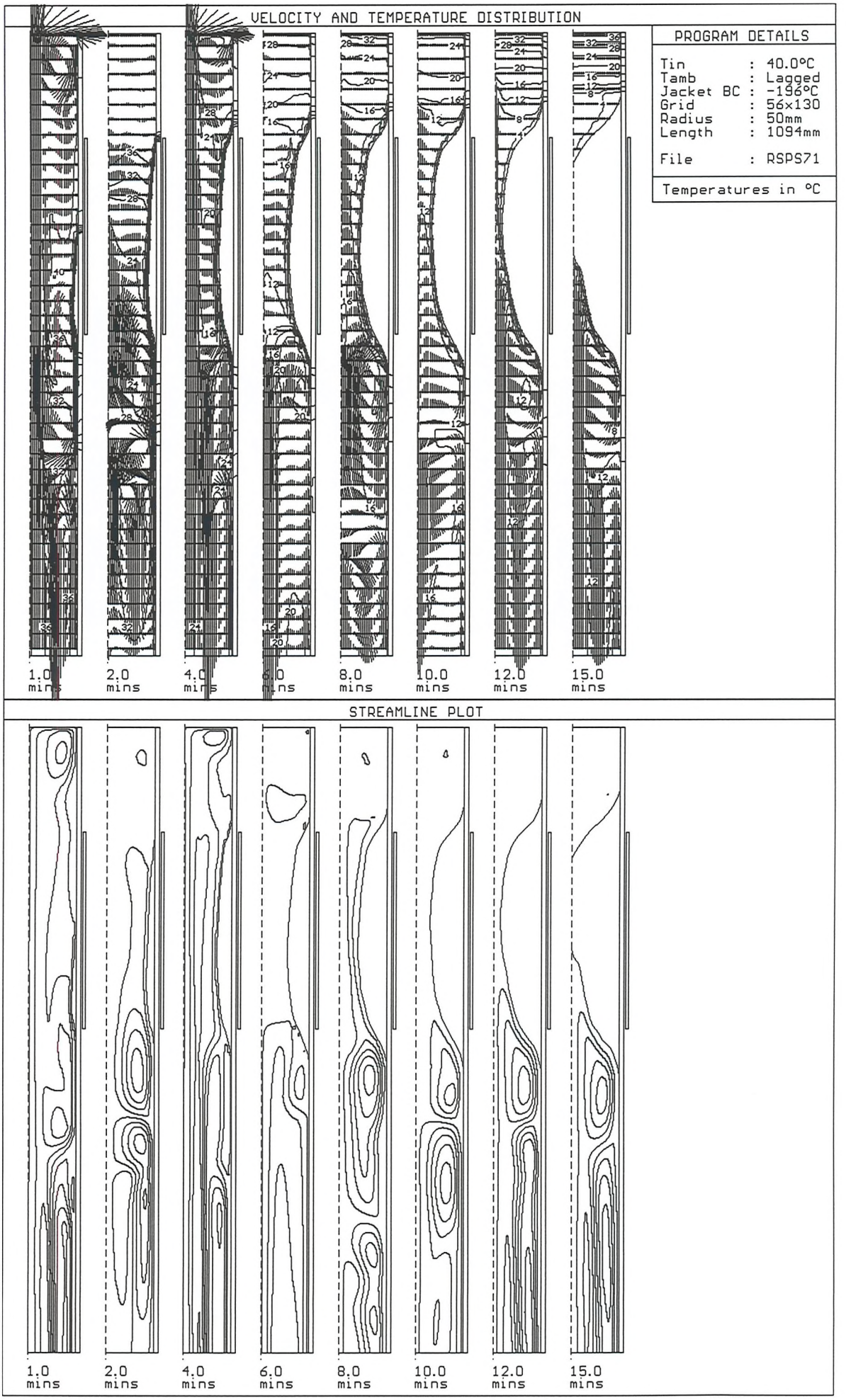

Figure 6.18c: Results from 40°C freeze; 'Long' pipe; -196°C jacket BC; Zoom on 'short' pipe domain

Relationship between Plug Neck Radius and Bulk Water Temperature

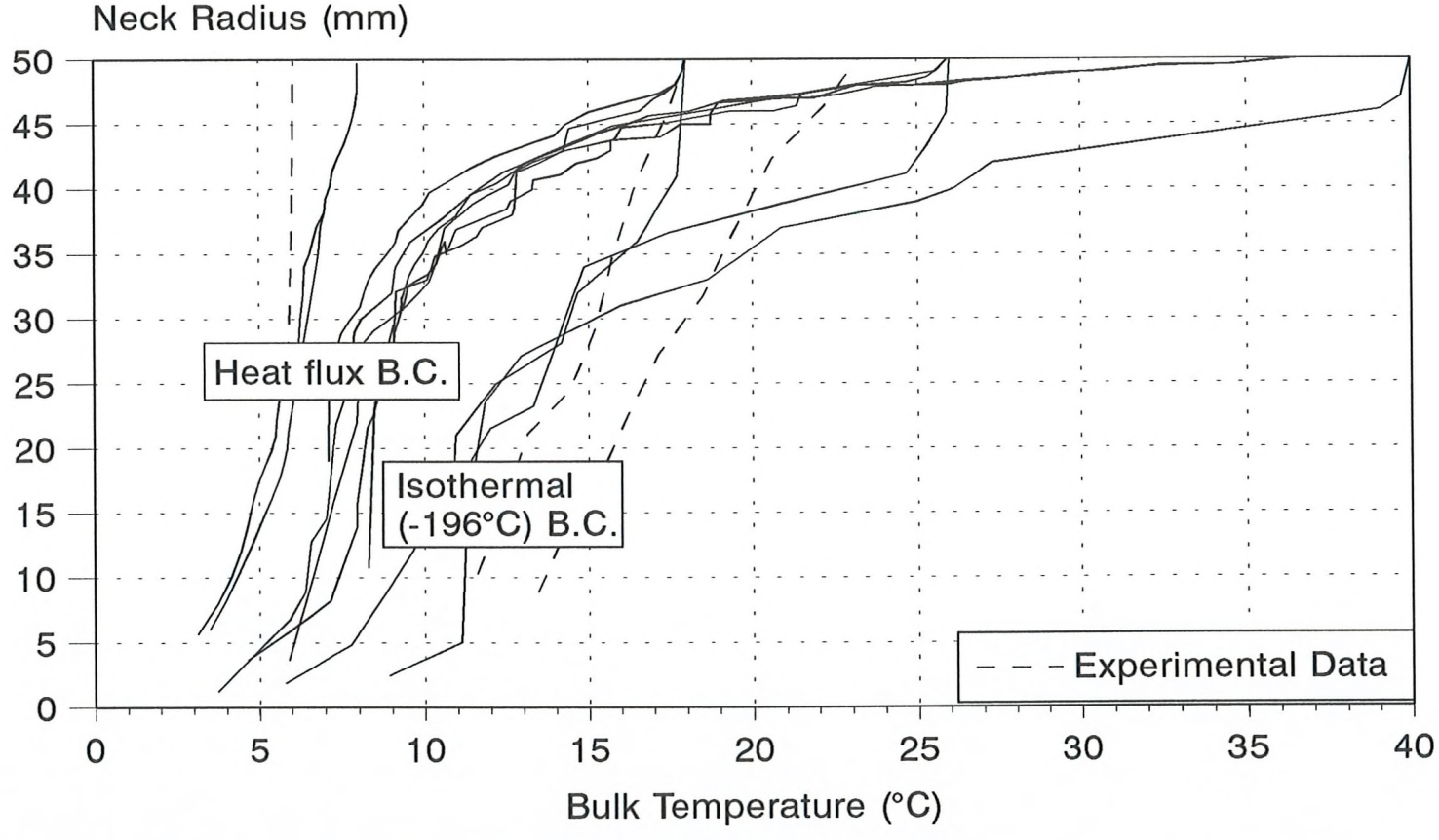

Tbulk evaluated away from ice; Measurements from Tavner[5]

Figure 6.19

Predicted Boundary Layer Velocities During Freezing Isothermal Jacket Boundary Condition

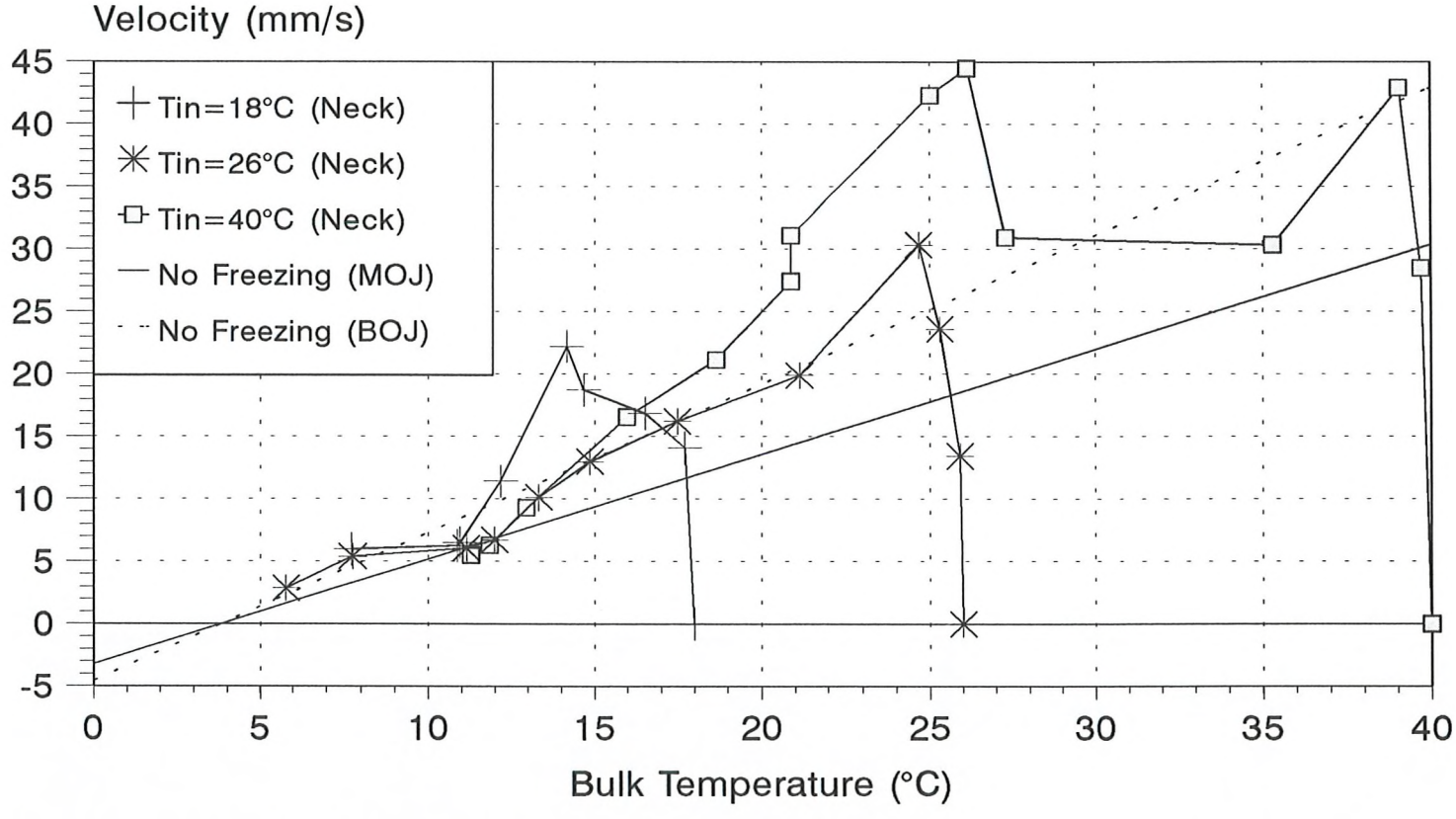

'Long' domain (L=1022mm)
(MOJ:Middle of jacket; BOJ:Bottom of jacket)

Figure 6.20

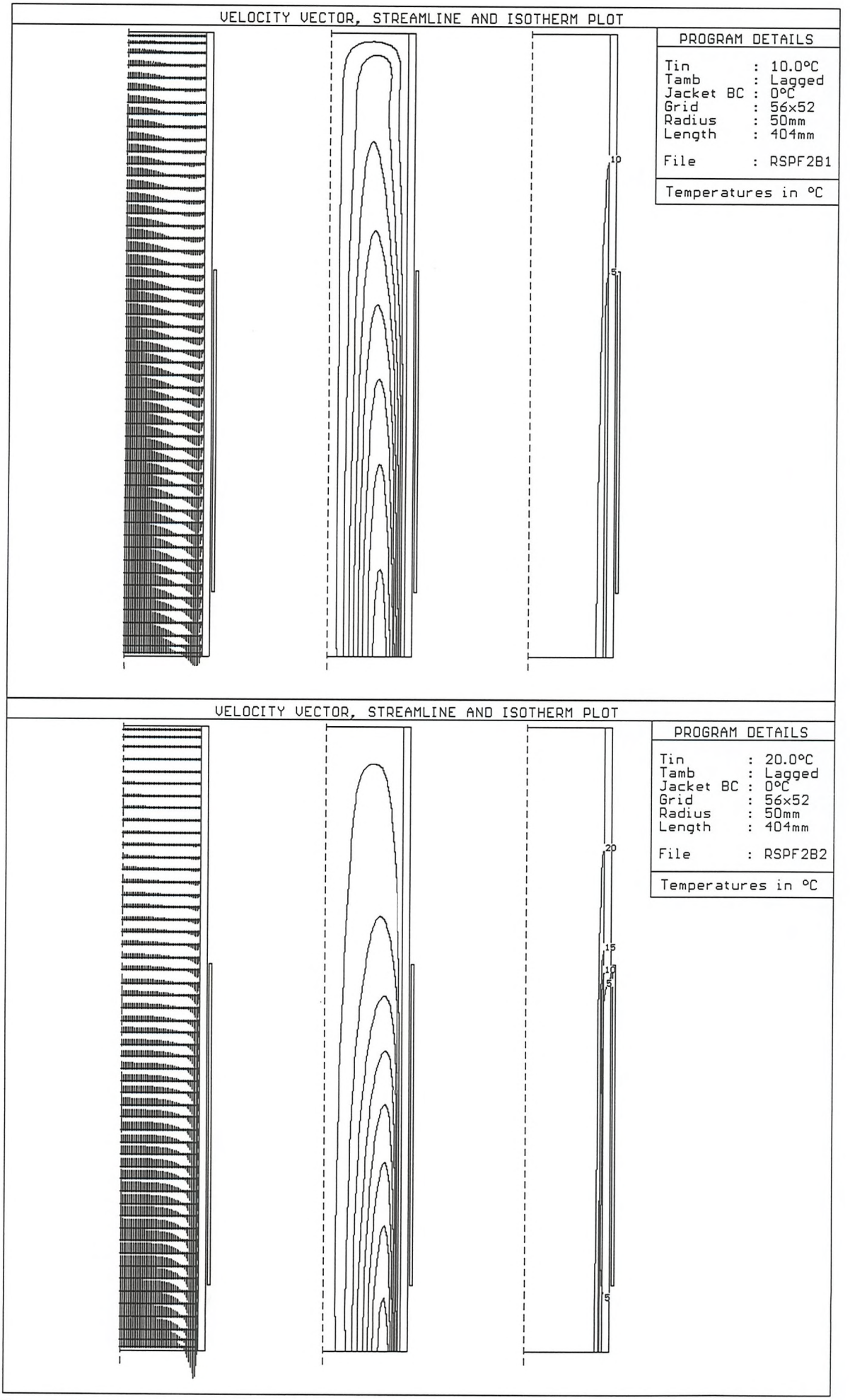

Figure 6.21a: Steady state convection; 0°C cooled wall; Bulk temps: 10°C (top), 20°C (bottom); Open pipe model

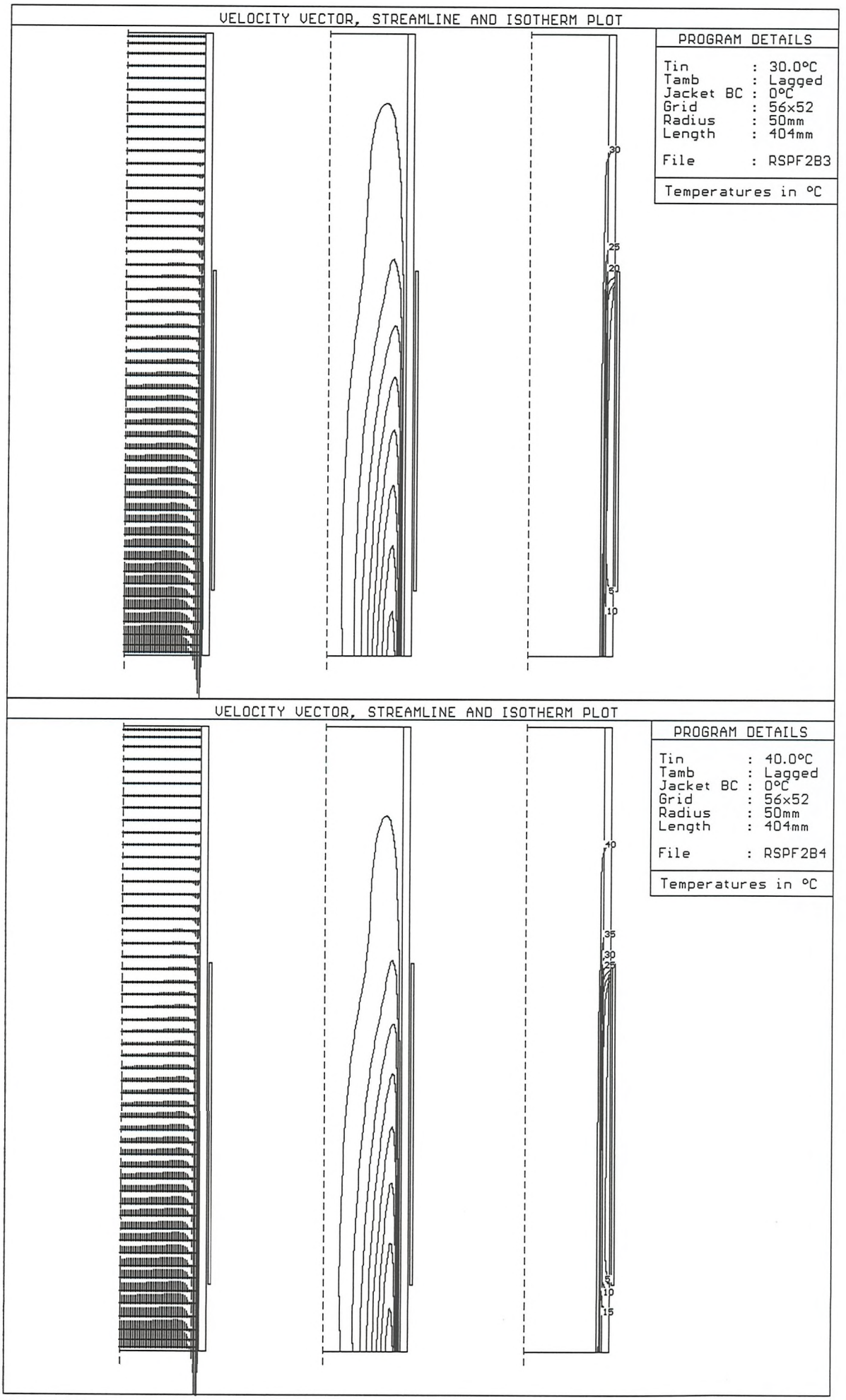

Figure 6.21b: Steady state convection; 0°C cooled wall; Bulk temps: 30°C (top), 40°C (bottom); Open pipe model

Predicted Boundary Layer Velocity
Closed and Open Pipe Models

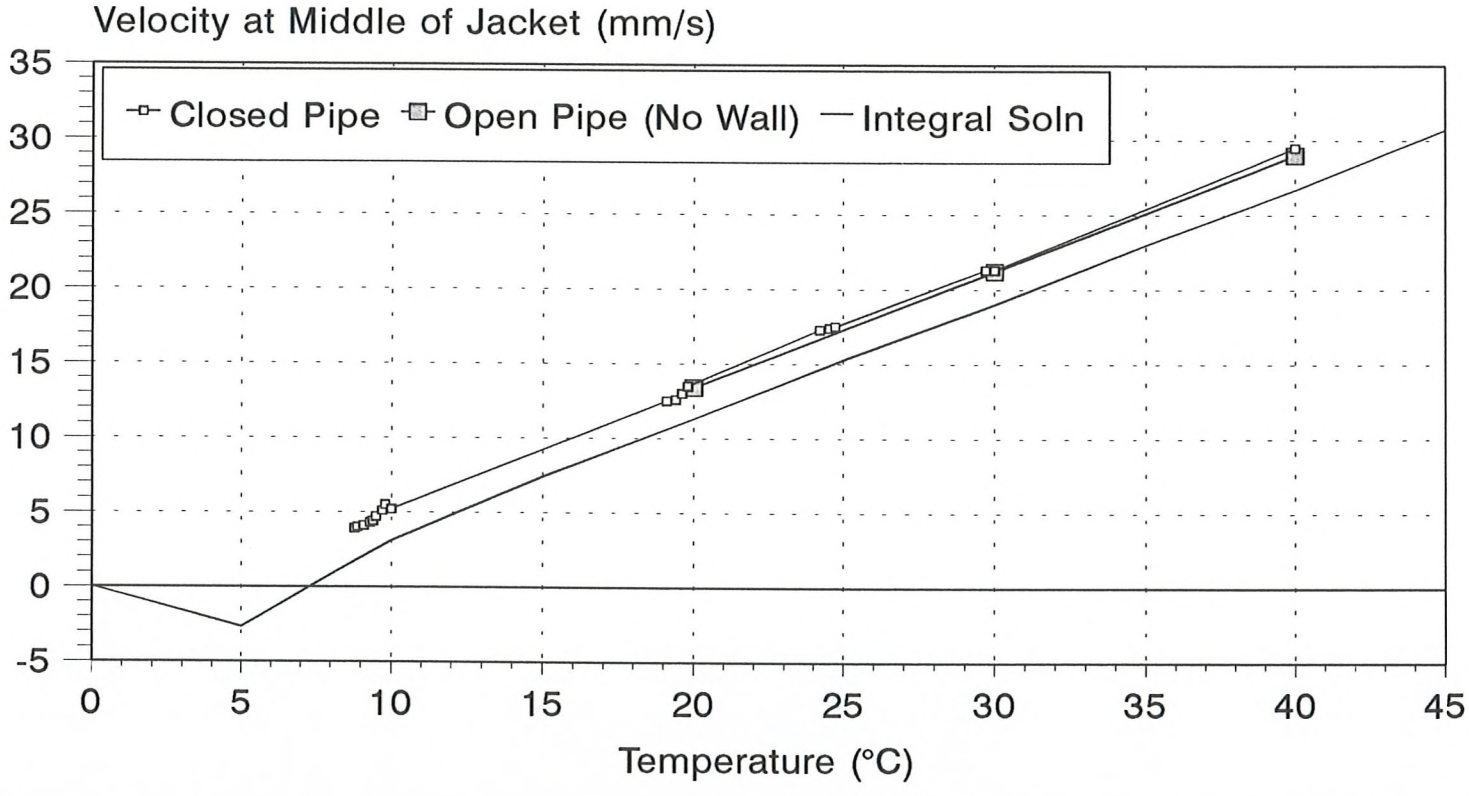

Radius 50mm; convection - no solidification; no wall; Twall=0°C in 'Jacket' (0.2m long)
Integral soln from Bejan[29] (velocities evaluated at $\frac{1}{2}T_b$)
- Predicted velocities extracted before flow reached bottom of domain -

Figure 6.22

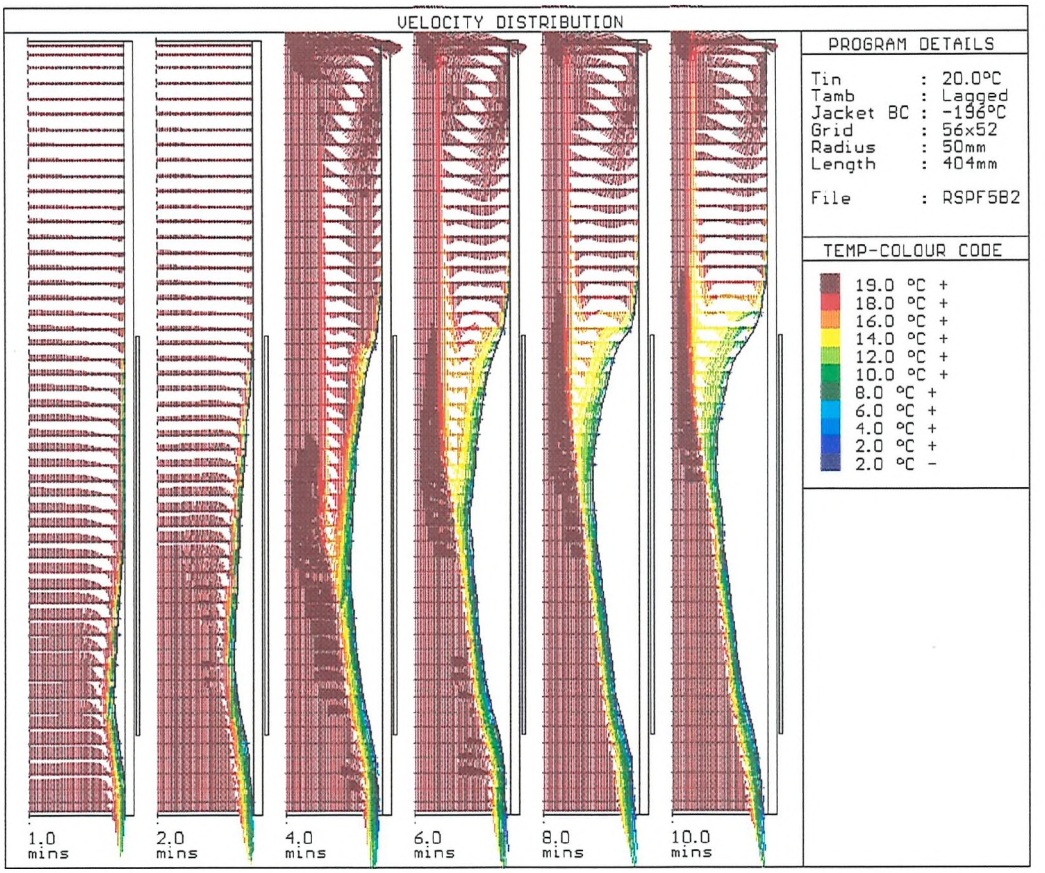

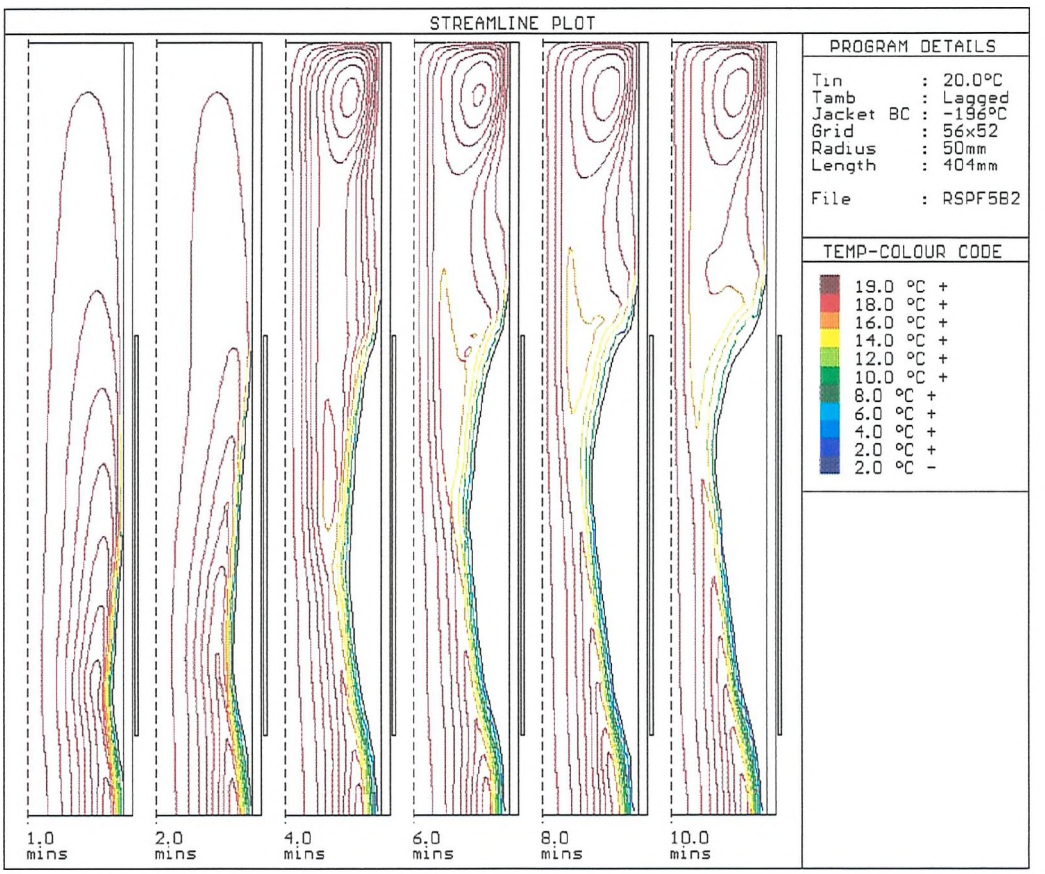

Figure 6.23a: Flow development with freezing (1..10mins); Open bottom domain; -196°C jacket BC; Tin=20°C

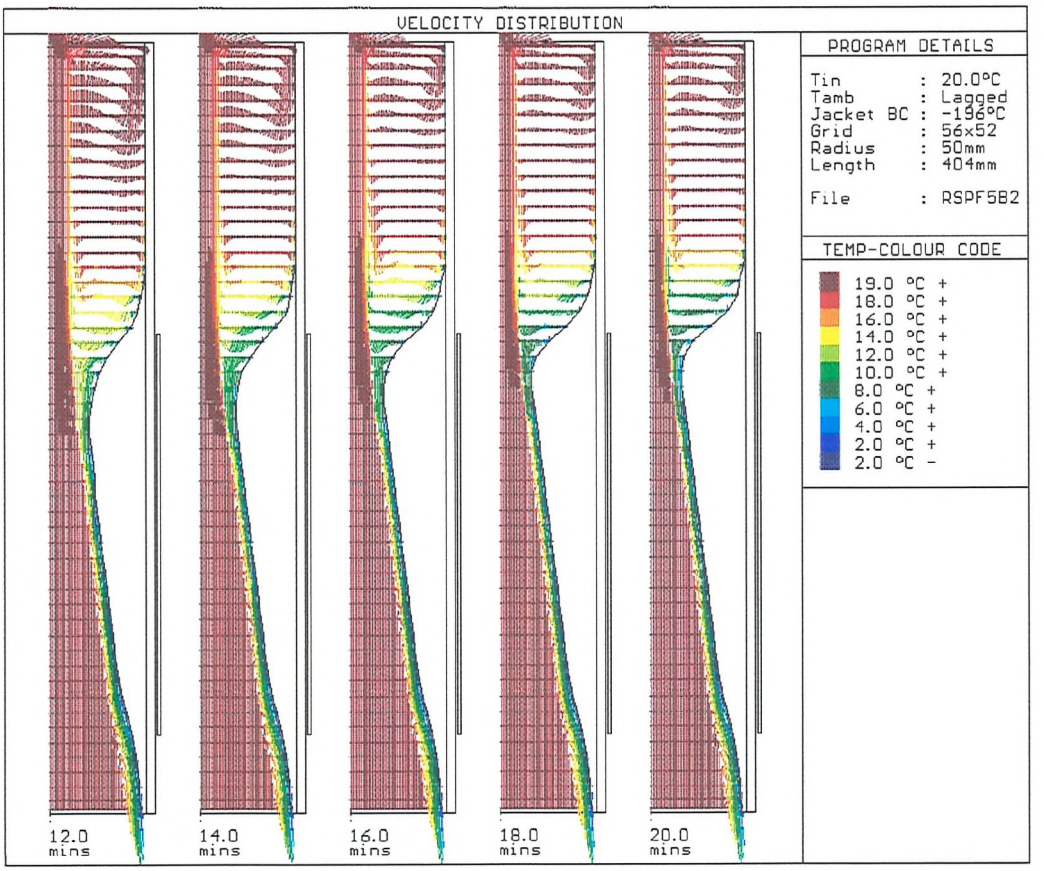

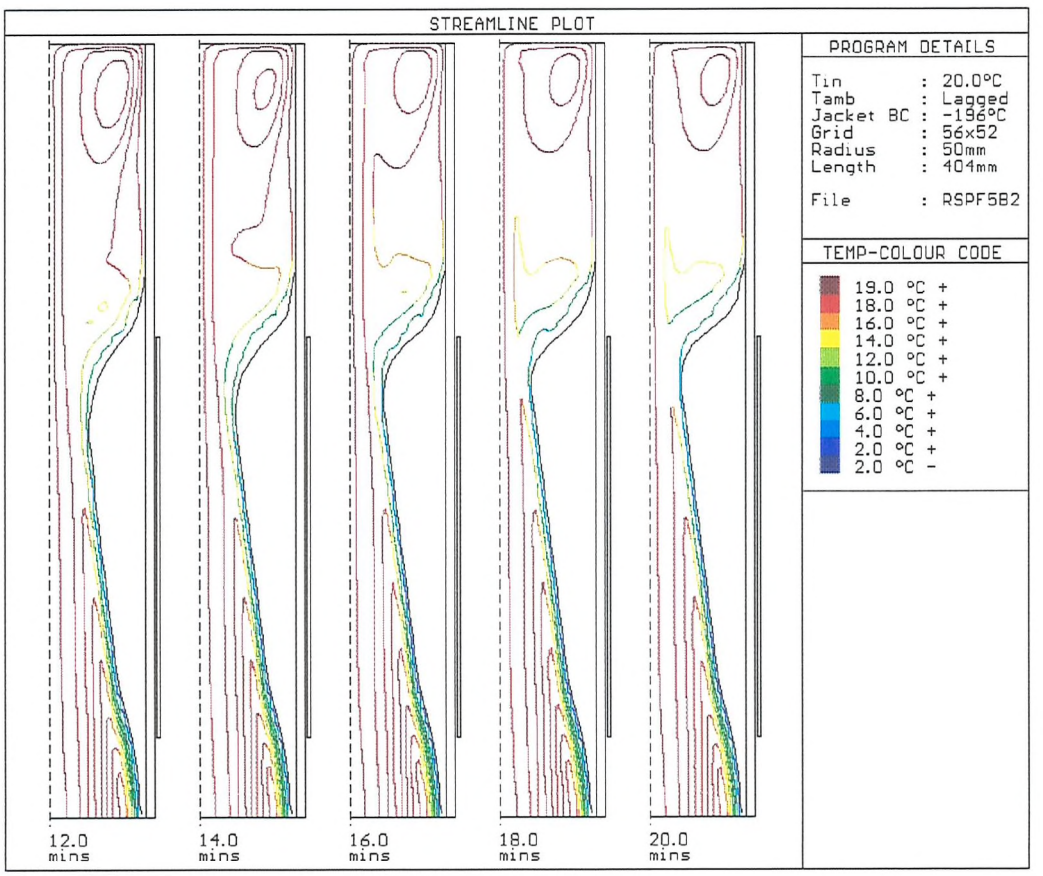

Figure 6.23b: Flow development with freezing (12..20mins); Open bottom domain; -196°C jacket BC; Tin=20°C

Effect of Natural Convection on Pipe Freezing
Selection of Appropriate Model Type

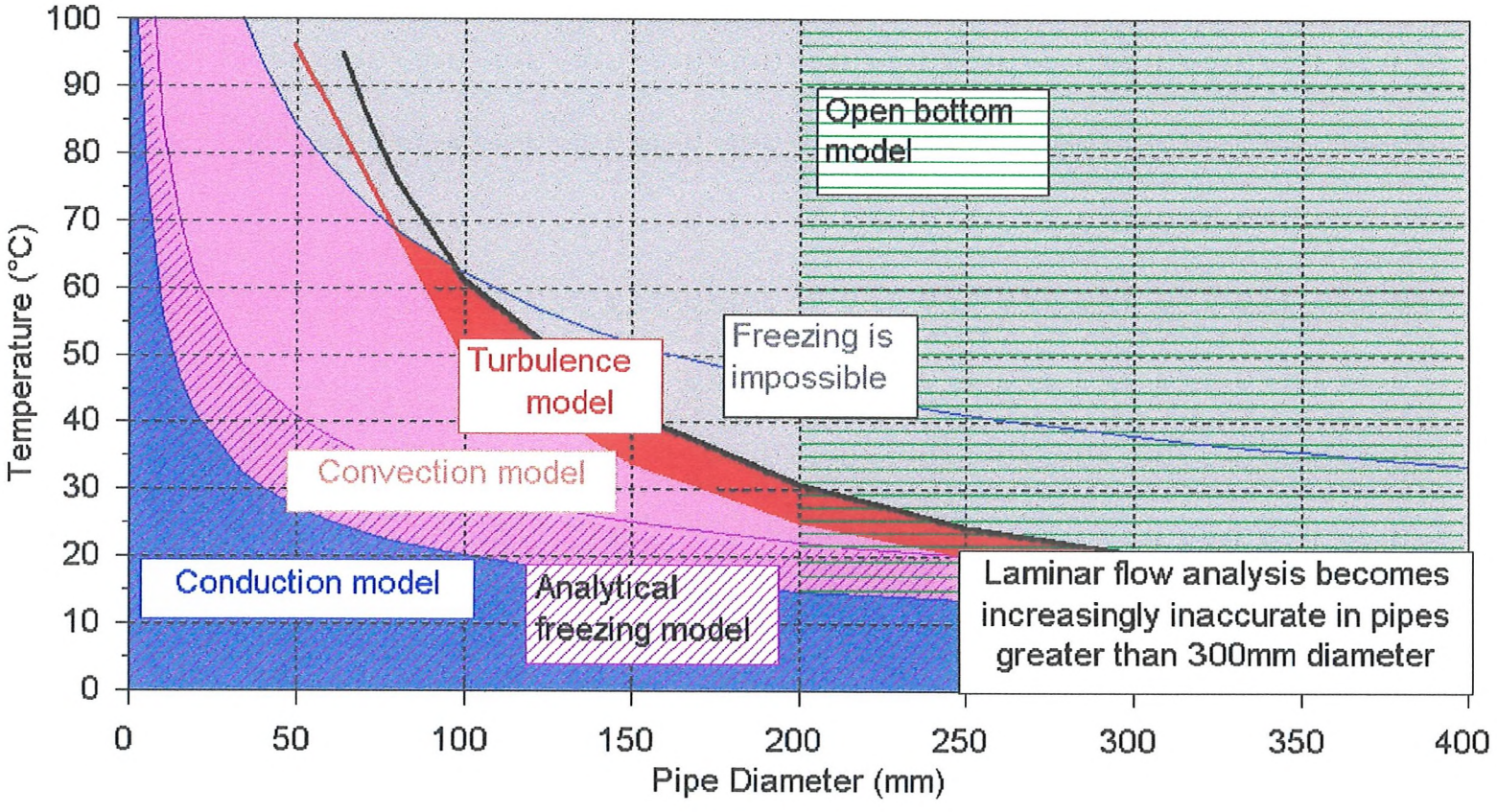

Jacket length=2xdia.; T_c =-196°C; h_c=BIG; see 6.4 for details on model selection

Figure 6.24

APPENDIX I
ANALYTICAL SOLUTION FOR BOUNDARY LAYER THICKNESS AND VELOCITY

Bejan[29] analysed the buoyancy driven flow over a heated vertical flat plate in a semi-infinite medium using both scale and integral analysis methods. The fluid was assumed to have constant properties and the flow was assumed laminar. This produced useful relationships for the velocity and boundary layer thickness in terms of the driving temperature difference, length of heated wall and the fluid properties. These relationships are used throughout this work and the derivation is therefore described in the following sections.

A1.1 SCALE ANALYSIS

In the boundary layer, the governing momentum and energy equations can be simplified to equation I.1.

$$u\frac{\partial v}{\partial x}+w\frac{\partial w}{\partial z}=\nu\frac{\partial^2 w}{\partial x^2}+g\beta(T-T_\infty)$$
$$u\frac{\partial T}{\partial x}+w\frac{\partial T}{\partial z}=\alpha\frac{\partial^2 T}{\partial x^2} \qquad \textbf{(I.1)}$$

In the thermal boundary layer, thickness δ_T (varies with z) and length H, the energy equation can be approximated to give the following balance (~ implies 'of the order of').

$$\underbrace{u\frac{\Delta T}{\delta_T},\ \frac{\Delta T}{H}}_{convection} \sim \underbrace{\alpha\frac{\Delta T}{\delta_T^2}}_{conduction} \qquad \textbf{(I.2)}$$

Mass conservation in the thermal boundary layer gives :

$$\frac{u}{\delta_T} \sim \frac{w}{H} \qquad \textbf{(I.3)}$$

From equations I.2 and I.3, it can be seen that both convection terms in equation I.1 are of order $w\Delta T/H$ and therefore the relationship between w and δ_T is given in equation I.4.

$$w \sim \frac{\alpha H}{\delta_T^2} \tag{I.4}$$

The momentum equation is governed by the inertia, friction and buoyancy forces in the thermal boundary layer, as shown in equation I.5.

$$\underbrace{u\frac{w}{\delta_T},\ w\frac{w}{H}}_{Inertia} \quad or \quad \underbrace{\frac{\nu w}{\delta_T^2}}_{Friction} \sim \underbrace{g\beta\Delta T}_{Buoyancy} \tag{I.5}$$

From mass conservation, the two inertia terms are of order w^2/H and $w \sim \alpha H/\delta_T^2$. Dividing equation I.5 by $g\beta\Delta T$ and substituting for w, gives the following balance.

$$\underbrace{\left(\frac{H}{\delta_T}\right)^4 Ra_H^{-1} Pr^{-1}}_{Inertia} \quad \underbrace{\left(\frac{H}{\delta_T}\right)^4 Ra_H^{-1}}_{Friction} \quad \underbrace{1}_{Buoyancy} \tag{I.6}$$

$$Ra_H = \frac{g\beta\,\Delta T\,H^3}{\alpha\nu}$$

The balance between inertia and friction is therefore decided by the Prandtl number: if the Prandtl number is high, the thermal boundary layer will be controlled by the friction-buoyancy balance whereas at low Prandtl number the inertia-buoyancy balance is important.

The Prandtl number of water varies between 13.4 at 0°C and 3.6 at 50°C, considerably greater than unity. The flow is therefore controlled by the friction-buoyancy balance, thus :

$$\delta_T \sim H\,Ra_H^{-0.25}$$
$$w \sim \frac{\alpha}{H} Ra_H^{0.5} \tag{I.7}$$

In addition to the thermal boundary layer, an extra (outer) layer of fluid is entrained by the viscous action by the thermal boundary layer; this layer is unheated and restrained by its inertia. The total velocity boundary layer thickness is δ_v.

$$w\frac{w}{H} \sim \nu\frac{w}{\delta_v^2} \qquad \therefore \quad \delta_v \sim H\, Ra_H^{-0.25} Pr^{0.5} \tag{I.8}$$

Thus, the ratio of velocity to thermal boundary layer thickness is of the order of ($\sqrt{Pr}$): the higher the Prandtl number, the larger the layer of entrained fluid.

A1.2 INTEGRAL ANALYSIS

The governing momentum and energy equations in the boundary layer are integrated from the wall (x=0) to a point (x=X) sufficiently far from the wall in the stagnant isothermal cold reservoir, to give equations I.9 and I.10.

$$\frac{d}{dz}\int_0^X w^2 dx = -\nu\left(\frac{\partial w}{\partial x}\right)_{x=0} + g\beta\int_0^X (T-T_\infty)\,dx \tag{I.9}$$

$$\frac{d}{dz}\int_0^X w(T_\infty - T)\,dx = \alpha\left(\frac{\partial T}{\partial x}\right)_{x=0} \tag{I.10}$$

The velocity and temperature distributions are *assumed* (note that V is a characteristic value of velocity and neither the maximum nor the average).

$$T-T_\infty = \Delta T\, e^{-x/\delta_T} \qquad \Delta T = T_o - T_\infty$$
$$w = V\, e^{-x/\delta_v}\,(1-e^{-x/\delta_T}) \tag{I.11}$$
$$V,\ \delta_v,\ \delta_T = f(z)\ (\textit{unknown})$$

A third equation is required to determine the three unknowns (V, δ_v, δ_T)[11]. Bejan suggests making use of the fact that the inertia terms are zero next to the wall, giving equation I.12.

[11] The established results obtained through integral analysis by Squire[66] assumed that the thermal and velocity boundary layer thicknesses were equal.

$$0 = \nu\frac{\partial^2 w}{\partial x^2} + g\beta(T_o - T_\infty) \tag{I.12}$$

The three equations can be solved for V, δ_v and δ_T, making use of the relationships $\delta \sim z^{1/4}$, $V \sim z^{1/2}$ (equation I.7-I.8).

The ratio δ_v/δ_T (=q) can be obtained by solving equation I.13.

$$Pr = \frac{5}{6}q^2\frac{q+\frac{1}{2}}{q+2} \qquad q = \frac{\delta_v}{\delta_T} \tag{I.13}$$

The equations for the boundary layer thicknesses, δ_v and δ_T and the velocity, V, are given by equation I.14.

$$\begin{aligned}
\delta_v(z) &= f_{\delta_v} Ra_z^{-0.25} Pr^{0.5} z \qquad f_{\delta_v} = \left(\frac{96(q+1)(q+2)^3}{25\ q^3(q+0.5)}\right)^{0.25} \\
\delta_T(z) &= f_{\delta_T} Ra_z^{-0.25} z \qquad f_{\delta_T} = \left(\frac{8(q+0.5)(q+1)(q+2)}{3q^3}\right)^{0.25} \\
V(z) &= f_v \frac{\alpha}{z} Ra_z^{0.5} \qquad f_v = \left(\frac{8(q+0.5)(q+1)}{3q(q+2)}\right)^{0.5}
\end{aligned} \tag{I.14}$$

The relationship between the characteristic velocity, V, and the maximum boundary layer velocity V_{max} is given in equation I.15.

$$V_{max} = V\ q\ (1+q)^{-(1+\frac{1}{q})} \tag{I.15}$$

The heat transfer coefficient at the cooled wall is defined by equation I.16 and increases with the length, z, raised to the power -0.25.

$$\begin{aligned}
h(z) &= \frac{k_l}{\Delta T}\frac{dT}{dx}\Big|_{x=0} \\
&= \frac{k_l}{\delta_T} \\
&= \frac{k_l\ Ra^{0.25}}{f_{\delta_T} z}
\end{aligned} \tag{I.16}$$

A1.3 PREDICTED VALUES FOR CONVECTION IN WATER

Equations I.14-I.16 were used to calculate the boundary layer thickness and velocities for various values of temperature difference. The wall temperature was assumed to be at 0°C and the water at 0°C, 10°C, 20°C, 30°C, 40°C and 50°C. The fluid properties were evaluated half-way between the water and the wall temperature. The cooled wall was 200mm long (equivalent to the length of a 2D jacket in 100mm (4") pipe).

ΔT (°C)	Pr	q	V_{max} (mm/s)	δ_v (mm)	δ_T (mm)	h (W/m²K)
0	13.4	4.6	0	0	0	-
10	11.2	4.2	3.1	12.4	3.0	192
20	9.5	3.9	11.3	6.1	1.6	370
30	8.1	3.6	19.0	4.2	1.2	484
40	7.0	3.4	26.7	3.5	1.0	580
50	6.1	3.2	35.1	2.9	0.9	671

A spreadsheet was set up which stored the properties of water and calculated the values of boundary layer thickness, velocity and heat transfer coefficient for given cooled wall lengths. An example of this (H=0.1m) is shown on the following page.

In order to manipulate the heat transfer coefficient more readily, an approximate relationship in terms of the length, z, and the bulk temperature was obtained. The length appears in the definition of h as ($z^{-0.25}$); a least squares regression was carried out to find the values of the two constants A and B for which ($h=AT_b^B z^{-0.25}$) for bulk temperatures from 10°C to 100°C. (The best fit line for the equation log ($h\ z^{0.25}$) = log A + B log T_b was found.) The resulting relationship is given in equation I.17; the two sets of data are plotted in figure I.1.

$$h(z) = 25.880\ T_b^{0.680} z^{-0.25} \qquad \textbf{(I.17)}$$

Example Spreadsheet : Bejan's Analytical Solution at z=0.1m

dT(=2Twork)	ß*1E6	dens	μ*1E3	k	c*1E-3	H	Rax1e-9	Gr	Pr	q	dv	dt	h (W/m²K)	wmax (mm/s)
0	-52	999.868	1.787	0.561	4.2177	0.1	0	0	13.43499	4.570685	ERR	ERR	ERR	0
5	-23.75	999.969	1.645	0.565	4.21	0.1	-0.00528	-0.00043	12.25743	4.384716	13.88921	3.167642	178.36609	2.706584
10	15	999.985	1.52	0.57	4.2022	0.1	0.007137	0.000637	11.20587	4.21058	12.44441	2.955511	192.86008	3.130275
15	52.5	999.895	1.408	0.575	4.1972	0.1	0.040042	0.003896	10.27767	4.04962	7.824505	1.932158	297.59475	7.371193
20	87.53	999.718	1.307	0.579	4.1922	0.1	0.095082	0.010048	9.463222	3.901979	6.110025	1.565878	369.76049	11.27837
25	122.57	999.458	1.219	0.584	4.189	0.1	0.176692	0.020208	8.74382	3.765905	5.080559	1.349094	432.88317	15.29288
30	150.13	999.12	1.139	0.588	4.1858	0.1	0.275658	0.033997	8.108208	3.640683	4.420198	1.214112	484.30451	18.97706
35	180.24	998.703	1.067	0.593	4.1839	0.1	0.408153	0.054217	7.528198	3.521811	3.898808	1.107046	535.65964	22.97509
40	204.37	998.22	1.002	0.597	4.1819	0.1	0.558638	0.079591	7.018867	3.413364	3.513194	1.029247	580.03588	26.71629
45	230.54	997.678	0.9439	0.601	4.1808	0.1	0.746565	0.113699	6.566152	3.313415	3.189125	0.962489	624.42285	30.70782
50	260.8	997.07	0.8908	0.606	4.1796	0.1	0.984645	0.160265	6.143874	3.216834	2.905167	0.903114	671.01187	35.11999
55	280.9	996.4	0.8422	0.61	4.1791	0.1	1.22402	0.212139	5.769898	3.128309	2.689894	0.859855	709.42153	38.94817
60	301	995.68	0.7975	0.613	4.1785	0.1	1.501259	0.276163	5.43614	3.046686	2.502173	0.821277	746.39861	42.85872
65	321.5	994.9	0.757	0.617	4.1784	0.1	1.815312	0.354104	5.126497	2.968534	2.336905	0.787225	783.76563	46.90423
70	342	994.06	0.7196	0.62	4.1782	0.1	2.173325	0.448163	4.849408	2.896432	2.190631	0.756321	819.75817	51.02431
75	357.31	993.18	0.685	0.624	4.1784	0.1	2.534931	0.55265	4.586865	2.826051	2.06711	0.731448	853.10221	54.86438
80	377.79	992.25	0.6529	0.627	4.1786	0.1	2.979671	0.684791	4.351209	2.761016	1.948977	0.705891	888.23867	59.15963
85	413.1815	991.26	0.6235	0.631	4.1791	0.1	3.59601	0.870825	4.129428	2.698059	1.825974	0.676773	932.36572	64.7388
90	432.4503	990.25	0.5962	0.634	4.1795	0.1	4.139811	1.053303	3.930312	2.639969	1.732931	0.656421	965.84358	69.12115
95	450.9636	989.2	0.5706	0.638	4.1801	0.1	4.722114	1.263103	3.738503	2.582494	1.64822	0.638228	999.64249	73.55911
100	468.7509	988.1	0.5468	0.64	4.1807	0.1	5.363564	1.501606	3.571886	2.531262	1.571833	0.620968	1030.6491	77.94384

Heat Transfer Coefficient
Integral Solution from Bejan[29]

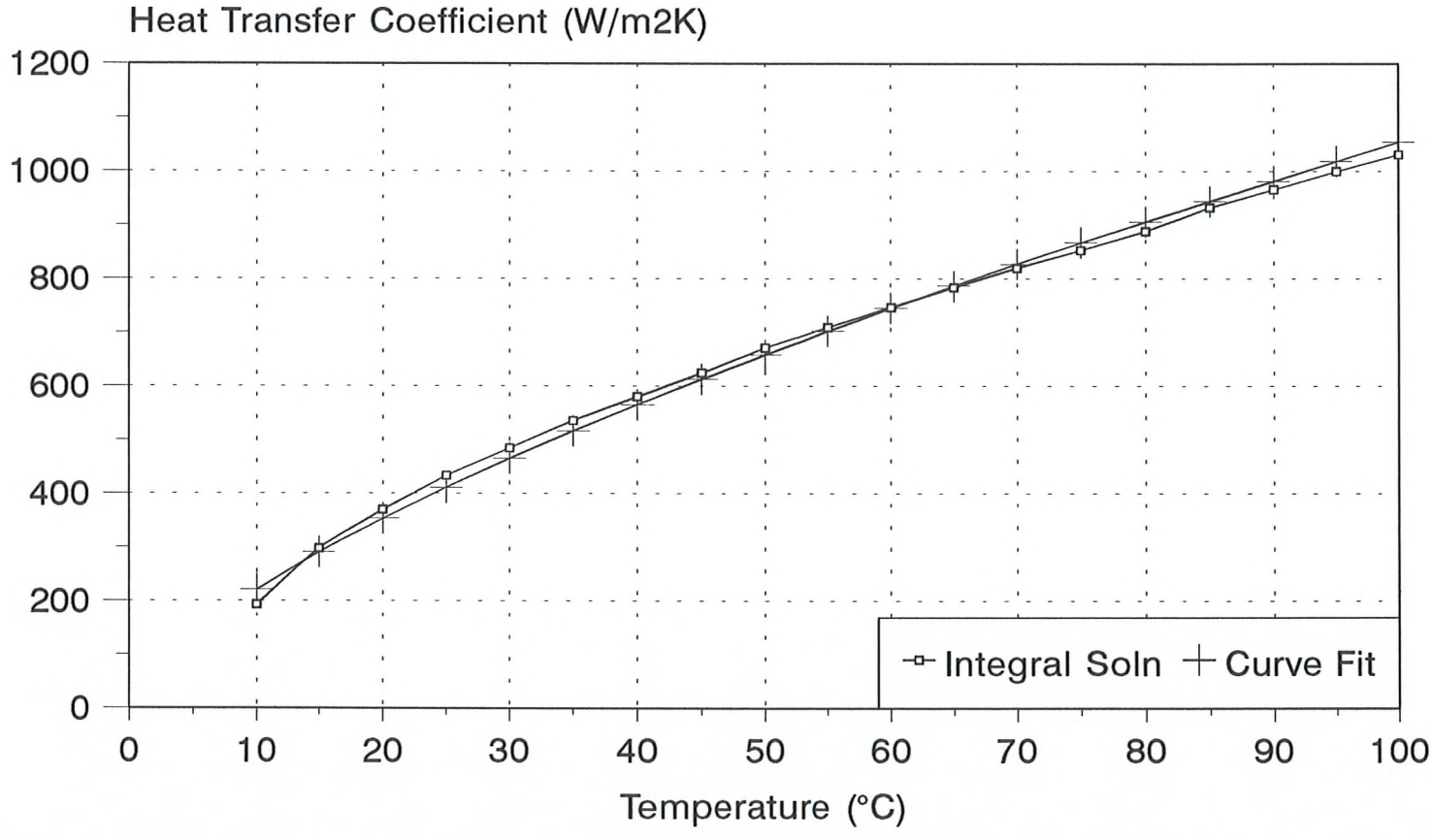

Heat transfer coefficient evaluated for z=0.1m; Curve fit: $h=25.88\ T_b^{0.680}\ z^{-0.25}$ Figure I.1

APPENDIX II
STREAMFUNCTION CALCULATION

In order to produce a streamline plot, the streamfunction distribution must be calculated from the velocity distribution. The relationship between streamfunction, S, and the two components of velocity (in radial co-ordinates) is given in equation II.1 (from Kakaç et al[65]).

$$u = -\frac{1}{r}\frac{\partial S}{\partial z} \qquad w = \frac{1}{r}\frac{\partial S}{\partial r} \tag{II.1}$$

This is manipulated as follows :

$$\nabla^2 S = \frac{1}{r}\frac{\partial}{\partial r}\left(r\frac{\partial S}{\partial r}\right) + \frac{\partial^2 S}{\partial z^2} = \frac{1}{r}\frac{\partial}{\partial r}(r^2 w) + \frac{\partial}{\partial z}(-ru) \tag{II.2}$$

$$\therefore \nabla^2 S = \ldots\ldots\ldots\ldots = i_1 + i_2$$

This gives the same equation as that which describes steady state conduction, formulated in terms of streamfunction rather than temperature and with a source term of $-(i_1+i_2)$. A simple finite volume method can be used to obtain the distribution of streamfunction inside the domain; a grid of control volumes (CVs) is defined, the integrated source term is evaluated for each CV, the boundary conditions are chosen and the equations are solved using an iterative (line-by-line - TDMA) method.

The integrated source term is given in equation II.3.

$$\int_V -(i_1+i_2)dV = -(I_1+I_2)$$

$$I_1 = \int_{r_w}^{r_e}\int_{z_s}^{z_n} \frac{1}{r}\frac{\partial}{\partial r}(r^2 w)\,dr\,dz \approx ([r^2 w]_e - [r^2 w]_w)\Delta z \tag{II.3}$$

$$I_2 = \int_{r_w}^{r_e}\int_{z_s}^{z_n} \frac{\partial}{\partial z}(-ru)\,dr\,dz \approx -r_e r_w \Delta r(u_n - u_s)$$

Evaluation of the source term is simpler if the control volumes for the streamfunction calculation are staggered from the 'main' control volumes (CVs), as shown in figure II.1. The radial velocity grid points are then located on the north and south sides of the CV and the vertical velocity grid points on the east and west sides; therefore no interpolation is required in order to calculate the integrated source term.

The boundary conditions for recirculating flow in a closed region are constant streamfunction on the external boundaries and also at the centre of the pipe, ie. no streamline will cross the boundary. The boundary condition for the open pipe calculation was $\partial S/\partial z=0$, ie. the streamlines were perpendicular to the bottom boundary.

The streamline figures were obtained by carrying out a contour plot of the streamfunction distribution. Eight equally spaced streamlines were plotted.

Figure II.1: Sketch Showing Staggered Control Volume Locations

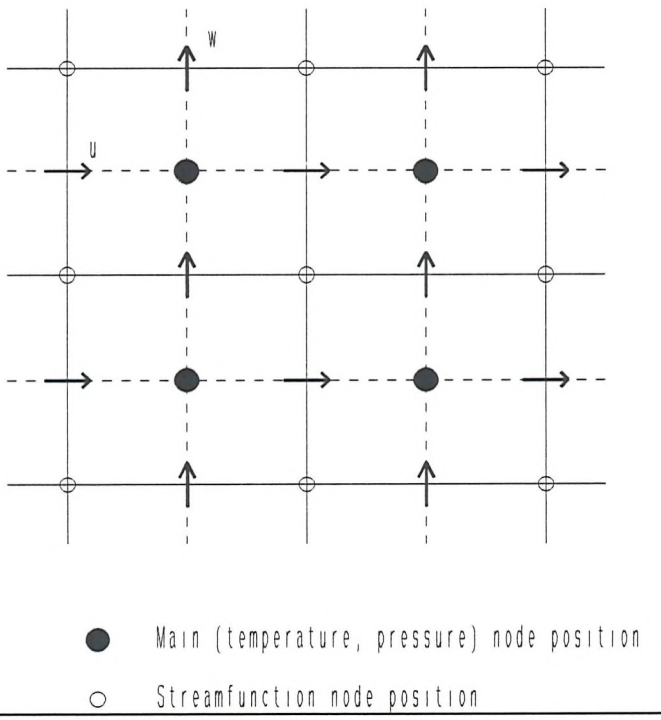

APPENDIX III
COMPARISON WITH FLOW DEVELOPMENT PREDICTED USING PHOENICS AND FLOW-3D

A3.1 COMPARISON WITH THE PREDICTIONS FROM PHOENICS

The CFD package PHOENICS-1.4 was used to predict the convection-driven flows inside a pipe with a section of cooled wall. The aim of this exercise was to check that the flow development predicted using the 'pipe freezing code' was not due to a mistake in the computer program.

PHOENICS was developed at Imperial College, London, and is distributed by CHAM Ltd. It is based on the finite volume method and uses the SIMPLEST algorithm to solve the governing equations. Version 1.4 is the shareware version of the 1987 code; it includes built-in models, such as turbulence and 2-phase flow, but the shareware version does not allow user-written FORTRAN routines.

A3.1.1 Description of Model

The pipe model was developed from case 251 in the library of examples; this modelled the steady state laminar natural convection in air in a two-dimensional square box with heated and cooled side walls. This was modified to describe transient convection in a cylindrical cavity containing water, with a section of the outer surface cooled to 0°C.

The pipe geometry was as follows :

- Radius 50mm (48x1mm,4x0.5mm) (as before)
- Length 480mm (70x8mm) (grid spacing as before)
- Cooled wall length 200mm (25x8mm) (as before)
- Distance between bottom of cooled wall and bottom of domain 280mm (35x8mm)

The boundary conditions were applied as follows :

- Initial temperature 20°C
- Adiabatic boundary condition applied above and below the cooled section
- Isothermal at the top and bottom (maintained at the initial temperature)
- Zero velocity parallel to the boundary on top, bottom and sides (symmetry condition at centre)

The Boussinesq velocity source term was used with constant properties (ß=2.1E-3/K)

because it was not possible to include temperature dependent properties. A transient simulation was used with the run terminating at the time specified in LSTEP (in seconds). The model was run for the cases LSTEP=15,20,25,30.

The input file (written in the PHOENICS Input Language (PIL)) is listed in III.1.2 and the results are described in III.1.3.

A3.1.2 PHOENICS Input File

```
 TALK=T;RUN( 1, 1);VDU=VGAMOUSE
    GROUP 1. Run title and other preliminaries
TEXT(NATURAL CONVECTION IN A VERTICAL PIPE
This is based on the PHOENICS-81 example 251 ('Laminar natural convection in a cavity')
The simulation is transient; the run stops at the time specified in LSTEP (in seconds).
    GROUP 2. Transience; time-step specification
STEADY=F;LSTEP=30;TFIRST=0.0;TLAST=1.0;TFRAC(1)=-LSTEP;TFRAC(2)=1.0
    GROUP 3. X-direction grid specification
CARTES=F
    GROUP 4. Y-direction grid specification
NY=52;YVLAST=1.0;YFRAC(1)=-48.0;YFRAC(2)=.001;YFRAC(3)=4.0;YFRAC(4)=.0005
    GROUP 5. Z-direction grid specification
NZ=70;ZWLAST=1.0;ZFRAC(1)=-70.0;ZFRAC(2)=.008
    GROUP 6. Body-fitted coordinates or grid distortion
    GROUP 7. Variables stored, solved & named
SOLVE(P1,V1,W1,H1);SOLUTN(P1,Y,Y,Y,N,N,N);NAME(H1)=TEMP
    GROUP 8. Terms (in differential equations) & devices
TERMS(TEMP,N,Y,Y,Y,Y,Y)
    GROUP 9. Properties of the medium (or media)
RHO1=1000.0;ENUL=1.002E-6;PRNDTL(TEMP)=7.0
    GROUP 10. Inter-phase-transfer processes and properties
    GROUP 11. Initialization of variable or porosity fields
FIINIT(P1)=0.0;FIINIT(V1)=0.0;FIINIT(W1)=0.0;FIINIT(TEMP)=20.0
    GROUP 12. Convection and diffusion adjustments
    GROUP 13. Boundary conditions and special sources
  * OUTER WALL - WITH FRICTION INNER WALL DEFAULTS TO SYMM
PATCH(OUTWALL,NWALL,1,1,NY,NY,1,NZ,TFIRST,LSTEP)
COVAL(OUTWALL,W1,1.0,0.0)
  * JACKET BC 0DEG 36--60
PATCH(JCKT,NWALL,1,1,NY,NY,36,60,TFIRST,LSTEP)
COVAL(JCKT,TEMP,1./PRNDTL(TEMP),0.0)
  * TOP OF DOMAIN - NO SLIP +ISOTHERMAL
PATCH(TOPDOM,HWALL,1,1,1,NY,NZ,NZ,TFIRST,LSTEP)
COVAL(TOPDOM,TEMP,1./PRNDTL(TEMP),20.0);COVAL(TOPDOM,V1,1.0,0.0)
  * BOTTOM OF DOMAIN - NO SLIP +ISOTHERMAL
PATCH(BOTDOM,LWALL,1,1,1,NY,1,1,TFIRST,LSTEP)
COVAL(BOTDOM,TEMP,1./PRNDTL(TEMP),20.0);COVAL(BOTDOM,V1,1.0,0.0)
  * BUILT-IN BOUSSINESQ APPROXIMATION FOR BUOYANCY SOURCE TERM
 PATCH(BUOY,phasem,1,1,1,NY,1,NZ,TFIRST,LSTEP);COVAL(BUOY,W1,FIXFLU,GRND3)
    GROUP 14. Downstream pressure for PARAB=.TRUE.
    GROUP 15. Termination of sweeps
LSWEEP=200
    GROUP 16. Termination of iterations
LITER(P1)=-30;ENDIT(P1)=1.E-3;LITER(V1)=30;LITER(W1)=30;LITER(TEMP)=30
    GROUP 17. Under-relaxation devices
RELAX(V1,LINRLX,0.1);RELAX(W1,LINRLX,0.1);OVRRLX=1.0
    GROUP 18. Limits on variables or increments to them
    GROUP 19. Special calls from EARTH to GROUND
 * FOLLOWING VALUES  ARE USED IN BOUSSINESQ FORMULA
 * RSG1=ABUOY*AGRAV*TREF
 * RSG2=-AGRAV*ABUOY
```

```
 * ABUOY=2.874E-3;AGRAV=-981.2;TREF=0.0
RSG1=0.0;RSG2=0.00210;RSG10=1.0
   GROUP 20. Preliminary print-out
ECHO=F
   GROUP 21. Print-out of variables
   GROUP 22. Spot-value print-out
IYMON=3;IZMON=20;NYPRIN=NY/5;NZPRIN=NZ/5;NPLT=1
   GROUP 23. Field print-out and plot control
 * TEMPERATURE AND VELOCITY PROFILES
PATCH(PROF,PROFIL,1,1,1,NY,NZ/2,NZ/2,TFIRST,LSTEP)
PLOT(PROF,W1,0.0,0.0);PLOT(PROF,TEMP,-10.0,10.0)
 * TEMPERATURE CONTOURS
PATCH(CONT,CONTUR,1,1,1,NY,1,NZ,TFIRST,LSTEP)
PLOT(CONT,TEMP,0.0,10.0)
STOP
```

A3.1.3 Results

The predictions of velocity and temperature distribution at 10, 15, 20, 25 and 30 seconds are included as figures III.a-e. The cooled wall section in indicated by the grey rectangle outside the domain; the centre line of the pipe is on the left-hand side. These images were produced by the PHOENICS post-processor, PHOTON.

These results were compared with the predicted velocity and temperature distributions shown in figures 6.1a and show excellent agreement. At 10 seconds (figure III.a) the cooled boundary layer falls down the wall, leaving the wall at around 17-20°C. At 15 seconds (figure III.b) the boundary layer is visibly thickened towards the bottom of the cell and the temperature of the upward-flowing water is less than 20°C. By 20 seconds (figure III.c) an upward flow is visible below the convection cell, with the boundary layer being pushed towards the centre of the pipe. This continues at 25 and 30 seconds (figures III.d-e), with the upward core flow increasing in velocity as it is pushed towards the centre of the pipe. A complex flow pattern inside the main convection cell is visible at 30 seconds (figure III.e), which agrees with the predictions obtained using 'pipe freezing' code (for instance, see figure 6.1a).

A3.2 COMPARISON WITH THE PREDICTIONS FROM FLOW-3D

The CFD package Flow-3D was developed by AEA Technology, Harwell. This was mounted on the University's Solaris computer service in late summer 1994. Flow-3D is a complex, state-of-the-art CFD package and was developed based on the finite volume approach. This package was used to predict the flow development over the first 30 seconds

in a 100mm (4") diameter pipe under the conditions described above (III.1.1).

The input file is listed below. Note that the properties of water were not specified directly; water was selected as the working fluid and Flow-3D assigned properties accordingly.

A3.2.1 Input (Command) File

```
/*********************************************************          */
/* NATURAL CONVECTION IN A PIPE WITH COOLED WALL                     */
/* ALISON KEARY 22/11/94                                            */
/*********************************************************          */
>>FLOW3D
  >>SET LIMITS
    TOTAL INTEGER WORK SPACE 5000000
    TOTAL CHARACTER WORK SPACE 2000
    TOTAL REAL WORK SPACE 2000000
    MAXIMUM NUMBER OF BLOCKS 1
    MAXIMUM NUMBER OF PATCHES 30
    MAXIMUM NUMBER OF INTER BLOCK BOUNDARIES 0
  >>OPTIONS
    TWO DIMENSIONS
    RECTANGULAR GRID
    CYLINDRICAL COORDINATES
    AXIS INCLUDED
    LAMINAR FLOW
    HEAT TRANSFER
    INCOMPRESSIBLE FLOW
    BUOYANT FLOW
    TRANSIENT FLOW
>>MODEL TOPOLOGY
  >>CREATE BLOCK
    BLOCK NAME 'BOX'
    BLOCK DIMENSIONS 70 52 1
  >>CREATE PATCH
    PATCH NAME 'CNTRE'
    BLOCK NAME 'BOX'
    PATCH TYPE 'SYMMETRY PLANE'
    LOW J
  >>CREATE PATCH
    PATCH NAME 'OJCKT'
    BLOCK NAME 'BOX'
    PATCH TYPE 'WALL'
    PATCH LOCATION 1 35 52 52 1 1
    HIGH J
  >>CREATE PATCH
    PATCH NAME 'JCKT'
    BLOCK NAME 'BOX'
    PATCH TYPE 'WALL'
    PATCH LOCATION 36 60 52 52 1 1
    HIGH J
  >>CREATE PATCH
    PATCH NAME 'AJCKT'
    BLOCK NAME 'BOX'
    PATCH TYPE 'WALL'
    PATCH LOCATION 61 70 52 52 1 1
    HIGH J
  >>CREATE PATCH
    PATCH NAME 'BTM'
    BLOCK NAME 'BOX'
```

```
    PATCH TYPE 'WALL'
    LOW I
   >>CREATE PATCH
    PATCH NAME 'TOP'
    BLOCK NAME 'BOX'
    PATCH TYPE 'WALL'
    HIGH I
 >>MODEL DATA
  >>AMBIENT VARIABLES
    U VELOCITY 0.0000E+00
    V VELOCITY 0.0000E+00
    PRESSURE 0.0000E+00
    TEMPERATURE 2.9300E+02
  >>TITLE
    PROBLEM TITLE 'CONVECTION IN A PIPE'
  >>PHYSICAL PROPERTIES
    >>STANDARD FLUID
      FLUID 'WATER'
      STANDARD FLUID REFERENCE TEMPERATURE 2.9300E+02
    >>BUOYANCY PARAMETERS
      GRAVITY VECTOR -9.810000E+00 0.000000E+00 0.000000E+00
      BUOYANCY REFERENCE TEMPERATURE 2.9300E+02
    >>TRANSIENT PARAMETERS
      >>FIXED TIME STEPPING
        TIME STEPS 30* 1.000000E+00
        INITIAL TIME 0.0000E+00
        BACKWARD DIFFERENCE
>>SOLVER DATA
  >>PROGRAM CONTROL
    MAXIMUM NUMBER OF ITERATIONS 50
    PRESSURE REFERENCE POINT BLOCK 'BOX'
    PRESSURE REFERENCE POINT 35 25 1
    OUTPUT MONITOR BLOCK 'BOX'
    OUTPUT MONITOR POINT 35 25 1
    MASS SOURCE TOLERANCE 1.0000E-07
    ITERATIONS OF VELOCITY AND PRESSURE EQUATIONS 5
    ITERATIONS OF TEMPERATURE AND SCALAR EQUATIONS 5
    ITERATIONS OF HYDRODYNAMIC EQUATIONS 1
    SOLVER DEBUG PRINT STREAM 20
  >>EQUATION SOLVERS
    U VELOCITY 'STONE'
    V VELOCITY 'STONE'
    PRESSURE 'STONE'
>>CREATE GRID
  >>SIMPLE GRID
    BLOCK NAME 'BOX'
    DX 70* 8.000000E-03
    DY 48* 1.000000E-03 4* 5.000000E-04
    DZ 1.000000E-02
>>MODEL BOUNDARY CONDITIONS
  >>WALL BOUNDARY CONDITIONS
    PATCH NAME 'BTM'
    TEMPERATURE 2.9300E+02
  >>WALL BOUNDARY CONDITIONS
    PATCH NAME 'OJCKT'
    HEAT FLUX 0.0000E+00
  >>WALL BOUNDARY CONDITIONS
    PATCH NAME 'AJCKT'
    HEAT FLUX 0.0000E+00
  >>WALL BOUNDARY CONDITIONS
    PATCH NAME 'JCKT'
    TEMPERATURE 2.7300E+02
  >>WALL BOUNDARY CONDITIONS
    PATCH NAME 'TOP'
    TEMPERATURE 2.9300E+02
>>STOP
```

A3.2.2 Results

The velocity and temperature distributions at 30 seconds are shown in figure III.2. This shows complete agreement with the existing predictions of the flow development. In particular, the cooled boundary layer can be seen to leave the wall before it had warmed up to the initial temperature and formation of the secondary region is visible.

A3.3 CONCLUSIONS

The CFD packages PHOENICS and Flow-3D were used to model the natural convection flows inside a 100mm (4") diameter pipe. Excellent agreement with the flow development predicted using the specific 'pipe freezing' code was obtained, giving confidence in the proposition of a three stage flow development and the existence of a 'choking' mechanism.

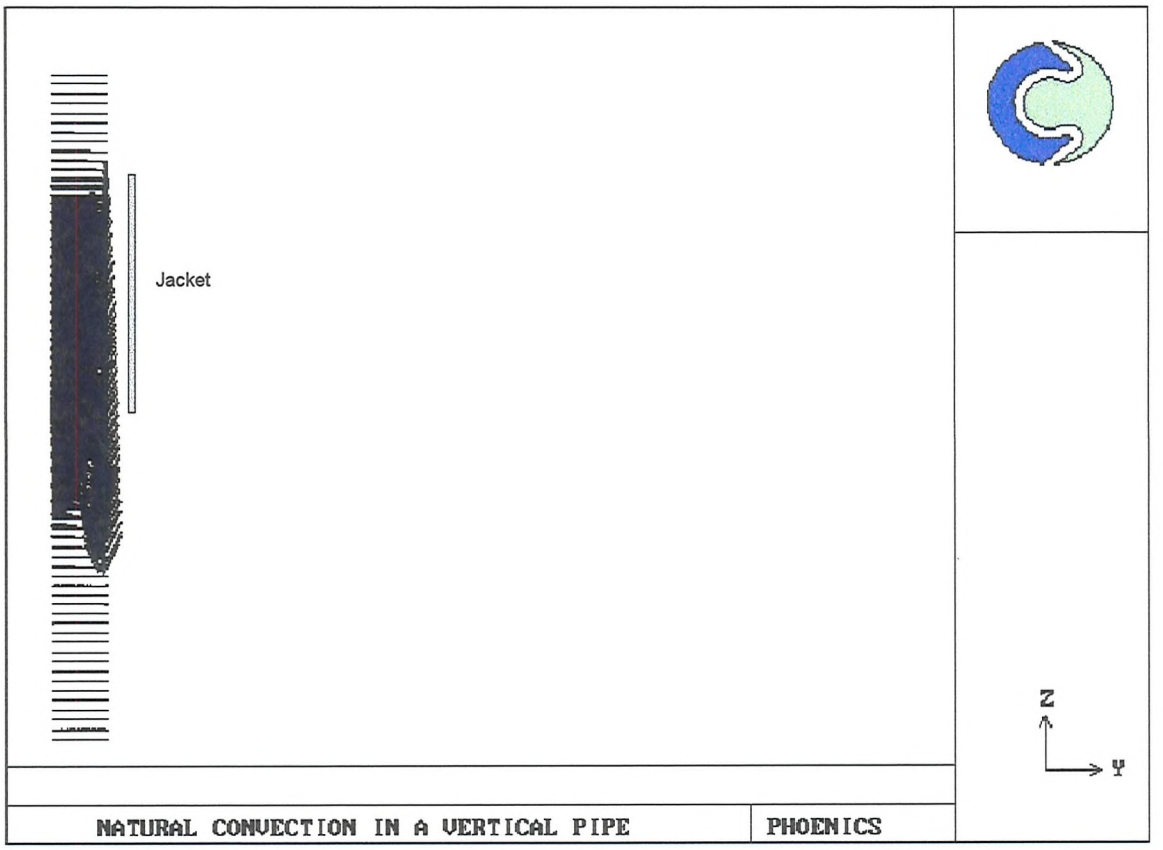

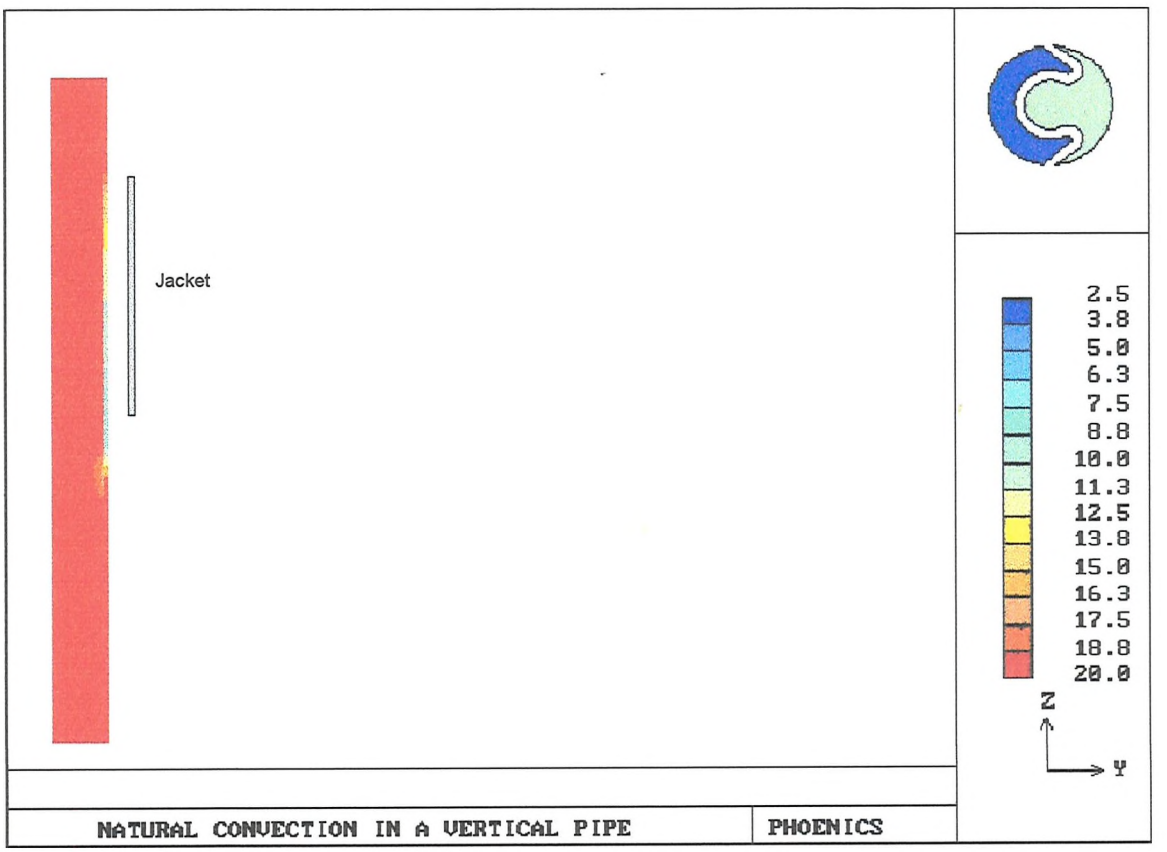

Figure III.1a: PHOENICS predictions: Velocity and temperature distributions at 10 seconds (centre line on left)

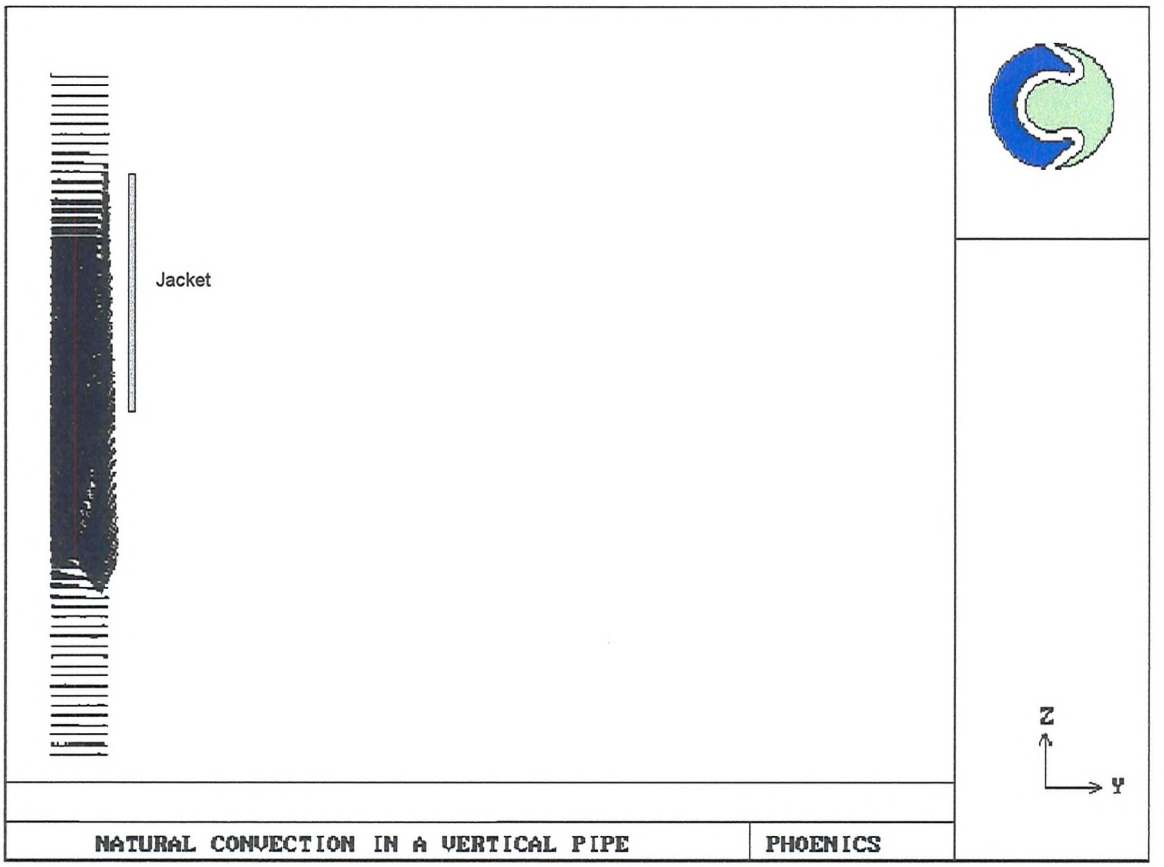

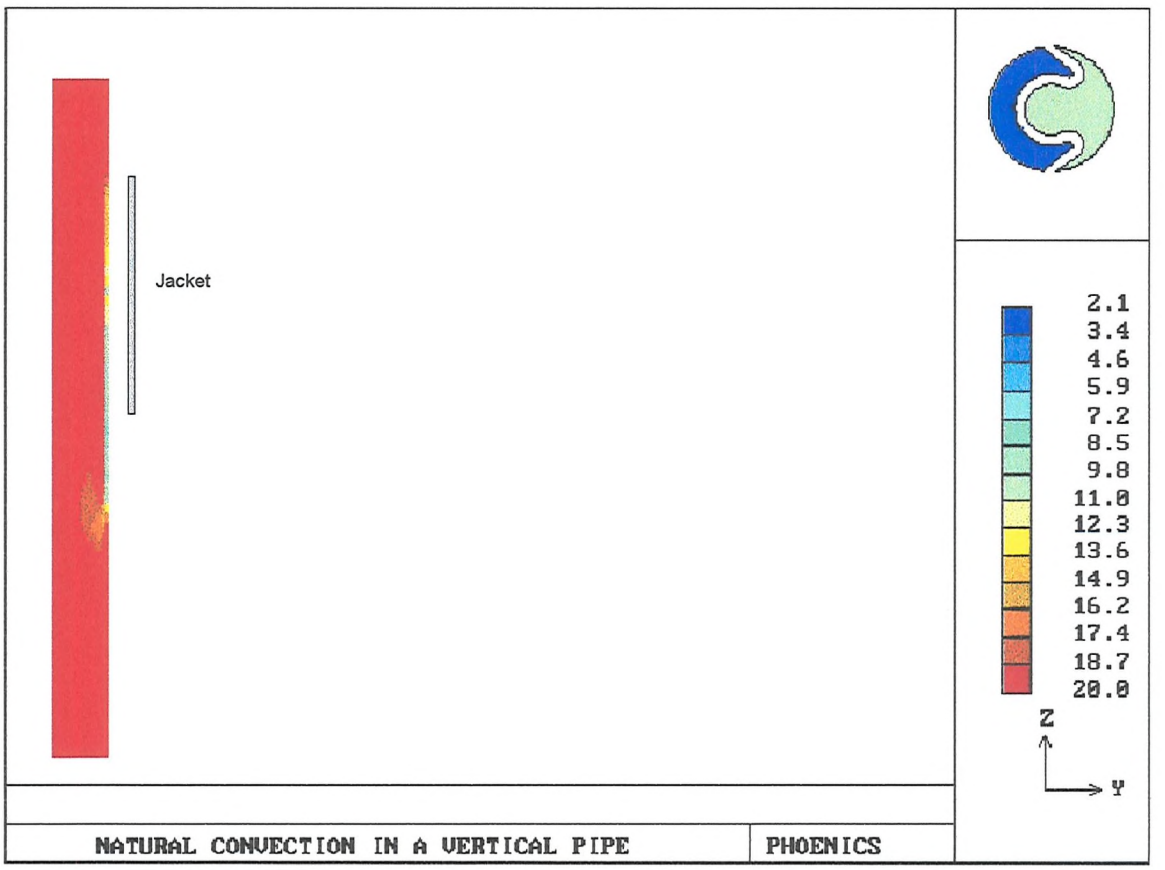

Figure III.1b: PHOENICS predictions: Velocity and temperature distributions at 15 seconds (centre line on left)

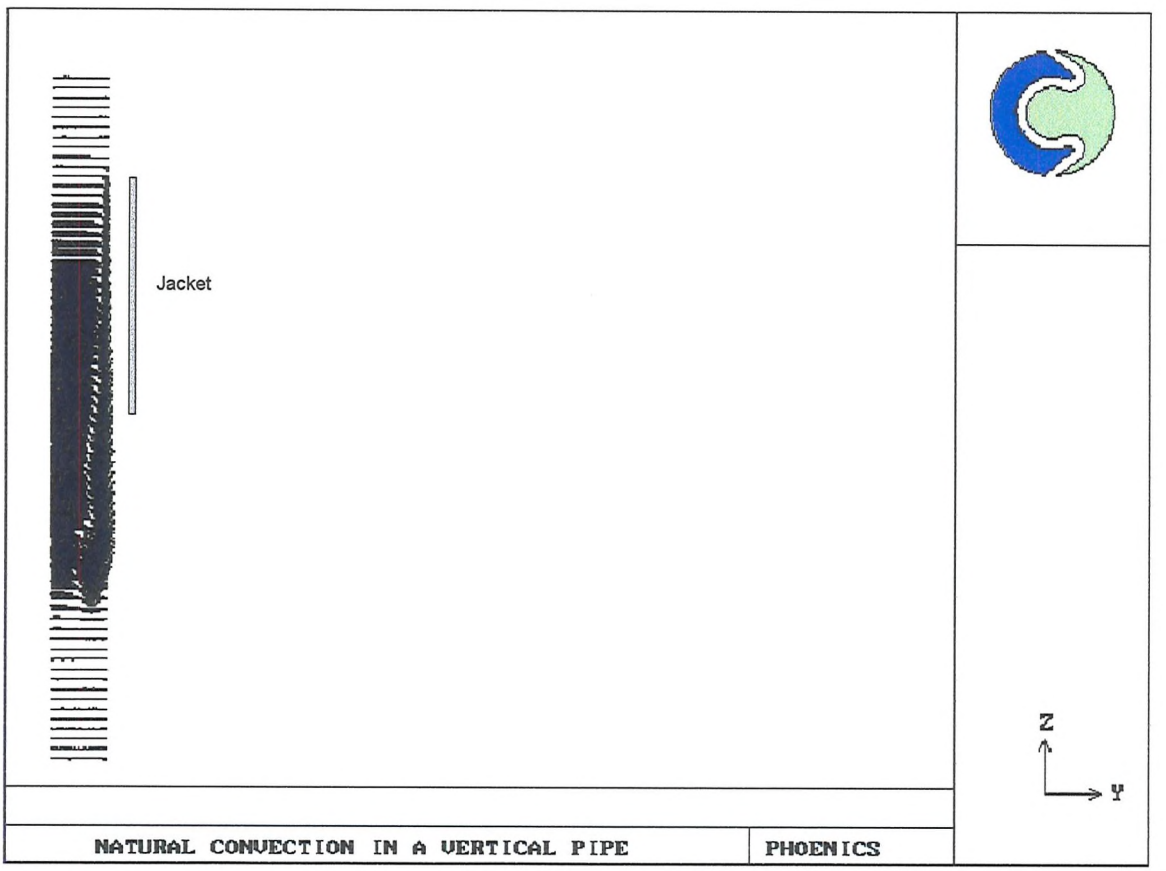

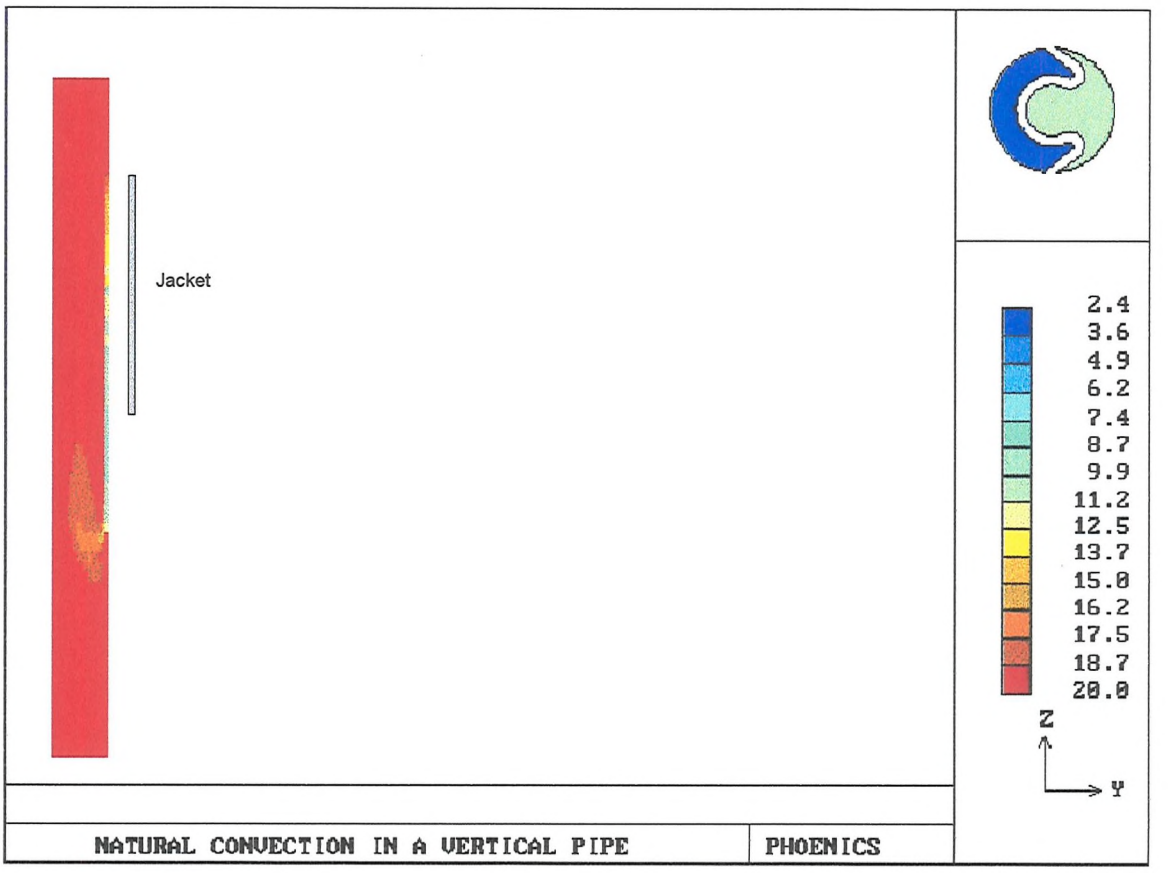

Figure III.1c: PHOENICS predictions: Velocity and temperature distributions at 20 seconds (centre line on left)

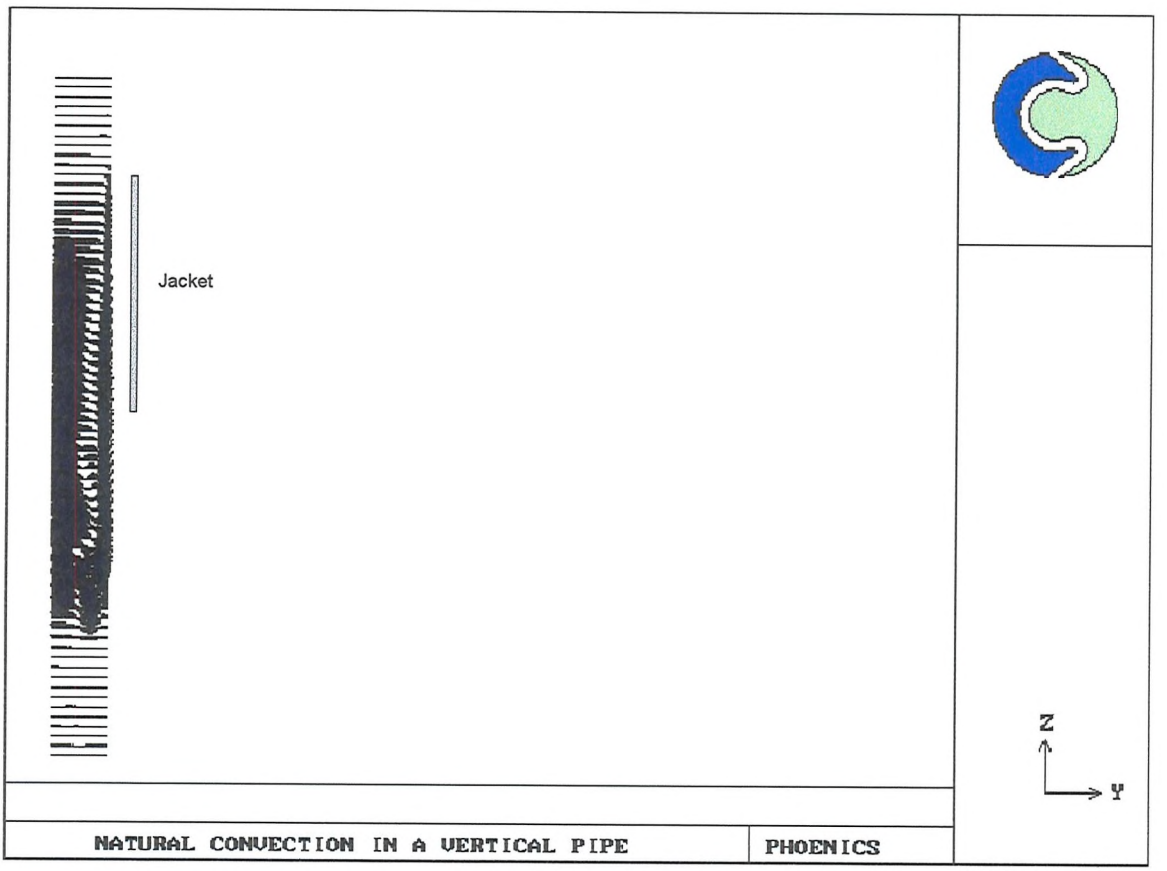

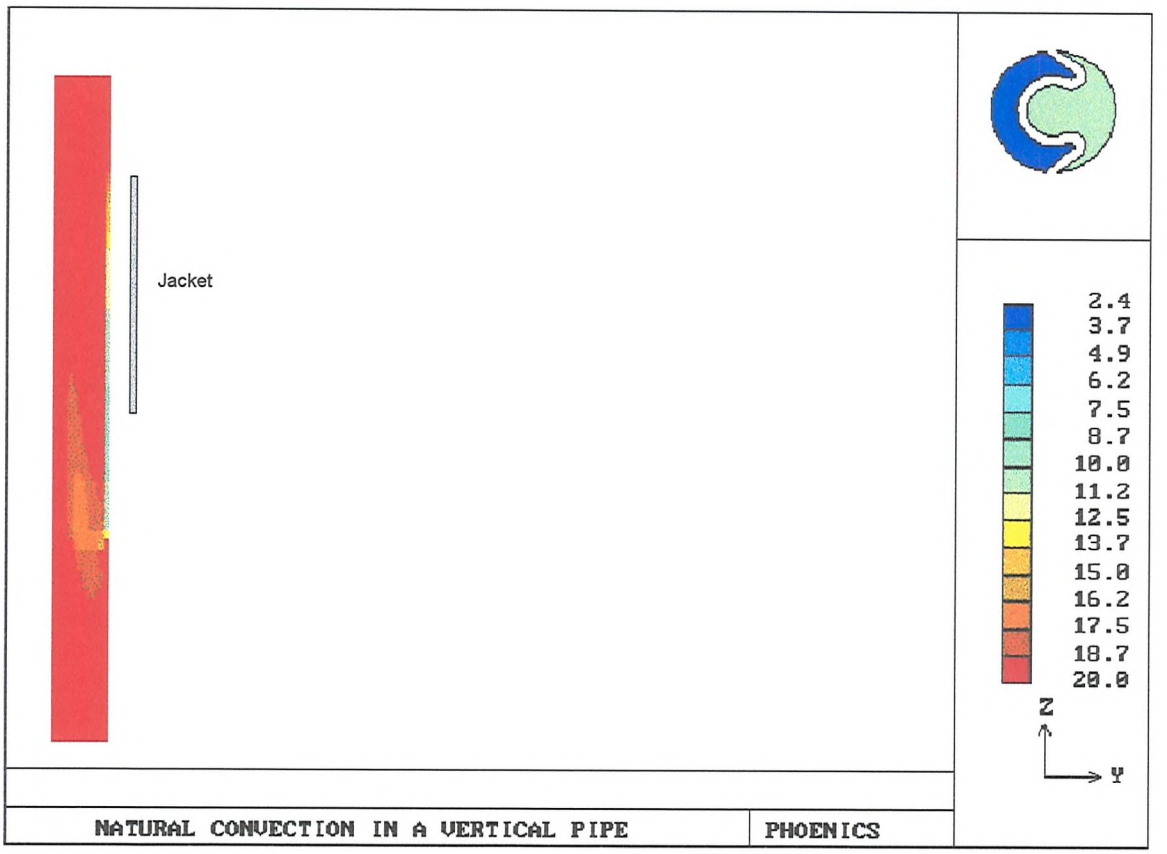

Figure III.1d: PHOENICS predictions: Velocity and temperature distributions at 25 seconds (centre line on left)

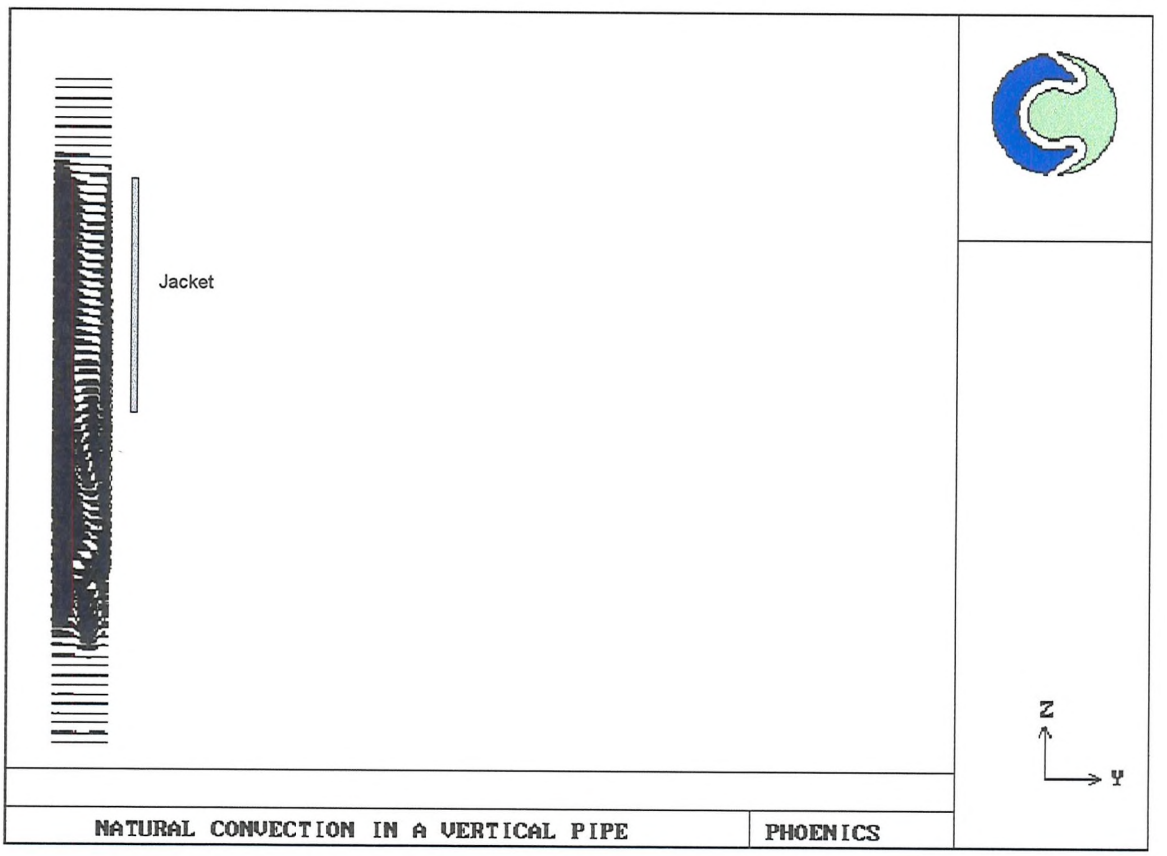

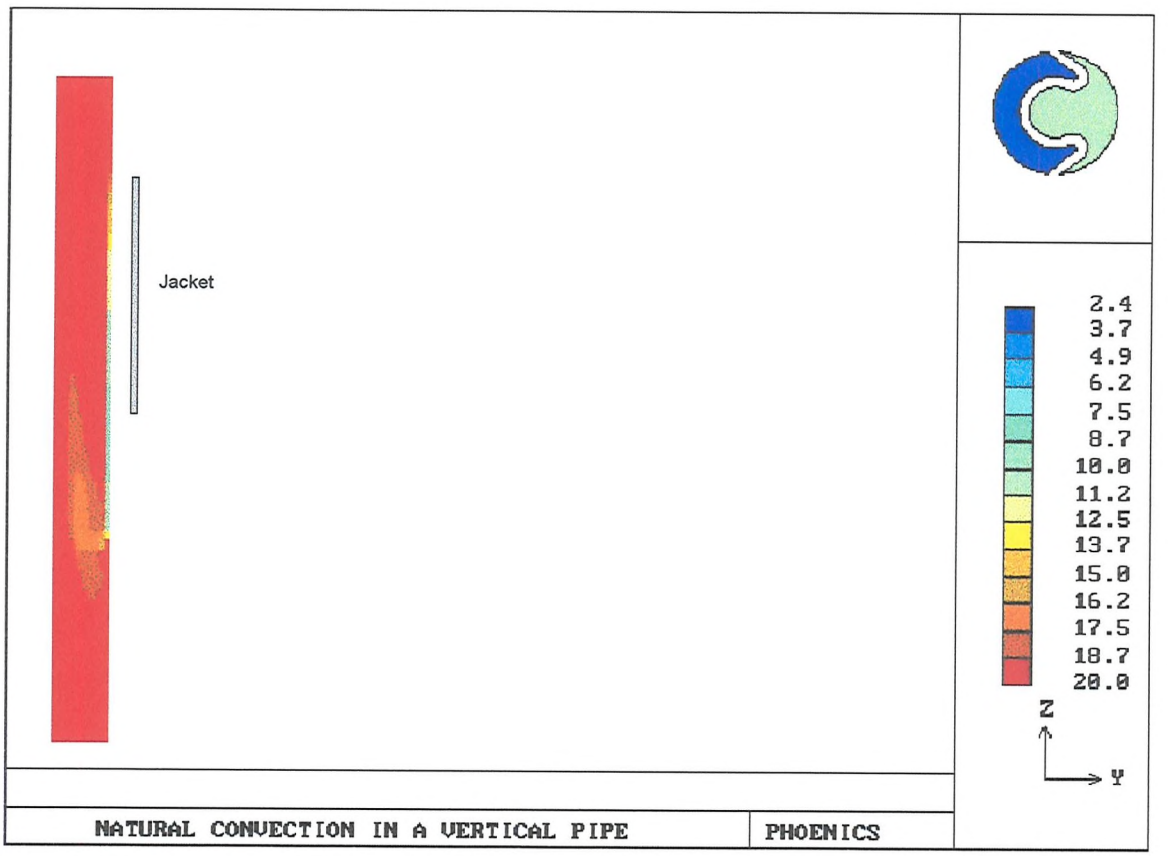

Figure III.1e: PHOENICS predictions: Velocity and temperature distributions at 30 seconds (centre line on left)

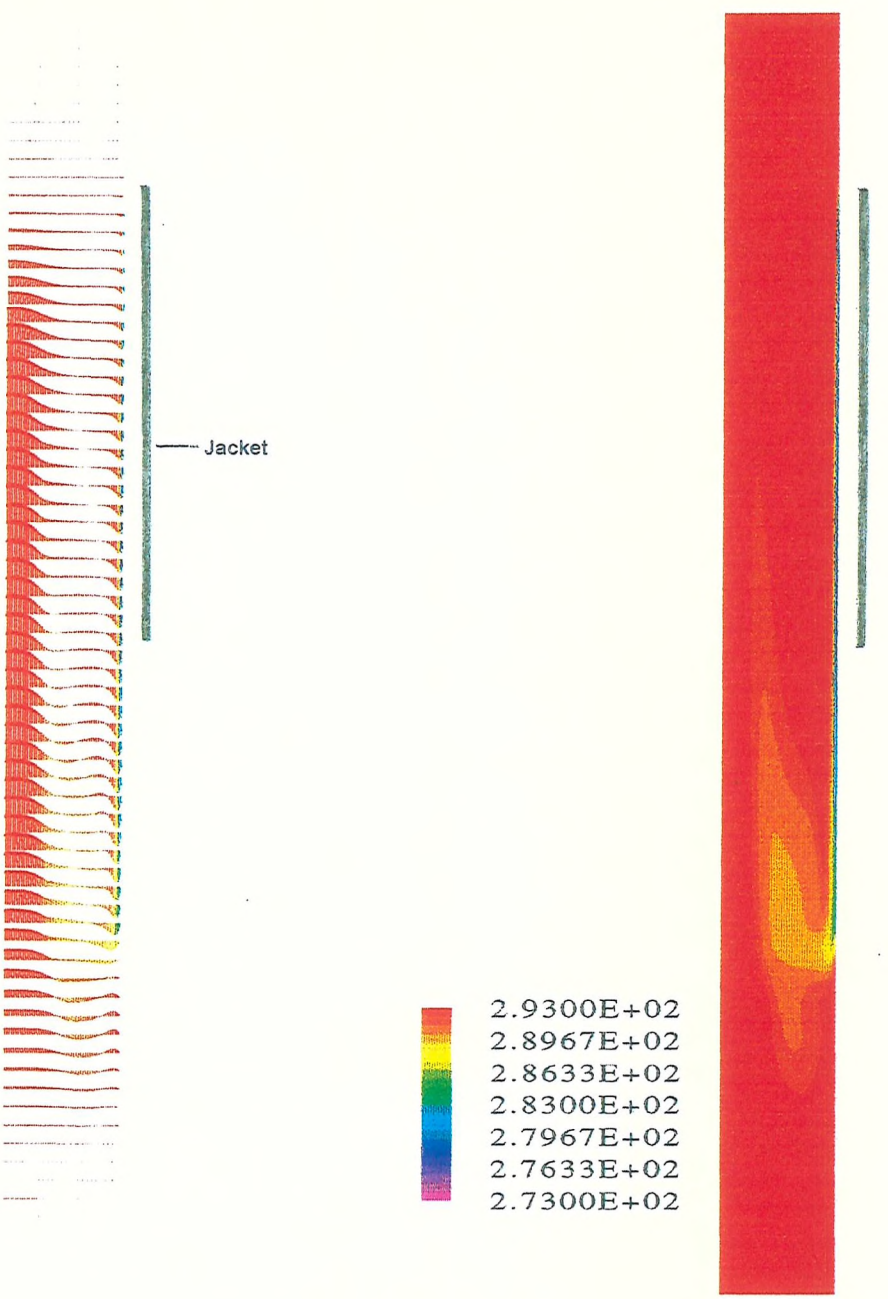

Figure III.2: Flow-3D predictions: Velocity and temperature distributions at 30 seconds (centre line on left, temperature in Kelvin)

APPENDIX IV
DIMENSIONLESS NUMBERS: DEFINITION AND TYPICAL VALUES

Pipe freezing is a transient process involving natural convection in the liquid, phase change and boiling heat transfer to the cryogen. In the following sections, the dimensionless numbers associated with the three main processes (natural convection, freezing and the heat transfer to the coolant) are summarised. Typical values for these numbers are included.

A4.1 Natural Convection

One component part to the problem is the effect of natural convection on the freezing process: the flow may be laminar or turbulent and will affect freezing to differing extents. The dimensionless groups describing natural convection driven flow are as follows; the Prandtl Number (which is the ratio of momentum to thermal diffusivity), the Grashof Number (relates buoyancy, inertia and viscous forces) and the Rayleigh Number (product of Grashof and Prandtl Numbers). (The Reynolds Number is used when there is flow in the pipe (ie. forced or mixed convection).) The Nusselt Number is used to describe heat transfer by natural or forced convection.

There are numerous experimental and also theoretical studies of the heat transfer over a heated or cooled vertical plate in a semi-infinite medium. These results (eg. Rogers and Mayhew[67] and Ösişik[68]) relate the average Nusselt number to Rayleigh number and Prandtl number. The characteristic dimension is the length of the heated (or cooled) plate. Theoretical analysis by Bejan[29] provided order of magnitude relationships for the boundary layer thickness and velocity in terms of the fluid properties and temperature difference.

The criterion listed by Bejan for transition between laminar and turbulent flow over an isothermal vertical flat plate is given as a Grashof number[IV.1] of 1.3×10^9 (data from Mahajan and Gebhart[49]).

Calculating values for the Prandtl, Rayleigh and Grashof numbers is complicated by variations in the properties of water over the temperature range, especially the viscosity and the volumetric expansion coefficient. The viscosity drops off markedly with increasing temperature (for instance, the viscosity at 27°C is roughly half of that at 0°C) whereas the

[IV.1] Note that the criteria for transition between laminar and turbulent flow may vary by up to an order of magnitude from one study to another.

expansion coefficient increases with temperature from less than zero at 0°C to greater than zero above 4°C. Thus the boundary layer next to the ice consists of an upwardly buoyant layer where the temperature is below 4°C and a downwards moving layer above 4°C. The way in which the values of the properties are chosen makes a significant difference to the values of Rayleigh and Grashof numbers (and to a lesser extent, the Prandtl number).

The Prandtl Number for water decreases with temperature from around 13 at 0°C to around 3.6 at 50°C. This shows that the thermal boundary layer will be thinner than the moving layer of water (the velocity boundary layer). The velocity boundary layer consists of two parts; a cooled layer and a further outer layer which is entrained by the moving cooled layer.

The values of Grashof and Rayleigh Numbers also depend strongly on the definition of a characteristic length. For pipe freezing, there are two dimensions of interest: the pipe diameter (or radius) and the jacket length. However, because the jacket length is normally proportional to the pipe diameter (normally 2 or 3D), either dimension can be used although a consistent definition must be used if comparing two situations. Values of Rayleigh, Prandtl and Grashof number were evaluated using fluid properties halfway between 0°C and the initial water temperature. Taking the case of a 100mm (4") diameter pipe with a 2D jacket (200mm long) and an initial water temperature of 20°C as an example, the Rayleigh and Grashof numbers are 760×10^6 and 80×10^6, respectively, based on the jacket length and 95×10^6 and 10×10^6, respectively, based on the pipe diameter.

The Grashof and Rayleigh numbers are used to express the transition between laminar and turbulent flow conditions. No experimental results were available which demonstrated the point at which the flow conditions change from laminar to turbulent and therefore experimental results obtained for natural convection over a cooled or heated vertical plate were considered. Kreith and Bohn[69] state that transition takes place at a Rayleigh number of 10^9. Bejan[29] however, suggests that transition takes place at a Grashof number of 1.5×10^9 with a Prandtl number of 0.71 (Rayleigh number of 1.1×10^9) and at a Grashof number of 1.3×10^9 with a Prandtl number of 6.7 (giving a Rayleigh number of 8.7×10^9). While it is recognised that such criteria are only order-of-magnitude estimates, it does appear that the Grashof number offers a better way of quantifying the transition criterion than the Rayleigh number.

The convected heat flux is expressed non-dimensionally using the Nusselt Number. Estimates for the heat transfer coefficient are available from experimental data, for instance Tavner calculated heat transfer coefficients from temperature measurements and obtained a wide scatter of values over the range 0 to 600 W/m^2K and Bowen et al[9] obtained values in

the range 5 to 315 W/m²K in the temperature range 10°C to 50°C. Bejan's integral analysis gives a value of around 370 W/m²K under these conditions. The resulting values of Nusselt numbers are 0-200 (Tavner), 2-105 (Bowen) and 135 (Bejan) (using the jacket length as the characteristic dimension). The empirical correlations provided by Rogers and Mayhew[67] and by Ösişik[68] give Nusselt Numbers of 96 and 104, respectively.

A4.2 **Freezing Process**

The dimensionless number used to characterise freezing is the Stefan Number which is the ratio of the sensible heat to the latent heat. For freezing using liquid nitrogen, typical values of Stefan Number are around 0.80 with a liquid temperature of 0°C and 1.05 at 20°C.

Another dimensionless number which is often used in conduction processes is the Fourier Number. This is a dimensionless time which indicates how far heating or cooling effects have penetrated a solid body. For phase change problems, the dimensionless time is modified to include latent heat effects by using the product of Fourier and Stefan Numbers.

Taking the characteristic length in the Fourier Number as the jacket length, the Fourier Number for freezing in a 100mm diameter pipe is ($7.4x10^{-5}t$) and the product (Fo.Ste) is ($5.9x10^{-5}t$) for an initial temperature of 0°C and ($7.8x10^{-5}t$) at 20°C (t is time in seconds).

A4.3 **Cooling Process**

The cooling process is governed by the liquid nitrogen boiling against the pipe wall. This is a complex process and the heat flux varies significantly with the wall temperature as the boiling process passes through the film and nucleate boiling stages.

The dimensionless number which is used to quantify the cooling process is the Biot Number. This is the ratio of internal thermal resistance in the solid to the surface resistance. Biot number expresses the ratio of conduction within a body (usually solid) to the convection at the surface (or at the boundary), its value indicates where the main resistance to heat transfer lies: for example Biot number less than 0.1 implies that most of the resistance is at the surface and therefore isothermal behaviour within the solid can be assumed.

In order to evaluate this an average heat transfer coefficient must be estimated from the heat flux-temperature boiling curve. Typical heat transfer coefficients for boiling nitrogen are 900 W/m²K and 2200 W/m²K in the film and nucleate boiling regimes (respectively) from

Lannoy and Flaix[11] giving a Biot Number of 3.5 and 8.5 for mild steel and 11.3 and 27.6 for stainless steel. If the thermal resistance of the pipe wall is neglected and the Biot Number is referenced to ice, values of 50 and 120 are obtained. This shows that the thermal resistance within the ice and steel cannot be neglected and the thermal resistance in the ice is more significant than that in the steel pipe wall.

APPENDIX V
PUBLICATIONS

Three papers were written and presented during the course of this research. They are reproduced and included in the following sections. Note that the reference and figure numbers for each paper apply to that specific paper.

A5.1 The development of a two dimensional numerical model of freezing in a vertical water filled pipe
A.C. Keary, R.J. Bowen, A.C.R. Tavner
Numerical Methods in Thermal Problems, Vol.VII, pp.175-185
Pineridge Press, Swansea, UK.

This was presented at the Seventh International Conference on Numerical Methods in Thermal Problems, held at Stanford University, California, U.S.A. on July 8-12th 1991.

THE DEVELOPMENT OF A TWO DIMENSIONAL NUMERICAL MODEL OF FREEZING IN A VERTICAL WATER FILLED PIPE

A.C.Keary, R.J.Bowen, A.C.R.Tavner

Department of Mechanical Engineering, University of Southampton, UK

SUMMARY

Cryogenic Pipe Freezing is a technique used for isolating sections of a liquid filled pipeline. A jacket is attached to the pipe and filled with a cryogen causing the liquid in the pipe to freeze and form a plug.

In order to obtain a clear understanding of this process, a finite-difference model was developed using the enthalpy formulation to predict the conduction and solidification processes in a vertical pipe. Experimental data were used for the wall temperatures in the cooled region and the predicted temperature distributions were found to compare well with those from the experiments. The model was run for a range of initial water temperatures and it was found that as the temperature increased the accuracy of the predictions became worse, showing the increasing importance of convection under these conditions.

NOMENCLATURE

H	Enthalpy	A	Area
T	Temperature	V	Volume
k	Thermal conductivity	δ	Distance between nodes
ρ	Density	T_f	Freezing temperature
c	Specific heat capacity	T_{ref}	Reference temperature
L	Latent heat		

Subscripts

E,W,N,S,P Neighbouring nodes

S Solid

L Liquid

Superscripts

' Value at last time step

1. INTRODUCTION

Cryogenic Pipe Freezing is a pipeline maintenance technique used for isolating sections of a liquid filled pipeline. A jacket is placed round the pipe and filled with a cryogen such as liquid nitrogen which cools the liquid in the pipe causing it to freeze and form a plug. By freezing two plugs, the section between them is isolated and work may be carried out on it. Once this has been completed, the jacket can be removed and the plugs allowed to thaw. This eliminates the need to drain the system and is inexpensive and uncomplicated compared to other plugging techniques.

Due to the general lack of understanding of the process and also the concern about the effect that the sudden cooling would have on the pipe itself, a research programme was started at Southampton in 1981. Over the past ten years a large amount of data has been collected from experimental investigations. Although a wide range of pipe conditions have been explored, it would not been feasible to investigate all possible variations. The development of a numerical model of the pipe freezing process was therefore considered essential.

Both experimental work and practical experience have demonstrated that convection from the liquid to the forming ice plug in the pipe is significant when the initial water temperature is above a certain level. Experimental results for a range of pipe sizes, figure(1), show that as the water temperature increases so

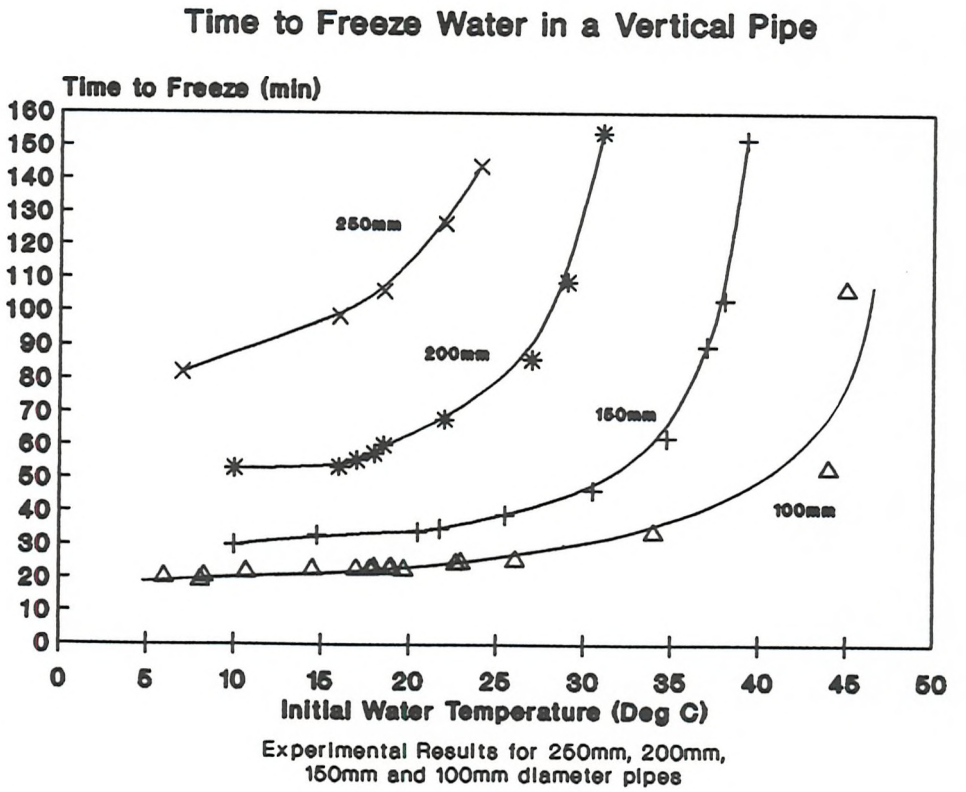

Figure 1 : Effect of Pipe Size on Freezing Time

the time to close the pipe off increases, eventually reaching a limiting temperature above which a solid plug cannot be formed.

A complete model of plug formation is being developed, however as a first step convection has been neglected and a model based only on the conduction and solidification processes has been developed. A finite volume approach has been taken incorporating the solidification using the enthalpy method and using experimental data for the wall conditions.

The experimental work was carried out using liquid nitrogen to freeze a vertical 100mm diameter pipe which provided temperature data and ice plug profiles for water with initial temperatures varying between 8°C and 26°C. This paper presents the development of a numerical model of ice plug formation in a pipe and compares the results with experimental data.

2. GOVERNING EQUATIONS

The geometry of the application suggests it should be modelled in two dimensions in radial coordinates. By applying conservation of energy in the absence of heat sources, sinks and convection, the relationship between enthalpy and temperature, in 2D radial (r,z) co-ordinates, is given by equation (1).

$$\frac{\partial}{\partial t}(\rho H) = \frac{1}{r}\frac{\partial}{\partial r}\left(rk\frac{\partial T}{\partial r}\right) + \frac{\partial}{\partial z}\left(k\frac{\partial T}{\partial z}\right) \qquad (1)$$

This is valid everywhere in the domain except on the solid/liquid interface itself, where the time derivative is not defined in the usual sense, since the value of enthalpy jumps by L on solidification. However, because the interface occupies zero volume, integrating over a control volume, using the finite volume method, results in a set of descretised equations which are valid over the entire domain. This is described in more detail by Shamsundar and Sparrow [1].

Taking the standard finite volume method [2] with an implicit formulation, equation (1) is descretised giving the following relationship between the temperature and enthalpy for the control volume ΔV around node P bounded by East, West, North and South nodes :

$$\frac{[(\rho H)_P - (\rho H)'_P]\,\Delta V}{\Delta t} = \left(\frac{Ak}{\delta}\right)_E T_E + \left(\frac{Ak}{\delta}\right)_W T_W + \left(\frac{Ak}{\delta}\right)_N T_N + \left(\frac{Ak}{\delta}\right)_S T_S - \left[\left(\frac{Ak}{\delta}\right)_E + \left(\frac{Ak}{\delta}\right)_W + \left(\frac{Ak}{\delta}\right)_N + \left(\frac{Ak}{\delta}\right)_S\right] T_P \qquad (2)$$

$$H_P + a_P T_P = \sum_i (a_i T_i) + b$$

$$a_i = \left(\frac{Ak}{\delta}\right)_i \frac{\Delta t}{\rho \Delta V} \qquad a_P = \sum_i a_i \qquad b = \frac{(\rho H)'_P}{\rho} \qquad i = E, W, N, S \qquad (3)$$

The relationship, therefore, between the temperature and enthalpy at P and the temperature at the neighbouring nodes is given in equation (3). This formulation is exactly the same as that in cartesian co-ordinates, except that areas of the control volume faces vary with the radial position of the volume.

The enthalpy at a point is related to the temperature by the following relationships :

$$H(T) - H_S(T) = \int_{T_{ref}}^{T} c\, dT \qquad T < T_f$$

$$H(T) - H_L(T) = \int_{T_{ref}}^{T} c\, dT + L \qquad T > T_f \tag{4}$$

3. SOLUTION METHOD

The method described by Shamsundar and Rooz [3] was used. At each node in the domain, the right-hand side of equation (3) is evaluated using the last values of the neighbouring temperatures and properties. Let this be called R. Tests are then carried out to find consistent values of enthalpy, temperature and state as shown in figure 2.

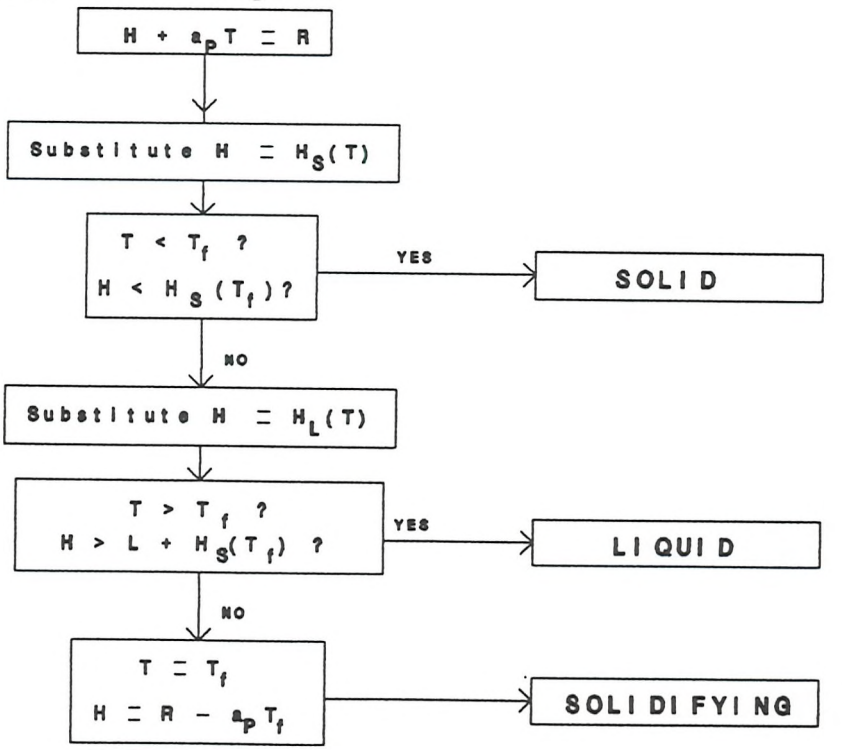

Figure 2 : Flowchart of Solution Method

The grid is swept several times and convergence is accepted when the maximum change in nodal enthalpy between sweeps falls below 1 J/kg which corresponds to a maximum temperature change of around 0.0005°C in the ice and 0.00024°C in the water.

4. VALIDATION TESTS

The method was first tested against the 1D analytical solution to the Neumann problem [4] for freezing in a semi-infinite domain. Several test cases were employed to cover a range of freezing rates. Predictions of interface position were found to be within 5% of the exact solution and, by selecting the grid spacing and time step correctly, the results became identical to the exact solution.

A two dimensional model in cartesian co-ordinates was also developed to predict the transient freezing of a substance initially at its freezing temperature in a square container and cooled by convection on the outer surface. The results were found to be within one percent of the published results [1,3].

5. DESCRIPTION OF EXPERIMENTAL RIG

A series of freezes of nominally static water were carried out which produced a collection of measurements which could be used for comparison with the numerical model. The experiments were conducted on a 100mm diameter vertical pipe with an 200mm freezing jacket. In order to observe the plug formation in the freezing section, the pipe was cut in half lengthways and a perspex window bolted on across the open side. Perspex is a poor conductor of heat so the heat transfer through the window was assumed to be minimal. This was confirmed by comparing the freezing times with those for similar freezes in a whole pipe and finding good agreement. This is described in more detail in [5].

A series of freezes was carried out with 20 thermocouples in the pipe. These were arranged in groups of five and positioned across the pipe at 0, 100mm, 150mm and 200mm above the bottom of the jacket. This provided measurement of the temperature at the pipe wall and inside the freezing section. The thermocouples were placed on a radius extending to the back of the pipe and so, with the exception of the more central ones, were mostly unaffected by the presence of the perspex wall.

6. DESCRIPTION OF MODEL

The solution domain is shown in figure 3. The boundary conditions for the domain indicated in the sketch are as follows:
(1) Wall temperatures obtained from the experimental data were imposed on the wall to simulate the presence of the jacket. The measured temperatures were recorded every 30 seconds so linear interpolation was used both in space and time to calculate the temperatures for the nodes lying on the boundary.
(2) The top and bottom of the domain were maintained at the initial water temperature to emulate the thermal mass of water above and below the modelled section.
(3) The centre of the pipe is naturally adiabatic. The wall above and below the jacket was assumed adiabatic for the sake of simplicity. The conduction of heat up and down the wall away from the jacket and the heat transfer through the wall to the ambient room temperature were neglected therefore and assumed to cancel out.

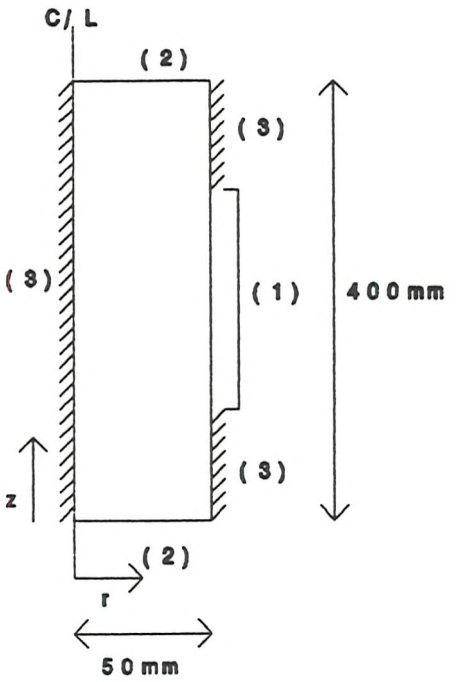

Figure 3 : Sketch of Domain

Investigations were carried out with 40x51, 40x102, 80x51 and 80x102 grids and time steps of 1 second and 0.5 second. These showed very little variation in predictions and it was therefore decided to use the 40x51 grid which gave a grid spacing of 10mm in the vertical (z) direction and of 1mm in the radial direction.

The physical properties of water and ice used in the model were obtained from Hobbs [6]. Since the density, specific heat capacity and conductivity in water vary little over the temperature range of interest they have been taken as constant. For ice the properties vary rather more and their temperature dependence has been included. This results in a quadratic relationship between enthalpy and temperature in the ice.

7. RESULTS

Temperature measurements were taken from seven freezes of static water with initial temperature varying between 8°C and 26°C. In addition, plug profile measurements were available from other freezes. Only the temperature profiles from the 8°C and 26°C freezes and the plug profiles from the 23°C freeze are compared here.

Figure 4 plots freezing time against initial temperature. The predicted freezing times increase in a generally linear fashion with initial temperature and are extrapolated, as indicated with the dashed line, to provide estimates of the freezing times for higher initial temperatures. At low temperatures, these are within a minute of the measured freezing times. As the temperature increases, the experimental results increase rapidly as convection in the water becomes more important. The under prediction of around a minute could be attributed to neglecting heat transfer through the wall and the perspex window. In addition, close-off was assessed visually at the window and so was subject to human error.

Figure 5 (a..d) show the temperature profiles across the pipe at 5,10,15 and 20 minutes for the 8°C freeze. This shows good agreement between measured and predicted results up until the ice front reaches the centre line.

Figure 6 (a..e) show the temperature profiles at 5 minute intervals for the 26°C freeze. Again the departure from the measured results after freeze-off can be seen. It is worth noting that the actual water temperature in the top half of the freezing zone is actually slightly lower than predicted and that the solidification at the bottom of the jacket is significantly slower than predicted.

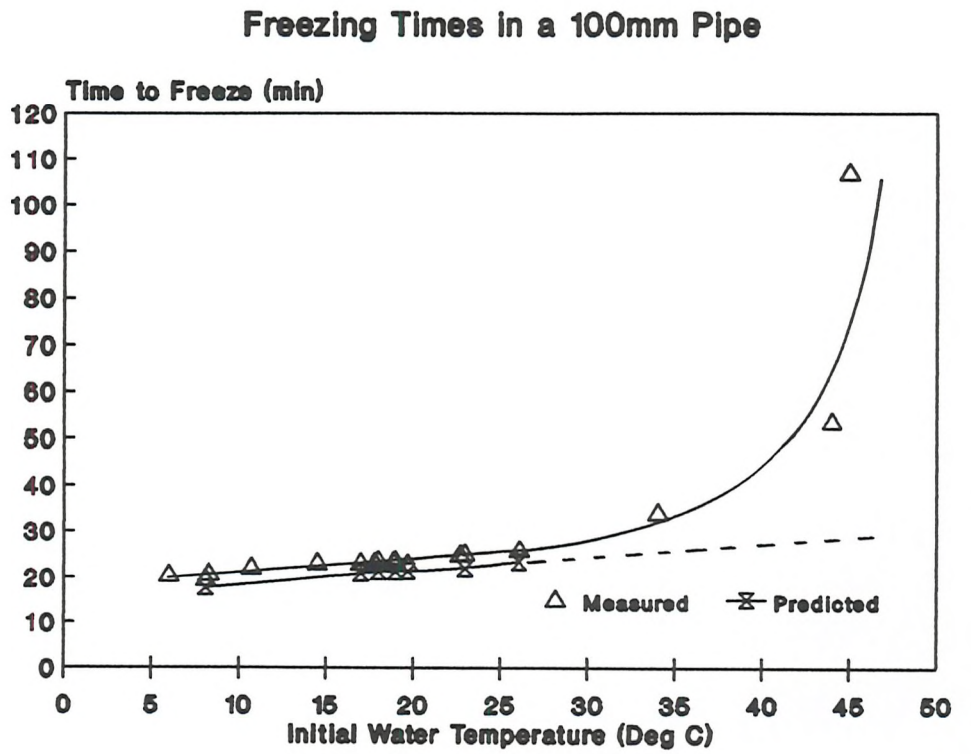

Figure 4 : Effect of Initial Temperature on Freezing Time

This is consistent with the existence of a recirculation cell caused by convection off the ice causing warmer water from beneath the plug to be returned to this region therefore maintaining the temperature and retarding the solidification rate near the bottom of the jacket. Conversely, the recirculation cell established above the plug causes the bulk water temperature drop, as seen here.

At first sight, the underprediction of temperature in the ice after freeze-off would appear to be a major failing in the model. In fact, earlier experimental work by Burton [7] showed similar flat temperature distributions to those predicted here. The difference between the measured temperatures reported here and the predicted values is probably due to heat transfer through the perspex window especially as the ambient temperature when these freezes were performed was high (23°-27°C). The effect of this heat leak was tested numerically by developing another model to describe a horizontal section through the pipe. A convective boundary condition was imposed on the outside of the perspex corresponding to free convection in air. Preliminary results from this model showed that, while the effect on the temperature of the water was small, once the water in contact with the window had solidified, the temperatures in the resulting ice were higher than those obtained with an adiabatic boundary and no window. This could not account for the whole difference between the predicted and measured temperature however, during the experiments condensation and freezing of water vapour from the air occurred which may have significantly affected the heat leak through the window and this effect was not included in the model. In addition, the temperature in a solid ice core falls rapidly so any slight differences in freeze-off time would cause a large

FIGURE 5 : TEMPERATURE PROFILES FOR 8° FREEZE

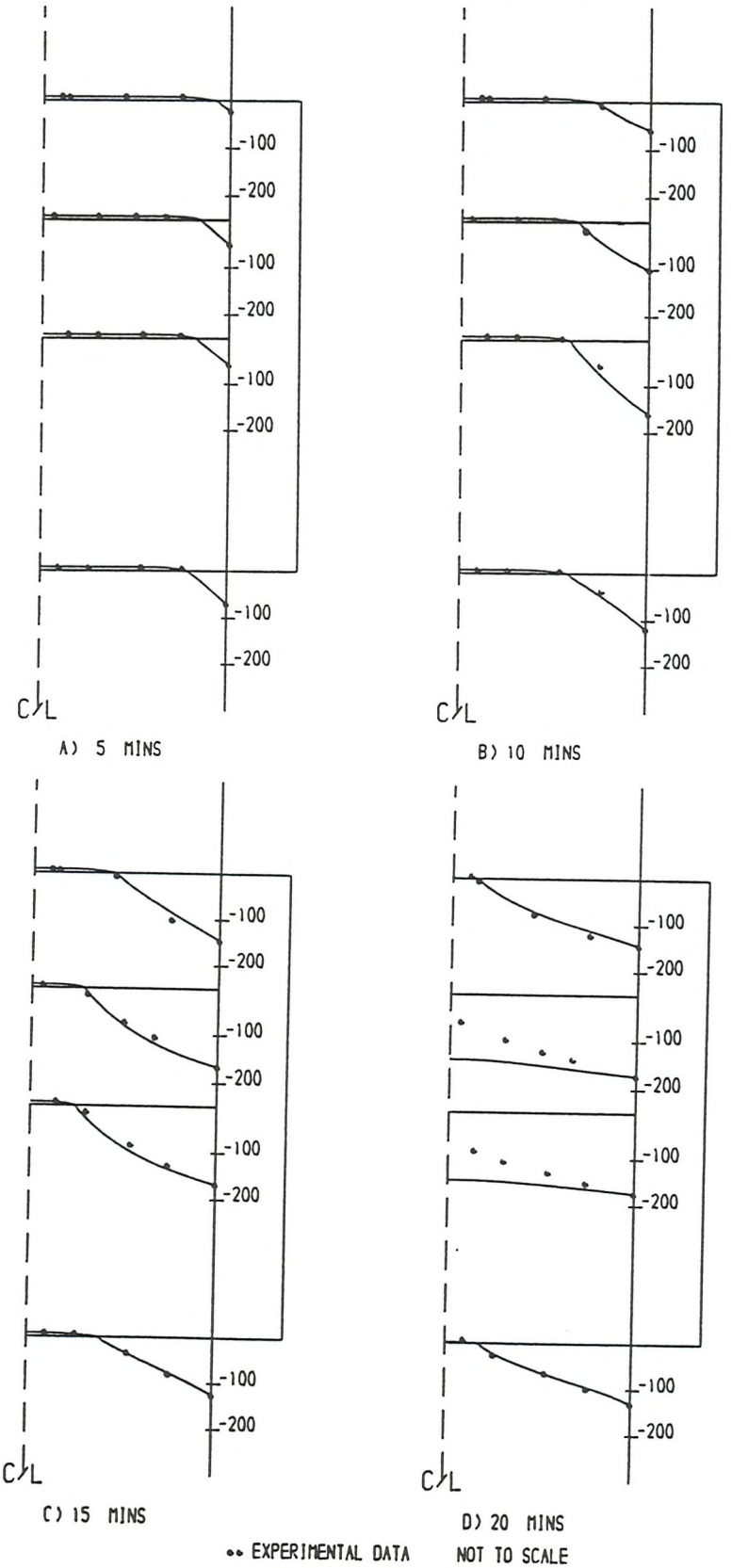

FIGURE 6 : TEMPERATURE PROFILES FOR 26° FREEZE

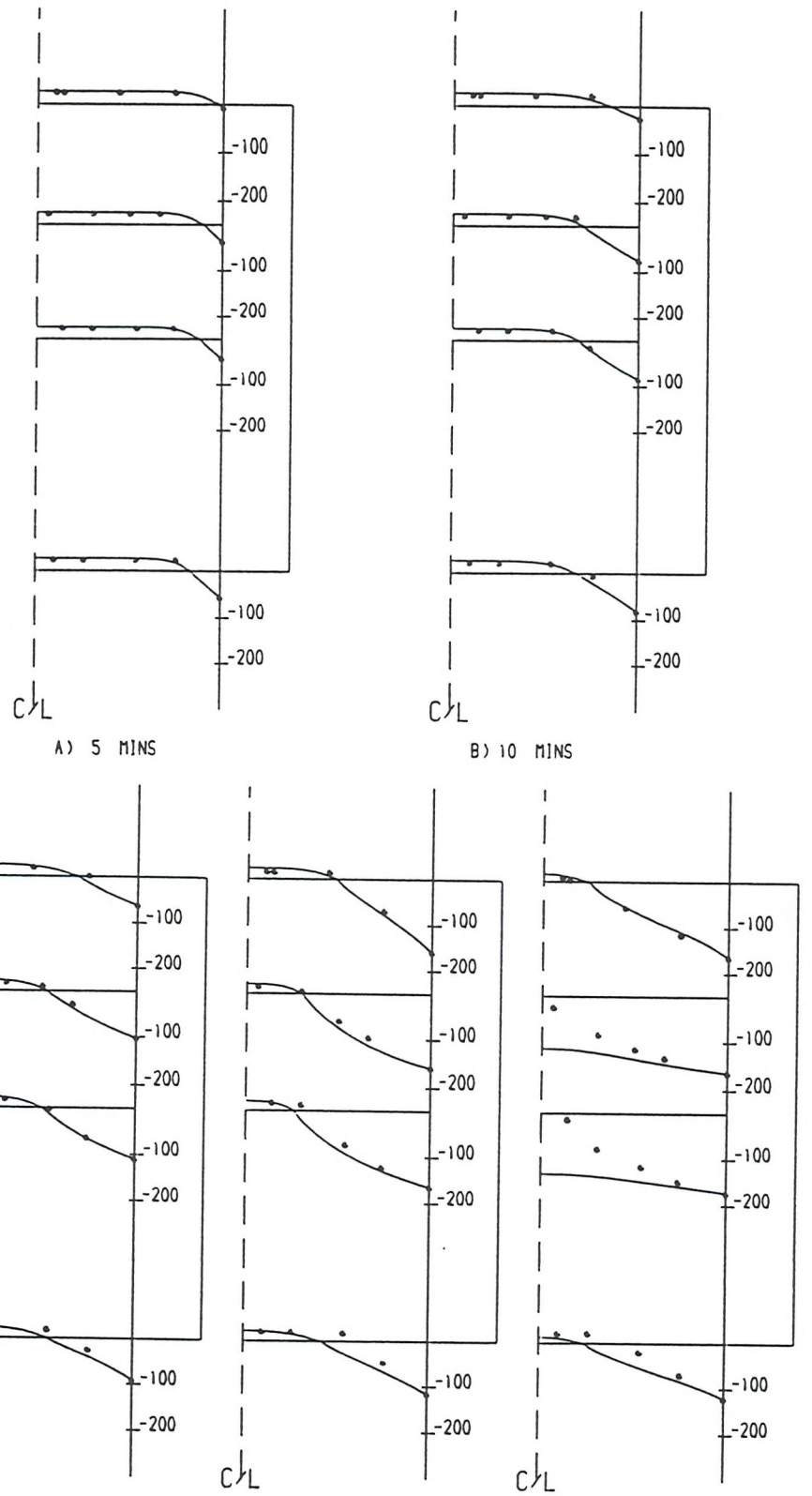

•• EXPERIMENTAL DATA NOT TO SCALE

FIGURE 7 : PLUG PROFILES FOR 23° FREEZE

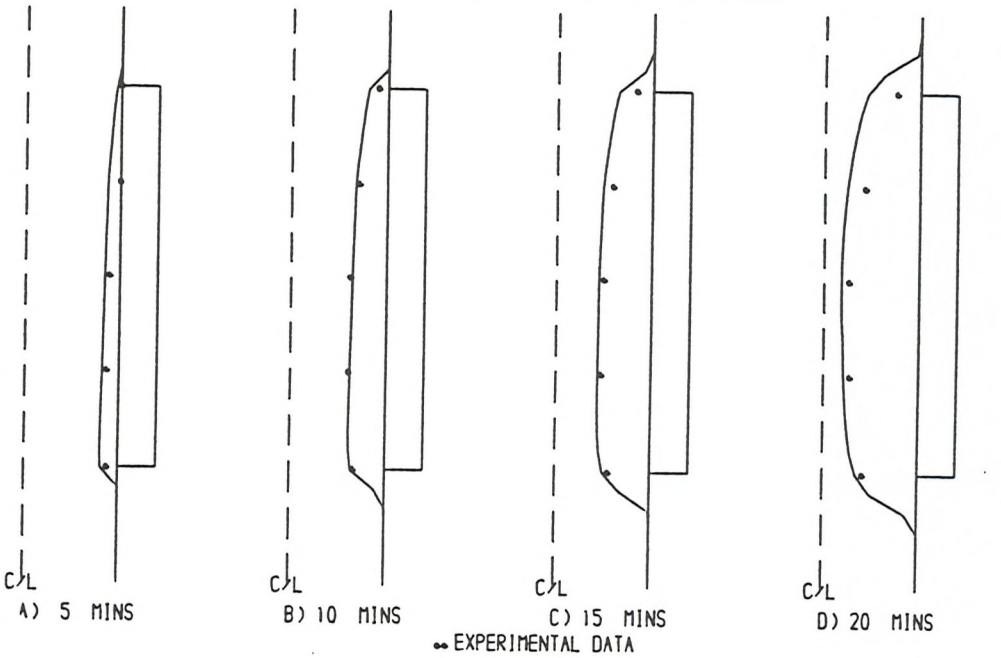

variation in temperature distribution.

The plug profiles for the 23° freeze (Figure 7 (a..d)) show good qualitative agreement. These were different freezes and inconsistencies in the method of maintaining the liquid nitrogen level account for the variations especially at the top of the jacket.

8. CONCLUSIONS AND FURTHER WORK

A model of the plug formation in a vertical pipe has been developed. A fixed grid, finite volume approach incorporating the enthalpy method was applied in two dimensional radial (r,z) co-ordinates to solve the conduction and solidification equations. Experimental work was carried out which provided temperature data and ice plug profiles from a series of freezes of water with initial temperatures varying between 8°C and 26°C. The wall conditions for the model were taken from the experimental results and the resulting temperature distributions and plug profiles were compared with the numerical results.

Agreement was excellent for the lower temperature freezes. Freezing times were predicted to within less than one minute and the measured temperatures lay on or close to the predicted temperature profiles. At higher temperatures, the freezing times recorded during experiments increase rapidly whereas the model predicted a linear increase. In addition, the predicted temperature distributions were less accurate, particularly at the bottom of the jacket where the measured solidification was slower than predicted. This indicates that at these temperatures convection is set up in the water which causes the movement of warmer water into the cooled section, thereby retarding solidification.

Experimental work has shown that the value of initial temperature at which convection becomes significant is lower for larger pipes. As the aim of this research is to develop a full model of pipe freezing which can be applied to any combination of pipe size and initial temperature, the next stage will be to introduce convection into the model.

ACKNOWLEDGEMENTS

The authors gratefully acknowledge the financial support of PowerGen, the S.E.R.C. (M.T.D.) and Conoco UK Ltd. Thanks are also due to The British Oxygen Company Ltd, Mobil UK, Shell UK, Britoil PLC, The CEGB, The Swedish State Power Board, Bishop Pipefreezing Ltd, The Department of Energy and The Health and Safety Executive, all of which helped to fund the project.

REFERENCES

1. SHAMSUNDAR, N. and SPARROW, E.M. - Analysis of MultiDimensional Phase Change via the Enthalpy Method, Journal of Heat Transfer, 97, n3, 333-340 (1975)

2. PATANKAR, S.V. - Numerical Heat and Mass Transfer, Hemisphere Publishing Corp, 1980

3. SHAMSUNDAR, N. and ROOZ, E. - 'Numerical Methods for Moving Boundary Problems', Handbook of Numerical Heat Transfer, Minkowycz, W.J., Sparrow, E.M., Schneider, G.E. and Pletcher, R.H., John Wiley and Sons, Inc., 1988, p.747

4. CARSLAW, H.S. and JAEGER, J.C. - Conduction of Heat in Solids, Clarendon Press, 1959

5. TAVNER, A.C.R. - The Effect of Convection on Ice Formation in a Vertical Pipe During Cryogenic Pipe Freezing : An Experimental Study, Ph.D Thesis, University of Southampton, (Pending)

6. HOBBS, P.V. - Ice Physics, Clarendon Press, Oxford, 1974

7. BURTON, M.J. - An Experimental and Numerical Study of Plug Formation in Vertical Pipes During Cryogenic Pipe Freezing, Ph.D Thesis, University of Southampton, 1986

A5.2 The development of a numerical model of freezing and convection in a vertical water filled pipe

A.C. Keary, R.J. Bowen, A.C.R. Tavner

Proceedings of Eurotherm 30: Heat Transfer in Phase-Change Processes: Melting and Solidification, Orsay, France. October 1992. (pp.49-52)

THE DEVELOPMENT OF A NUMERICAL MODEL OF FREEZING AND CONVECTION IN A VERTICAL WATER FILLED PIPE

A C Keary, R J Bowen and A C R Tavner
Department of Mechanical Engineering
University of Southampton
UK

INTRODUCTION

Cryogenic Pipe Freezing is a pipeline maintenance technique used for isolating sections of a liquid filled pipeline without requiring that the system is drained. A jacket is attached to the pipe and filled with a cryogen such as liquid nitrogen causing the liquid in the pipe to freeze. By freezing two plugs, the section between them is isolated and work may be carried out on it. Once this has been completed, the jacket can be removed and the plugs allowed to thaw. This process is inexpensive and uncomplicated compared to other plugging techniques; however, the success of the method is sensitive to the flow and temperature of the liquid in the pipe.

Due to the general lack of understanding of the process, a research programme was started at Southampton in 1981. Over the past eleven years, a large amount of data has been collected from experimental investigations. Although a wide range of pipe conditions have been explored it would not have been feasible to investigate all possible variations. The development of a numerical model of the pipe freezing process was therefore considered essential.

DEVELOPMENT OF THE MODEL

The finite volume approach was used and the development of a full model of plug formation was tackled in stages. The case of a vertical pipe was chosen so that the problem was two-dimensional. Firstly, a model was developed which predicted the convection inside the pipe using the SIMPLER algorithm proposed by Patankar [1]. Next a model of the solidification and conduction processes, neglecting the effects of convection, was developed using the enthalpy method [2] to solve the phase change problem.

The final stage was to couple the two models together in order to investigate the effect of convection on the plug formation. The fluid velocity in a solidifying control volume was forced to zero as the volume froze by imposing a velocity source term. This is described by Hibbert et al [3] who used it to model solidifying water and metals.

The convection and the solidification solution methods were tested against the appropriate available benchmark tests and showed good agreement with the published data. The solidification model was used to predict plug formation and was also tested extensively against experimental data. A paper [4] describing this work was presented at the 7th International Conference in Numerical Methods in Thermal Problems in July 1991.

DESCRIPTION OF THE EXPERIMENTAL RIG

Experimental research provided measurements of freezing times, plug profiles, and temperature and velocity distributions inside a 1m length of 100mm diameter pipe with a 200mm jacket placed centrally on the pipe. In order to observe the plug formation and any flows inside the freezing section, the pipe was cut in half lengthways and a perspex window bolted across the open side. The pipe was placed over a tank of water to simulate the thermal mass of the liquid in the pipeline. By using flow visualisation techniques, the convective flows inside the pipe could be measured and photographed together with the plug shape. In addition, a series of freezes on nominally static water with thermocouples inside the pipe were carried out, using water of varying initial temperatures. This is described in more detail in [5].

DESCRIPTION OF THE MODEL

For the test runs, a 654mm length of 100mm diameter pipe was modelled, with the top of the jacket 111mm from the top of the pipe. There was therefore 343mm of pipe below the jacket compared to 400mm in the experimental rig. No tank was included in the domain, although the bottom wall was maintained isothermal. The outer wall condition above and below the freezing zone was assumed to be adiabatic.

A 56x82 grid was chosen, giving a grid spacing of 1mm in the radial direction and of between 5mm and 10mm in the vertical direction with the spacing set at 8mm inside the freezing zone. A time step of one second was used.

The physical properties of water and ice vary with temperature and these variations were incorporated into the model. The nitrogen boiling in the jacket was simulated by formulating a relationship between heat flux and wall temperature which resulted in good agreement between the measured and predicted values of the wall temperatures throughout the freeze.

Experimental work has demonstrated that, for a 100mm diameter pipe, the time to freeze increases in a generally linear fashion for initial temperatures below 25°C and then increases more rapidly until a limiting temperature of around 50°C is reached beyond which a solid plug cannot be formed. The model was run for initial water temperatures of 8°C, 18°C, 26°C and 40°C to investigate this behaviour.

RESULTS AND DISCUSSION

Figure 1 shows the flow field and temperature distribution developing during the 26°C freeze. The results are plotted at two minutes intervals up to 10 minutes and 5 minute intervals after that until plug closure. The plots show a slice through the pipe with the wall on the left and the centre of the pipe shown as a dashed line on the right.

Cooling the wall inside the freezing zone causes a downwards flow of water at the wall. When the plume leaves the freezing zone the flow next to the wall slows down as it is no longer being cooled. This trips up the plume, forcing it to flow inwards. Thus two convection cells are established with an upper cooled cell supported on top of a lower cell. A complicated mixing zone develops below the forming plug where the two cells meet with pockets of warmer water trapped inside cooler fluid. When the ice reaches a critical thickness the flow through the neck decreases, isolating the liquid above the plug from that below.

Figure 2 shows the measured and the predicted values of boundary layer velocity as the freeze progresses. The prediction is excellent, with the two values lying within 0.5mm/s of each other. With the exception of the 40°C freeze, the predicted freeze times lie within a minute of the measured freezing times and they increase more rapidly with initial temperature than those obtained when convection is ignored.

When the bulk temperature of the water inside the freezing zone was examined, it was observed that the predicted value dropped more rapidly than the measured value. An isothermal outer boundary condition was incorporated into the model in order to test whether this was due to heat flux through the wall above and below the freezing zone, but this was found to have no effect on the decay of bulk temperature.

The temperature of the water inside the freezing zone is controlled by the temperature of the core flow of water returning up the pipe. At about 5 minutes, the two convection cells become established which then control the temperature of the return flow. In the experiments, the presence of a tank resulted in the temperature of the lower cell being maintained. By using a closed domain in the numerical work, a smaller mass of water was cooled and therefore the temperature of the lower cell, and hence of the mixing region and return flow, dropped more rapidly.

The water temperature inside the freezing zone controls the rate at which freezing occurs and at higher values of initial temperature, when convection is more important, the freeze time is markedly affected. In the 40°C case, the predicted freezing time was around 30 minutes, some 5 minutes slower than when convection was not included but still 23 minutes faster than the measured value.

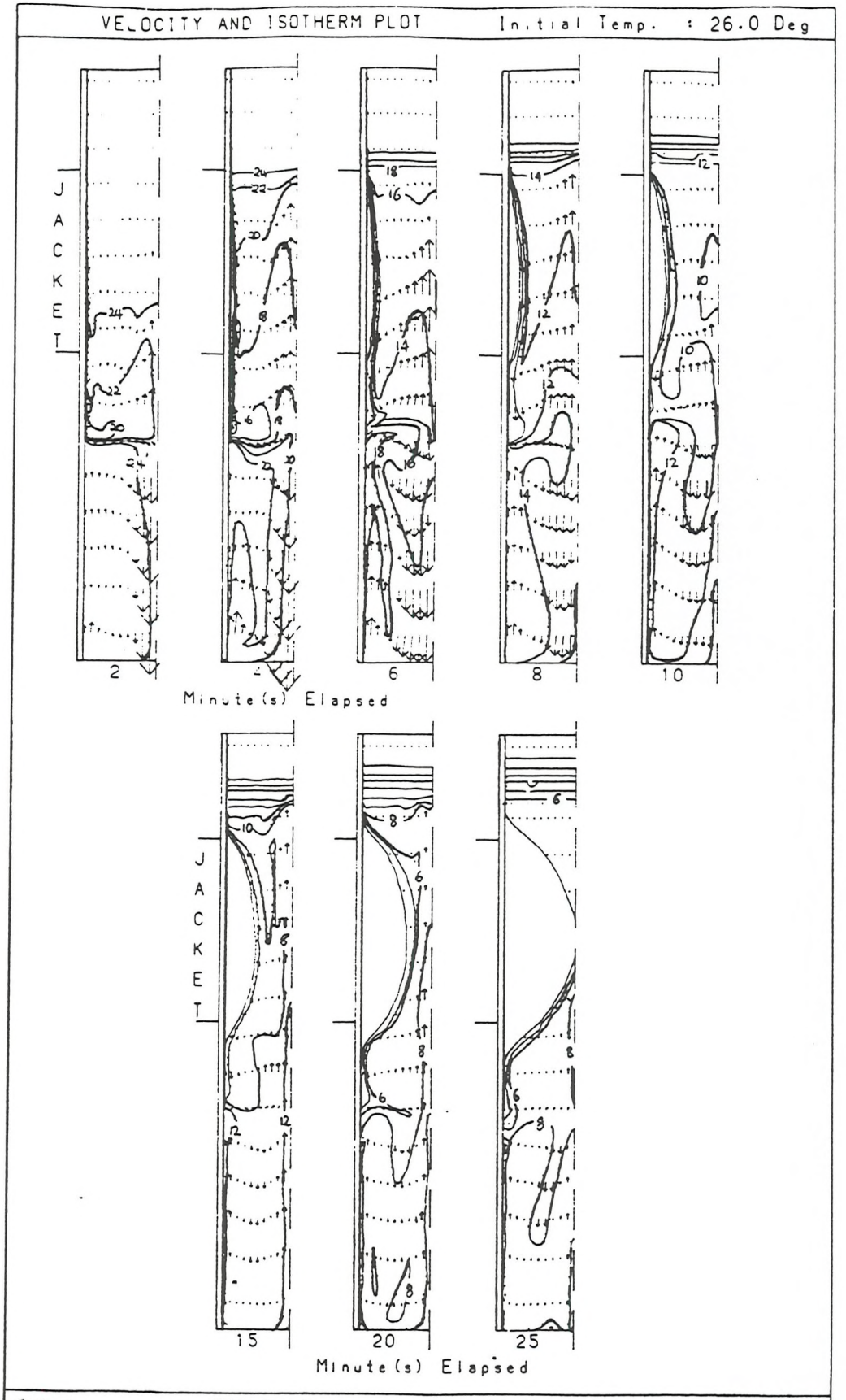

FIG. 1 NOT To Scale Not All Points Plotted

Burton [5] investigated the effect on plug formation of including a tank in the experimental rig and experienced similar effects. He found that not including a tank led to faster freezing and a higher limiting value of temperature beyond which freezing is impossible. This clearly demonstrates that the predictions are accurately modelling freezing in a closed length of pipe.

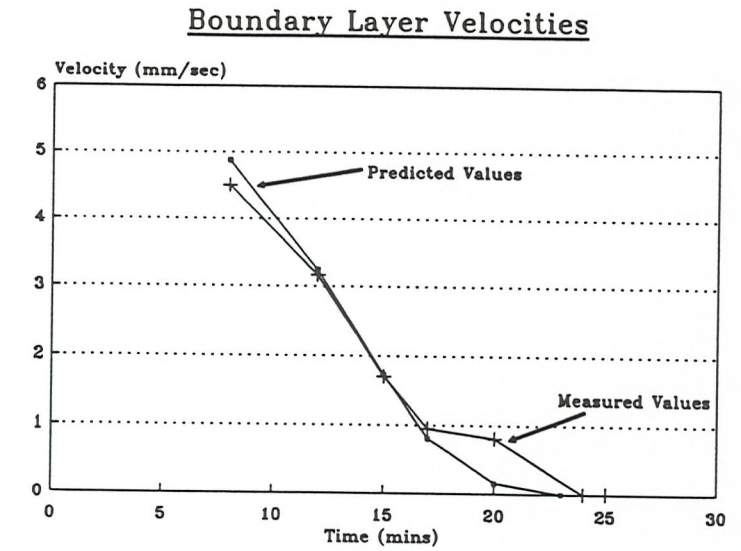

Comparison for 18 Deg Freeze

Figure 2

CONCLUSIONS

A model was developed which predicts the formation of a plug in a pipe including the effects of convection. This has given good results for velocity and plug growth in freezing water at temperatures below 30°C and has aided the understanding of the mixing mechanisms which take place between the cooled water and surrounding water near the ice plug.

It has been observed from the predictions that a complex mixing region is set up below the forming plug where the cooled water from the freezing zone interacts with the surrounding water. This region is responsible for setting the temperature of the water returning up the centre of the pipe, which is itself crucial to the rate at which the plug freezes.

ACKNOWLEDGEMENTS

The authors gratefully acknowledge the financial support of PowerGen, the S.E.R.C. (M.T.D.) and Conoco UK Ltd.

REFERENCES

1. PATANKAR, S.V. - Numerical Heat and Mass Transfer, Hemisphere Publishing Corp, 1980
2. SHAMSUNDAR, N and SPARROW, E.M. - Analysis of MultiDimensional Phase Change Via the Enthalpy Method, Journal of Heat Transfer, 97, n3, 333-340 (1975)
3. HIBBERT, S.E., MARKATOS, N.C. and VOLLER, V.R. - Computer Simulation of Moving-Interface, Convective, Phase-Change Processes, Int. J. Heat and Mass Transfer, 31, n8, p1709-1718, 1988
4. KEARY, A.C., BOWEN, R.J. and TAVNER, A.C.R. - The Development of a Two Dimensional Numerical Model of Freezing in a Vertical Water Filled Pipe, 7th Int. Conf. Numerical Methods in Thermal Problems, Pineridge Press, Swansea, 1991
5. TAVNER, A.C.R. - An Experimental Study if Ice Formation and Convection During Cryogenic Pipe Freezing, Ph.D Thesis, University of Southampton, 1992
5. BURTON, M.J. - An Experimental and Numerical Study of Plug Formation in Vertical Pipes During Cryogenic Pipe Freezing, Ph.D Thesis, University of Southampton, 1986

A5.3 The effect of free convection on plug formation during cryogenic pipe-freezing: a numerical study

Tenth International Heat Transfer Conference

Brighton, UK. 1994. (pp.55-60)

THE EFFECT OF CONVECTION ON PLUG FORMATION DURING CRYOGENIC PIPE-FREEZING : A NUMERICAL STUDY

A C Keary and R J Bowen

Department of Mechanical Engineering
University of Southampton
UK

ABSTRACT

A numerical model was developed in order to investigate the effect of convection on freezing during cryogenic pipe freezing in a vertical pipe. In order to simulate an infinite length of pipe, flow was allowed across the bottom boundary of the numerical domain. The temperature of the water entering the domain was kept fixed at the initial water temperature and the interaction between the flow and the forming plug was predicted. The developing plug was found to distort the convection cell, causing the regions above and below the plug neck to become more and more isolated as the plug developed. Cooled water was trapped above the neck and the bulk of the relatively warm water entering the domain was turned at the plug neck, maintaining the temperature of the region below the plug neck. When the temperature and velocities were significantly large, the ice formation in the region below the neck was retarded, causing the position of the neck to move up the plug.

The results obtained in this investigation were limited by the simplifications made in formulating the velocity boundary condition. However, the predicted plug profiles resembled those measured during experiments and therefore the results can be considered as giving a qualitative description of the processes involved during freezing in a vertical pipe.

1. INTRODUCTION TO PIPE FREEZING

Cryogenic pipe freezing is a pipeline maintenance technique used for isolating sections of a liquid filled pipeline without requiring that the system is drained. A jacket is attached to the pipe and filled with a cryogen such as liquid nitrogen. The liquid inside the pipe is cooled and starts to freeze, forming a plug which grows inwards from the wall to block the pipe. Freezing two plugs isolates the section of pipe between the plugs which can then be worked on. Once the work has been completed, the jackets are removed and the plugs allowed to thaw. This process is inexpensive and uncomplicated compared to other plugging techniques; however, the success of the method is sensitive to the flow and temperature of the liquid in the pipe.

Due to the general lack of understanding of the process, a research programme was started at Southampton in 1981. Over the past twelve years, a large amount of data has been collected from experimental investigations. Although a wide range of pipe conditions have been explored it would not been feasible to investigate all possible variations. The development of a numerical model of the pipe freezing process was therefore considered essential.

2. DEVELOPMENT OF THE NUMERICAL MODEL

A model was developed to predict the formation of an ice plug in a vertical pipe including the effects of convection. The finite volume approach was used and the velocity and pressure equations for the buoyancy driven flow in the water were solved using the SIMPLER algorithm proposed by Patankar (1980). The energy equation was formulated in terms of enthalpy and solved using the method described by Shamsundar and Sparrow (1977) and Shamsundar and Rooz (1988). The variation with temperature of the conductivity and specific heat capacity of ice and the viscosity of water was incorporated into the model and the definition of the buoyancy source term included the density inversion at 4°C.

During the development of the model, it was tested against published, analytical and experimental results. The convection model was used to predict convection in a square cavity for comparison with the results of Markatos and Pericleous (1984) and de Vahl Davis (1983) and also compared with the results of Huang and Hsieh (1987) for convection in a cylinder. A one-dimensional solidification model was tested using the analytical solution to the Neumann problem; the two-dimensional model was used to predict freezing in a square cavity for comparison with the results of Shamsundar and Sparrow (1975). The solidification model was then used to predict freezing in a pipe in the absence of convection and the results compared with experimental results, as described by Keary et al (1991).

In order to model an infinite length of pipe, the problem was initially formulated as a long length of pipe with closed ends. The aim was to position the top and bottom of the domain sufficiently far from the freezing zone so that they would have a negligible effect on the flow and the freezing.

The pipe wall was included in the domain and the presence of a jacket was simulated by a cooled section of the pipe wall. When the resulting predictions of convection and freezing were examined, it was noted that the cooled flow dropped rapidly down the pipe and therefore the use of a closed boundary condition at the bottom of the domain led to a decrease in the bulk temperature inside the pipe because the finite mass of water was being cooled. This problem became more important at higher values of initial temperature, when the use of a limited mass of water resulted in much faster freezing times than those recorded in the experiments. In particular, the experimental results showed a rapid rise in the freezing time when the initial temperature was greater than 30°C in a 100mm diameter pipe, which led to a limiting value of initial temperature above which it was not possible to form a plug. The predicted freezing times showed a nearly linear increase in freezing time with initial temperature.

Attempting to extend the length of pipe which was modelled increased the computer power and memory requirements with very little improvement in the predictions because the cooled flow dropped rapidly down the pipe. In addition, because the flow field was complex, it was not possible to coarsen the grid without decreasing the accuracy.

3. DESCRIPTION OF THE OPEN PIPE MODEL

In order to improve the predictions, it was clearly necessary to be able to control the bulk temperature inside the freezing region. This controls the heat flux arriving at the ice-water interface which, together with the rate at which the heat is removed through the ice layer to the cryogen, controls the rate of ice formation. The model was modified to allow flow in and out across the bottom of the domain. The temperature of the water flowing into the domain could then be specified which effectively controlled the temperature of the water inside the freezing zone.

The open pipe boundary was positioned a short distance below the freezing jacket. The definition of the velocity on this boundary required large simplifications to be made. The radial component of velocity was assumed to be zero, therefore only allowing flow in the vertical direction. Initially, the gradient of vertical velocity in the vertical direction ($\partial w/\partial z$) was set to zero but this was found to predict velocities which increased rapidly over the first minute to values one or two times greater than those obtained in a closed pipe. This was attributed to a failure to take account of the initial development of the flow field, during which the convection cell forms and stretches down the pipe. The model was then modified to use a closed long pipe to predict the initial development of flow field and then switch to an open pipe to predict the rest of the freezing process.

The boundary condition inside the jacket was formulated in various ways in order to try to simulate the complex process of the cryogen, nitrogen, boiling inside the jacket. The results presented and discussed here are for the 'best case' jacket where the temperature on the outside of the pipe wall falls to -196°C immediately that the jacket is filled. A fill time of 2 minutes was assumed, with the boundary condition above the nitrogen level assumed to be adiabatic. The boundary condition on the wall above and below the jacket was adiabatic. The top of the domain was maintained at the initial water temperature. The boundary condition on the bottom of the domain was defined to allow the temperature of the upwards core flow to be set; the boundary condition was adiabatic where the flow direction was downwards and isothermal at the initial temperature when the flow direction was upwards.

4. RESULTS

The model was used to predict the flow and plug formation with initial water temperatures of 10°C and 20°C. The resulting plug form and flow field at one minute intervals throughout the freeze are shown in figures 1 and 2 for the 10°C and 20°C freezes. Each plot shows a slice through the pipe, with the centre of the pipe on the left and marked by a dashed line and the position of the 'jacket' marked outside the pipe on the right hand side. The development of the velocity and temperature distributions throughout the freeze is shown by the velocity vector plots (1.a and 2.a), streamline plots (1.b and 2.b) and isotherm plots (1.c and 2.c). The isotherms inside the ice region are not shown and the plug outline is also shown on the vector, streamline and isotherm plots. The streamfunction was computed from the velocity distributions and the streamline plots are shown here because they provide a clearer picture of the flow field than the velocity vector plots. In all cases, eight equally spaced streamlines were plotted.

The results at 10°C are shown in figure 1.a-c. The effect of simulating the action of filling of the jacket can be seen, with the ice first forming near the bottom of the jacket and then spreading upwards over the first two minutes. This causes the asymmetry in the plug profile, with the position of maximum ice thickness (the plug neck) offset towards the bottom of the plug. This general shape is maintained throughout the freeze, with the plug finally closing off less than halfway up the jacket. The development of the flow field can be examined in more detail by looking at the streamline plots. The convection cell is formed when the wall is cooled. The boundary layer at the bottom of the plug is colder and therefore thicker and faster than that in the top half of the plug and therefore a major proportion of the core flow feeds the flow at the bottom of the plug, as shown by the greater density of streamlines in this region. As the plug develops, the distortion of the water region near the plug neck causes some interaction between the down- and up- flow as it passes through the plug neck and a subcell forms inside the main convection cell above the plug neck. This is visible at 2 minutes, after which it becomes bigger, so that an increasing proportion of the cooled flow is turned at the plug neck. This affects the temperature distribution because cooled water is trapped above the plug neck and the bulk temperature in this region drops. As the plug grows, the bulk of the flow entering the domain is turned at the plug neck and flows back down the ice front. The temperature below the neck is therefore maintained while the

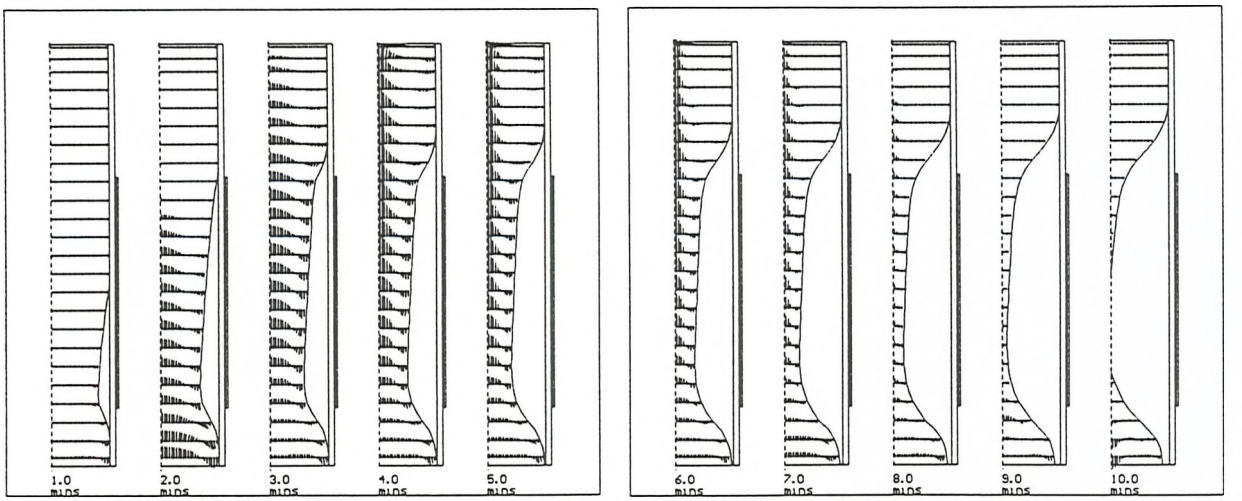

Figure 1.a :Development of Flow Field During 10°C Freeze; Velocity Vector Plot

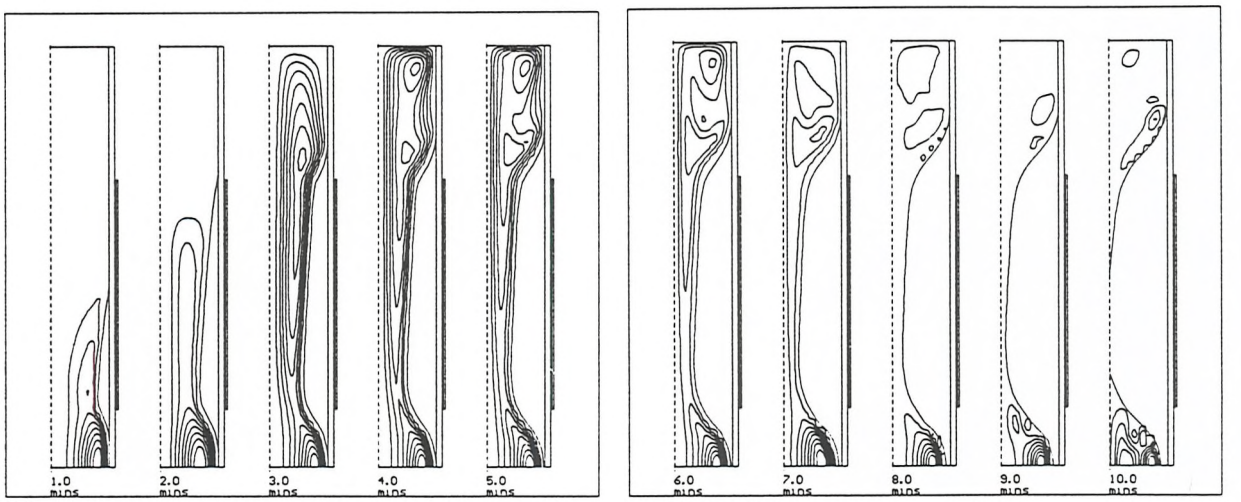

Figure 1.b :Development of Flow Field During 10°C Freeze; Streamline Plot

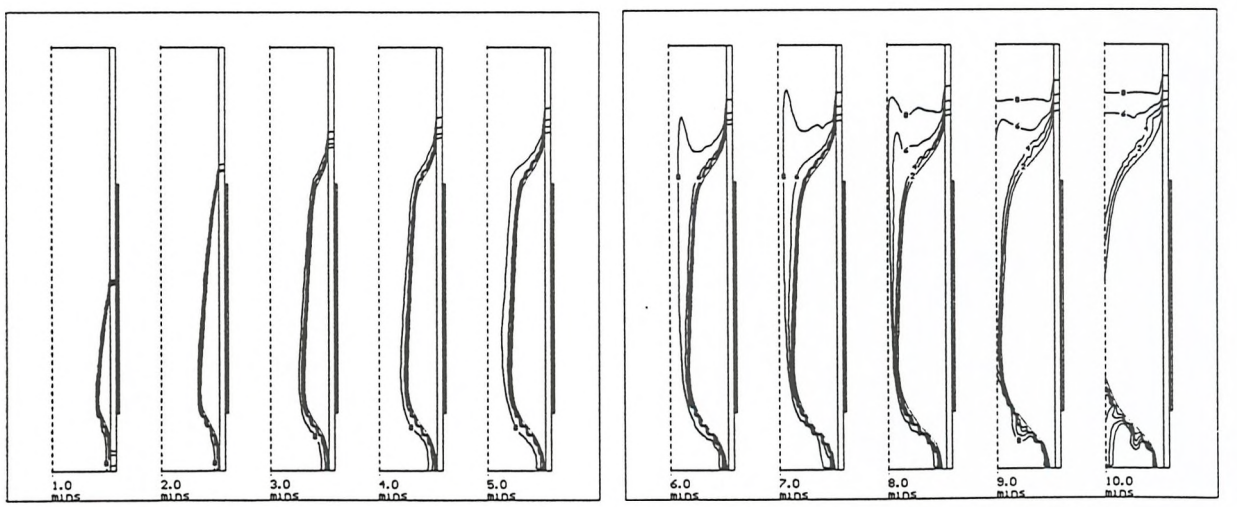

Figure 1.c :Development of Temperature Distribution During 10°C Freeze; Isotherm Plot (2,4,6,8°C)

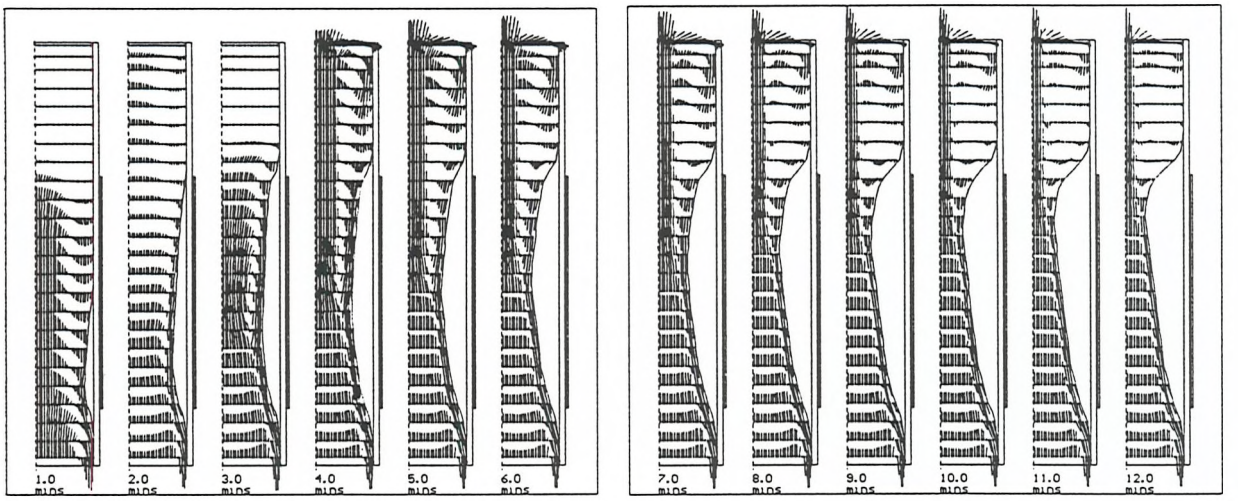

Figure 2.a :Development of Flow Field During 20°C Freeze; Velocity Vector Plot

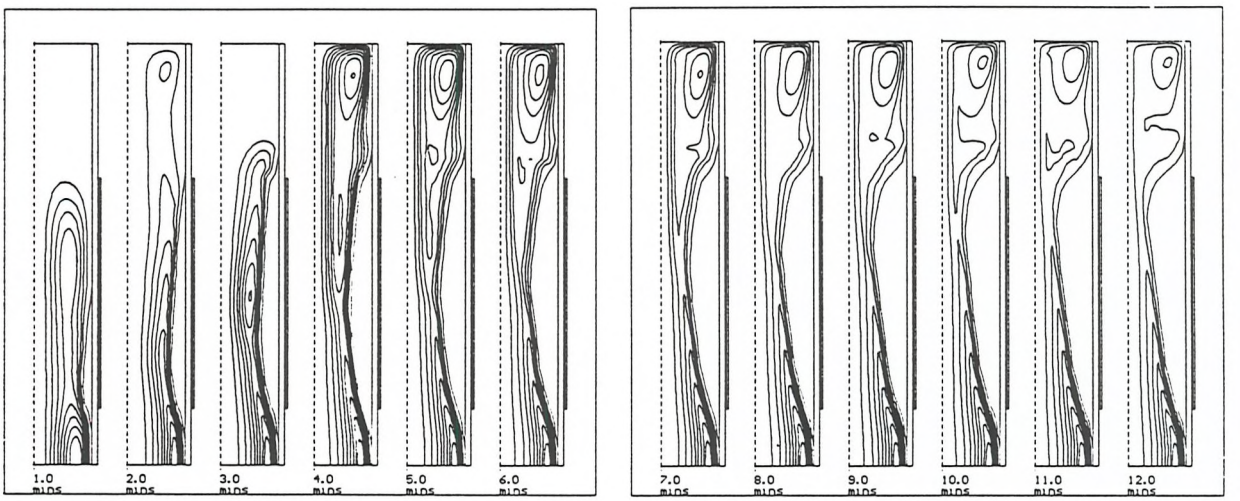

Figure 2.b :Development of Flow Field During 20°C Freeze; Streamline Plot

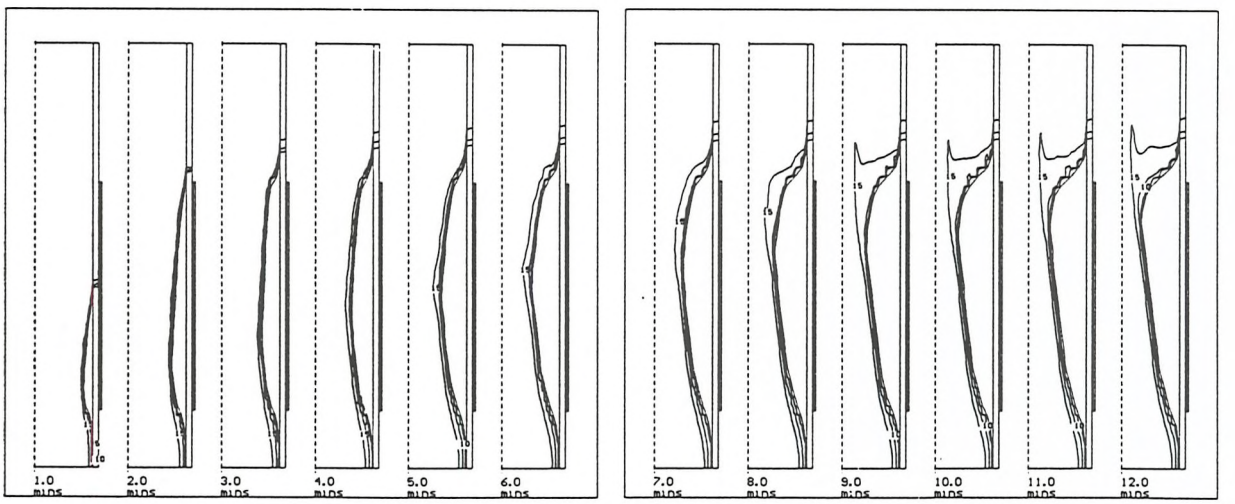

Figure 2.c :Development of Temperature Distribution During 20°C Freeze; Isotherm Plot (5,10,15°C)

region above the neck becomes increasingly isolated and the temperature decreases.

In the 20°C freeze, the development of the flow field is similar, however because the temperature and velocities are greater, the heat transported to the ice/water interface below the neck is more significant. This retards the solidification in this region and causes the position of the plug neck to move up the plug. This can be seen in figures 2.a-c, which show the neck near the bottom of the plug at the beginning of the freeze and then moving up the plug, being approximately halfway up the plug at 6 minutes and being located towards the top of the jacket by ten minutes.

These plug profiles resemble those formed in experiments carried out by Burton (1986) and Tavner (1992). Both Burton and Tavner observed that water is trapped above the forming plug and Burton noted that the position at which the plug froze off was over halfway up the jacket when the bulk temperature inside the freezing zone was maintained.

5. DISCUSSION

The interaction between the plug formation and the development of the convection driven flow field has been examined for two values of initial temperature. This has given a good insight into the mechanisms involved in plug formation, however, these results can only be considered as qualitative because great simplifications were made concerning the flow at the bottom boundary. The predicted velocities were larger than those predicted in a long closed pipe and therefore the effect of increasing the temperature was exaggerated.

This problem was caused by the simplifications which were made in formulating the velocity boundary condition. The predictions obtained using a closed pipe showed that the flow field was complex and therefore the assumption of zero velocity gradient in the vertical direction on the bottom boundary is not adequate. Mixing between the cooled down flow and the upward core flow, which is expected in smaller pipes (when the thickness of the boundary layer is significant is comparison to the pipe radius) was also found to be important in a 100mm diameter pipe, causing a complicated flow field. This effect decreases as the pipe size increases and the flow field becomes less complex. It is therefore expected that it will be possible to formulate a boundary condition which predicts the velocity distribution adequately in larger pipes.

6. CONCLUSION

A model has been developed which predicts plug formation in a vertical pipe without the limitations of a closed pipe length. The effect of convection on the forming plug can be seen, with the plug forming more rapidly near the top of the plug when the initial temperature is significant. The accuracy of the results is limited by the difficulty in defining the velocity boundary condition on the open boundary because the flow field inside a 100mm pipe is complicated because mixing takes places between the cooled boundary layer and the core flow.

One of the main motivations for developing a numerical model was to be able to predict the plug formation in larger pipes. It would require a massive increase in computer power to model a closed large diameter pipe and therefore the open pipe model will be essential. Fortunately, because the flow is less complicated in larger pipes, it is anticipated that it will be easier to obtain an adequate formulation for the boundary condition. The next stage is therefore to develop the model further with the aim of predicting freezing in large pipes.

ACKNOWLEDGEMENTS

The authors wish to thank PowerGen for providing financial support for this work.

REFERENCES

Patankar,S.V. 1980, Numerical Heat and Mass Transfer, Hemisphere Publishing Corp.

Shamsundar,N. & Sparrow,E.M. 1975, Analysis of MultiDimensional Phase Change via the Enthalpy Method, Journal of Heat Transfer, vol.97, n3, pp333-340

Shamsundar,N. & Rooz,E. 1988, Numerical Methods for Moving Boundary Problems, in Handbook of Numerical Heat Transfer, ed. Minkowycz,W.J., Sparrow,E.M., Schneider,G.E. & Pletcher,R.H., pp747-765, John Wiley and Sons, Inc.

Markatos,N.C. & Pericleous,K.A. 1984, Laminar and Turbulent Natural Convection in an Enclosed Cavity, Int. J. Heat Mass Transfer, vol.27, n5, pp755-772

de Vahl Davis,G. & Jones,I.P. 1983, Natural Convection in a Square Cavity : a Benchmark Numerical Solution, Int. J. Num. Method Fluids, vol.3, pp249-264

Huang,H.Y. & Hsieh,S.S 1987, Analysis of Natural Convection in a Cylindrical Enclosure, Num. Heat Transfer, vol.12, pp121-135

Keary,A.C., Bowen,R.J. & Tavner,A.C.R. 1991, The Development of a Two Dimensional Numerical Model of Freezing in a Vertical Water Filled Pipe, Proc. 7th Int. Conf. Numerical Methods in Thermal Problems, San Francisco, vol.1, pp.175-185, Pineridge Press, Swansea

Burton,M.J. 1986, An Experimental and Numerical Study of Plug Formation in Vertical Pipes During Cryogenic Pipe Freezing, Ph.D. thesis, University of Southampton, U.K.

Tavner,A.C.R. 1992, An Experimental Study of Ice Formation and Convection During Cryogenic Pipe Freezing, Ph.D thesis University of Southampton, U.K.

APPENDIX VI
NOTES ON THE FIGURES

The figures showing the numerical predictions of the flowfield and the temperature distribution were produced using post-processing software which was developed as part of this project. This software is briefly described in chapter 4 and in more detail by Keary[2].

The velocity distributions are presented using velocity vector or streamline plots; the temperature distribution is indicated either by isotherms (in the black and white figures) or by colour coding. Although the colour plots have greater initial visual impact, they actually convey less information; the difference of several degrees may lie in the ability to distinguish between different shades of orange. Both methods are used in the following set of figures; colour plots were used where visual impact was required and the black and white plots were preferred where more detail was needed.

A6.1 General Format

Three different methods were used to prepare these figures; the bulk of the figures show the development over a period of time, however, some figures show a zoom of the results obtained for one point in time either with or without the whole-field results.

The results (vectors, isotherms, streamlines) are shown for each point in time superimposed on the boundaries of the numerical domain. This shows a section through the pipe, with the centre line on the left hand side denoted by a dashed line. The position of the jacket, or cooled wall section, is indicated by a rectangle on the right hand side. If the numerical domain included the pipe wall this is included in the figure.

The velocity vectors are plotted from the grid point, position of which is denoted by a filled circle at the grid point, pointing in the direction of the flow and proportional to the speed of the flow in length. Arrow heads were not used because they were found to obscure the vectors (see the output from PHOENICS, Appendix III). Isotherms, where used, are labelled with the appropriate temperature (in degrees Celsius) wherever possible without obscuring the other results. Streamlines are drawn using eight evenly spaced values of streamfunction; the value of streamfunction represented by a streamline will therefore vary from plot to plot.

The plug profile, where applicable, is included in the plot. No vectors (grid point) or isotherms are plotted within the plug and therefore it is visible as a block white area.

A6.2 Figures showing Development over a Period of Time

The general layout used in the preparation of these figures was to show the results twice; the velocity and temperature distributions (isotherms or colour-coding) are plotted above the streamline plot (colour-coded for colour plots). Streamline plots were included as well as velocity vectors plots because they were found to convey more information on the flowfield; this was partially due to the long-thin domain which meant that the vertical component of velocity conceals the horizontal flows in vector plots. The velocity vector plots show the direction of the flow.

Multiple plots show the development over a period of time. The time interval between plots is normally uneven, being closer at the beginning of the simulation. The aim in preparing each figure was to display the important stages during the flow development and/or freeze *on one page*. Thus the plots are reduced in size if necessary. In several cases, the results in an 'area of interest' (for instance, the freezing zone) are plotted separately (for example, the predictions obtained for the 'long' domain).